Unravelling metabolism of *Leishmania* by metabolomics

Julie Kovářová, Mgr.

Submitted in fulfilment of the requirements for the degree of Doctor in Philosophy

School of Life Sciences

College of Medical, Veterinary and Life Sciences

University of Glasgow

March 2016

Abstract

The leishmaniases are neglected tropical diseases with an urgent need for effective drugs. Better understanding of the metabolism of the causative parasites will hopefully lead to development of new compounds targeted at critical points of the parasite's biochemical pathways. In my work I focused on the pentose phosphate pathway of *Leishmania*, specifically on transketolase, sugar utilisation, and comparison between insect and mammalian infective stages of the parasites.

The pentose phosphate pathway (PPP) is the major cellular source of NADPH, an agent critical for oxidative stress defence. The PPP uses glucose, reduces the $NADP^+$ cofactor and produces various sugar phosphates by mutual interconversions. One of the enzymes involved in this latter part is transketolase (TKT). A *Leishmania mexicana* cell line deleted in transketolase (Δtkt) was assessed regarding viability, sensitivity to a range of drugs, changes in metabolism, and infectivity. The Δtkt cell line had no obvious growth defect in the promastigote stage, but it was more sensitive to an oxidative stress inducing agent and most of the drugs tested. Most importantly, the Δtkt cells were not infective to mice, establishing TKT as a new potential drug target.

Metabolomic analyses revealed multiple changes as a consequence of TKT deletion. Levels of the PPP intermediates upstream of TKT increased substantially, and were diverted into additional reactions. The perturbation triggered further changes in metabolism, resembling the 'stringent metabolic response' of amastigotes. The Δtkt cells consumed less glucose and glycolytic intermediates were decreased indicating a decrease in flux, and metabolic end products were diminished in production. The decrease in glycolysis was possibly caused by inhibition of fructose-1,6-bisphosphate aldolase by accumulation of the PPP intermediates 6-phosphogluconate and ribose 5-phosphate. The TCA cycle was fuelled by alternative carbon sources, most likely amino acids, instead of glucose. It remains unclear why deletion of TKT is lethal for amastigotes, increased sensitivity to oxidative stress or drop in mannogen levels may contribute, but no definite conclusions can be made.

TKT localisation indicated interesting trends too. The WT enzyme is present in the cytosol and glycosomes, whereas a mutant version, truncated by ten amino acids, but retaining a C-terminal targeting sequence, localised solely to glycosomes. Surprisingly, cells expressing purely cytosolic or glycosomal TKT did not have different phenotypes regarding growth, oxidative stress sensitivity or any detected changes in metabolism. Hence, control of the subcellular localisation remains unclear as well as its function. However, these data are in agreement with the presumed semipermeable nature of the glycosome.

Further, *L. mexicana* promastigote cultures were grown in media with different combinations of labelled glucose and ribose and their incorporation into metabolism was followed. Glucose was the preferred carbon source, but when not available, it could be fully replaced with ribose.

I also compared metabolic profiles from splenic amastigotes, axenic amastigotes and promastigotes of *L. donovani*. Metabolomic analysis revealed a substantial drop in amino acids and other indications coherent with a stringent metabolic response in amastigotes. Despite some notable differences, axenic and splenic amastigotes demonstrated fairly similar results both regarding the total metabolic profile and specific metabolites of interest.

Contents

List of tables

List of figures

Acknowledgements

I would like to thank to everybody who helped me and supported me during my PhD.

Authors' declaration

I declare that, except where explicit reference is made to the contribution of others, that this dissertation is the result of my work and has not been submitted for any other degree at the University of Glasgow or any other institution.

Julie Kovářová

Abbreviations

Δtkt	transketolase knock-out
1,3bPGH	1,3-bisphosphoglycerate
2PG	2-phosphoglycerate
3PG	3-phosphoglycerate
6PG	6-phosphogluconate
6PGDH	6-phosphogluocnate dehydrogenase
AA	amino acid
AAP	amino acid permease
AmB	Amphotericin B
AMP	adenosine monophosphate
ATP	adenosine triphosphate
Ax Am	axenic amastigotes
BALB/c	“Bagg albino ‘colour’ locus” mouse line
CL	cutaneous leishmaniasis
cyto	cytosolic
DAT	Direct Agglutination Test
DHEA	Dehydroepiandrosterone
DTH	Delayed-type hypersensitivity
E4P	erythrose 4-phosphate
EC_{50}	half maximal effective concentration
EI	electron impact
F1,6bP	fructose 1,6-bisphosphate
FbPase	fructose-1,6-bisphosphate aldolase
F6P	fructose 6-phosphate
FCS	foetal calf serum
G3PDH	glycerol-3-phosphate dehydrogenase
G6P	glucose 6-phosphate
G6PDH	glucose 6-phopshate dehydrogenase
GA3P	glyceraldehyde 3-phosphate
GA3PDH	glyceraldehydes-3 –phosphate dehydrogenase
GC-MS	gas chromatography – mass spectrometry
GDH	glycerol-3-phosphate dehydrogenase
GDP-Man	guanosine diphosphate mannose
GFP	green fluorescence protein

GFAT	glutamine:Fru6P aminotransferase
Glu	glucose
GlcN	glucosamine
GlcNAc	N-acetylglucosamine
GlcN6P	glucosamine 6-phosphate
GlcNAc6P	N-acetylglucosamine 6-phosphate
glyco	glycosomal
GNAT	glucosamine-6-phosphate acetylase
GND	glucosamine-6-phosphate deaminase
GOX	glucose oxidase
GSK	GalaxoSmithKline
HK	hexokinase
HPLC	high performance liquid chromatography
IDEOM	Identification and evaluation of metabolomics data from LC-MS
IFA	immunofluorescence assay
KO	knock-out
LC-MS	liquid chromatography – mass spectrometry
MOI	multiplicity of infection
Man6P	mannose 6-phosphate
MPGT	mannose-1-phosphate guanylyltransferase
mRNA	messenger ribonucleic acid
N9P	nonulose 9-phosphate
NADH	nicotinamide adenine dinucleotide
NADPH	nicotinamide adenine dinucleotide phosphate
NAGD	N-acetylglucosamine 6-phosphate deacetylase
ND	not detected
NMR	nuclear magnetic resonance
NTD	neglected tropical diseases
NS	not significant
O8P	octulose 8-phosphate
PBS	phosphate-buffered saline
PC	principal component
PCA	principal component analysis
PCR	polymerase chain reaction
PEP	phosphoenolpyruvate
PEX	peroxisomal biogenesis factor

PGI	glucose 6-phosphate isomerase (phosphoglucose isomerase)
PKDL	post kala-azar dermal leishmaniasis
Pm	promastigotes
PMA	phorbol 12-myristate 13-acetate
PMM	paromomycin
PPP	pentose phosphate pathway
PTS	peroxisomal targeting sequence
R5P	ribose 5-phosphate
Rib	ribose
RNAi	ribonucleic acid interference
RPI	ribose-5-phosphate isomerase
RT	room temperature
Ru5P	ribulose 5-phosphate
S7P	sedoheptulose 7-phosphate
Sp Am	splenic amastigotes
TAL	transaldolase
TCA	tricarboxylic acid
THP1	“T-lypmocyte human peripheral” cell line
TEA	triethanolamine
TIM	triosephosphate isomerase
TKT	transketolase
TKTL	transketolase-like protein
TPI	triose phosphate isomerase
TPP	thiamine pyrophosphate
UDP-GlcNAc	uridine diphosphate N-acetylglucosamine
UL	unlabelled
UTP	uridine triphosphate
VL	visceral leishmaniasis
WB	Western blot analysis
WT	wild-type
X5P	xylose 5-phosphate
Xu5P	xylulose 5-phpsphate
ZIC-pHILIC	polymer based – Hydrophilic Interaction Liquid Chromatography Column

1 Introduction

Leishmaniasis is a neglected tropical disease affecting millions of people worldwide and causing immense harm (Uniting to Combat NTDs, 2014; WHO, 2010). *Leishmania* parasites are transmitted between their mammalian hosts by sandflies, hence they encounter completely different conditions in each of their hosts, for which they have evolved numerous adaptations. The promastigote stage lives inside the insect's digestive system, whereas the mammalian infecting amastigote stage resides inside phagocytic immune cells. After successful hijacking of macrophages, *Leishmania* spread through the body into skin, mucocutaneous tissues, internal organs or even bone marrow, depending on the species and host status. The final manifestation of the disease is highly variable depending on the specific *Leishmania* species, immune response of each individual, malnutrition, combined infection with other diseases and additional aspects. All of these factors plus the poor socio-economic conditions in most of the affected countries hinder the efforts to bring leishmaniasis under control.

1.1 Leishmaniasis

Leishmania parasites cause a wide range of diseases in terms of clinical manifestation, severity and geographical area concerned. Leishmaniasis occurs in 98 countries worldwide, where 350 million people live under threat of the disease, and the overall prevalence is estimated about 12 million people infected in total, 1.8 million people are newly infected and about 40,000 die because of leishmaniasis each year (Alvar et al., 2012; Palumbo, 2008). Approximately half of these cases are children (Palumbo, 2008; WHO, 2010). As with the other neglected tropical diseases, leishmaniasis is associated with poor living conditions and insufficient medical help available. Predominantly, patients live in developing countries with very poor health care without appropriate management and funding available to control the disease. Major risk factors for the

infection are poor socioeconomic conditions, malnutrition, population mobility, environmental and climate changes, and animal reservoirs (Savoia, 2015). Malnutrition is a very strong risk factor for development of the clinical disease after leishmania infection (Cerf et al., 1987; Harrison et al., 1986), probably due to failure of lymph node barrier (Anstead et al., 2001). Untreated patients seem to be the major infection reservoir for anthroponotic leishmaniasis and increase the risk of infection 26-fold within the household (Alvar et al., 2006). Poor housing conditions are associated with increased exposure to sand flies, lack of bed nets and sanitation. The total disease burden is substantially higher for women than men due to prejudices and stigma (Alvar et al., 2006). Basically, leishmaniasis and poverty create a positive feedback loop, especially strong because of high cost of the treatment compared to other infectious diseases (Alvar et al., 2006).

Manifestation of leishmaniasis is highly variable ranging from a mild, self-healing skin disease to a lethal visceral form, depending mostly on the parasite species but additional factors, including host immune status are involved. Cutaneous leishmaniasis affects about 0.7 – 1.2 million people each year and causes skin lesions, often self-healing and without any long-term effects, unless the scars become disfiguring, or can be debilitating if the lesions are multiple. Areas of occurrence are widely distributed, with approximately one third of the cases found in Latin America, one third in western Africa and the rest stretching from the Middle East to Central Asia (Alvar et al., 2012). 70% of cutaneous leishmaniasis cases are confined to Afghanistan, Algeria, Brazil, Colombia, Ethiopia, Iran, North Sudan, Peru, Syria, and Costa Rica (Fig 1.1) (Alvar et al., 2012). The major causing agents are *L. major, L. tropica, L. infantum* and *L. aethiopica* in the Old World; *L. mexicana, L. amazonensis, L. braziliensis, L. panamensis*, *L. peruviana*, and *L. guyanensis* in the New World (Pace, 2014; WHO, 2010).

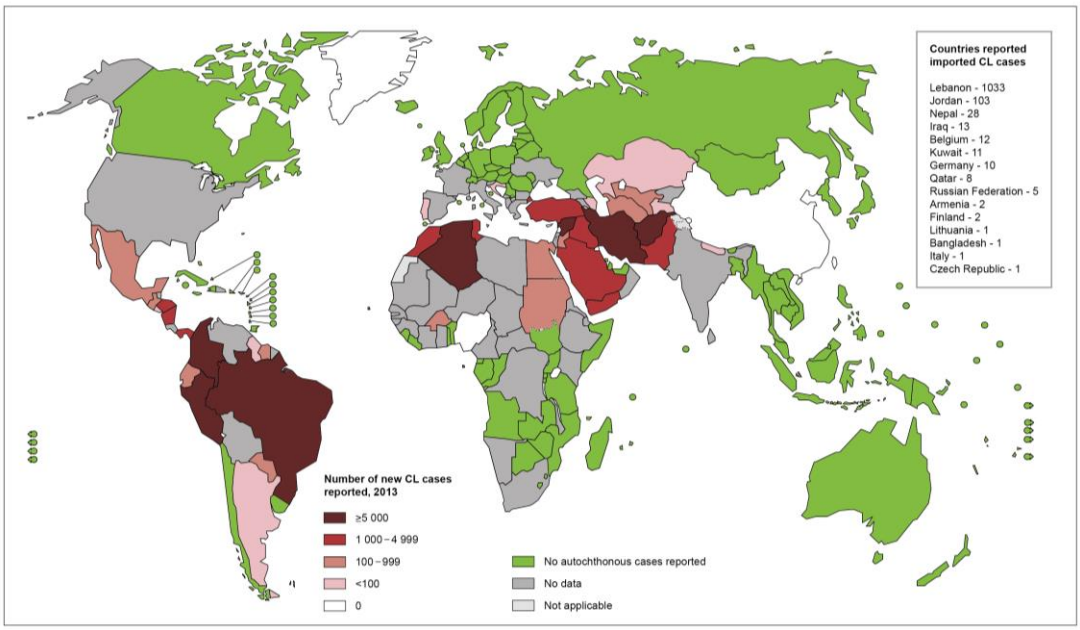

Figure 1.1. Distribution of cutaneous leishmaniasis. WHO 2013.

Mucocutaneous leishmaniasis is a relatively rare variant of the disease, when the parasites reside in mucocutaneous tissues of oral-nasal and pharyngeal cavities and can cause awful damage, disfiguring lesions or permanent deterioration of the face. 35,000 mucocutaneous leishmaniasis cases are reported each year in Peru, Bolivia and Brazil (Pace, 2014). The main species responsible are *L. braziliensis* and *L. guyanensis* in the New World, and *L. donovani*, *L. major*, and *L. infantum* in the Old World (Desjeux, 2004). Interestingly, recent findings show that especially severe cases of *L. braziliensis* and *L. guyanensis* infection are related to an RNA virus residing inside the parasites (Ives et al., 2011). The exact mechanisms of the viral effects and relevance to the disease outcome have not been elucidated so far.

About 0.2 - 0.4 million people are infected with visceral leishmaniasis each year, called by the original Hindi name kala-azar, the most severe form when the parasites infect spleen, liver or bone marrow. Visceral leishmaniasis is caused by *L. donovani* in the Indian subcontinent, parts of Asia and east Africa, *L. tropica* in the Middle East, and *L. infantum* in the Mediterranean region, south-west and central Asia, and South America (Murray et al., 2005; Pace, 2014) (Fig 1.2). The illness manifests with undulating fever, loss of weight, enlargement of the spleen and liver, anaemia before turning into a

multisystem disease which becomes lethal if not treated. Whereas hepatic infection is usually self-limiting, infection in spleen becomes persistent, reflecting the important role played by respective immune responses (reviewed in Engwerda and Kaye, 2000). An estimated 90% of visceral leishmaniasis cases are found in rural and suburban areas of Bangladesh, India, Sudan, South Sudan, Ethiopia and Brazil (Alvar et al., 2012; Uniting to Combat NTDs, 2014). Mortality of visceral leishmaniasis is estimated as 10%, but seems to be highly variable depending on the region (reviewed in Alvar et al., 2012).

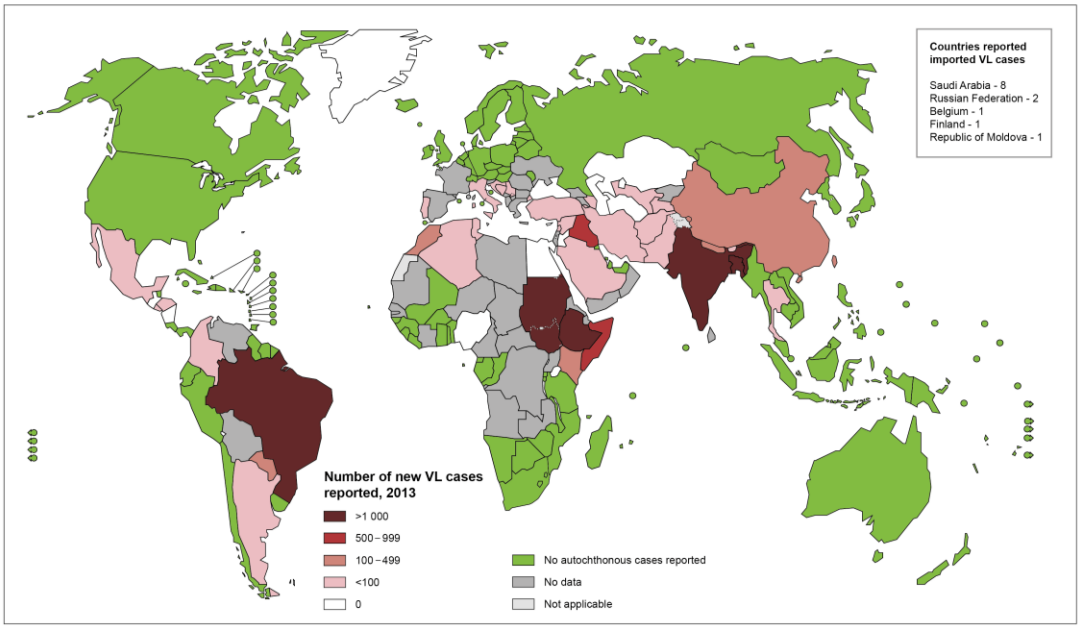

Figure 1.2. Distribution of visceral leishmaniasis. WHO, 2013.

Next to these major types of the illness, less common forms can develop if the immune system is impaired. Diffuse cutaneous leishmaniasis, for example, develops if the cell-mediated immune response is defective, and lesions are disseminated with patients suffering from relapses. When visceral leishmaniasis is not cured to completion with therapy, the so called post kala-azar dermal leishmaniasis (PKDL) syndrome can occasionally follow. Significant differences were reported for PKDL development between cases from Sudan and India with regard to the proportion of visceral leishmaniasis patients affected, the time scale of disease appearance and its severity (reviewed in Murray et al., 2005).

There are numerous aspects that contribute to the outcome of the disease. First, the specific parasite species is crucial, because it determines the type of disease. Despite intense efforts, including whole genome sequencing and the latest –omics techniques, to compare the species, the specific factors underlying the differences remain unresolved. A relatively small number of species-specific genes exist, but considerable variability in chromosome copy numbers, thus gene dosage is suspected to play the predominant role (reviewed in Cantacessi et al., 2015). Moreover, considering heterogeneity within sequence of individual genes and also the potential of interactions between variants within a system, clearly a systems wide appreciation of the parasite, and its interaction with the host, is needed before true understanding is possible.

Leishmania parasites infect macrophages and other phagocytic immune cells and the individual immune response is crucial in determining the outcome of the infection, for example whether the cutaneous disease will be asymptomatic, self-healing or relatively severe diffuse type. HIV co-infected patients experience especially severe development of the disease, another strong risk factor is malnutrition (Savoia, 2015).

Desjeux (2004) warned of a disturbing increase in the prevalence of leishmaniasis as a consequence of changes to living conditions in affected areas, such as fast urbanization, environmental and climatic changes or migration of people. Cases of cutaneous leishmaniasis doubled in Brazil from 1998 to 2002 to 40,000 cases, increased four times in Kabul, Afghanistan from 1994 to 2002, and numbers of VL patients rose four times in north-east Brazil between 1998 and 2002. A major hindrance in bringing the disease under control is lack of data and missing knowledge of the actual situation. Ostyn and colleagues (2011) reported 100,000 cases of VL in Indian subcontinent due to *L. donovani* infection, but they argue that the real situation may be 5 – 8 times higher. The total numbers of infected cases are only estimates, because proper and adequate records are missing. Studies aiming to calculate the exact numbers of infected patients draw a conclusion that the official numbers may be 4 – 8 times underestimated compared to the real situation (reviewed in Alvar et al., 2012). The authors declined to make estimates from sub-Saharan Africa, from where no data are available at all. Currently, the numbers currently appear to be in decline, for example Murray reported expected toll of 70,000 in 2005, while Alvar (2012) estimated only 20,000 – 40,000 deaths annually. The latest report by the NTD Initiative (2014) is optimistic, especially in south-east Asia, there is

an obvious progress towards elimination, since incidence dropped by 60% and number of fatality cases by 81% between 2011 and 2013. A big improvement is noted in monitoring and supplying updated statistics in the poorest areas, which are the first steps necessary for control of the disease.

Note, however, that circumstances can lead to a rapid change in fortune, as evidenced in the increasing incidence in Syria associated with the collapse of health services due to the state of war existing there. Movement of people due to war from nonendemic to endemic areas can lead to exposure of susceptible population to the parasites and high increase of the cases. In southern Sudan between 1984 -1994, it caused an estimated 100,000 deaths due to VL. In Afghanistan, approximately 300,000 people were affected with CL probably after exposure to the parasites in Pakistan (reviewed in Alvar et al., 2006). In the 2000's an outbreak of CL took place after the war in Iraq (Du et al., 2016).

Over the last 20 years, numbers of CL cases in Syria have been increasing from 3,900 newly reported cases in 1998, to 23,000 cases in 2008, to 53,000 cases in 2012 in consequence of socioeconomic changes, rapid urbanization, migration of people into new suburbs with inadequate hygiene and sanitation condition, and migration of non-immune people into *Leishmania* endemic areas (Hayani et al., 2015; Salam et al., 2014). The numbers continued to increase with the onset of the civil war in March 2011 reaching 41,000 in the first half of the year 2013, with leishmaniasis emerging even in new areas (Du et al., 2016). In addition, WHO estimated that the numbers may be three to five fold underestimated (Alvar et al., 2012). It has been reported numerous times in the past that war conflicts are accompanied with neglected tropical disease outbreaks, mostly because of insufficient health care, migration of people into and from endemic areas, poor living conditions, malnutrition and general weakening of the immune system (reviewed in Du et al., 2016). Despite recent progress in diagnosis and treatment, in Syria microscopy is used for diagnosis and antimonial-based drugs for treatment, whilst AmbiSome or miltefosine are not available (Hayani et al., 2015). With migration of refugees from Syria, leishmaniasis is emerging in neighbouring countries (Alawieh et al., 2014; Inci et al., 2015), *L. tropica* is spreading which is less sensitive to antimonial treatment (Hadighi et al., 2006, 2007) and patients from younger groups are the most effected as not being immune (Du et al., 2016). Other areas threatened with leishmaniasis increase are Libya, Tunisia, or Yemen (Du et al., 2016).

1.1.1 Diagnosis, treatment, vaccination

The statistics available are problematic, partly because the numbers of cases are underestimated due to misdiagnosis and lack of reporting of the cases, asymptomatic cases and discontinuous distribution of the disease. Due to high numbers of asymptomatic cases, proper tests are crucial in controlling the disease, since the individuals may possibly serve as reservoirs for further infection. Fortunately, there are new, cheap, easy to use and reliable serological tests available now, including DAT (Direct Agglutination Test), various ELISA based tests, a rapid strip test for rK39 antigen, the latex agglutination urine test, and a DTH (delayed-type hypersensitivity) test (Ostyn et al., 2011; Savoia, 2015). Use of these tests has confirmed high numbers of positive individuals who never reported clinical disease (Ostyn et al., 2011). However, the drawback of serological tests is that high levels of the specific antibodies remain in blood years after cure, so the tests cannot distinguish between present and past infection. Moreover, the tests are not reliable for HIV-coinfected patients due to immunosuppressive effect of the virus (reviewed in Savoia, 2015). The most widely used and reliable diagnostic technique remains detection of parasites in infected tissues by microscopy. Molecular tests such as PCR give good results regarding sensitivity under laboratory conditions but wider use is currently precluded by technical difficulties of PCR-based approaches in the affected areas (Savoia, 2015).

Vaccines have been always considered as having potential to combat leishmaniasis. So called, leishmanization - inoculation with virulent parasites, has been used since ancient times as a confirmed, reliable prevention. Inoculum is implemented on a selected, hidden body part, where a self –healing lesion forms after which the person is protected from future infections. The method was mostly abandoned due to safety issues, but is still used in high risk areas of Uzbekistan with a mixture of live and killed parasites (reviewed in Evans and Kedzierski, 2012). It is believed that 80 – 90% of natural cases are asymptomatic, suggesting cell-mediated immunity can combat the parasites (reviewed in Evans and Kedzierski, 2012). In most cases, people who overcome a primary cutaneous leishmaniasis skin lesion are protected from future infections, unless complications occur such as in the diffuse form. The prevailing evidence thus indicates that hopes for a vaccine as effective tool against leishmaniasis are not without basis. However, despite long lasting multiple efforts, no vaccine has been approved for humans until now. The

research and development in this area has included recombinant proteins, polyproteins, liposomal formulations of antigens and dendritic cell vaccine delivery systems (reviewed in Evans and Kedzierski, 2012). The last cutting-edge approach is usage of DNA vaccines, which are expected to induce Th1 responses leading to strong cytotoxic T-cell immunity (Das et al., 2014). There are two vaccines available for dogs, which contain the protein A2 antigen but their efficacy is only about 40% (Savoia, 2015). On the other hand, the caveat is that the parasites affect the immune system itself in multiple ways, efficiently blocking and inhibiting the normal immune response. This could mean that stable vaccines that behave consistently across the population will continue to confound efforts at their development (reviewed in Savoia, 2015).

1.1.2 Drugs

The first-line treatment against leishmaniasis has been different formulations of antimony-containing drugs for decades. Due to emerging resistant parasitic lines, as well as their intrinsic toxicity, they are being replaced with new, potentially more efficient and safer drugs such as AmbiSome, miltefosine or paromomycin (Fig 1.3). Crucially, drug treatment for leishmaniasis must be applied according to the specific species, given different species respond differently to drugs, but simple speciation is currently difficult in the field (reviewed in de Vries et al., 2015). Combinations of drugs are discussed and recommended due to the reduced risk of development of resistance, moreover, they seem to provide more effective treatment with fewer side effects (Seifert and Croft, 2006). Increasingly, the future of leishmaniasis chemotherapy would appear to be in combination chemotherapy (Melaku et al., 2007; Sundar et al., 2011; Trinconi et al., 2016).

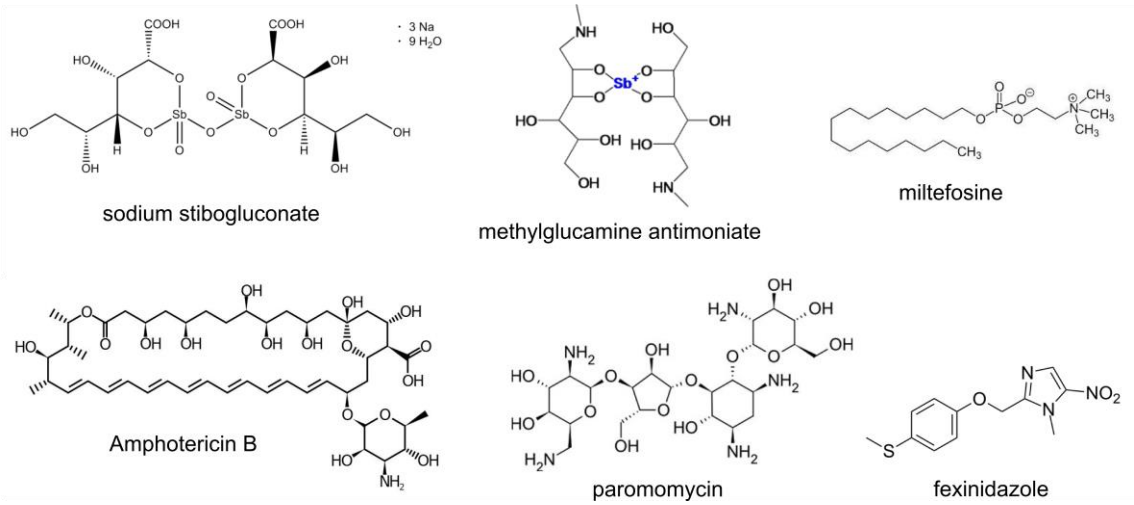

Figure 1.3. The drugs used against leishmaniases.

Several drugs contain pentavalent antimony (sodium stibogluconate, methylglucamine antimoniate), which is a prodrug and needs to be converted into the trivalent form inside macrophages to exert a toxic effect. Exactly how trivalent antimonials kill cells is not known, although depletion of trypanothione, the major antioxidant of trypanosomatids accompanies cell death (Croft et al., 2006). These drugs are effective as direct injections into skin lesions, even though painful. A strain resistant to antimonials spread in Bihar, India, causing the efficacy to drop to 35% (Murray et al., 2005), thus they are being replaced with amphotericin B, particularly in the liposomal formulation, AmbiSome where possible. Interestingly, it has recently been suggested that high levels of arsenic, a heavy metal in the same group as antimony in the periodic table, in ground water in parts of India might have led to selection of resistance to antimonial drugs (Perry et al., 2013, 2015). Other drawbacks of antimony are long duration of the treatment and adverse reactions (Murray et al., 2005).

Amphotericin B acts by binding selectively to ergosterol which is present in *Leishmania* but not in mammalian hosts where cholesterol is the primary membrane sterol (Croft et al., 2006). Even though this compound is not very well tolerated by patients, its liposomal formulation AmbiSome causes fewer and less severe adverse effects and seems to be more effective even in short (5 – 10 days) regimes (Murray et al., 2005), but is more costly. In Asia, AmbiSome is increasingly being used as the first line treatment in a single

intravenous dose (Uniting to Combat NTDs, 2014). There has been a single clinical resistance case reported so far but numerous resistant cell lines were selected in *in vitro* conditions (Al-Salabi and De Koning, 2005; Mbongo et al., 1998; Purkait et al., 2012; Srivastava et al., 2011) and attention must be paid to the risk of selection and spread of resistance, especially in light of the single-dose policy.

Miltefosine is the first oral drug available for use against leishmaniasis. It is active; effective in 90% cases of childhood visceral leishmaniasis (Palumbo, 2008), has a long half-life (~8 days) (Sundar et al., 2002), but the disadvantages are teratogenicity, gastrointestinal adverse reactions and relapse in 5-10% of obviously cured patients (Murray et al., 2005). Moreover, its availability as an oral drug, but requiring relatively long administration regimens, has made compliance of full dosing an issue and resistance is relatively easy to select (Croft et al., 2006). Its mode of action is not known. It has been proposed that it acts through inhibition of a glycosomal alkyl-specific-acyl CoA acetyltransferase, an enzyme involved in ether-lipid remodelling (Lux et al., 2000), among other potential mechanisms. In addition it stimulates T-cells and macrophages to secrete activating cytokines (Palumbo, 2008).

Paromomycin can be used in topical formulation against cutaneous leishmaniasis. It is expected to be very promising thanks to high-level efficacy, minimal toxicity and low cost (Murray et al., 2005). It is an aminoglycoside-aminocyclitol antibiotic, inhibiting protein synthesis in bacteria and the mode of action against *Leishmania* seems to be the same, since it was shown to bind to an rRNA model and inhibit translation (Shalev et al., 2015). There were resistant bacteria cases reported, caused by decreased uptake and some other reasons (Croft et al., 2006), and reduced uptake was also shown to associate with resistance in laboratory selected *Leishmania* lines (Jhingran et al., 2009; Maarouf et al., 1998).

There are several potential drugs in the pipeline, which is absolutely necessary. Fexinidazole is currently in trials against human African trypanosomiases and may be effective against leishmaniasis as well (Savoia, 2015). Nifurtimox is in clinical trials against visceral leishmaniasis, other interesting effective compounds should be on the way (Savoia, 2015). Pentamidine represents another treatment option but it is not widely used, so far as treatment outcomes are not really satisfactory (Murray et al., 2005). An

appreciation of the biology of the parasites offers a means to determine potential drug targets that may then enable the improvement of the drugs available to treat the disease.

1.2 *Leishmania* biology

1.2.1 Life cycle

Leishmania parasites are transmitted between mammalian hosts by female sand flies of the genus *Phlebotomus* in the Old World and *Lutzomyia* in the New World. There are about 800 known sand fly species in total and 93 of them were reported as vectors for *Leishmania* (WHO, 2010). When feeding on a host, the insect makes a wound and the tissue damage attracts macrophages (Fig 1.4). If the individual is infected, the macrophages are picked up by a sand fly including the internalized *Leishmania* (Bates, 2007). After entering the insect, temperature and pH changes cause transformation of amastigote *Leishmania* into promastigotes which settle first in the midgut and derive nutrition from the ingested blood meal. Afterwards, they migrate towards the foregut and attach to the gut epithelium which is a crucial step in determining if the parasites complete their lifecycle and the insect will serve as a true vector. After a couple of days, the parasites start secreting a so-called promastigote secretory gel composed of high molecular weight glycoproteins, creating a plug in the digestive tract (Ilg et al., 1996; Rogers et al., 2002). Over time, they change their body shape as they progress through different subtle life cycle stages, the last being the metacyclic epimastigotes, which are infective for a new mammalian host. When biting next time, the fly needs to clear the way in its digestive tract, thus the gel plug is egested together with the parasites (reviewed in Bates, 2007).

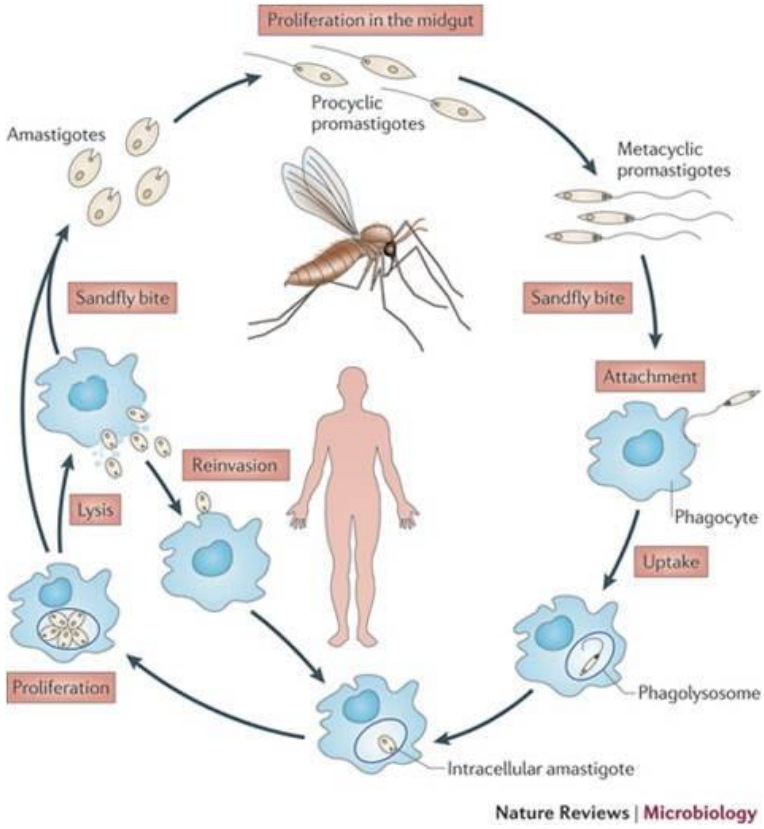

Figure 1.4. *Leishmania* life-cycle. Adapted from Kaye and Scott (2011), permission to reproduce this image has been granted by Nature Publishing Group.

Enclosure within sand fly saliva and the promastigote secretory gel supports the parasites in further establishment of infection. Significant differences were observed in mouse models, if the injection mixture contained extracts of salivary glands, which appear to induce immunomodulatory effects (Titus and Ribeiro, 1988). After recognition by the immune system, *Leishmania* are engulfed by phagocytic immune cells. Macrophages are preferred as the host cells but it has been reported that neutrophils may absorb the parasites first, serving as "Trojan horses", and when they undergo apoptosis and are ingested by macrophages later, *Leishmania* survive the process and establish infection in macrophages (Laskay et al., 2003; Peters et al., 2008). However, results from different *Leishmania* species vary and depend on the type of inbred mice used for each study, thus the definitive picture is still unclear (reviewed in Kaye and Scott, 2011). How the pathogens survive within the hostile conditions inside the phagocytic vacuole which are meant to destroy them has also not been resolved. Some *Leishmania* species prevent fusion of the primary endocytic vesicles with the phagosome vacuole while for others it

was suggested that the large volume of their parasitophorous vacuoles allows dilution of the detrimental enzymes and reactive chemical species (reviewed in Cecilio et al., 2014). Once inside macrophages, *Leishmania* differentiate into the amastigote stage which has smaller rounded cells without a protruding flagellum. The parasites multiply, eventually causing the host cell to burst, disseminating the pathogens around body, infecting lymph nodes, skin, liver, spleen or bone marrow depending on the *Leishmania* species (reviewed in Kaye and Scott, 2011).

1.2.2 Specific traits in morphology and molecular biology

Trypanosomatid parasites are considered to be one of the earliest branching groups of eukaryotes (Cavalier-Smith, 2010), which may explain the absence of some aspects considered normal in model eukaryotic cells and by contrast the presence of various unique molecular traits.

Leishmania are unicellular organisms with an elongated body shape in the promastigote stage and a circular morphology in the amastigote stage. Promastigotes have a flagellum at the anterior end of the cell to enable directed swimming or attachment. In the amastigote stage the flagellum is greatly diminished in size, and the arrangement of microtubules is altered (reviewed in Gluenz et al., 2010). Close to the flagellar attachment zone is the kinetoplast, a body of mitochondrial DNA composed of dozens of maxicircles and thousands of minicircles, highly condensed and thus easily stained with DAPI and other DNA staining dyes (Stuart, 1983). The prominence of the kinetoplast is responsible for the phylogenetic order containing the *Leishmania* species to have been classified as the Kinetoplastida. Only a single mitochondrion is present in each cell, but it is large, reticulated and stretches across the whole cell. In addition to the common organelles of eukaryotic organisms (e.g. endoplasmic reticulum, Golgi apparatus and lysosomes), various other organellar systems exist including acidocalcisomes and glycosomes (Coombs et al., 1982; Vercesi et al., 1994).

Organization of chromosomes and genes and their expression is very specific in trypanosomatids. *Leishmania* have a relatively flexible genome, meaning that whole chromosome duplications or fusions are common (Pages et al., 1989). Chromosome rearrangements happen relatively frequently during prolonged laboratory cultivation and the extent to which such flexibility is evolutionary advantageous, or merely an *in vitro*

artefact deserves attention. Protein coding genes do not have canonical transcription factors, but instead are transcribed into long polycistronic units, which need to be processed subsequently (Clayton, 2002; Ivens et al., 2005). During the process of *trans*-splicing, the large transcript is cleaved into single gene mRNAs and a common 39 nucleotide splice leader sequence is added to the 5' end of each transcript and poly-A tail at the 3' end (LeBowitz et al., 1993). Due to the absence of transcription factors, it remains unclear how gene expression is regulated. Control of mRNA stability and degradation and regulation of translation (Vasquez et al., 2014) have been described in *T. brucei* (reviewed in Clayton, 2014). A key role for 3'- untranslated region was demonstrated in posttranscriptional regulation of Hsp70 gene in *L. infantum* (Quijada et al., 2000), a paraflagellar rod component (Mishra et al., 2003), or a 600-4 gene in *L. mexicana* (Murray et al., 2007). Various proteins are supposed to be binding to these regions and influence mRNA stability and degradation, however, the overall process seems to be highly complex and only few of these proteins have been functionally characterised so far in *T. brucei* (reviewed in Clayton, 2013, 2014).

1.3 Metabolism

Published data has led to a depiction of *Leishmania* metabolism (McConville et al., 2015; Opperdoes and Coombs, 2007; Saunders et al., 2011, 2014). However, it needs to be noted that practically all of the work has been done on *in vitro* grown cultures and the conditions inside a fly's midgut or macrophage are most likely different, but practically unknown (McConville et al., 2015; Opperdoes and Coombs, 2007). The promastigote stage of *Leishmania* has been studied in more detail, given the easier cultivation of these cells (Opperdoes and Coombs, 2007; Pan et al., 1993; Trager, 1957). Axenic amastigote cultures can be obtained, but it remains a matter of dispute how biologically relevant they are (Holzer et al., 2006; Pan et al., 1993; Pescher et al., 2011; Pral et al., 2003). Different types of cultivated macrophages can be infected with *Leishmania*, but it is very difficult to separate the parasites subsequently and dissecting metabolism of macrophage resident *Leishmania* parasites is very difficult. Here, I will briefly describe the main aspects of the promastigote and amastigote central metabolism as it is currently understood.

1.3.1 Promastigotes

Under optimal growth conditions the major carbon source for a promastigote cell is glucose, and aspartate to a limited extent. Additional amino acids and fatty acids are taken up as well, but not incorporated into the tricarboxylic acid cycle (TCA) intermediates (Saunders et al., 2011). Glucose is used in glycolysis, the pentose phosphate pathway and for a succinate fermentation pathway and the derived products, acetyl-CoA and malate are further channelled into the TCA cycle. The major ultimate source of ATP is the respiratory chain, which was validated when inhibition of the separate complexes was shown to be lethal to the parasites, as was inhibition of mitochondrial aconitase from the TCA cycle (Hellemond and Tielens, 1997; Saunders et al., 2011). The alternative oxidase of the respiratory chain, characteristic of *T. brucei*, is not present in *Leishmania* (Opperdoes and Coombs, 2007). The major metabolic end products are CO_2, acetate, alanine and succinate (Saunders et al., 2011).

The standard metabolism can be altered substantially in cells grown under suboptimal conditions, for example cells depleted for glucose transporters can use various sources (alanine, acetate, aspartate, glycerol) for mannogen biosynthesis, indicating that these substrates can be used as general carbon sources (Rodriguez-Contreras and Landfear, 2006). Promastigotes scavenge fatty acids from medium but do not incorporate the carbons into the TCA cycle intermediates or sugars, even in the absence of glucose. When amino acids were depleted, fatty acid utilisation was not increased, rather lipogenesis was reduced (Naderer et al., 2006). The parasites have amylase and sucrase enzymes (Blum and Opperdoes, 1994), functions of which were suggested in degradation of starch and sugar polymers after sand fly plant meal (Opperdoes and Coombs, 2007), or in degradation of extracellular matrix glycosaminoglycans in the amastigote stage (Naderer et al., 2015).

Leishmania are auxotrophic for many nutrients, including specific amino acids, vitamins, or purines and in other cases uptake and *de novo* biosynthetic pathways overlap (McConville et al., 2015; Opperdoes and Coombs, 2007). Pyrimidines can be obtained by either *de novo* biosynthesis or salvage pathways. Disruption of each of the branches is fully compensated by the other, but cells with deletions in both the pathways were viable only in the promastigote stage but not infective to mice (Wilson et al., 2012). The purine ring cannot be synthesized by the parasite. Its salvage pathway is complex and

redundant with various alternative routes, with the majority being confined to glycosomes and some enzymes present in the cytosol (reviewed in Boitz et al., 2012). Amino acid metabolism of *Leishmania* was described based on genome analysis, excluding the capacity to synthesize aromatic and branched chain amino acids, histidine, and lysine (Opperdoes and Coombs, 2007). However, the presence of additional enzymes with non-canonical sequences cannot be excluded until tested experimentally, especially regarding the high number of hypothetical proteins with unknown function present in the genome (Ivens et al., 2005). Degradation pathways for tryptophan and arginine were dissected by LC-MS metabolomics revealing substantial differences between three different *Leishmania* species (Westrop et al., 2015).

Biosynthesis of mannogen (Fig 1.5), a storage sugar polymer, represents a significant and important part of sugar metabolism in *Leishmania* (Ralton et al., 2003). Activated mannose can be used for biosynthesis of mannogen or various mannose-conjugated glycolipids or proteoglycans. Deletions of different genes from the aminosugar pathway (GDP-mannose pyrophosphorylase (GDPMP), dolicholphosphate-mannose synthase (DPMS), phosphomannomutase (PMM)) caused no obvious defects in promastigote cultures, but the cells were not infective to macrophages or mice (Garami and Ilg, 2001; Garami et al., 2001). The defect seems to be due to deficiency in mannogen rather than loss of mannose conjugates of the cell surface (Ralton et al., 2003), although lipophosphoglycan together with other glycoconjugates is essential for the parasites' survival in the sand fly's midgut, attachment to the walls and protection from digestive enzymes present there (Sacks et al., 2000). In addition to glucose, glucosamine or N-acetylglucosamine can be used as substrates for mannogen biosynthesis (Naderer et al., 2010). Through gluconeogenesis it can also be synthesised from glycerol, alanine and aspartate, and in amastigotes from lactate too (Rodriguez-Contreras and Hamilton, 2014; Rodriguez-Contreras and Landfear, 2006).

Mannogen accumulates during promastigote to amastigote transformation, or in response to stress, and the intracellular levels are higher in the mammalian infective stage (Ralton et al., 2003). If sugars are not available, mannogen is rapidly consumed, and the cells become more sensitive to various types of stress in its absence (Ralton et al., 2003). Deletion of glucosamine-6-phosphate deaminase (GND) caused decrease in infectivity of amastigotes, whereas promastigotes were still able to grow, if glucose but not amino

sugars were supplemented. Deletion of glutamine:fructose-6-phosphate amidotransferase (GFAT) provoked auxotrophy for amino sugars, loss of surface lipid-linked oligosaccharides and hypersensitivity to increased temperatures. The mutant promastigotes were unable to infect macrophages *ex vivo*, but established infection in mice and once transformed into amastigotes, the growth was comparable to WT cells (Naderer et al., 2008). A similar phenotype was observed in N-acetylglucosamine acetyltransferase (GNAT) deficient *L. major* mutant which was auxotrophic for N-acetylglucosamine and caused skin lesions in mice, but was unable to infect macrophages *ex vivo* (Naderer et al., 2015). This may be explained by a premise that hyaluronan and other sugar polymers are available *in vivo*, cleaved by various hydrolases inside the parasitophorous vacuole and used by the parasites (Naderer et al., 2015). It also indicates that even though the mannogen biosynthetic pathway seems redundant (Fig 1.5), free N-acetylglucosamine is not abundant, and in addition the branch via mannose (bottom part in Fig 1.5) is not sufficient to compensate for the whole biosynthesis. Why mannogen is essential in amastigotes is still not fully resolved. It may possibly be used during transformation of promastigotes into amastigotes or under stress conditions when usual carbon sources are limited, and after establishing of macrophage infection, the intracellular pool of mannogen is replenished. The nutritional status of the parasitophorous vacuole remains a matter of speculation (McConville et al., 2015), and may be variable i.e. when sugars are available mannogen may be synthesised, then consumed if sugars are depleted.

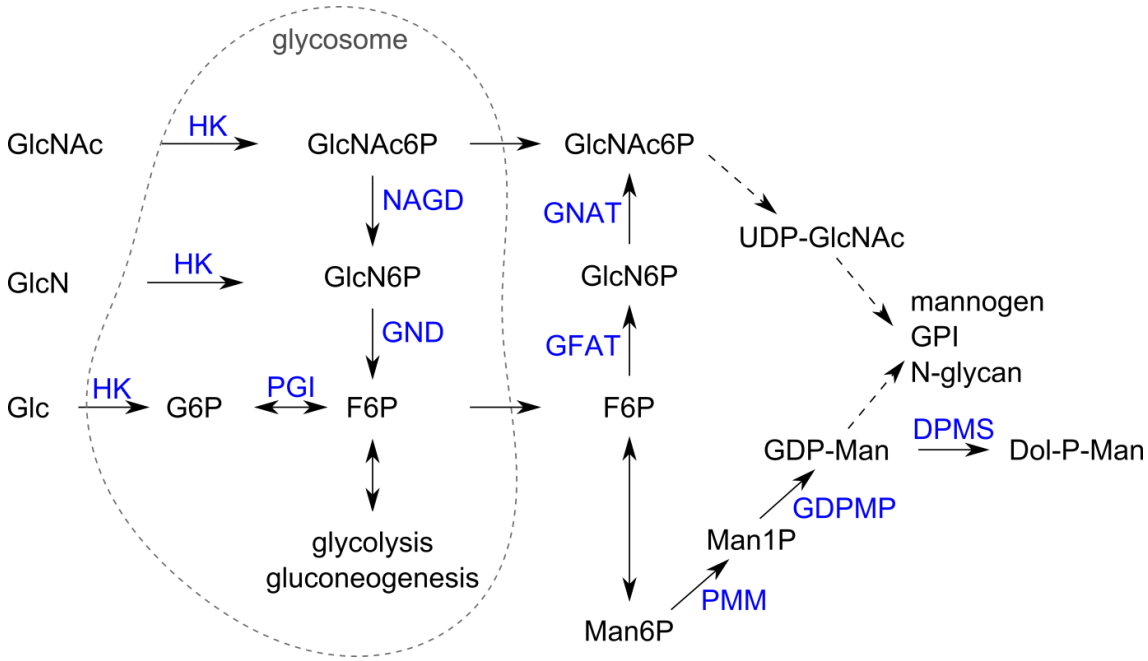

Figure 1.5. Scheme of mannogen biosynthesis. GlcNAc – N-acetylglucosamine, GlcNAc6P - N-acetylglucosamine 6-phosphate, GlcN – glucosamine, GlcN6P – glucosamine 6-phosphate, Glc – glucose, G6P – glucose 6-phosphate, F6P – fructose 6-phosphate, Man6P – mannose 6-phosphate, Man1P – mannose 1-phosphate, UDP-GlcNAc - uridine diphosphate N-acetylglucosamine, GDP-Man – guanosine diphosphate mannose, GPI – glycosylphosphatidylinositol, Dol-P-Man – dolicholphosphate mannose. Enzymes are depicted in blue: HK – hexokinase, PGI – glucose-6-phosphate isomerase, NAGD – N-acetylglucosamine-6-phosphate deacetylase, GND – glucosamine-6-phosphate deaminase, GNAT – glucosamine-6-phosphate acetylase, GFAT – glutamine:Fru6P aminotransferase, PMM – phosphomannomutase, GDPMP – GDP-mannose-pyrophosphorylase, DPMS – dolicholphosphate-mannose synthase; dashed arrows indicate multiple enzymatic steps; based on Naderer, 2010 and Garami, 2001.

1.3.2 Amastigotes

The major difference in metabolism of the amastigote stage is that it has been described as stringent given its apparent nutrient sparing nature (Saunders, 2014). When compared to promastigotes, the cells consume less glucose (30 times) and glutamate, use it more efficiently and secrete less end products (Saunders, 2014). They secrete practically no

partly oxidised end products, such as succinate, alanine, or malate (McConville et al., 2015; Saunders et al., 2014). These metabolic changes seem to be tightly linked to the specific life stage, since they take place even in rich culture conditions (McConville et al., 2015; Saunders et al., 2014). In addition, lesion amastigotes grow extremely slowly with a doubling time of approximately 12 days, as was estimated based on DNA, RNA, and protein turnover, suggesting that the parasites enter a semi-quiescent state (Kloehn et al., 2015). Even axenic amastigotes have DNA turnover about four times lower than promastigotes (Saunders et al., 2014). The fact that all cellular processes are very slow may enhance persistence of the parasites and negatively impact on drug efficiency.

It was suggested by Hart and Coombs (1982) that amastigotes use fatty acids as source of carbon. This was confirmed in a current study comparing metabolism of the two life stages by untargeted GC-MS metabolomics, when medium was supplemented with a mixture of ^{13}C labelled fatty acids, and the labelling was detected in the TCA cycle intermediates in amastigotes but not in promastigotes (Saunders et al., 2014). The overall labelling patterns seemed quite similar between promastigotes and amastigotes when labelled glucose or amino acids were used, confirming that glucose is still the main carbon source, used for glycolysis, succinate fermentation and the TCA cycle. The TCA cycle is essential and sensitivity to an inhibitor (fluoroacetate) of mitochondrial aconitase is 100 times higher than in promastigotes (Saunders et al., 2014). Gluconeogenesis becomes essential in amastigotes, since mutants lacking its key enzyme, fructose-1,6-bisphosphatase, did not multiply inside macrophages. In the promastigote stage the same deletion caused a growth defect in medium containing glycerol as the major carbon source, whereas glucose supplementation rescued the phenotype (Naderer et al., 2006). Levels of mannogen are much higher in amastigotes than promastigotes and it is crucial for survival inside macrophages (Ralton, 2003; Naderer, 2010). As an example of the differences between *in vitro* and *in vivo* conditions a recent experimental observation revealed that when amastigotes grow inside macrophages, they consume polymers of saccharides and glycoproteins from the extracellular matrix, possibly thanks to activity of secreted digestive enzymes (Naderer, 2015).

1.3.3 Glycosomes

Glycosomes are small organelles characteristic for trypanosomatids and originally derived from peroxisomes. They are surrounded by a semipermeable membrane equipped with specific transmembrane channels and import machinery for proteins (Achcar 2013, Gualdron-Lopez, 2012; reviewed in Michels, Bringaud, 2006). Proteins are imported into glycosomes based on presence of the peroxisomal targeting sequence (PTS). PTS1 type is composed of the last three amino acid residues –SKL, or similar (Gould et al., 1989), whereas PTS2 is close to the N-terminus, is bipartite and more variable (Swinkels et al., 1991). In addition, several non-canonical targeting sequences were detected, and import of protein complexes, where not all components contain distinguishable PTS can also occur (Opperdoes and Szikora, 2006). Once a PTS is recognized by a PEX receptor, it is connected with a docking complex on the glycosomal membrane and transferred across the membrane (reviewed in Gualdrón-López et al., 2013).

Part of the glycolytic pathway is located inside glycosomes and such compartmentalisation compensates for allosteric regulation which is missing for glycolytic enzymes of trypanosomatids (or completely different from the described types). Another advantage is that because investment of ATP is required for initialisation of glycolysis, thanks to compartmentalisation the flux through the pathway is independent of outside conditions, which are variable (Bakker et al., 2000; Haanstra et al., 2008).

Bigger molecules such as nucleotide cofactors cannot cross the membrane freely, thus the balance of NAD(P)/H and ADP/ATP needs to be maintained inside the organelle. That is probably the purpose for the presence of the succinate fermentation pathway inside these organelles, to ensure recycling of these molecules needed for glycolysis (Fig 1.6). Various metabolic pathways have dual subcellular localisation, being present both in the cytosol and glycosomes, for example the pentose phosphate pathway, purine salvage, pyrimidine biosynthesis, β-oxidation of fatty acids or trypanothione pathway (reviewed in Michels et al., 2006). The purpose is mostly suspected to be connection with glycolysis but it becomes questionable if we consider the semipermeable character of the glycosomal membrane. Various sugar kinases have been identified in the *Leishmania* genome, functions of which are not exactly clear but all of them carry a PTS, indicating

a possible connection with the PPP or mannogen biosynthesis (Opperdoes and Coombs, 2007). Glycosomal localisation is essential for some but not all enzymes. For example, for the enzymes of the purine salvage pathway tested, glycosomal localisation was not necessary (Carter et al., 2008). Cells containing mislocalised glucosamine-6-phosphate deaminase of mannogen biosynthetic pathway were viable, but dependent on glucose supplementation unless the WT localisation was restored (Naderer et al., 2010). A mutated cytosolic version of hexokinase caused swelling and death of cells (Kumar et al., 2010). Glycosomes vary during the life cycle, while promastigotes contain around 20, there are only 10 in amastigotes (Cull et al., 2014), and their enzyme content changes probably as well (Mottram and Coombs, 1985a).

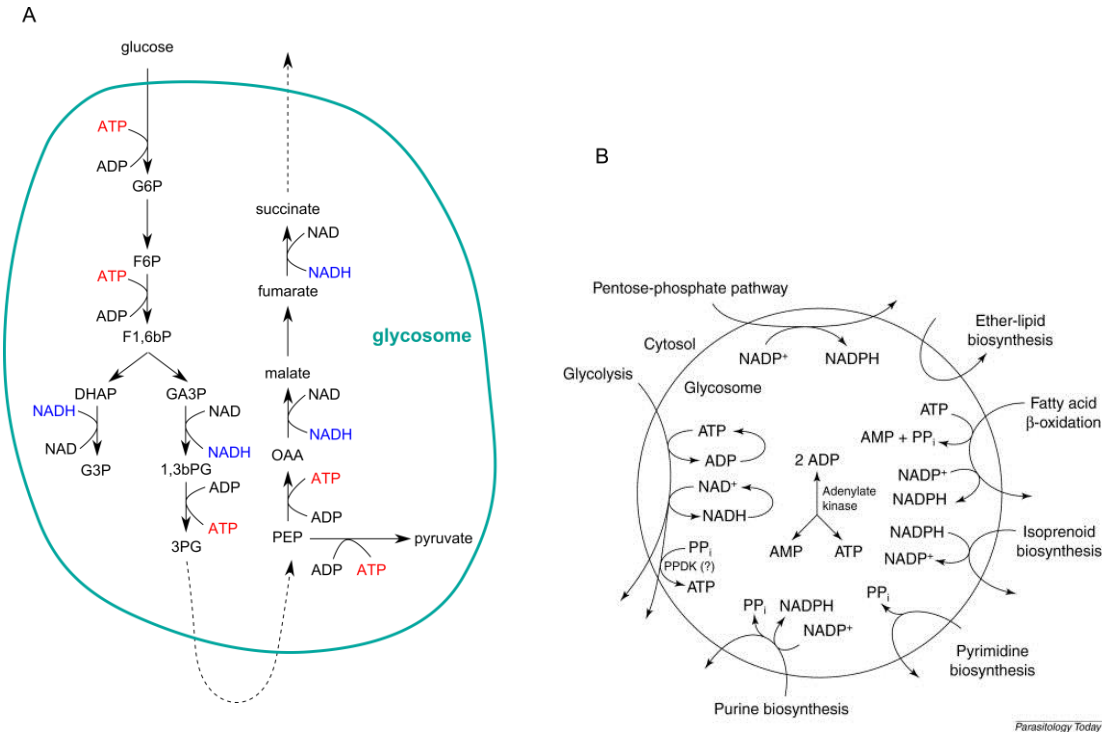

Figure 1.6. Metabolism compartmentalisation in the glycosome. A – The greater parts of glycolysis and the succinate fermentation pathway are confined to the glycosome, ensuring ADP/ATP and NAD/H balance; adapted from Michels et al. (2006). B – Glycosomal pathways contributing to nicotinamide and ATP cofactors pools in the glycosome; adapted from Michels et al. (2000). Permission to reproduce this image has been granted by Elsevier.

1.4 The pentose phosphate pathway

The pentose phosphate pathway (PPP) is a key component of cellular metabolism, tightly connected to glycolysis as a key consumer of glucose. Its primary roles are to generate NADPH as a source of reducing power and other products that feed diverse parts of metabolism. These include ribose 5-phosphate (R5P) for nucleotide synthesis and erythrose 4-phosphate (E4P) for aromatic amino acid and various vitamin biosyntheses (Braus, 1991; Lam and Winkler, 1990; Zhao and Winkler, 1994). The PPP has long been considered to offer potential drug targets and the recently invigorated quest for inhibitors of enzymes of the pathway in cancer means that new possibilities to seek compounds that might inhibit the pathway in the parasites are emerging.

First reports demonstrating the PPP in trypanosomatids emerged in 1960's. Studies used glucose labeled with ^{14}C at either position 1 or position 6 to feed the parasites after which the ratios between $^{14}CO_2$ produced under either condition were interpreted as pointing to the respective fluxes via the PPP and glycolysis. Values between 10% and 41% flux into the PPP were reported for *T. cruzi* (Mancilla and Naquira, 1964; Maugeri and Cazzulo, 2004), and 6% for *Leishmania* (Mancilla et al., 1965; Maugeri et al., 2003). However, since various degree of incomplete oxidation of glucose occur in all trypanosomatids, these numbers may be inaccurate estimates. Specific activities of each enzyme of the canonical PPP (Fig 1.7) were measured in the four major life stages of *T. cruzi* (Maugeri and Cazzulo, 2004), and in promastigote *L. mexicana, L. braziliensis*, *L. donovani*, and *L. tropica* (Martin et al., 1976; Maugeri et al., 2003). In *T. brucei*, all of the enzyme activities were measured in the procyclic stage (PCF) while transketolase and ribulose 5-phosphate epimerase were absent in the bloodstream form (BSF) (Cronín et al., 1989). A kinetic model of the PPP in BSF *T. brucei* was constructed (Kerkhoven et al., 2013), extending the previous model of BSF trypanosome glycolysis (Bakker et al., 1997, 1999; Haanstra et al., 2008) and pointing at gaps in our understanding of the system, particularly with regard to how the bound phosphate pool within the glycosome is maintained if a proportion of the glycolytic glucose 6-phosphate is shunted through the oxidative branch of the PPP (Fig 1.8). The PPP of trypanosomatids has been reviewed with focus on structures of the enzymes, comparison with mammalian counterparts and search for potential inhibitors (Comini et al., 2013).

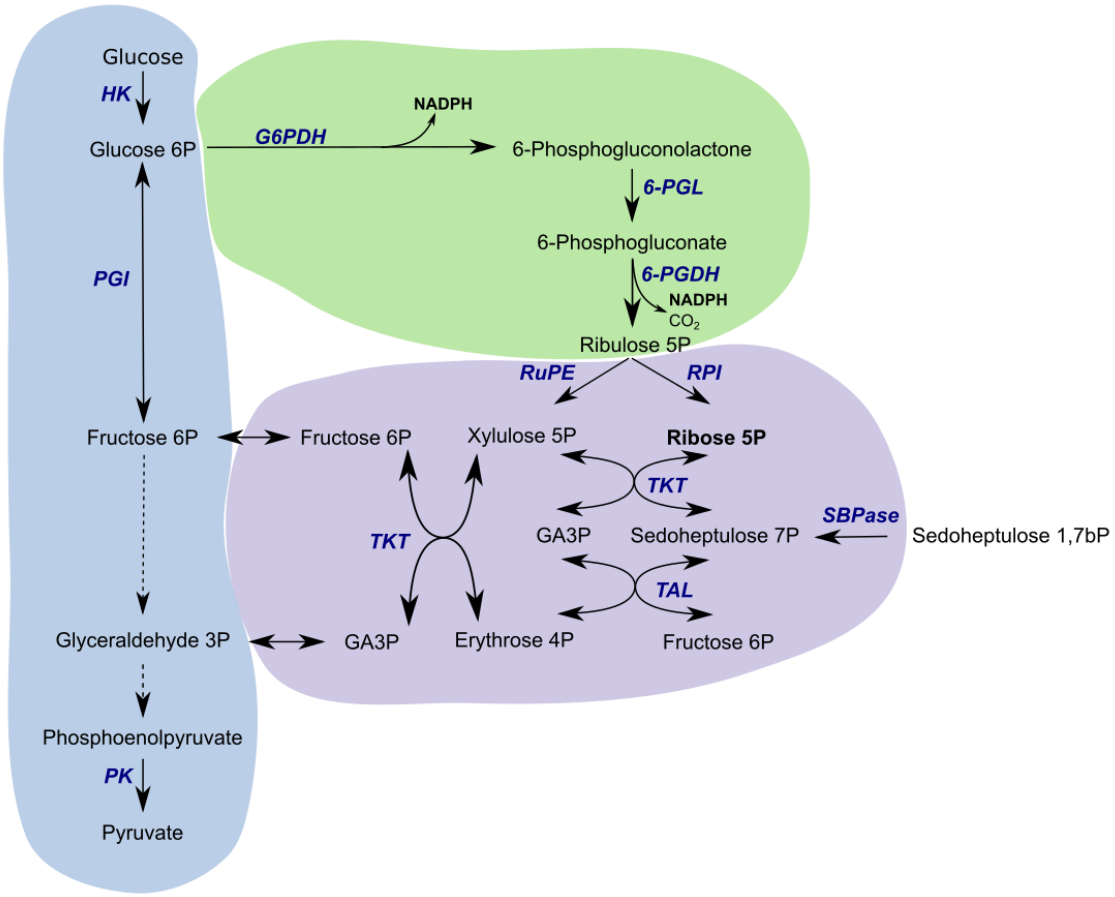

Figure 1.7. The pentose phosphate pathway. Glucose can be metabolized via glycolysis or through the pentose phosphate pathway, branching at glucose 6-phosphate. The glycolytic pathway is shaded in blue and enzymes hexokinase (HK), phosphoglucose isomerase (PGI) and pyruvate kinase (PK) are marked. Other reactions between fructose 6-phosphate and glyceraldehyde 3-phosphate (GA3P) are summarized through the presence of dotted lines. The oxidative branch of the pentose phosphate pathway, shaded in green, comprises the enzymes glucose-6-phosphate dehydrogenase (G6PDH), 6-phosphogluconolactonase (6-PGL) and 6-phosphogluconate dehydrogenase (6-PGDH). The non-oxidative branch, shaded in lilac comprises the enzymes ribulose-5-phosphate epimerase (RuPE), ribose-5-phosphate isomerase (RPI), transketolase (TKT) and transaldolase (TAL). Sedoheptulose-1,7-bis-phosphatase (SBPase) which can introduce sedoheptuolse 1,7-bisphosphate to the pathway is also depicted.

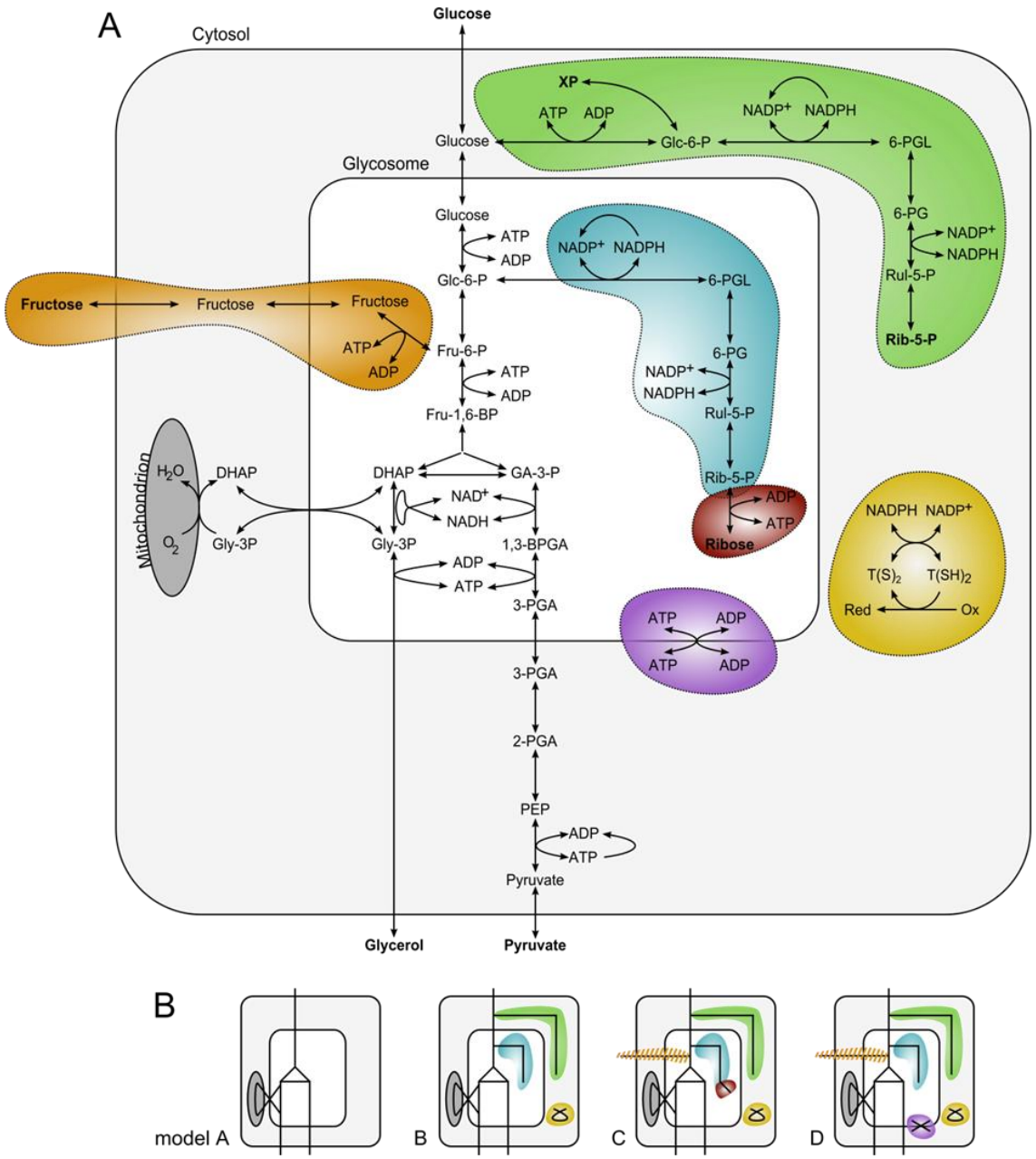

Figure 1.8. A mathematical model of the PPP in bloodstream form *T. brucei*. A - Scheme of the modeled metabolic pathways. B - A mathematical model of glycolysis in *T. brucei*, based on kinetic measurements of activities of each enzyme, had proven successful in describing glucose metabolism in these cells (model A) (Bakker et al., 1997, 1999; Haanstra et al., 2008). As kinetic parameters of the pentose phosphate pathway enzymes became available it was possible to add these to the model (model B). However, the addition of the pentose phosphate pathway created a potentially fatal leak of bound phosphate from the metabolite pool in the glycosome of these cells. It was necessary, therefore, to evoke possible

solutions to this, which are shown as models C and D. Cytosolic PPP is shaded in green, glycosomal PPP in blue, ribokinase reaction in crimson, ATP:ADP antiporter in purple, trypanothione recycling in yellow, and fructose utilization in orange. 1,3-BPGA – 1,3-bisphosphoglycerate, 2-PGA – 2-phosphoglycerate, 3-PGA – 3-phosphoglycerate, 6-PG - 6-phosphogluconate, 6-PGL – 6-phosphogluconolactone, ADP – adenosine diphosphate, AMP – adenosine monophosphate, ATP – adenosine triphosphate, DHAP – dihydroxyacetone phosphate, Fru-1,6-BP – fructose 1,6-bisphosphate, GA-3-P – glyceraldehyde 3-phosphate, Glc-6-P – glucose 6-phosphate, Gly-3P – glycerol 3-phosphate, NADP(H) – nicotinamide adenine dinucleotide phosphate, T(SH)2 – trypanothione, T(S)2 – trypanothione disulfide, Rib-5-P – ribose 5-phosphate, Rul-5-P – ribulose 5-phosphate. The figure was adapted from Kerkhoven et al. (2013).

1.4.1 Biochemical roles of the PPP and its substrates

The pathway is conventionally divided into two branches (Fig 1.7), the first three reactions comprising the oxidative PPP while the following sugar interconversions make up the non-oxidative PPP. The oxidative branch uses glucose 6-phosphate (G6P) from glycolysis and converts it to 6-phosphoglucono-1,5-lactone using glucose-6-phosphate dehydrogenase (G6PDH) (*EC* 1.1.1.49) with NADP as a cofactor. The second enzyme, 6-phosphogluconolactonase (6PGL) (EC 3.1.1.17) produces 6-phosphogluconate (6PG). Following 6-phosphogluconate dehydrogenase (6PGDH) (*EC* 1.1.1.44) produces a CO_2 molecule and ribulose 5-phosphate (Ru5P) while creating another molecule of NADPH.

Ru5P is further converted through the non-oxidative PPP, either by ribose-5-phosphate isomerase (RPI) (EC 5.3.1.6) into ribose 5-phosphate (R5P), a critical cellular metabolite used in nucleotide synthesis, or to xylulose 5-phosphate (Xu5P) by ribulose-5-phosphate epimerase (EC 5.1.3.1). Both of these products serve as substrates for the following enzyme, transketolase (TKT) (EC 2.2.1.1), which transfers a two carbon keto unit from a ketose to an aldose, producing, in this case, sedoheptulose 7-phosphate (S7P) and glyceraldehyde 3-phosphate (GA3P). These are further used by transaldolase (EC 2.2.1.2), which transfers a three carbon aldol unit from S7P to GA3P, producing erythrose 4-phosphate (E4P) and fructose 6-phosphate (F6P). The latter re-enters glycolysis, whereas E4P is used in a further TKT reaction with Xu5P, resulting in GA3P and F6P. In this canonical scheme all of the final products feed back into glycolysis. However, as

Kleijn and colleagues have suggested, this scheme is an over simplification, and the non-oxidative PPP could be better considered as a sum of half-reactions, where TKT and TAL can use a diversity of substrates ranging from 2 or 3 to 8 or more carbons and combine any suitable substrate and product pair (Kleijn et al., 2005). This model of a dynamic junction-centre driven by substrate availability seems to offer a better description.

Metabolomic analyses of PCF (Creek et al., 2012a) and BSF *T. brucei* (Creek et al., 2015) revealed larger monosaccharides including S7P, octulose 8-phosphate (O8P) and nonulose 9-phosphate (N9P). Their production from the non-oxidative branch was shown in experiments where 50% of glucose in the medium had all six carbons labelled (U-^{13}C-glucose). The distribution of labelled carbons in metabolic products indicates that O8P derives primarily from addition of a 3 carbon unit to R5P while N9P derives from addition of a 3 carbon unit to G6P, using TAL (Creek et al., 2012a, 2015). In plants O8P has been shown to play a role in sugar cycling in the Calvin cycle (Williams and MacLeod, 2006), but roles for these larger monosaccharides are not known in trypanosomatids; indeed it is possible that they are merely an inevitable consequence of the promiscuous shuffling of carbons carried out by the non-oxidative branch.

Additional enzymes, which were not regarded as part of the classical pathway, but which produce PPP intermediates, and thus should be taken in consideration as well, are being discovered in various systems. For example, sedoheptulokinase (SHK) in mammalian cells (previously known as CARKL) catalyses the phosphorylation of sedoheptulose to S7P (Kardon et al., 2008). In trypanosomatids, although sedoheptulose and S7P can be detected in cell extracts, genes with clear orthology to SHK are not known. In *Leishmania*, a variety of different pentose kinases have been inferred from sequence analysis and these are assumed to broaden the range of carbohydrates available for use from plant fluids consumed by the sand fly vectors of the parasites (Opperdoes and Coombs, 2007).

In yeast, a pathway termed riboneogenesis was described recently, including sedoheptulose-1,7-bisphosphatase (SBPase) which removes one phosphate group from sedoheptulose 1,7-bisphosphate in order to produce S7P. This step allows creation of R5P independent of NADP/NADPH balance (Clasquin et al., 2011). An orthologous gene is present in trypanosomes, and the enzyme contains a predicted PTS (Igoillo-

Esteve et al., 2007), and was detected in glycosomes in two independent proteomic studies of PCF *T. brucei* (Colasante et al., 2006; Guther et al., 2014).

In addition to its role in creating carbohydrates as precursors in various synthetic processes and acting as a "carbon exchange centre" to shuffle carbohydrates to glycolysis, the pathway plays a key role in recycling of NADP to NADPH, an essential reducing agent for reductive biosynthesis and protection against oxidative stress. In trypanosomatids, NADPH is the cofactor for trypanothione reductase, the enzyme that catalyses reduction of trypanothione, the central thiol reductant in these cells (Fairlamb et al., 1985).

1.4.2 The role of the oxidative PPP in NADPH synthesis

The proportion of the cellular NADPH contributed by the PPP varies in different cell types and other enzymes also contribute to the production of this crucial cellular reductant. A technique tracing deuterium from labelled glucose indicated that between 25% - 50% of cellular NADPH derives from the PPP in different mammalian cell types (Fan et al., 2014). The PPP is subject to rapid regulation in response to prevailing conditions and cellular needs. For example, oxidative stress activates the pathway as NADPH is consumed in providing defense against such stresses. As NADPH levels rise, they contribute to inhibition of the two oxidative branch dehydrogenases, again dampening flux through the pathway. Activation under oxidative stress was clearly observed in *T. cruzi* and *L. mexicana* (Maugeri and Cazzulo, 2004; Maugeri et al., 2003).

The second most important source of NADPH in trypanosomatids is malic enzyme. In *Leishmania* this enzyme is present in the cytosol, using malate to produce pyruvate and NADPH. *T. brucei* and *T. cruzi* have a second malic enzyme gene encoding a mitochondrial isoform. In PCF *T. brucei*, the mitochondrial enzyme is essential, whereas the cytosolic one is dispensable (Allmann et al., 2013). However, simultaneous depletion of cytosolic malic enzyme and G6PDH is lethal which demonstrates the joint contribution of the PPP and malic enzyme in fulfilling cytosolic NADPH needs (Allmann et al., 2013). The authors speculated that malic enzyme may take on the dominant role in NADPH production when glucose is scarce in environments inhabited by particular life cycle stages. Mitochondrial isocitrate dehydrogenase, an enzyme of the TCA cycle, also produces NADPH, but since the cofactor cannot cross membranes, the NADPH pools

are independent in the respective compartments. Methylene tetrahydrofolate dehydrogenase from the folate metabolic pathway also makes a significant contribution to NADPH production in mammalian cells (Fan et al., 2014), but a contribution of this pathway to NADPH production has not been ascertained for trypanosomatids (Vickers and Beverley, 2011).

In humans, partial deficiencies in several enzymes of the pathway are known. The role of G6PDH partial deficiency, selected originally in West Africa by resistance to malaria for example is a widely spread human inborn error of metabolism. Other deficiencies are known too, including 6PGDH, TAL and RPI, and some of them cause severe genetic disorders (reviewed in Stincone et al., 2014). The lack of reported deficiencies for other enzymes indicates that their loss is lethal during development. A number of studies have characterized individual enzymes of the pathway, and their cellular roles, in different trypanosomatids.

1.4.3 Subcellular localization of the PPP in trypanosomatids

In most organisms the PPP is present in the cytosol, and this is also the primary location in trypanosomatids, although *in silico* predictions found peroxisomal (i.e. glycosomal) targeting sequences (PTS) on many of the PPP enzymes. Subcellular localisation experiments have confirmed the presence of many enzymes of the PPP in glycosomes, although most of those activities are found in the cytosol too, indicating a dual localisation.

Digitonin fractionation followed by enzyme assay in *T. cruzi* localized the majority of each PPP enzyme to the cytosol, with a minor glycosomal fraction representing 35% for G6PDH and TAL, 20% for RPI and TKT, 15% for 6PGDH and 10% for lactonase, respectively. Ru5PE was released at very low digitonin concentration (Maugeri and Cazzulo, 2004) which might indicate a unique localisation, or represent an example of the limitations of the approach.

Colasante performed a proteomics study of separated glycosomes and detected G6PDH, TKT, SBPase and ribokinase in PCF *T. brucei* but only ribokinase in BSF (Colasante et

al., 2006). In another study, 6PGDH, ribokinase and RPI were detected in both stages of *T. brucei*, G6PDH only in BSF and TKT and TAL only in PCF (Vertommen et al., 2008). A highly purified glycosomal fraction, from organelles pulled down using epitope tagging on the glycosomal membrane protein PEX13 confirmed a glycosomal localisation for G6PDH, 6PGL, SBPase and ribokinase with high confidence in PCF *T. brucei*. The other enzymes showed predominant signal in the cytosol, which may mask a minor fraction present in glycosomes (Guther et al., 2014). Glycosomes from promastigote *L. donovani* were separated on sucrose gradients and subjected to proteomics where 6PGDH and TKT were detected (Jamdhade et al., 2015).

1.4.4 The enzymes of the PPP in trypanosomatids

1.4.4.1 Glucose-6-phosphate dehydrogenase (G6PDH)

G6PDH is of central importance due to its high control coefficient for the PPP (Kacser, 1995). G6PDH or 6PGDH depletion in *T. brucei* indicates no obvious phenotype in PCF but loss of either enzyme is lethal for BSF (Cordeiro et al., 2009; Kerkhoven et al., 2013). A genome scale RNAi screen, however, did not show immediate lethality, although for G6PD differentiation from BSF to PCF was prevented (Alsford et al., 2011). Intermediates of human steroid metabolism, dehydroepiandrosterone (DHEA), epiandrosterone (EA) and derived 16α-bromoepiandrosterone (16BrEA) are known to be uncompetitive inhibitors of mammalian and trypanosome G6PDH. DHEA inhibits the *T. cruzi* enzyme and kills both the epimastigote stage parasites and BSF *T. brucei* in *in vitro* culture (Cordeiro and Thiemann, 2010; Cordeiro et al., 2009). These compounds also reduce parasite levels in mice infected with *T. cruzi* (Cordeiro and Thiemann, 2010; Cordeiro et al., 2009). However, the same molecules do not inhibit the *Leishmania* enzyme, presumably due to alterations in the as yet unknown hormone binding site. In an elegant experiment showing that the anti-trypanosomal activity of DHEA related to G6PDH inhibition, the leishmanial enzyme was expressed in *T. brucei* and these cells became insensitive to DHEA (Gupta et al., 2011).

Interestingly, the genes in both trypanosomes have two alternative start codons and the longer protein product contains cysteine residues within an N-terminal 37 amino acid sequence preceding a second putative start codon. Versions of the *T. cruzi* enzyme either

containing the 37 amino acid N-terminal domain, or not, were expressed in *E.coli* and purified proteins compared. The longer, but not the shorter version, was inhibited by various reducing agents (DTT, glutathione, 2-mercpatoethanol), potentially due to their binding to a pair of cysteine residues within the domain. NADPH also inhibited the long form of the enzyme. The *T. brucei* and leishmania enzymes lack those cysteines within the homologous N-terminal region and are presumed, therefore, to lose this reductive regulation (Igoillo-Esteve et al., 2006). The longer variant of the protein is expressed predominantly in all four major life stages of *T. cruzi*, being most abundant in metacyclic trypomastigotes and amastigotes, lower in cultured trypomastigotes and negligible in epimastigotes, which seems to correlate with oxidative stress levels encountered in the parasite's natural environment (Igoillo-Esteve and Cazzulo, 2006). The enzymatic activity correlates with protein levels but not exactly with mRNA levels, indicating post-transcriptional control (Igoillo-Esteve and Cazzulo, 2006). Moreover, exposure to reactive oxygen species triggered increases in G6PDH expression in metacyclic trypomastigotes, but had detrimental effects on epimastigotes, suggesting the adaptation to be stage specific (Igoillo-Esteve and Cazzulo, 2006).

G6PDH has a dual subcellular localization, with a higher glycosomal proportion than other PPP enzymes. Almost 50% of the activity was measured inside glycosomes by Heise and Opperdoes in PCF *T. brucei* (Heise and Opperdoes, 1999) while Duffieux *et al.*(2000) also reported over 40% of the activity in glycosomes.

The sensitivity of *T. brucei* and *T. cruzi* to DHEA indicates that G6PDH can represent a druggable target in these cells. However, the steroid inhibitors are relatively toxic and of limited efficacy. Mercaldi *et al.*(2014) recently performed a screen of 30,000 compounds from the Chemridge DIVERSet in an assay designed to seek other uncompetitive inhibitors of the enzyme. After several rounds of screening a series of quinazolines were selected with activity against *T. cruzi*, for consideration for further development towards new chemical entities.

In *L. donovani*, overexpression of G6PDH de-sensitised these cells to reactive oxygen species (Ghosh et al., 2015). Mukherjee *et al.* (2013) also showed that the G6PDH gene locus, along with ascorbate peroxidase, was amplified in *L. major* strains selected for resistance to Sb^{3+} and the associated chromosomal amplification containing these linked

genes decreased reactive oxygen species accumulation in cells exposed to Sb^{3+}. Null mutants of G6PDH were then generated in *L. major* and the promastigote forms grew more slowly than wild-type (WT) cells and were of three fold increased sensitivity to Sb^{3+}. Moreover, reactive oxygen species accumulated more in the knockout cells (1.5 fold) in comparison to WT when treated with Sb^{3+} (Mukherjee et al., 2013).

1.4.4.2 6-phosphogluconolactonase (6PGL)

6-phosphogluconolactonase accelerates the hydrolysis of 6-phosphogluconolactone to 6-phosphogluconic acid (6PG). The genome wide RNAi target sequencing (RITseq) in *T. brucei* indicated a small growth defect in PCF but no phenotype in BSF related to 6-PGL loss (Alsford et al., 2011). Targeted analyses on the function of the gene have not been carried out in any of the trypanosomatids though. Subcellular fractionation of PCF *T. brucei* cell extracts on sucrose gradients indicated that about 15% of the total activity was associated with glycosomes (Duffieux et al., 2000). An NMR study on the reaction catalyzed by the *T. brucei* enzyme was very informative. The half-life of the lactone was shown to be non-negligible and given its being a highly reactive electrophile a need for an enzyme to prevent accumulation of this potentially toxic species was proposed. The version of the lactone formed from G6P is the δ-form. This form may spontaneously hydrolyse, or else form a γ-form by intramolecular rearrangement. This latter form is not spontaneously hydrolysed, hence the lactonase appears to be required to convert the δ-form to 6-PG before the γ-form emerges (Miclet et al., 2001).

Structural studies on lactonase from *T. brucei* provided an X-ray crystal structure of the enzyme at 2.1 Å resolution, showing that it binds zinc, possibly for a structural rather than catalytic role. *In silico* docking studies were used to show how the lactone orientates in the active site (Delarue et al., 2007). Further studies have investigated dynamics of the protein associated with catalysis (Calligari et al., 2012).

1.4.4.3 6-phosphogluconate dehydrogenase (6PGDH)

The next enzyme in the pathway, 6-phosphogluconate dehydrogenase, enables decarboxylation of 6PG into Ru5P with concomitant reduction of NADP. The 6PGDH gene was identified first in *T. brucei* using a functional complementation approach expressing a library of trypanosome DNA fragments in *E. coli* (Barrett and Le Page,

1993). It was a failure to find 6PGDH activity in BSF *T. brucei* (Ryley, 1962) that led to the pathway being largely ignored until Cronín *et al.* (1989) clearly reported activities of each enzyme. The use of 6PGDH as an isoenzyme marker in studies into genetics of *T. brucei* went unnoticed (Tait et al., 1985).

RNAi indicates no defect associated with 6PGDH loss in PCF, while its absence is lethal in BSF *T. brucei* (Kerkhoven et al., 2013). The gene deletion is lethal in yeast and in drosophila, however, since loss of G6PD rescues these cells from loss of the 6PGDH, it was proposed that it is accumulation of 6PG *per se* that is lethal, rather than reduced production of NADPH through the oxidative branch (Hughes and Lucchesi, 1976; Lobo and Miatra, 1982). Nevertheless, that mechanism was disproven for BSF *T. brucei* (Kerkhoven et al., 2013).

The structure of the trypanosome enzyme was resolved by X-ray crystallography at 2.8 Å resolution (Phillips et al., 1998). The *T. brucei* crystal structure then allowed modelling of the *T. cruzi* and *Leishmania* proteins too (Esteve and Cazzulo, 2004; González et al., 2010). Its high level of sequence divergence from the mammalian enzyme indicated that selective inhibitors may be possible. Several screens were made (Dardonville et al., 2003; Pasti et al., 2003) and particularly interesting was a reaction-based approach to inhibitor design (Dardonville et al., 2004; Ruda et al., 2007, 2010a, 2010b). The reaction mechanism involves a high energy 1,2-*cis*-enediol intermediate (Fig 1.9 A). Gilbert and colleagues (Dardonville et al., 2004) reasoned that hydroxamate analogues of the enediol might have potent activity. This was proven to be the case. Moreover, the inhibitors demonstrated substantially enhanced inhibitory activity of the trypanosome enzyme over a mammalian version (Dardonville et al., 2004). The most potent inhibitor discovered was 4P-D-erythronohydroxamate with Ki = 10 nM with 250-fold selectivity over the sheep enzyme (Fig 1.9 B) (Dardonville et al., 2004). In spite of the potent inhibition of the enzyme these molecules had no efficacy against trypanosomes, attributable to the failure of phosphorylated compounds to cross the parasite membrane. Gilbert's team then added various groups to mask the charged phosphate moiety and among these series arylphosphoramide derivatives (Fig 1.9 C), designed for ester cleavage of the prodrug, yielded compounds with pronounced trypanocidal activity (Ruda et al., 2007). Unfortunately, the presence of esterases in serum probably de-mask the prodrugs in

blood, reducing *in vivo* activity, hence further developments are required to bring compounds derived for this rational approach towards clinical development.

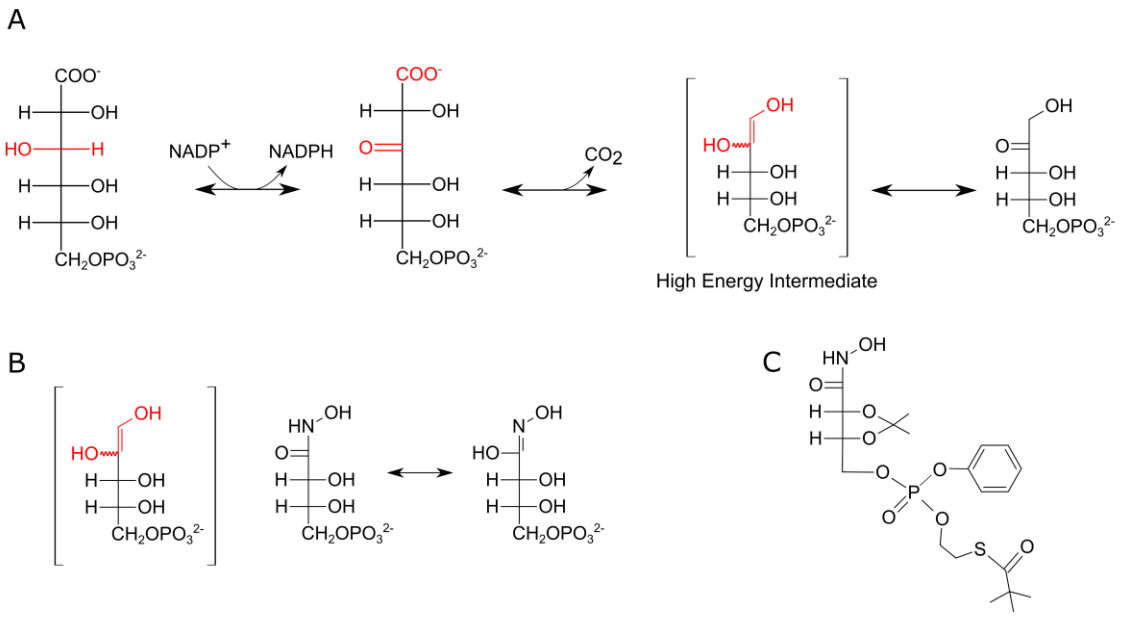

Figure 1.9. Inhibitor design based on the reaction mechanism of 6-PGDH. A - The reaction mechanism that converts 6-PG on the far left to Ru5P on the far right, is proposed to involve the production of a high energy enediol intermediate (marked). B - Hydroxamate analogues of the enediol intermediate were producted and shown to be potent inhibitors of the *T. brucei* enzyme (Dardonville et al., 2003). C - In order to produce cell permeant derivatives of the hydroxamate analogues, ester-based masking groups were added to neutralize the charge on the phosphate groups. The masking groups are cleaved by esterases post cell entry and this endowed the inhibitors with trypanocidal activity (Dardonville et al., 2004).

Activity in the reverse direction, from Ru5P to 6PG could be measured in the enzyme from sheep liver and *Candida* (Silverberg and Dalziel, 1975; Villet and Dalziel, 1969). We have observed in *Leishmania* parasites that accumulation of pentose phosphates can cause the reaction to run in reverse, and in *T. brucei* too, it was possible to find small amounts of 6PG with five labelled carbons in cells grown in glucose containing 6 labelled carbons, indicating the reverse reaction can operate with fixation of CO_2 and consumption of NADPH (Creek et al., 2015).

There is no obvious PTS in the *T. cruzi* enzyme but *L. mexicana* contains a non-canonical internal PTS1 and in *T. brucei* a possible PTS1 was suggested to exist on an exposed loop (Greenblatt et al., 2002). 6PGDH activity was located almost exclusively in the cytosol in PCF *T. brucei* (Heise and Opperdoes, 1999) as well as in *T. cruzi* (Esteve and Cazzulo, 2004), although digitonin permeabilisation experiments with Western blot analysis using an antibody to 6PGDH indicated that small amounts might be found in glycosomes in BSF *T. brucei* (Kerkhoven et al., 2013).

1.4.4.4 Ribose-5-phosphate isomerase (RPI)

The trypanosomatid version of RPI clusters phylogenetically with the B isoform of prokaryotes, while the mammalian version clusters with the A isoform, hence the trypanosomatid and mammalian versions are divergent (Greenblatt et al., 2002; Loureiro et al., 2015). RITseq experiment indicated a strong growth defect after depletion of RPI mRNA in *T. brucei* (Alsford et al., 2011), although depletion of RPI by a targeted RNAi caused only mild growth phenotype in BSF *T. brucei in vitro* and lower parasitemia with delayed onset and slower progression of the disease in mice (Loureiro et al., 2015), hence its utility as a target for drugs remains equivocal. RPI is expressed in all four major stages of *T. cruzi* with higher protein levels in metacyclic trypomastigotes and trypomastigotes (Stern et al., 2007). In *T. brucei,* localisation was shown to be mostly cytosolic but with a small fraction in glycosomes in both stages as determined by immunofluorescence microscopy and digitonin permeabilisation (Loureiro et al., 2015). Structure of the *T. cruzi* enzyme has been resolved, including binding with substrates and its low potency inhibitor, 4-phospho-D-erythonohydroxamic acid (Stern et al., 2011).

An alternative route to create R5P is via ribokinase activity using free ribose, that can be accumulated from blood or else derived from nucleosides through the action of nucleoside hydrolases (Parkin, 1996). Although gene knockout of the *T. brucei* ribokinase was not possible, RNAi indicated that the RNA could be depleted below detection limits without an effect on phenotype (Kerkhoven et al., 2013), which was also the conclusion in the genome wide study for BSF, although it appeared essential in PCF (Alsford et al., 2011).

1.4.4.5 Ribulose-5-phosphate epimerase (RuPE)

Ribulose-5-phosphate epimerase has not been subject to a targeted study in any trypanosomatid so far. The *T. brucei* RITseq experiment indicated that mRNA depletion did not cause any growth defect (rather a gain in fitness phenotype was seen in both BSF and PCF) (Alsford et al., 2011). In the absence of TKT in BSF *T. brucei*, its role is not immediately obvious since its product Xu5P is technically a dead end, unless other enzymes, for example a Xu5P phosphoketolase, as described in bacteria (Petrareanu et al., 2014) were operative. Such an enzyme would create GA3P and acetyl phosphate. However, genome searches have not yielded any strong candidates based on homology to bacterial variants of the enzyme.

1.4.4.6 Transketolase (TKT)

In addition to TKT itself, two additional gene paralogues called transketolase-like proteins (TKTL1 and TKTL2), are known in humans and, although TKT activity is associated with these proteins, controversy exists as to their true biochemical function (Coy et al., 1996; Meshalkina et al., 2013; Schneider et al., 2012). A number of studies clearly link over-expression of TKTL1 with cancer (Langbein et al., 2006; Staiger et al., 2006a) which is fuelling renewed interest in TKT.

In yeast, the phenotype of TKT mutants is dependent on the carbon source. Growth is reduced on fermentable, but not on gluconeogenic substrates, indicating a role for TKT in regulating glycolysis (Sundström et al., 1993). Simultaneous G6PDH and TKT depletion is lethal in yeast (Schaaff-Gerstenschläger and Zimmermann, 1993). TKT uses thiamine pyrophosphate (TPP) as a cofactor and analogues, including oxythiamine (which is phosphorylated inside cells) have been proposed as inhibitors of TKT with promising preliminary results as inhibitors of cancer cell growth (Rais et al., 1999). However, oxythiamine-PP inhibits other enzymes that use TPP as a cofactor, including pyruvate dehydrogenase and oxoglutarate dehydrogenase, hence TKT may not be the primary target (Chan et al., 2013). Oxythiamine was active against *P. falciparum* but the presence of thiamine in the medium diminished the effect and toxicity (weight loss) associated with oxythiamine administration to infected mouse models diminishes the compound's attractiveness for further consideration as a therapeutic against malaria (Chan et al., 2013).

BSF *T. brucei* lack TKT and knock-out of the gene in PCF *T. brucei* led to no obvious growth defect or morphological change, but metabolomic analysis showed significant changes in metabolites of glycolysis and the PPP (Stoffel et al., 2011). The enzyme contains a PTS1 sequence and localisation was measured to be 70% cytosolic and 30% glycosomal in *L. mexicana* (Veitch et al., 2004) and 10% glycosomal in PCF *T. brucei* (Stoffel et al., 2011). The crystal structure of the *Leishmania* enzyme was resolved at 2.2 Å (Veitch et al., 2004).

1.4.4.7 Transaldolase (TAL)

A gene annotated as TAL was cloned from *T. brucei* and the protein expressed then used to determine the ability of the enzyme to create O8P using R5P and F6P as acceptor and donor substrates respectively (Creek et al., 2015). This indicates TAL as a likely source of the higher carbon content carbohydrates referred to above. It is unclear what the function of TAL in BSF *T. brucei* is, in the absence of TKT and RuPE. RITseq experiments indicated the gene to be essential to PCF but not BSF *T. brucei* (Creek et al., 2015). Out of three independent proteomics experiments (Colasante et al., 2006; Guther et al., 2014; Vertommen et al., 2008), only Vertommen *et al*., (2008) detected the protein within PCF *T. brucei* glycosomes.

1.5 Metabolomics

Metabolomics refers to high-throughput techniques aiming to dissect the composition of metabolites and quantifying them within a single experiment. This is a very challenging task compared to other –omics (genomics, transcriptomics, proteomics), because metabolites are small molecules of diverse biophysical characteristics, thus they cannot all be characterised by a single method. However, current techniques can confidently determine hundreds of small molecules and the numbers are still increasing (Bouatra et al., 2013). The experimental approach undertaken can be untargeted, represented by semi-quantitative analyses of the total cellular metabolome, or targeted, aiming at precise quantification of a limited group of compounds of interest.

The two most widely used platforms are nuclear magnetic resonance (NMR) and mass-spectrometry (MS). While NMR can provide precise absolute quantification and it is usually highly reproducible, the number of metabolites detected is relatively low given poor sensitivity, and data analysis becomes difficult in complex samples. Prior to MS analysis, the samples are separated by gas or liquid chromatography (GC or LC) or capillary electrophoresis with numerous variations, enabling a focus on specific target groups of compounds. Usage of GC requires derivatization of the samples accompanied with more complicated sample preparation and subsequent data analysis, but it achieves high quantitative accuracy and reproducibility. LC can be targeted either at hydrophilic or lipophilic compounds, which determines the method of choice. HILIC (hydrophilic interaction liquid chromatography) columns are commonly used for metabolomics as they are suitable for most cellular metabolites, unless lipidomics analysis is desired (reviewed in Creek et al., 2012b; Shulaev, 2006). The approach is semi-quantitative but absolute quantification can be obtained if labelled standards are included (Kim et al., 2015). Despite persisting drawbacks (high costs, data analysis and interpretation, uncertainty with compound identification), the positives of metabolomics approaches prevail and popularity and usage of metabolomics is growing rapidly. Improvement in the technology and decrease in cost coincide with these developments.

1.5.1 Metabolomics applied to trypanosomatid protozoa

A range of high-throughput –omics techniques enables to study organisms on different levels from the genome towards the final phenotype, and they have been applied to

trypanosomatid parasites over the last years. A number of trypanosomatid genomes have been sequenced, unravelling a huge number of genes for hypothetical proteins, to which is extremely difficult to assign a function (Berriman et al., 2005; Ivens et al., 2005). When transcriptomics became available, numerous studies were performed on *Leishmania* comparing promastigote and amastigote life stages, but the extent of differences detected was surprisingly small and it was generally concluded that because trypanosomatids do not have control on transcriptional level, RNAseq data cannot provide much information relevant to the biology (Akopyants et al., 2004; Cohen-Freue et al., 2007). Thus, proteomics and especially metabolomics may point to profound differences in parasite biology that are not evident through gene expression analysis, because metabolomics is closest to the final phenotype of the omics technologies. Metabolomics may, therefore, enable us to shed light on persistent questions behind the parasite's biology and point to metabolic weak points offering targets for treatment.

Numerous metabolomics analyses of trypanosomatids have been performed including a comprehensive depiction of central metabolism in *T. brucei* (Creek et al., 2013, 2015) including precise quantification of metabolic end-products by LC-MS (Kim et al., 2015) while NMR has been extensively used to dissect pathways of glucose and proline metabolism of PCF *T. brucei* (Mazet et al., 2013; Millerioux et al., 2013). A comprehensive overview of *L. mexicana* metabolism was obtained by GC-MS on promastigote (Saunders et al., 2011) and amastigote stages (Saunders et al., 2014). In addition, changes in metabolism during development were investigated (Silva et al., 2011), while study on amino acid metabolism revealed substantial changes between three different species (Westrop et al., 2015). Further, metabolomics can answer specific questions such as drug target deconvolution (Trochine et al., 2014; Vincent et al., 2010, 2012), interaction with the host (Caradonna et al., 2013) or specific amino acids utilisation (Johnston, 2015). Concerning *Leishmania*, in addition to the publications mentioned above, there is for example an interesting work tracing labelled deuterium, which provided information on turnover of DNA, RNA, protein and lipids in parasites both from a culture and lesions and showed how much slower the growth is *in vivo* (Kloehn et al., 2015).

1.6 Scope of this thesis

My general aim of this thesis was to use metabolomics approach to study *Leishmania* parasites. I compared promastigote and amastigote cells, assessed utilisation of different sugars, and performed analysis of transketolase knock-out cells. Untargeted LC-MS approach was used first, and based on the data obtained, further targeted analyses were performed focused on specific questions. Additional experiments were performed in order to complete the studies and bring as much comprehensive results as possible.

A comparative metabolomics analysis was performed of *L. donovani* promastigotes, axenic amastigotes and splenic amastigotes. To the best of my knowledge this is the first metabolomic analysis of amastigotes obtained directly from an animal tissue. The main objective of this study was to evaluate differences between the two types of amastigotes, since axenic parasites are cultured in conditions very different form their natural environment, especially regarding nutrient availability. Hence, I wanted to compare the metabolomes of the cells, which should give us indications if cell metabolism is changed in consequence of the specific environment. The data should provide clues useful for future studies, i. e. if axenic amastigotes are a good model for studies focused on metabolism, or testing potential drugs targeted on metabolism.

Further, I performed a metabolomics analysis of *L. mexicana* promastigotes grown in media containing different labelled sugars, and afterwards I assessed incorporation of carbons from these sugars into metabolism. Maugeri *et al*. (2003) cultured *L. mexicana* promastigotes in medium containing radiolabelled glucose and calculated the flux in the PPP from incorporation of the label into nucleic acids. However, this estimation may be inaccurate and highly dependent on glucose and ribose concentrations in the medium. In the PPP glucose is turned into R5P which is essential for nucleotide biosynthesis. In addition ribose can be taken up from medium and directly phosphorylated into R5P by ribokinase, thus we hypothesized that presence of ribose would influence the utilisation of glucose for nucleotide biosynthesis. In order to assess that, I cultured cells in medium containing labelled glucose, ribose and combinations of the two sugars and analysed utilisation of carbons from the sugars into metabolism.

Previously *L. mexicana* transketolase knock-out (Δtkt) cell line was obtained in the promastigote stage and I performed phenotypic characterisation of the parasites. The aim was to assess its sensitivity to various drugs, infectivity and potential utilisation as a drug target. I performed an untargeted LC-MS metabolomics analysis of the cell line and since the results indicated major changes in the metabolism beyond the PPP, I performed further studies to validate these observations. Additional analyses followed with an aim to elucidate the mechanism driving these changes and potential regulatory mechanisms of metabolism.

Preliminary studies on TKT sparked a hypothesis that binding of various sugar substrates has an influence on conformation of the protein, especially the C-terminus (Wildridge, 2012). The C-terminus is flexible and bears a PTS1, hence a change in its conformation could have an impact on the subcellular localisation. I prepared a series of constructs of TKT with alternations to the C-terminus and examined their localisation by immunofluorescence microscopy. One of these constructs appeared to be present solely in glycosomes, so subsequently I made an additional construct with purely cytosolic TKT and compared phenotypes and metabolomes of cells expressing TKT in a single compartment.

2 Materials and Methods

2.1 Ethics statement

All animal experiments were performed in accordance with the Animals (Scientific Procedures) Act 1986 and the University of Glasgow care and maintenance quidelines. All animal protocols and procedures were approved by The Home Office of the UK government and the University of Glasgow Ethics Committee (or Institut Pasteur, Paris, France).

2.2 Cell culture and cell growth

2.2.1 Cell culture

Leishmania mexicana M379 promastigote cells were cultured in Homem medium (Berens et al., 1976; GE Healtcare) at 25°C supplemented with 10% heat–inactivated foetal calf serum (FCS; Thermo Fisher Scientific) at density 10^5 – 2 x 10^7 cells/ml. For transgenic cell lines antibiotics were added as required, for Δtkt cells 25 µg/ml nourseothricin (Sigma-Aldrich) and 25 µg/ml hygromycin (Roche), for Δtkt + TKT re-expressor 25 µg/ml puromycin (Sigma-Aldrich) in addition. For cells expressing GFP-TKT episomal constructs 25 µg/ml G418 (Sigma-Aldrich) was added.

L. mexicana amastigote cells were cultured in Schneider's Drosophila Medium (Sigma-Aldrich) supplemented with 20% FCS (Thermo Fisher Scientific) and 15 mg/l hemin (Sigma-Aldrich), at 32°C, 5% CO_2, pH 5.5 (Bates et al., 1992). Cells were maintained at density 10^6 – 3 x 10^7 cells/ml.

L. donovani 1S2D promastigotes were cultured in M199 medium supplemented with 10% FCS, 25 mM Hepes pH 6.9, 4mM $NaHCO_3$, 1 mM glutamine, 1x RPMI-1640

vitamin mix, 0.2 µM folic acid, 100 µM adenine, 7.6 mM hemin, 8 µM biopterin, 50 U/ml penicillin and 50 µg/ml streptomycin.

L. donovani amastigotes were cultured at 37°C and 5% CO_2 in RPMI-1640 supplemented with 1 mM glutamine, 1x RPMI-1640 vitamin mix, 0.2 µM folic acid, 100 µM adenine, 20% FCS, 1x RPMI-1640 amino acid mix, 28 mM MES, 50 U/ml penicillin and 50 µg/ml streptomycin.

Macrophage THP-1 cell line was cultured in RPMI-1640 medium (Sigma-Aldrich) supplemented with 10% FCS (Thermo Fisher Scientific) and 2 mM glutamine. Cells were maintained at density 10^5 – 10^6 cells/ml.

Cell density was estimated using Neubauer haemocytometer under a light microscope.

2.2.2 Alamar Blue Assays

Toxic effects of various compounds were tested using Alamar Blue Assays in various alternations (Allmann et al., 2013; Räz et al., 1997). Compounds were diluted serially across 96-well culture plates in appropriate medium, alternatively glucose oxidase (Sigma-Aldrich) was added in required dilutions to the medium. Cells were added to the plates at the final density 5 x 10^5 cells/ml for promastigotes and 10^6 cells/ml for amastigotes. Cells were cultured in the plates for 72 hours and subsequently 0.48 mM resazurin was added to all wells. After additional 48 hours of incubation, absorbance in plates was measured with fluorescence spectrometer FLUOstar OPTIMA (BMG Labtech) at excitation wavelength 544 nm and emission wavelength 590 nm. Data were analysed with GraphPad Prism software to obtain EC_{50} values. Technical duplicates were collected for each reading and biological triplicates for most experiments, if not stated otherwise.

2.2.3 Macrophage infections

THP-1 macrophages were activated with 20 ng/ml phorbol 12-myristate 13-acetate (Sigma-Aldrich) for 3 days, afterwards the cells were washed with RPMI-1640 medium twice, transferred into 16-well tissue culture slides (Lab-tek), 100 µl/well at density 2 x 10^5 cells/ml and incubated at 37°C, 5% CO_2 overnight. *L. mexicana* promastigotes in the stationary phase were used for infections, at a ratio of 5 or 10 parasites per macrophage.

Leishmania cells were washed with PBS and resuspended in RPMI-1640 medium to the appropriate density, finally adding 100 µl of parasites per well. Slides were incubated at 32°C, 5% for 6 hours and subsequently extracellular parasites were washed by slowly adding 200 µl PBS to each well and decanting, repeating this step three times. Cells were incubated at 32°C, 5% for 24 hours or as required. Finally, cells were fixed by adding 70% methanol for 1 min and subsequently washed with water. 2.5 µM DAPI (4',6-diamino-2-phenylindole) was used for staining of nuclei, visualised with fluorescent microscope Axioplan2 (Zeiss) and Volocity software, and the macrophage infection was counted.

2.2.4 Animal infections

For mouse infection assessment, BALB/c mice and *L. mexicana* promastigotes in stationary phase were used. 2 x 10^6 cells in total volume of 40 µl PBS were inoculated into the right food pad, and the size of ensuing lesions were measured at least once a week. When the food pad lesions reached above 4 mm in size, the animals were culled.

2.3 Molecular biology

2.3.1 DNA isolation

For genomic DNA isolation 10 ml of *Leishmania* culture in logarithmic growth phase was used, equivalent to approximately 10^8 cells in total. A NucleoSpin Tissue kit (Macherey-Nagel) was used following the manufacturer's standard protocol. Final DNA concentration was measured using Nanodrop1000 Spectrophotometer (Thermo Fisher Scientific).

2.3.2 GFP-TKT constructs

In order to express TKT with an N-terminal GFP tag, the pNUS-GFPnH plasmid was used (http://www.ibgc.u-bordeaux2.fr/pNUS/greenvectors.html ; based on Tetaud et al., 2002). Primers used for the amplification are listed in Tab 2.1.

gene	label	sequence	restriction site
WT TKT	MB0766	TAAGATCTATGGCCTCCATTGAGAAGGTGG	*Bgl*II
WT TKT	MB0767	TACTCGAGTTACATCTTGCTGAATGAAGA	*Xho*I
cyto TKT	MB0812	TACTCGAGGAATGAAGAGTTCTTGAGCGGCG CC	*Xho*I

Table 2.1. List of primers used for PCR. All primers were purchased from Sigma-Aldrich.

2.3.3 High-fidelity PCR

For error-prone PCR, 50 µl of PCR reaction mixture contained 0.4 mM dNTPs, 1 µl of each primer, 2 µl of genomic DNA, 0.5 µl of Phusion HF DNA Polymerase (Biolabs), 1x Phusion DNA Polymerase buffer (Biolabs). The cycling program used consisted of the following: heated lid at 112°C, denaturation at 98°C for 1 min, then 35 cycles of denaturation at 98°C for 15 sec, annealing at 59°C for 30 sec, elongation at 72°C for 2 min, and final elongation at 72°C for 10 min, using a Thermal Cycler (G-Storm). The PCR products were purified using Nucleospin Gel and PCR Clean-up kit (Macherey-Nagel), following the manufacturer's protocol. In order to amplify TKT without the PTS1, a combination of primers MB0766 and MB0812 was used.

2.3.4 Ligation and restriction digest

Prior to ligation into the pGEM-T Easy vector, single adenosine overhangs were added to the PCR products by incubating a mixture of 20 µl PCR product, 0.5 µl GO Taq DNA Polymerase (Promega), 0.1 mM dATPs and 1x GO Taq Buffer, at 72°C for 30 min.

For ligation into pGEM-T Easy vector (Promega), 100 ng of vector and 200 ng of insert was incubated with 1 µl of T4 DNA Ligase (Promega) in 1x ligase buffer (Promega) for 1 hour at room temperature (RT).

For a typical restriction digest reaction, 1 µl of each enzyme, appropriate buffer and 50 µl of plasmid DNA was used in total volume of 60 µl. Ligation reactions contained the

following: 1 µl of T4 DNA ligase (Promega), 1x ligase buffer (Promega), DNA in a ratio 2:1 of the insert and plasmid, in total volume of 10 µl.

2.3.5 Transfection into *Escherichia coli*

In order to transfect a construct into *E.coli* cells, 50 µl of competent cells were used, mixed with 2 µl of ligation reaction, incubated at 42°C for 45 sec, subsequently on ice for 2 min, and supplemented with 600 µl of SOC medium. After 1 h incubation at 37°C shaking, bacteria were spread on agar plates with appropriate antibiotics and incubated overnight at 37°C. Subsequently, the obtained colonies were screened by PCR. Bacteria containing positive plasmids were cultured in 5 ml of LB medium at 37°C shaking overnight and the plasmids were isolated using NucleoSpin Plasmid kit (Macherey-Nagel) following the manufacturer's protocol, and the integrated genes verified by sequencing at MWG, UK.

2.3.6 Screen PCR

In order to screen bacteria for insert integration, 25 µl of PCR reaction mixture contained GoTaq DNA Polymerase (Promega), 0.4 mM of dNTPs, 1 µl of each primer, template DNA, and 1x GoTaq DNA polymerase buffer (Promega). The following cycling program was used: heated lid at 112°C, denaturation at 98°C for 2 min; 25 cycles of denaturation at 95°C for 30 sec, annealing at 59°C for 45 sec, elongation at 72°C for 2 min, and final elongation at 72°C for 5 min, using Thermal Cycler (G-Storm).

2.3.7 GFP-TKT with mutated C-termini

In order to prepare mutated constructs of TKT with altered C-termini, dsDNA constructs containing the respective sequences were purchased from GenScript, USA. These DNA fragments were cloned into pNUS-GFPnH vector containing WT TKT gene using TKT internal restriction site for *Fsp*AI (Biolabs) and *Xho*I (Biolabs) restriction site of the vector.

2.3.8 Transfection of *Leishmania* with episomal constructs

In order to transfect *Leishmania* with an episomal vector, about 10 µg of DNA is required. Constructs verified by sequencing were grown as mini-preps, plasmid DNA purified with NucleoSpin Plasmid kit (Macherey-Nagel) and precipitated with ethanol in

a volume ratio 10:1:3 containing DNA, 3 M sodium acetate and 100% ethanol. The mixture was incubated at -20°C for 15 min, centrifuged at 14,000 g, 4°C for 30 min, the obtained pellet rinsed with 70% ethanol, and following centrifugation at 14,000 g, 4°C for 15 min, the pellet was dried and resuspended in sterile water. 5 x 10^7 *Leishmania* cells were centrifuged at 1,300 g for 10 min, resuspended in 100 µl of Human T Cell Nucleofector Solution (Lonza) in transfection cuvettes. The plasmid DNA was added, and cuvette placed into Nucleofector Amaxa (Lonza) using program U-033. The cuvette was immediately placed on ice and cells subsequently transferred into 10 ml of fresh Homem medium. Following overnight incubation at 25°C, the required antibiotic was supplemented at 50 µg/ml and cells cultured at 25°C until selected cells emerged.

2.4 Metabolomics

2.4.1 Sample preparation

Preparation of metabolomic samples was adapted from method described by Creek et al. (2011). For all metabolomic experiments 4 biological replicates were prepared for each condition. Cell cultures were started 2 – 3 days prior to sample preparation at cell density 5 x 10^5 cells/ml, subsequently cells in logarithmic growth phase were harvested. 10^8 cells were collected for each final 200 µl sample. Cells were rapidly cooled in a dry ice/ethanol bath to 4°C and kept at 4°C for the rest of the preparation. Cells were centrifuged at 1,250 g, 4°C for 10 min (spent medium was kept for analysis when required) and washed with PBS. The cell pellet was resuspended in extraction solvent (chloroform:methanol:water, 1:3:1 volume ratio) and extracted by shaking vigorously for 1 h at 4°C. Subsequently, samples were centrifuged at 16,000 g, 4°C for 10 min and obtained supernatant collected and stored at -80°C under argon atmosphere until the LC-MS analysis. For medium analysis 10 µl of medium was mixed with 190 µl of extraction solvent.

For experiments with labelling, the respective labelled sugars were added to the medium from the beginning of cell cultivation. U-^{13}C-glucose, U-^{13}C-ribose, or 1,2-^{13}C-glucose (all Cambridge Isotope Laboratories, Inc.) were used and mixed in the media as appropriate for each experiment.

2.4.2 LC-MS

The analyses were performed using liquid chromatography coupled to mass spectrometry on the platform at Glasgow Polyomics. All samples were separated with high performance liquid chromatography (HPLC) on ZIC-pHILIC (polymer based – Hydrophilic Interaction Liquid Chromatography Column, Merck) using an ICS-5000 system (Dionex Corporation) prior to mass detection on an Orbitrap Exactive mass spectrometer (Thermo Fisher). The samples were run alongside 248 authentic standards at 10 µM each for further data analysis. Analysis was performed in positive and negative modes, using 10 µl injection volume and a flow rate of 100 µl/min. For HPLC gradient solvent A was 20 mM ammonium carbonate in H_2O and solvent B was 100% acetonitrile.

2.4.3 Data analysis for LC-MS

The raw data were processed and analyzed using Identification and evaluation of metabolomics data from LC-MS (IDEOM, Creek et al., 2012). IDEOM uses MZmatch software (Scheltema et al., 2011) in the R environment. For analysis of experiments with labelling, mzMatchISO software (Chokkathukalam et al., 2013) was used. Standards were processed with ToxID software (Thermo Scientific). For further analyses and data visualisation MetaboAnalyst interface was used (Xia et al., 2015).

2.4.4 Derivatisation of samples for GC-MS

For GC-MS analysis, the samples were prepared following the same protocol as for LC-MS, the further derivatisation, analysis and data processing was performed by Dr. Stefan Weidt at Glasgow Polyomics.

A retention index mix was prepared from pure alkanes dissolved in hexane to a final concentration of 6 mg/ml. Stock solutions were prepared for each from neat reference standards in water. A custom standard mixture of sugars, sugar phosphates, and pentose phosphate pathway intermediates was then prepared by mixing the stock solutions together and diluting with water.

30 µl of extracted sample, as well as each of the custom standard mix of sugars, sugar phosphates, and pentose phosphate pathway intermediates, were transferred to a 300 µl KIMSHIELD™ deactivated glass polyspring insert (National Scientific). Internal

standards $^{13}C_6$-Glucose (2 nmol), D_{27}-Myristic acid (2 nmol) and Scyllo-Inositol (1 nmol) were added to each sample. Samples were then dried in a Savant SPD1010 SpeedVac concentrator (Thermo Scientific) for 90 min. Inserts were then placed into a 9 mm screw cap amber borosilicate glass 1.5 ml vial (Thermo Scientific). 50 µl of 20 mg/ml (w/v) methoxyamine HCl in pyridine was added to each dried sample and sealed. The vial and insert were vortexed for 10 seconds and incubated at 60°C for 120 min. Following the methoximation step, 90 µl of MSTFA + 1% TMCS (N-Methyl-N-(trimethylsilyl) trifluoroacetamide + 1% trimethylchlorosilane) was added, followed by a further 10 second of vortexing. Silylation was performed by incubation at 80°C for further 120 min. Samples were cooled to room temperature. 10 µl of retention index alkane mixture was added to each sample. Samples were then ready for injection.

2.4.5 GC-MS analysis

1µl of derivatized sample was injected into a Split/Splitless (SSL) injector at 280°C using a 1 in 50 split flow using a Trace 1310 gas chromatograph (Thermo Scientific). Helium carrier gas at a flow rate of 1.2 ml/min was used for separation on a TraceGOLD TG-5SILMS 30 m length × 0.25 mm inner diameter × 0.25 µm film thickness column (Thermo Scientific). The initial oven temperature was held at 70°C for 4 min, followed by an initial gradient of 20°C/min ramp rate. The final temperature was 320°C and held for 5 min. Eluting peaks were transferred through an auxiliary transfer temperature of 250°C into a GC-QExactive mass spectrometer (Thermo Scientific). Electron impact (EI) ionisation at 70 eV energy, emission current of 50 µA with an ion source of 230°C. A filament delay of 5.3 min is used to prevent excess reagents from being ionised. High resolution EI fragment spectra were acquired using 60,000 resolution with a mass range of 50-650 *m/z.* The best internal lock mass from 207.0324, 281.0511 or 355.0699 *m/z* was used to maintain mass accuracy throughout the chromatogram.

2.5 RNA sequencing

For the RNAseq experiment 5 x 10^7 cells were used for each sample in biological triplicates. RNA was isolated using RNeasy Mini Kit (Qiagen) following the manufacturer's protocol. The concentration of the obtained RNA was determined using a Nanodrop1000 Spectrophotometer (Thermo Fisher Scientific).

The sequencing was performed at Glasgow Polyomics on the NextSeq500 platform, using library preparation by polyA selection, paired-end samples with 13 million reads per sample.

The analysis was performed using the Galaxy interface (Afgan et al., 2012; Giardine et al., 2005), using Bowtie2 software (Langmead and Salzberg, 2012) and Cufflinks package (Trapnell et al., 2010).

2.6 Biochemistry

2.6.1 Glucose consumption assay

In order to quantify the consumption of glucose by promastigotes, Homem medium was prepared containing just 1mM glucose and supplemented with 10% FCS as usual. *L. mexicana* cells were grown up to logarithmic phase, centrifuged at 1,300 g for 10 min, washed with PBS, and resuspended in fresh Homem with 1mM glucose. Subsequently, at selected time points (12, 15, 18, 21, and 24 hours), cell density was established and a sample of medium collected and stored at -20°C. Subsequently, the concentration of glucose in the samples was measured using a Glucose oxidase kit (Sigma-Aldrich). Four biological replicates were prepared for each group.

2.6.2 Enzyme activity assays

For all enzyme activity assays, cells at logarithmic growth were collected, 2 x 10^7 cells were used to create a final 100 µl of cell extract. Cells were centrifuged at 1,300 g, 16°C for 10 min and washed with PBS, and resuspended in 100 µl TE lysis buffer (10 mM Tris-HCl pH 8, 1 mM EDTA) with 0.15% Triton and Complete protease inhibitor cocktail (Roche). Samples were incubated at room temperature (RT) for 20 min, centrifuged at 16,000 g, 16°C for 5 min and supernatant collected. Subsequently, the protein concentration was established by Bradford Assay using a Bio-Rad Protein Assay reagent (Bio-Rad).

All the reactions described here are coupled to another enzyme in a way to produce or consume NAD(P)H which can be easily detected as change in absorbance at $\lambda = 340$ nm

by UV-VIS Spectrophotometer (Shimadzu). All the chemicals and enzymes were purchased from Sigma-Aldrich, if not stated otherwise.

2.6.2.1 Transketolase

In order to measure TKT activity, its reaction is coupled in a way allowing its substrate GA3P, to be used by triose phosphate isomerase in order to make DHAP, which is then used by glycerol-3-phosphate dehydrogenase in a reaction producing NADH (Brin, 1974). The reaction mixture was prepared containing 100 mM Tris.HCl pH 8.0, 1.2 mM $MgCl_2$, 10 µM TPP, 100 µM NADH, 10 mM R5P, 1 mM Xu5P, 1 U triose phosphate isomerase (Sigma-Aldrich) and 1 U glycerol-3-phosphate dehydrogenase (Sigma-Aldrich) and 100 µl of cell extract in 1 ml of total volume. Consumption of NADH was measured by UV-VIS Spectrophotometer (Shimadzu) at $\lambda = 340$ nm.

2.6.2.2 Hexokinase

Hexokinase produces G6P, thus its activity measurement is coupled with the G6PDH reaction producing NADPH. The reaction mixture was prepared containing 300 mM Tris-HCl pH 7.5, 25 mM NaCl, 3 mM glucose, 2 mM ATP, 2 mM $MgCl_2$, 1 mM NADP and 1U G6PDH in 1 ml total volume.

2.6.2.3 Glucose-6-phosphate isomerase

The assay for PGI uses F6P as a substrate which leads to production of G6P, and thus can be coupled with G6PDH producing NADPH, which is detected. The reaction mixture contained 100 mM triethanolamine (TEA) pH 7.5, 7 mM $MgCl_2$, 1.3 mM F6P, 0.4 mM NADP, and 1 U of G6PDH in 1 ml total volume.

2.6.2.4 Glucose-6-phosphate dehydrogenase and 6-phosphogluconate dehydrogenase

Both G6PDH and 6PGDH reactions produce NADPH which can be easily measured, however, since the product of the first reaction is spontaneously converted into the substrate of the latter, sum activity of the two enzymes has to be measured, and separately activity of 6PGDH, and G6PDH is calculated from the difference. For 6PGDH activity measurement, the reaction mixture contained 50 mM TEA pH7.5, 5 mM $MgCl_2$, 2mM 6PG and 1 mM NADP. For measurement of both enzymes, 1mM G6P was also supplied.

In order to measure the 6PGDH reaction in the reverse direction, an assay was used as described (Villet and Dalziel, 1969). The mixture contained 130 mM triethanolamine, 2 mM Ru5P, 68 mM $NaHCO_3$, and 50 µM NADPH.

2.6.2.5 Fructose-1,6-bisphosphate aldolase

The assay for FbPase activity determination is coupled with TPI and G3PDH consuming NADH. The reaction mixture contained 10 mM TEA pH 7.6, 2 µM EDTA, 10 µM F1,6bP, 1 U TPI, 1 U G3PDH and 100 µM NADH in 1 ml total volume.

2.7 Techniques for determination of subcellular localisation

2.7.1 Immunofluorescence microscopy

For preparation of samples for immunofluorescent microscopy, 200 µl of cell culture was used for each sample. Cells were centrifuged at 1,300g, 10 min, washed in PBS twice and resuspended in 100 µl of PBS. 100 µl of 2% formaldehyde was added (methanol free, Thermo Fisher) and samples were incubated for 30 min. Triton X-100 was added to 0.1% final concentration, incubated for 10 min, and glycine was added to 0.1 M final concentration. Following 10 min incubation, samples were centrifuged at 1,300 g, for 10 min, resuspended in 200 µl of PBS, spread on a microscope slide and left to dry at RT. Subsequently, slides were washed in PBS and blocked in TB solution (1x PBS with 0.1% Triton X-100, 0.1% BSA) for 1h at RT. The primary antibody was added to the desired concentration (1:100 dilution for α-*Tb*TIM polyclonal, kindly provided by Prof. Paul Michels, University of Edinburgh (Helfert et al., 2001)) in TB solution and incubated at 4°C overnight. Cells were washed three times in PBS, and incubated with secondary antibody (1:1000, AlexaFluor 594 anti-rabbit, Molecular Probes) for 1 h at RT. Slides were washed three times in PBS and let to dry at RT, subsequently mounted with 2.5 µM DAPI, and covered with cover slides. Cells were visualised using Axioplan2 (Zeiss) and Volocity software.

2.7.2 Digitonin fractionation

For digitonin fractionation, cells were collected, washed with PBS and 10^9 cells resuspended per 1 ml of STE buffer. Subsequently, a series of samples was prepared

containing 100 µl of cell suspension each and increasing concentrations of digitonin from 0.04 to 1.6 mg/ml. Samples were incubated at RT for 4 min, centrifuged at 14,000g for 2 min, and the obtained supernatant collected and used for Western blot analysis.

2.7.3 Western blot analysis

For Western blot (WB) analysis, cells were harvested, washed in PBS and samples were prepared with SDS loading buffer, using 10 µl per 5 x 10^6 cells and incubation at 95°C for 10 min. Samples were loaded on a NuPage Protein gel (Thermo Fisher) and separated at 100 mA, using manufacturer's 1x NuPage running buffer. Subsequently, proteins were transferred onto a nitrocellulose membrane (Hybond ECL, GE Healthcare Life Sciences) at 40 V for 2 h in 1x transfer buffer. Membranes were blocked in 5% milk solution in PBS-T (1x PBS, 0.05% Tween X-100) for 30 min at RT, and subsequently incubated with the required primary antibody at 4°C overnight. α-GFP (Sigma-Aldrich) was used in 1:5,000, α-TKT (Veitch et al., 2004) in 1:2,000,and α-GDH (kindly provided by Prof. Paul Michels, University of Edinburgh (Kohl et al., 1996)) in 1:1000 dilution, respectively. Following three washes in PBS-T for 10 min each, the membrane was incubated with the secondary antibody (goat α-rabbit, 1:20,000, Invitrogen) for 1h at RT. Following additional three washes in PBS-T, the membrane was mounted with 1 ml of ECL Western Blotting Substrate (Thermo Fisher), incubated for 1 min and visualised using gel doc.

2.8 Separation of amastigotes from hamster liver

Isolation of amastigotes from hamster spleen was performed as described previously by Pescher *et al.* (2011). Isolated spleen was added to a tube with 4.5 ml PBS and 0.5 ml of 25mg/ml saponin then homogenised using a gentleMACS Dissociator (MACS Miltenyi Biotec). After adding 20 ml of PBS, samples were centrifuged at 2,000g, 4°C for 10 min. Supernatant was collected and cooled in a dry ice/ethanol bath to 4°C. The samples were again centrifuged at 2,000g, 4°C for 10 min and the pellet resuspended in 2 ml of PBS and 25 ml of PBS with saponin (1mg/ml) then added. Following 5 min incubation on ice, samples were centrifuged at 2,000 g, 4°C for 10 min, the pellet resuspended in 50 ml PBS and this step repeated twice. Finally, the pellet was separated on 45-90% Percoll gradient by centrifugation at 2,500 g, 15°C for 35 min. The layer containing amastigotes

was collected, resuspended in 50 ml of PBS and centrifuged at 2,000 g, 4°C for 10 min, and this step then repeated. The cells were counted and used for metabolite extraction as described in part 2.3.1.

2.9 Buffers and solutions

Homem medium, 1l

0.2 g	$MgSO_4 . 7 H_2O$
0.4 g	KCl
6.8 g	NaCl
0.3 g	$NaHCO_3$
1.58 g	$Na_2HPO_4 . 2 H_2O$
0.292 g	glutamine
1 mg	*p*-aminobenzoic acid
0.1 mg	D-biotin
3 g	glucose
5.9575 g	HEPES
0.11 g	sodium pyruvate
0.01 g	phenol red Na^+ salt
2 mg	inositol
0.1 mg	riboflavin
1 mg	thiamine HCl
1 mg	nicotinamide
1 mg	D-calcium pantothenate
1 mg	folic acid
1 mg	choline chloride
1 mg	pyridoxal HCl
0.0224 g	methionine
0.0706 g	valine
0.0153 g	tryptophan
0.0797 g	leucine
0.0543 g	tyrosine
0.0787 g	isoleucine
0.0495 g	phenylalanine
0.0629 g	histidine HCl
0.1096 g	lysine
0.0715 g	threonine
0.036 g	cystine
0.1896 g	arginine HCl
0.0089 g	alanine
0.0132 g	asparagine
0.0075 g	glycine
0.0105 g	serine
0.0133 g	aspartic acid
0.0147 g	glutamic acid
0.0115 g	proline

Schneider's Drosophila Medium, 1l

0.25 g	glycine
0.4 g	arginine
0.4 g	apspartic acid
0.06 g	cysteine
0.1 g	cystine
0.8 g	glutamic acid
1.8 g	glutamine
0.4 g	histidine
0.15 g	isoleucine
0.15 g	leucine
1.65 g	lysine HCl
0.8 g	methionine
0.15 g	phenylalanine
1.7 g	proline
0.25 g	serine
0.35 g	threonine
0.1 g	tryptophan
0.5 g	tyrosine
0.3 g	valine
0.5 g	β-alanine
0.6 g	$CaCl_2$
1.807 g	$MgSO_4$
1.6 g	KCl
0.45 g	KH_2PO_4
0.4 g	$NaHCO_3$
2.1 g	NaCl
0.7 g	Na_2HPO_4
0.2 g	α-ketoglutaric acid
2 g	D-glucose
0.1 g	fumaric acid
0.1 g	malic acid
0.1 g	succinic acid
2 g	trehalose
2 g	yeastolate

PBS, 1l

8.0 g	NaCl
0.2 g	KCl
1.42 g	Na_2HPO_4
0.24 g	KH_2HPO_4

STE buffer for digitonin fractionation

250 mM	sucrose
25 mM	Tris-HCl pH7.4

1mM	EDTA
150	mM NaCl
1mM	DTT

4x SDS Loading Buffer for Western Blot

4ml	100% glycerol
2.4 ml	1M Tris pH 6.8
0.8 g	sodium dodecyl sulfate
3.1 ml	H_2O
0.5 ml	β-mercaptoethanol

bromphenol blue

Transfer buffer for WB

3.03 g	Tris
14.4 g	glycine
200 ml	methanol
800 ml	H_2O

3 Metabolomic comparison of promastigote and amastigote *Leishmania donovani*

3.1 Introduction

One of the persisting questions in *Leishmania* biology is that of how transformation of promastigotes into amastigotes occurs. It is well established that increased temperature and decreased pH trigger the transformation, but the underlying molecular mechanisms are unknown (Alcolea et al., 2010a; Debrabant et al., 2004; Pan et al., 1993; Saar et al., 1998). In addition, the extent to which the two life stages are physiologically distinct remains unclear. Numerous investigators have performed various high-throughput studies, which collectively are contributing to create a comprehensive explanation.

Transcriptome analysis by Akopyants and colleagues (2004), detected only about 1% of nuclear DNA as being expressed differentially between *L. major* promastigotes, metacyclics, and amastigotes isolated from macrophages. The authors also analysed transcription of kinetoplast maxicircles, which encode genes for several subunits of complexes of the respiratory chain, and this was found to be increased in amastigote and metacyclic stages (Akopyants et al., 2004). Another study found that changes in expression of particular respiratory chain subunits (including those encoded in the nucleus) were not consistent between separate complexes and stages (Alcolea et al., 2010b). Microarray analysis of *L. mexicana* showed only 17 genes to be expressed differentially between promastigotes and axenic amastigotes, but 288 (3.5% of all genes analysed) when comparing promastigotes with lesion derived amastigotes (Holzer et al., 2006). Another study compared *L. major* stages by a cDNA microarray approach and identified 430 stage-specific genes, 35% of which were increased in amastigotes, includng ribosomal proteins, heat shock proteins and surface antigens (Almeida et al.,

2004). Thus, the authors concluded that there was high degree of gene expression regulation in that stage. DNA microarray assays focused on *L. major* differentiation from promastigotes to metacyclics detected 15% of DNA to change significantly, but the magnitude of the changes was low, since only 1% (corresponding to 108 genes) were upregulated two times or more, and 0.14% (13 genes) were downregulated (Saxena et al., 2003). DNA oligonucleotide genome microarrays representing 8,160 genes were used to analyse mRNA expression profiles of *L. major* promastigotes and lesion derived amastigotes. In general, a low degree of differential mRNA expression was detected, 1.5% in each stage corresponding to approximately 120 genes (Leifso et al., 2007). Genes upregulated in amastigotes were associated with metabolism, translation, and a substantial number encoded hypothetical proteins. Promastigotes harboured higher levels of tubulins, leishmaniolysin, glucose transporters, heat shock proteins, or SHERP (Leifso et al., 2007). Microarrays were used to investigate a diverse range of sample types: amastigote *L. major* from mice footpads, *L. infantum* from spleen and *L. braziliensis* from RAW 246.7 macrophages, but only a small number of the target genes were transcribed differentially (Depledge et al., 2009). Very few differences were detected when *L. major* amastigotes grown in two different mice strains were analysed, suggesting that transcription does not change in response to the host's immune system (Depledge et al., 2009). Global RNA expression profiling was performed to compare *L. infantum* amastigotes cultivated axenically or inside macrophages, and major differences were detected in fatty acid metabolism, intracellular transport, membrane vesicular fusion, and proteolysis (Rochette et al., 2009). 12.5% of genes were differentially expressed between promastigotes and amastigotes, when fold changes higher than 1.7 were considered, whilst the proportions of up- and down-regulated genes were the same (Rochette et al., 2009). The genes increased in promastigotes were, for example, associated with translation, whereas in amastigotes it was amastins, A2 protein, SHERP, fatty acid and trypanothione metabolism that increased (Rochette et al., 2009), which corresponds with other studies and later metabolomic work on amastigotes by Saunders (2014). Similar results were obtained in a study focused on differentiation of promastigotes into amastigotes under different conditions, where amastigotes upregulated expression of amastin-like and hypothetical proteins or trypanothione reductase and downregulated numerous nucleotidases, glucose transporters, two glycolytic enzymes and the heme biosynthetic pathway (Alcolea et al., 2010a).

A proteomic analysis of *L. infantum* detected about 6% of proteins to be upregulated in promastigotes, whereas 12% were up in amastigotes, but only 220 proteins were detected in total (McNicoll et al., 2006). The proteins increased in the amastigote stage were classified mostly as heat shock proteins, involved in stress response and protein folding. The correlation between mRNA and protein levels was poor, and the fold changes were higher at the protein than mRNA levels (McNicoll et al., 2006). Another proteomic analysis of *L. infantum* promastigotes and amastigotes detected 91 proteins in total, 72% of which were constitutively expressed, 8% (7 proteins) elevated in amastigotes, and 20% (18 proteins) increased in promastigotes, including paraflagellar rod components, leishmaniolysin and enolase (Leifso et al., 2007). A 2D gel proteomic study comparing promastigote and amastigote *L. donovani* detected about 2,000 protein spots in total, 31 of which were specific for promastigotes, 65 increased during differentiation into amastigotes and 4 decreased (Bente et al., 2003). The stage specific proteins were classified mostly into groups related to stress response, cytoskeleton and cell membrane, energy metabolism, cell cycle and proliferation, and amino acid metabolism (Bente et al., 2003). Another study using the same technique on axenically differentiated *L. mexicana* visualised twice as many protein species in total, 47 of which were stage-specific and an additional 100 spots changed in intensity during differentiation (Nugent et al., 2004) .

Collectively, these studies consistently show a rather low degree of differentially expressed genes, approximately only 0.2 – 5% at the mRNA level (reviewed in Cohen-Freue et al., 2007). In addition, the stage specific genes are unique for each species, for example only a few common genes are differentially expressed when comparing *L. major* and *L. mexicana* (Cohen-Freue et al., 2007). Not a single gene was found to be upregulated in common between *L. major* and *L. mexicana* amastigotes, whereas 51 genes were common for promastigotes, including tubulins, calmodulins, and the paraflagellar rod proteins (Cohen-Freue et al., 2007). Alcolea and colleagues (2014) compared results of their differential expression study with previous data and concluded that 95% of upregulated genes were different, but they observed lower upregulation in amastigotes, consistent with other studies. The correlation between RNA and protein expression is low, the proteomic studies detected around 5 – 12% proteins showing differential expression between stages (Cohen-Freue et al., 2007). Most of the genes seem to be transcribed constitutively during the whole life cycle, which is expected given that transcription is polycistronic in trypanosomatids (Ivens et al., 2005). Even post-

transcriptional control, represented by mRNA stability and degradation (Clayton, 2014), however, appears to play a relatively minor role in distinguishing phenotypic differences between different life cycle stages. Translational and post-translational regulation of proteins therefore may play major roles in determining phenotypes of the respective stages.

Comparing the outcomes from the various studies needs to be carried out with some caution since many aspects of the methods differ. On the other hand, it should be possible to draw general conclusions for the major changes determining the respective stages. Whereas some of the studies used freshly differentiated amastigotes, others used established cultures, and it is unknown how different or similar they are. Further, the specific methodology, statistics and its stringency applied plays a crucial role for the final outcome and data interpretation.

The knowledge and understanding of amastigote metabolism progressed substantially with the publication of work by Saunders and colleagues (2014), who performed GC-MS metabolomics on different life cycle stages of *L. mexicana*. They focused on the major trends of carbon metabolism in amastigotes when compared to promastigotes and coined the term the 'stringent metabolic response' to describe it. Compared to promastigotes, consumption of glucose and amino acids was decreased as well as production of organic acids and other metabolic end products. Fatty acid utilisation by β-oxidation was increased and these fuelled the TCA cycle, which is repressed in cultured promastigotes (Saunders et al., 2014). The cells were much more sensitive to inhibition of aconitase of the TCA cycle, suggesting that oxidative phosphorylation plays a more important role in amastigotes (Saunders et al., 2014). These data correspond with results from several transcriptomic analyses, which reported general downregulation of gene expression in amastigotes, and drop in expression of glucose transporters and some other carbon metabolism enzymes (Alcolea et al., 2010b, 2014; Holzer et al., 2006; Leifso et al., 2007).

3.2 Aims

- Prepare metabolomics samples from *L. donovani* promastigotes, axenic amastigotes, and splenic amastigotes
- Analyse obtained LC-MS metabolomics data with focus on comparison of the two types of amastigotes

3.3 Results

Although numerous transcriptomic studies have been performed, focusing on differences between the individual *Leishmania* life stages, they do not provide satisfactory and intuitive explanations for the diversity of phenotypes that distinguish life cycle stages (reviewed in Cohen-Freue et al., 2007). More information was obtained by proteomics, but metabolomics may offer a superior approach for this question. Of all the omics techniques it is the one closest to the final phenotype, and there is a good example represented by the metabolomic work by Saunders and colleagues (2014), which provided lot of new and concise information.

Thanks to collaboration with Gerald Spath and Pascale Pescher from the Institut Pasteur in Paris, we were able to prepare metabolomic samples from *L. donovani* amastigotes isolated from spleen of infected hamsters. In addition, we prepared samples from axenically cultured amastigotes and promastigotes and analysed them by LC-MS metabolomics. In this chapter, I present metabolomics data comparing these three sample groups. Since these cells differ significantly in their size (Pescher et al., 2011), protein content was measured and the metabolomic data were normalised per unit of intracellular protein.

A general overview of the data shows that the three sample groups are separated and based on principal component analysis (PCA) that the two amastigote groups are closer to each other than either is to promastigotes (Fig 3.1). The PCA plot shows that one of the splenic amastigote samples is separated from the other three, which are positioned close to all the axenic amastigote samples (Fig 3.1A). Promastigotes are further apart but they are barely distinguished from axenic amastigotes based on principal component 1, represented by the *x* axis.

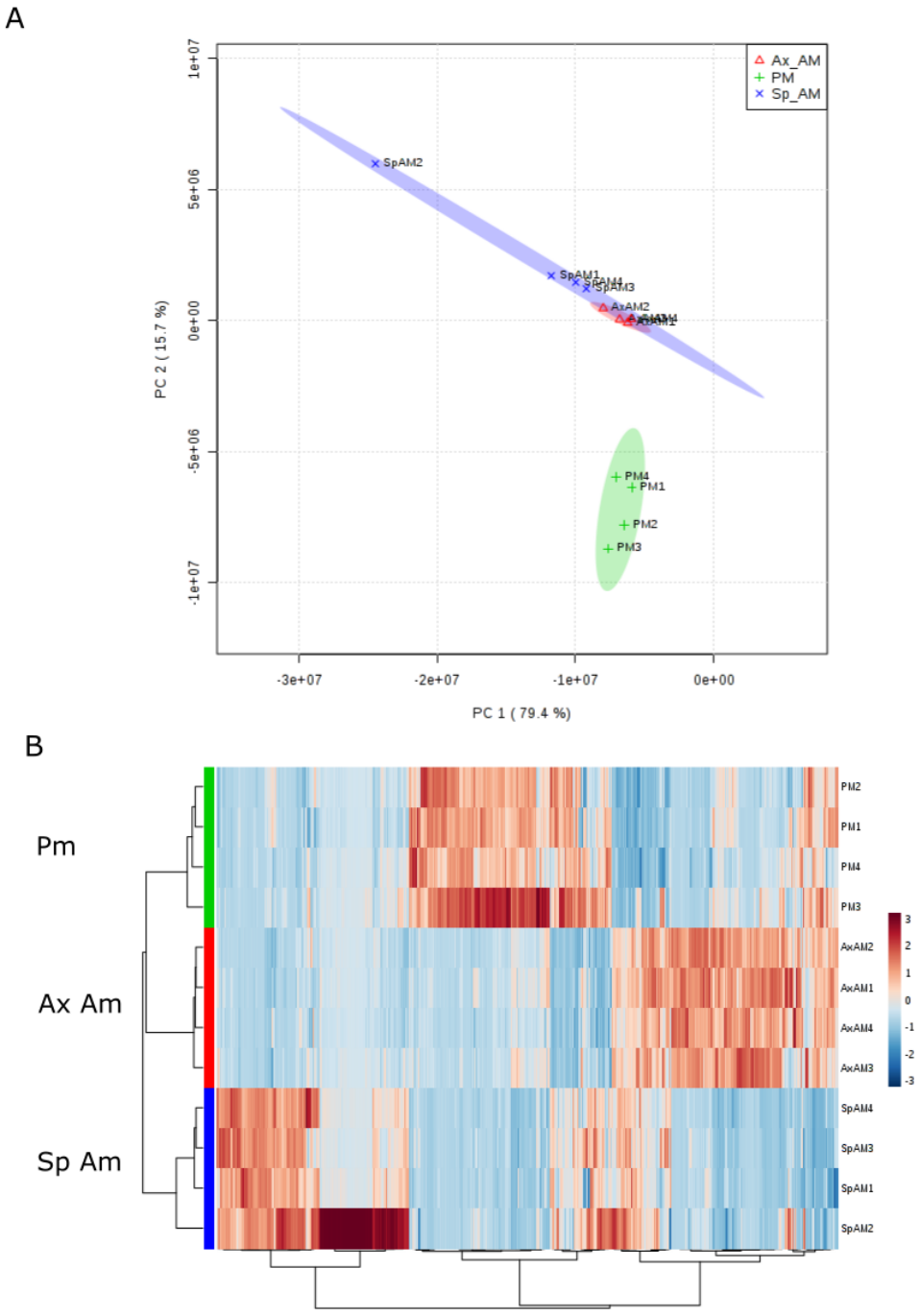

Figure 3.1. Overview of the LC-MS metabolomic data comparing L. donovani axenic amastigotes, splenic amastigotes and promastigotes. A – PCA plot, colour ellipses indicate 95% confidential interval; B – A heat map based on all the metabolites identified, the bar on the right indicates fold change; Pm – promastigotes, Ax Am – axenic amastigotes, Sp Am – splenic amastigotes. Graphs were made using MetaboAnalyst.

The most plausible explanation for the splenic amastigote outlier sample is contamination with host cells. However, no obvious contaminants (i.e. mammalian specific metabolites) were found in the metabolite list, although a group of metabolites was found exclusively in splenic amastigotes, but they were not elevated in the outlier sample. For example several fatty acids are substantially increased in that sample.

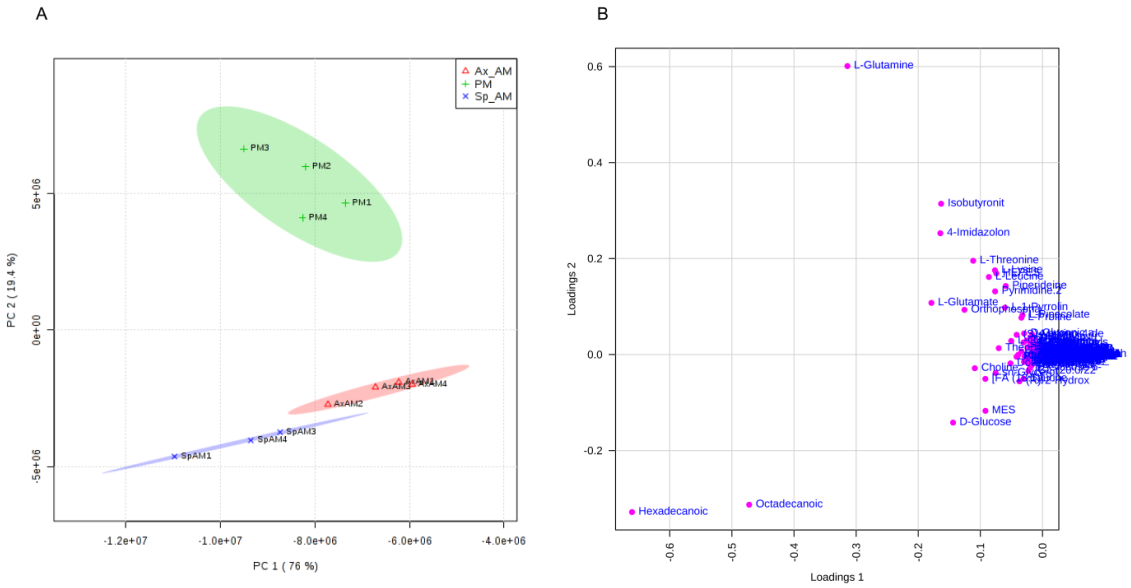

Figure 3.2. PCA plot and corresponding loading plot. A – PCA plot without Sp Am2 outlier; B - Loading plot for the PCA plot shown in A. Graphs were made using MetaboAnalyst.

I obtained an additional PCA plot, this time excluding the single splenic amastigote outlier sample (Fig 3.2A). Positions of the samples are only slightly changed relative to the previous PCA plot (Fig 3.1A), but the 95% confidence regions of amastigotes are contained and do not overlap. The loading plot for this PCA plot is shown in Fig 3.2B and the metabolites mostly determining separation of principal components (PC) 1 and 2 are listed in Appendix A5. Metabolites appearing among the top 20 important for separation of both PC 1 and PC 2 are hexadecanoic acid, octadecanoic acid, glucose, MES (probably a contaminant from the medium), octadec-9-enoic acid, glycerol 3-phosphate, and choline. Other fatty acids and amino acids are represented substantially too.

Visualisation of the total metabolomic profile on a heat map confirms that one of the splenic amastigote samples is substantially different from others (Fig 3.1B). Each of the groups is clearly separated, but a substantial group of metabolites similar between any two groups is distinguishable (in the left part of the heat map for promastigotes and axenic amastigotes, in the middle for both amastigote groups, and in the right part for promastigotes and splenic amastigotes). Prior to sample extraction, promastigotes were cultured in M199 medium with 10% FCS and additional supplements, axenic amastigotes in RPMI-1640 medium with 20% FCS and added amino acids and vitamins, and splenic amastigotes were purified directly from the spleen into PBS. Hence, the overall profile shows that the metabolomics reflects truly intracellular metabolism, with the environment or medium used for cultivation playing a minor role.

I focused further on comparison between axenic and splenic amastigote cells. Metabolites changing the most between axenic and splenic amastigotes are listed in Tab 3.1, (regardless of the change relative to promastigotes). On the other hand, metabolites indicating the same trend in both amastigote groups are listed in Tab 3.2. Compounds identified as glycogen and cellopentaose are sugar polymers and probably represent mannogen in *Leishmania*. Altogether, it is difficult to draw clear conclusions from this data, the metabolites represented do not indicate any specific pathway being clearly similar, or diverse between the two types of amastigotes.

formula	**putative identification**	**relative abundance**		
		PM	Ax AM	Sp AM
C5H8O4	2-Acetolactate	1.00	**2.35**	**165.45**
C10H19N3O5	Lys-Asp	**0.00**	**0.00**	**6.75**
C5H9NO5	L-erythro-4-Hydroxyglutamate	**0.00**	**0.00**	**3.01**
C6H10O7	D-Glucuronate	1.00	**2.34**	**96.62**
C5H8O6	2-Dehydro-D-xylonate	**0.00**	**0.00**	**55.26**
C6H13O8P	L-Fucose 1-phosphate	**0.00**	**0.00**	**7.28**
C5H11NO	Betaine aldehyde	**0.00**	**0.38**	**38.29**
C25H44NO7P	[PE (20:4)] 1-(5Z,8Z,11Z,14Z-eicosatetraenoyl)-sn-glycero-3-phosphoethanolamine	1.00	0.80	**130.72**
C5H6O4	2,5-Dioxopentanoate	1.00	**0.22**	**10.19**
C6H6O6	L-Dehydroascorbate	**0.00**	**0.00**	**54.29**
C20H25N7O6	5-Methyltetrahydrofolate	**0.00**	**3.35**	**0.00**
C6H8O4	2,3-Dimethylmaleate	1.00	**22.25**	**4.16**
C4H4O2	3-Butynoate	**0.00**	**1.65**	**101.74**
C2H7NO3S	Taurine	1.00	1.33	**288.08**
C15H24O	2-trans,6-trans-Farnesal	1.00	**3.85**	0.52
C5H8O5	**(R)-2-Hydroxyglutarate**	1.00	1.25	**28.11**
C4H9NO4	4-Hydroxy-L-threonine	**0.00**	**0.00**	**10.13**
C4H7NO	2-Pyrrolidinone	1.00	**20.04**	0.96
C5H6O5	Methyloxaloacetate	**0.00**	**0.00**	**17.73**
C20H18O9	1-Hydroxy-2-(beta-D-glucosyloxy)-9,10-anthraquinone	1.00	0.71	**42.80**

Table 3.1. Metabolites showing the biggest changes detected between the two amastigote groups. The identifications are only putative based on mass, metabolites highlighted in bold were confirmed with standards.

formula	**putative identification**	**relative abundance**		
		PM	Ax AM	Sp AM
C18H13NO4	Stealthin C	0.00	119.92	31.60
C24H42O21	Glycogen	1.00	34.74	20.70
C30H52O26	Cellopentaose	0.00	28.63	10.26
C43H81O13P	[PI (16:0/18:1)] 1-hexadecanoyl-2-(9Z-octadecenoyl)-sn-glycero-3-phospho-(1'-myo-inositol)	0.00	27.87	16.14
C2H6O4S	2-Hydroxyethanesulfonate	1.00	19.69	21.61
C17H29N5O6	Asn-Leu-Gly-Pro	1.00	9.33	4.85
C24H46O2	[FA (24:0)] 15Z-tetracosenoic acid	1.00	8.65	30.08
C4H8O3	4-Hydroxybutanoic acid	1.00	6.36	5.69
C10H18N4O6	N-(L-Arginino)succinate	1.00	5.45	13.56
C5H4N4O3	Urate	0.00	5.37	3.35
C6H11NO2	L-Pipecolate	1.00	0.00	0.00
C5H11NO4	4-amino-4-deoxy-L-arabinose	1.00	0.00	0.02
C28H40N10O5S	Arg-Met-Trp-His	1.00	0.00	0.00
C7H15NO3	**L-Carnitine**	1.00	0.00	0.00
C21H32O4	11beta,21-Dihydroxy-5beta-pregnane-3,20-dione	1.00	0.00	0.00
C6H13NO3	N-hydroxyisoleucine	1.00	0.00	0.00
C6H13NO2	L-Isoleucine	1.00	0.00	0.00
C8H12N2O2	Pyridoxamine	1.00	0.00	0.00
C14H20N6O4S2	Ovothiol A disulfide	1.00	0.00	0.00
C9H17NO8	Neuraminic acid	1.00	0.00	0.00

Table 3.2. Metabolites showing similar changes in axenic and splenic amastigotes relative to promastigotes. The identifications are only putative based on mass, metabolites highlighted in bold were confirmed with standards.

3.3.1 Amino acids

Probably the most striking change in the whole dataset is a general drop in amino acid levels in amastigotes. Basically all of the amino acids decreased substantially in both amastigote types as can be viewed in the total comparison (Fig 3.3).

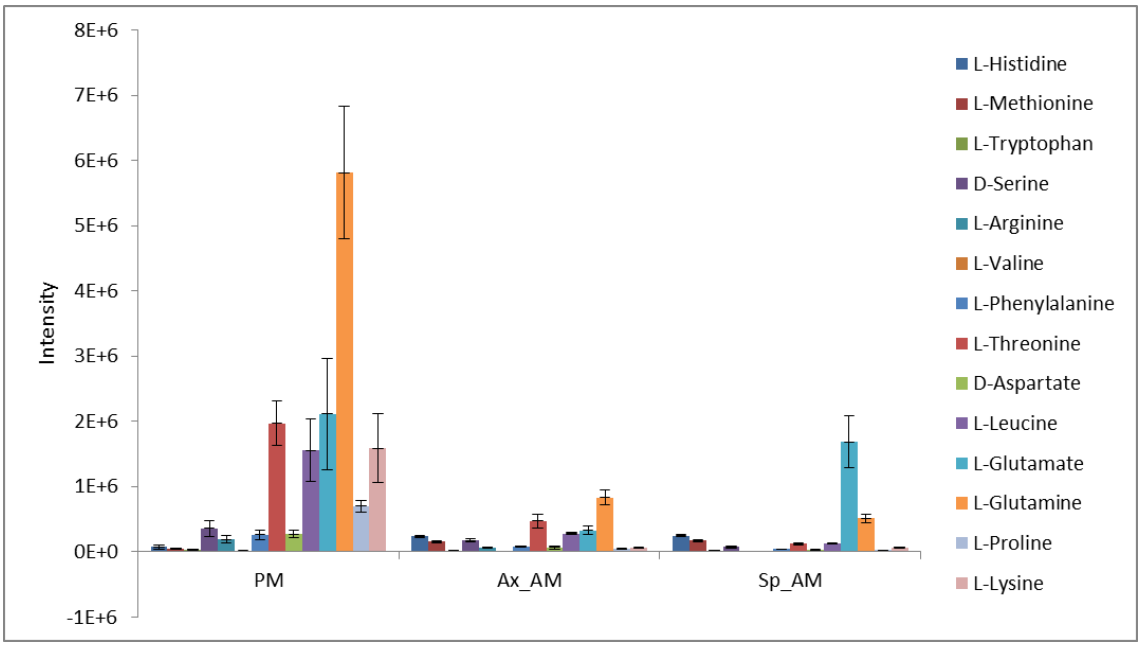

Figure 3.3. Relative levels of all the amino acids detected by LC-MS. PM – promastigotes, Ax_AM – axenic amastigotes, Sp_AM – splenic amastigotes.

In almost all cases, amino acid levels are decreased to the same extent in both axenic and splenic amastigotes when compared to promastigotes. One group of amino acids is decreased around ten fold in both types of amastigotes compared to promastigotes, including glutamine, proline, leucine, and lysine. About a four-fold decrease was observed for threonine, phenylalanine, arginine, and aspartate. In both amastigote groups, tryptophan reaches levels half those of promastigotes. Glutamate is decreased six fold in axenic amastigotes, but in splenic amastigotes returned to the same level as in promastigotes. Serine is decreased two fold in axenic, and five fold in splenic amastigotes, respectively. Two amino acids, histidine and methionine, are three fold increased in both types of amastigotes (Fig 3.4).

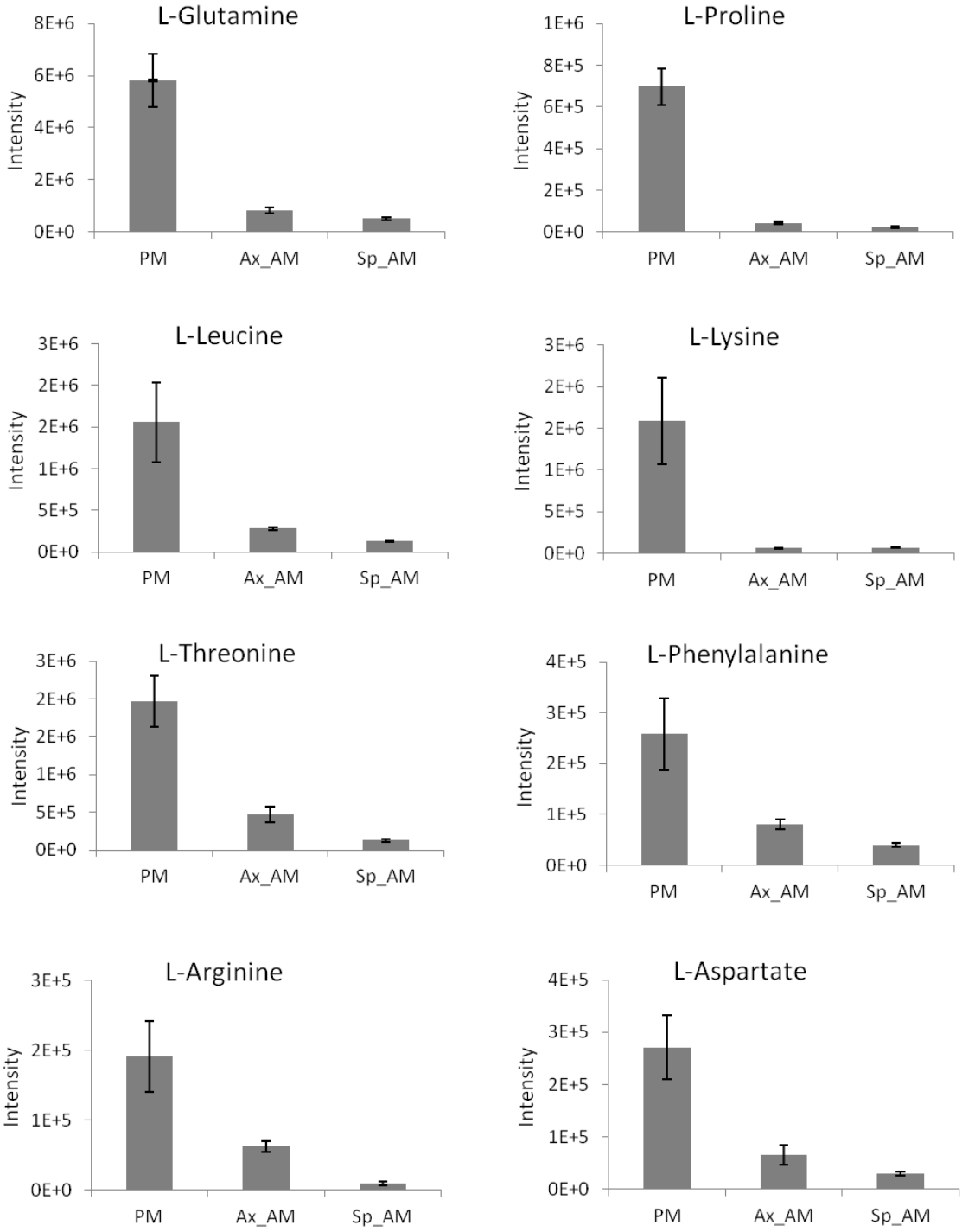
L-Glutamine
Intensity
8E+6
6E+6
4E+6
2E+6
0E+0
PM
Ax_AM
Sp_AM
L-Proline
Intensity
1E+6
8E+5
6E+5
4E+5
2E+5
0E+0
PM
Ax_AM
Sp_AM
L-Leucine
Intensity
3E+6
2E+6
2E+6
1E+6
5E+5
0E+0
PM
Ax_AM
Sp_AM
L-Lysine
Intensity
3E+6
2E+6
2E+6
1E+6
5E+5
0E+0
PM
Ax_AM
Sp_AM
L-Threonine
Intensity
3E+6
2E+6
2E+6
1E+6
5E+5
0E+0
PM
Ax_AM
Sp_AM
L-Phenylalanine
Intensity
4E+5
3E+5
2E+5
1E+5
0E+0
PM
Ax_AM
Sp_AM
L-Arginine
Intensity
3E+5
2E+5
1E+5
0E+0
PM
Ax_AM
Sp_AM
L-Aspartate
Intensity
4E+5
3E+5
2E+5
1E+5
0E+0
PM
Ax_AM
Sp_AM

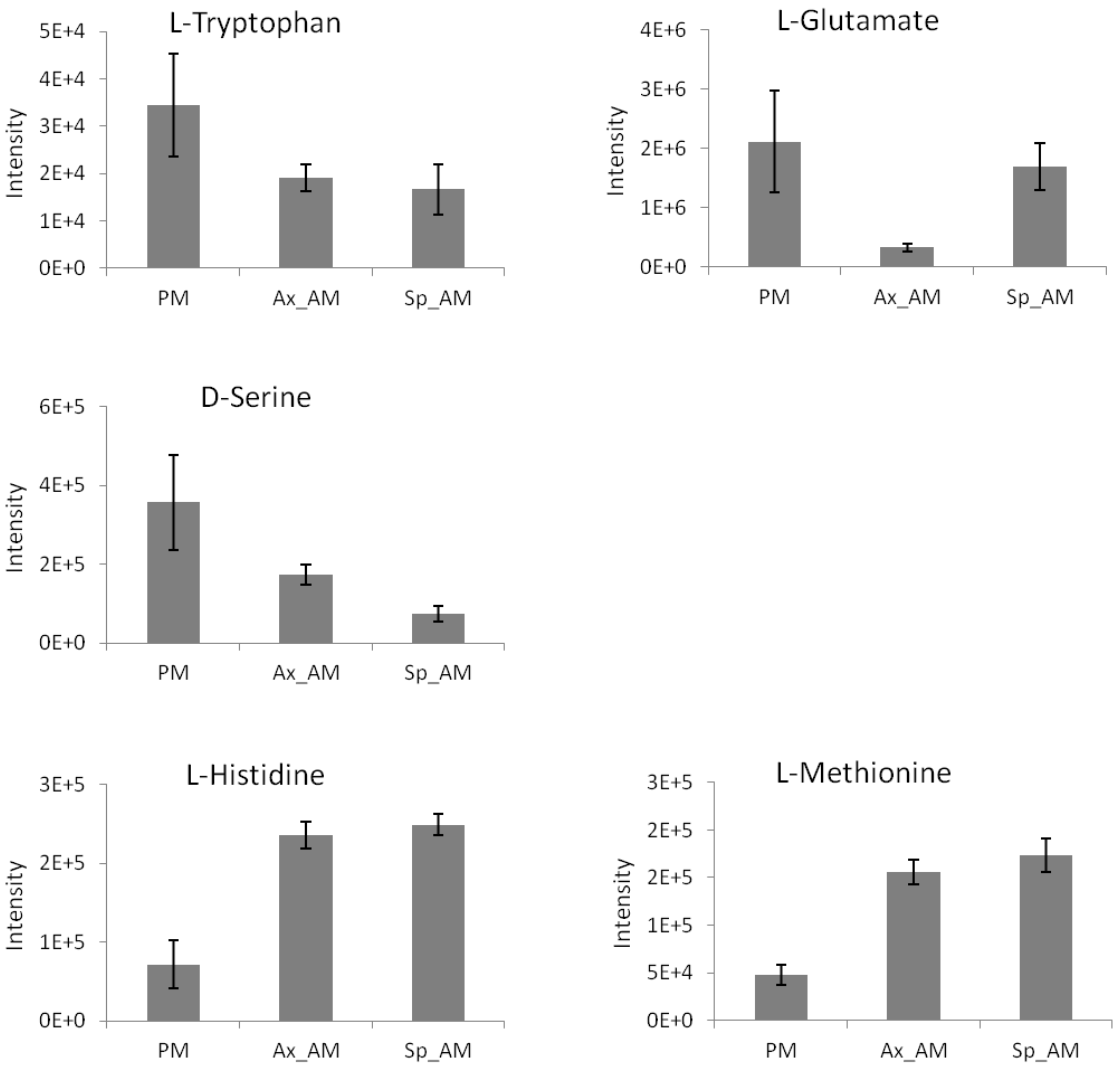

Figure 3.4. Relative changes in all amino acids detected by LC-MS. PM – promastigotes, Ax_AM – axenic amastigotes, Sp_AM – splenic amastigotes, error bars represent standard deviation, n = 4.

3.3.2 Carbon metabolism

Central carbon metabolism is especially important, because it involves glycolysis and the TCA cycle, the canonical major energy sources. From glycolysis, we detected glucose, G6P, PEP and pyruvate. Glucose and G6P are increased in both amastigote samples, while PEP is decreased, which may be interpreted as decreased flux through glycolysis, since the inputs at the top of the pathway are accumulated while the output at the bottom of the pathway is decreased (Fig 3.5). Pyruvate is 25 fold elevated in axenic amastigotes and two fold decreased in splenic amastigotes compared to promastigotes, which is very difficult to explain and interpret, and we cannot exclude some kind of artefact, however, the low amount of pyruvate present in the medium, comes only from FCS.

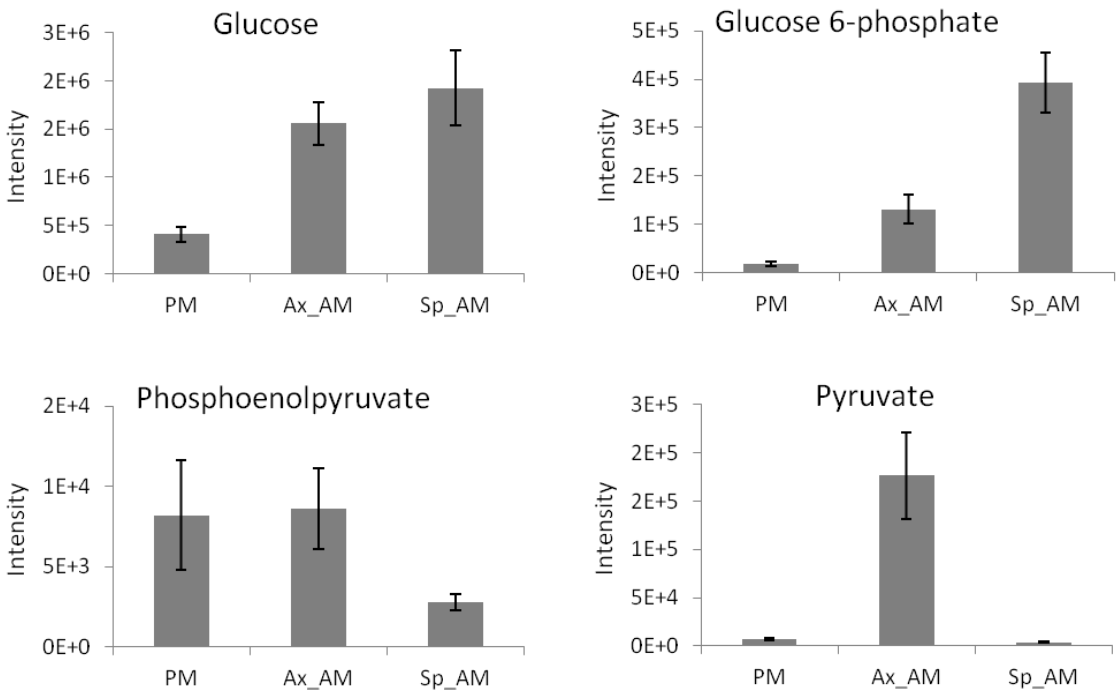

Figure 3.5. Relative changes in metabolites from glycolysis detected by LC-MS. PM – promastigotes, Ax_AM – axenic amastigotes, Sp_AM – splenic amastigotes, error bars represent standard deviation, n = 4.

Not many metabolites from the PPP were detected in this dataset. Ribose decreased to the detection limit in both amastigote samples, but R5P was not detected. S7P was detected and reaches the same levels in promastigotes and splenic amastigotes, but is two fold increased in axenic amastigotes (Fig 3.6). Three metabolites, possibly related to mannogen, were detected, corresponding to trimeric, tetrameric and pentameric hexose polymers, all of which are highly increased in both types of amastigotes (axenic even more than in splenic) (Fig 3.6).

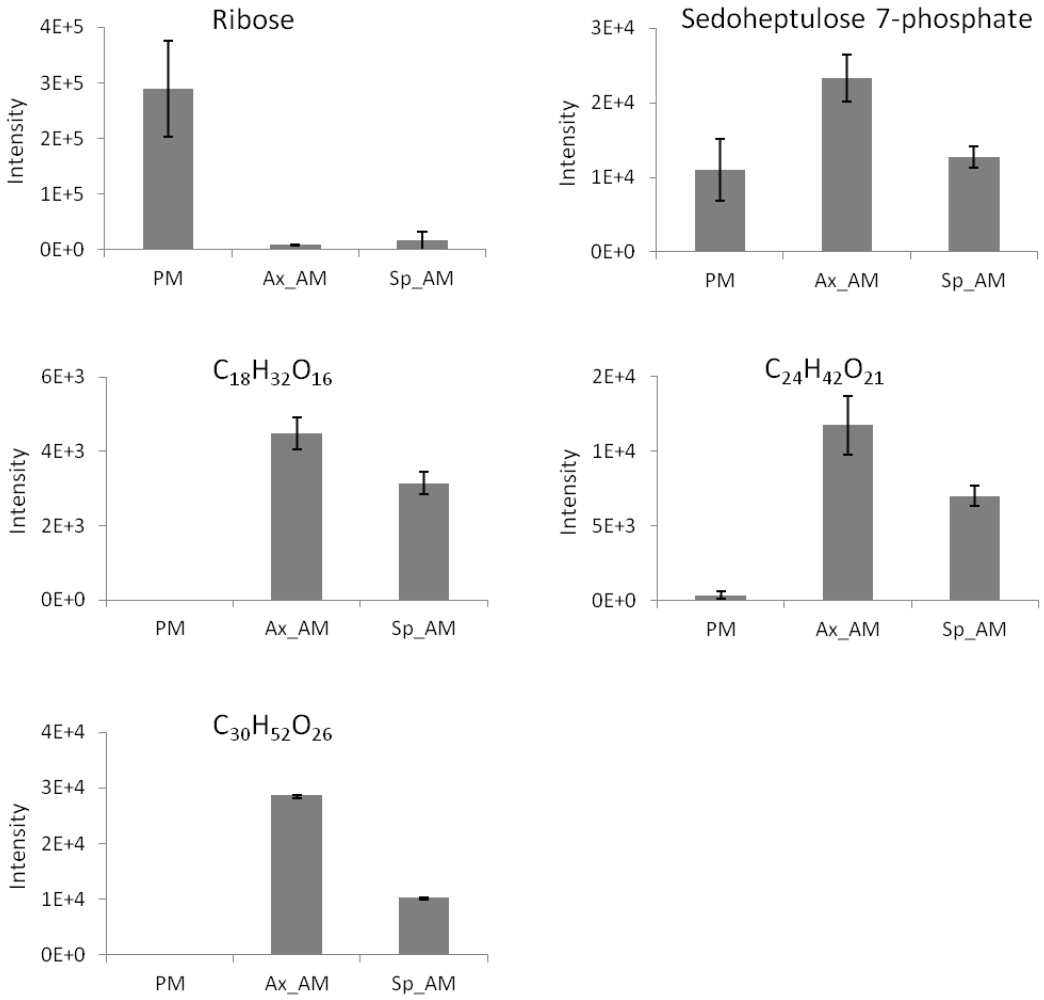

Figure 3.6. Relative changes in metabolites from the PPP and substitutes for mannogen detected by LC-MS. PM – promastigotes, Ax_AM – axenic amastigotes, Sp_AM – splenic amastigotes, error bars represent standard deviation, n = 4.

Both malate and succinate are decreased three fold in splenic amastigotes, which corresponds with the stringent metabolism phenotype, these organic acids being secreted as metabolic end products when metabolism is more profligate. In axenic amastigotes, malate was decreased two fold while succinate reached the same levels as in promastigotes (Fig 3.7). Two metabolites of the TCA cycle were detected, citrate and *cis*-aconitate. Both of them showed the same trend, i.e. a minor increase in axenic amastigotes and more than three-fold increased levels in splenic amastigotes (Fig 3.7).

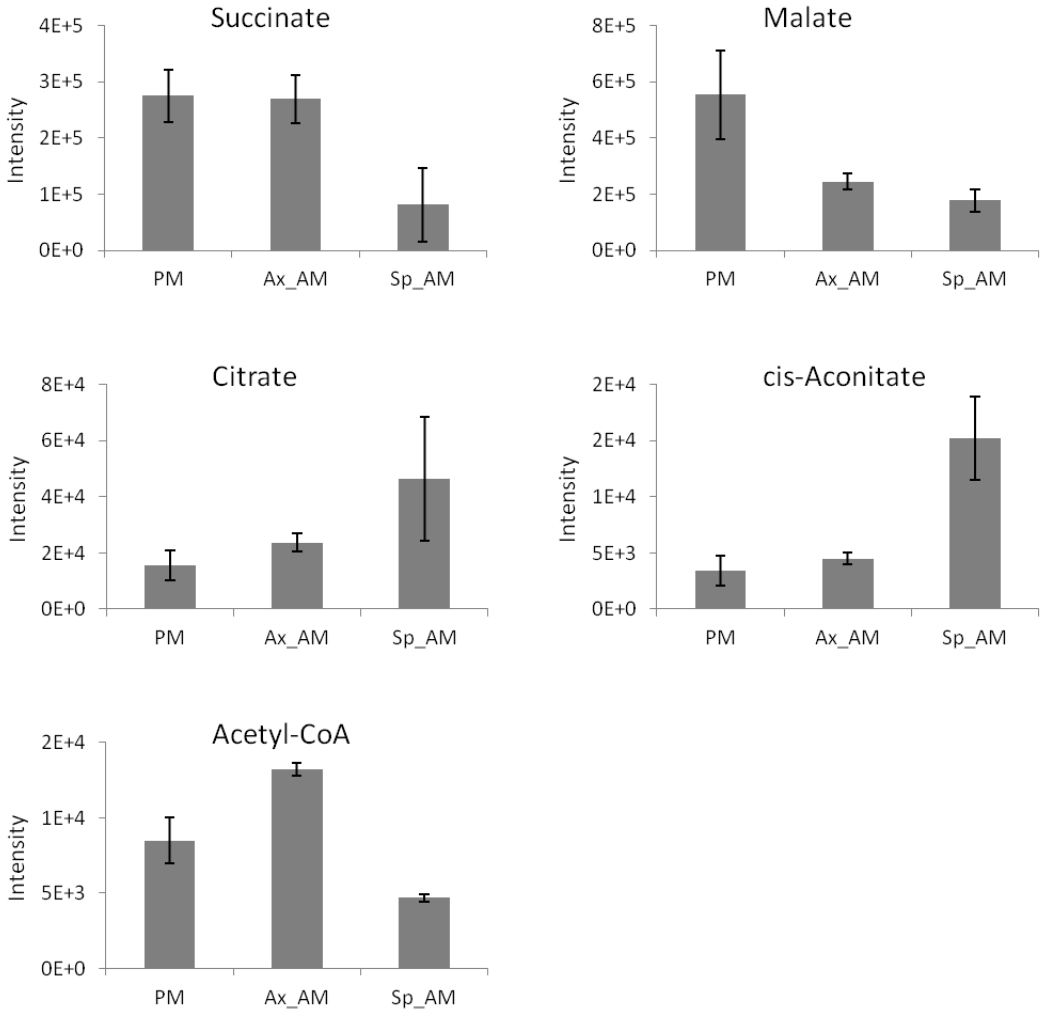

Figure 3.7 Relative changes in succinate, malate and metabolites from the TCA cycle detected by LC-MS. PM – promastigotes, Ax_AM – axenic amastigotes, Sp_AM – splenic amastigotes, error bars represent standard deviation, n = 4.

It was suggested that fatty acid degradation may play an important role in amastigote metabolism (Hart and Coombs, 1982; Saunders et al., 2014). Even though the metabolomic method used here is not optimal for fatty acid and other lipid identification (which resolve better using reverse phase chromatography), we can still obtain a general overview. Acetyl-CoA, the major intermediate of fatty acid degradation, which can be channelled into the TCA cycle, is slightly increased in axenic and decreased two fold in splenic amastigotes compared to promastigotes (Fig. 5.7).

The general overview of lipid metabolism, however, does not show any substantial change in these metabolites in amastigotes (Fig 3.8). A heat map constructed from metabolites classified as part of lipid metabolism does not indicate any striking increase in amastigotes (Fig 3.8 A). The sample from splenic amastigotes which stood as an outlier in considering the total metabolome also stands apart in the lipid analysis, indicating that lipids make a primary contribution to this discriminatory effect.

A volcano plot offers a different perspective on the data, considering metabolites in promastigote as equal to one and indicating relative changes in the two types of amastigote samples, and p-values associated with these changes (Fig 3.8 B). A substantial group of metabolites whose fold change is increased in splenic amastigotes fail to reach statistical significance ($p>0.1$). Whereas metabolites from axenic amastigotes seem to be distributed evenly on both sides of the plot from one, splenic samples are more abundant in the right half of the graph, indicating accumulation. These are mostly glycerolipids and derivatives of choline. However, most of these data points are associated with high p-values and may be possibly caused by the one odd sample with high levels of lipids, which causes increase with high variance and thus is not significant (after removing the outlier sample, the change is smaller but still not significant).

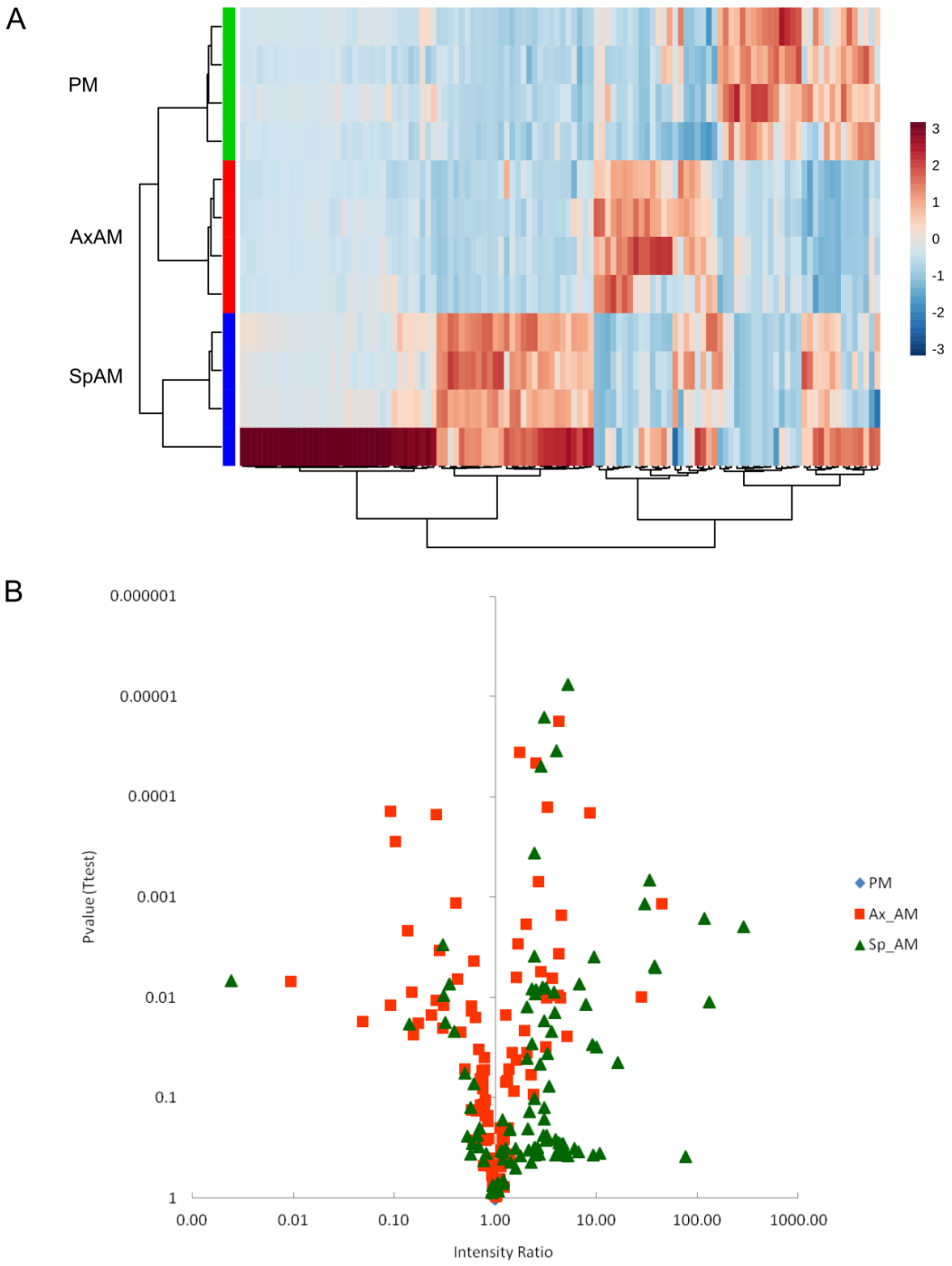

Figure 3.8. Overview of lipid metabolism. A- heat map based on metabolites classified as part of lipid metabolism, the bar on the right indicates fold change; B – volcano plot showing changes in amastigote samples relative to promastigotes. Pm – promastigotes, AxAm – axenic amastigotes, SpAm – splenic amastigotes. The heat map was created with MetaboAnalyst, using Euclidean distance measure and Ward clustering algorithm.

3.4 Discussion

The aim of this study was to gain insight into the status of different types of amastigotes (axenic versus spleen-derived) using metabolomic analysis. There has been debate as to whether axenic amastigotes are really representative of splenic amastigotes or whether, instead, they are more akin to promastigotes, only altered in morphology (Holzer et al., 2006; Pan et al., 1993; Pescher et al., 2011; Pral et al., 2003). As mentioned earlier, hindrances in working with axenic amastigotes include the risk of introducing artefacts during cell cultivation, their relatively large size, their production of promastigote stress factors and decreased virulence (Pescher et al., 2011). On the other hand, it is difficult to purify amastigotes from macrophages and maintain them pure and intact. The group of Gerald Spath established a protocol for purification of amastigotes from mammalian tissue with use of a mild detergent, saponin and gradient centrifugation (Pescher et al., 2011 and Methods 2.7). Hence, we used this protocol to prepare cells for metabolomic analysis. We cannot guarantee absolute purity of the obtained samples, and it was not possible to perform controls for contamination with mammalian tissue simultaneously (for example by Western blot analysis). Moreover, amastigotes take up small molecules present in their environment, and distinguishing these from components naturally present inside the parasites is impossible. In spite of these caveats, a general overview of the final data can be used as a quality control and seems robust (i.e. the splenic amastigote samples are not completely different and levels of individual metabolites are similar). In addition, the samples were not profoundly influenced by the culture medium, since splenic amastigotes were not kept in any medium and still cluster close to axenic amastigotes. To the best of my knowledge, direct metabolomic analysis of lesion derived amastigotes has not been performed to date, as Saunders (2014) cultivated the amastigotes in culture previous to the analysis.

The general analysis of the whole metabolomic dataset shows that the sample replicates group together well (except from one sample) and the respective groups clearly separate from each other, which is a good quality control of the analysis. Two different statistical methods give slightly different outputs. In the PCA plot the two different types of amastigotes are placed closer to each other with promastigotes further separated (Fig 3.1), whereas the heat map shows the three groups distinctly separated. A PCA is based on differences and the final outcome may be driven by a few species which change

dramatically. In contrast, a heat map provides visualisation of all the metabolites detected, hence both similar and different species are represented. Since it is difficult to make any conclusions based on these analyses only, especially if they give different results, I focused further on metabolites of central metabolism which we can match with standards, i. e. central carbon metabolism, amino acids.

The most prominent change in the dataset is observed for amino acids. With the exception of histidine and methionine, all of the amino acids were decreased in both types of amastigotes. Amastigotes probably consume amino acids to a much lesser extent than promastigotes, irrespective of their availability, since the medium for axenic culture is more rich (Methods 2.2.1). This corresponds with the observation that amastigotes have reduced capacity to scavenge glutamate and feed it into the TCA cycle (Saunders et al., 2014). Some of the amino acids show similar patterns and can be grouped together, but these groups do not reflect chemical properties and thus do not seem to be associated with specific transporters. mRNA for one putative amino acid transporter was found to be 2 fold decreased in promastigotes compared to amastigotes (Leifso et al., 2007). Two amino acid permeases were found among the genes whose RNA abundance was most decreased in amastigote *L. major* (Rochette et al., 2008), and one amino acid permease was downregulated in amastigote *L. infantum* (Alcolea et al., 2010b). On DNA microarrays, two different amino acid permeases were found to be upregulated and two others to be downregulated after transformation of promastigotes into amastigotes, leading to speculation that different transporters are used in each stage (Alcolea et al., 2010a). However, the substrate specificity of these permeases is unclear. There is no obvious explanation for the increase in histidine and methionine. Amino acid transporters of *Leishmania* are not well defined functionally and it is not known if, for example, they possess a broad spectrum transporter, common for histidine and methionine. A permease which can import both of these amino acids was found in yeast (Isnard et al., 1996) and for example, the eflornithine transporter TbAAT6 of *T. brucei* was proven to have low substrate specificity (Mathieu et al., 2014).

It is difficult to make any conclusions about the PPP, but since S7P is a metabolite specific for this pathway, it suggests that the flux is comparable in amastigotes and promastigotes. Considering that most of the metabolic pathways are decreased in amastigotes, we could say then that the PPP may be increased relative to other pathways,

which would be expected due to increased demand for NADPH in response to high oxidative stress inside macrophages. On the other hand, the GC-MS analysis of *L. mexicana* with labelled glucose did not identify relatively high levels of PPP intermediates (Saunders et al., 2014).

An interesting observation is the increased levels of *cis*-aconitate and citrate in amastigotes, suggesting increased flux through the TCA cycle. When labelled glucose was used for GC-MS metabolomics in promastigotes, metabolites from the TCA cycle were labelled less than from glycolysis, whereas in amastigotes the labelling was more similar in both pathways (Saunders et al., 2014). At the same time, amastigotes were shown to be more sensitive to inhibition of aconitase in the TCA cycle (Saunders et al., 2014). Different labelling patterns in TCA cycle metabolites were observed between promastigotes and amastigotes, and the data were interpreted to indicate that the full cycle operates in promastigotes, whereas an anabolic mode of operation dominates in the amastigote stage, providing intermediates for subsequent synthesis. The increase in the TCA cycle intermediates observed here agrees with an increase in TCA cycle flux in amastigotes over promastigotes.

Evidence is also accumulating that suggests increased fatty acid β-oxidation in *Leishmania* amastigotes when compared to promastigotes. Hart and Coombs (1982) observed that amastigotes consumed free fatty acids up to 10-fold faster than promastigotes. Activities of enzymes of fatty acid β-oxidation were shown to be higher in amastigotes than promastigotes, in contrast to glycolytic enzymes (Coombs et al., 1982). Oxidation of fatty acids was measured in promastigote cultures over time from rapidly growing to late stationary phase cultures, and later cultures consumed fatty acids faster, which may suggest a trend towards amastigotes (Blum, 1990). In proteomic analysis, enzymes of fatty acid catabolism were detected to be more abundant in amastigotes, specifically those of unsaturated fatty acid degradation (Paape et al., 2008). Utilisation of carbons from fatty acids in the TCA cycle was clearly proven in axenic amastigotes using GC-MS based metabolomics and, even though the signal was lower, it was still clear in lesion derived amastigotes (Saunders et al., 2014). Activity of both salvage and *de novo* biosynthesis of fatty acids was detected in lesion amastigotes, but the turnover was much slower than in other stages (Kloehn et al., 2015). Increased levels of some metabolites associated with lipid metabolism in amastigotes were detected in

this dataset, which may indicate increased lipid metabolism in total, but no clear conclusions can be made, the method used (LC-MS with ZIC pHILIC column) not being optimal for lipid analysis, because hydrophobic compounds elute prior to resolution in chromatography.

The so-called stringent metabolic response is the main characteristic of amastigote metabolism according to Saunders and colleagues (2014). From this data, a consistent decrease in amino acids, significantly decreased levels of succinate and malate, important metabolic end products, and a potential decrease in the glycolytic flux are traits clearly coherent with that hypothesis.

A few genes are consistently detected in the comparative transcriptomic and proteomic studies mentioned earlier. For example, heat shock proteins, stress response proteins, amastins and high number of hypothetical proteins are consistently overexpressed in amastigotes. However, these are not directly connected with metabolism and cannot be related to metabolomics data. On the other hand, downregulation of glucose transporters and some enzymes of carbon metabolism in amastigotes, as well as general downregulation of expression (Alcolea et al., 2010b) seems to be consistent with the stringent metabolic response. Most of the proteins specific for promastigotes, such as tubulins, calmodulins or components of the paraflagellar rod cannot be directly related to metabolism.

In general, my data show splenic amastigotes, axenic amastigotes and promastigotes as three distinct groups. They are consistent with the work by Saunders and colleagues (2014), and support the stringent metabolism hypothesis suggested for amastigotes. We provide an interesting novel observation of consistent and significant decrease in amino acid levels in amastigotes, regardless of their growth environment.

There are some indications (PCA, amino acids, mannogen) that at the metabolic level axenic amastigotes are more closely related to splenic amastigotes than they are to promastigotes, on the other hand, the total metabolome overview contradicts that and no profound conclusions can be made at this point. These results contribute to the so far scarce knowledge of amastigotes and give indications which may be considered in future studies using axenic amastigotes as a model. It would be desirable, but technically

challenging, to perform similar metabolomics analyses of metacyclic cells or promastigotes from sand flies in the future.

4 Utilisation of glucose and ribose by wild-type *Leishmania mexicana*

4.1 Introduction

As with most eukaryotic organisms, glucose is the major carbon source for trypanosomatids and the extent of its utilisation in metabolism was confirmed by metabolomics. When either bloodstream or procyclic form *T. brucei* cells were grown in the presence of U-^{13}C-glucose, a significant proportion of labelling was detected in glycolysis and the succinate fermentation pathway and the label was subsequently detected in remote metabolic branches (Creek et al., 2012, 2015). Similarly, promastigote *L. mexicana* incorporated carbons from glucose for example into nucleotides (Saunders et al., 2014). However, in some conditions, for example different anatomical locations within arthropod vectors, and in some *in vitro* conditions less glucose is available and additional substrates, including amino acids and other sugars can be present in abundance (Van Grinsven et al., 2009; Opperdoes and Coombs, 2007). Tsetse flies, for example, use proline as their primary energy source (Bursell et al., 1973) and procyclic African trypanosomes use this as their main source of energy, although they prefer glucose if available (Lamour et al., 2005). In the case of *Leishmania*, the sandfly host feeds primarily on plants and accumulates a variety of sugars. In *Leishmania* it is clear that glucose can be replaced by other substrates, since WT *Leishmania* can grow in absence of glucose (Burchmore et al., 2003), but it is unclear which sources can be used instead and what changes in metabolism are triggered.

The *Leishmania* genome encodes three separate genes for different glucose transporters. Concomitant deletion of all of them leads to a growth defect (Burchmore et al., 2003). The spontaneous expression of an alternative glucose transporter (LmGT4) from an

extrachromosomal element can relieve that growth defect (Feng et al., 2009). All three transporters can import glucose, fructose, mannose and galactose (Rodriguez-Contreras et al., 2007) but there seems to be some differential preference for other substrates among the transporters, for example glucose transporter 2 is more efficient for import of ribose (Naula et al., 2010). Expression of sugar and other nutrient transporters reflects substrate availability, as they are upregulated under substrate starvation conditions and depleted when substrate is in excess, offering means to achieve stable uptake of given substrates (Rodriguez-Contreras et al., 2015; Seyfang and Landfear, 1999). Utilisation of sugars by the PPP was previously assessed indirectly in *L. mexicana*, and it was calculated that 57% of radiolabelled ribose and 11% of glucose is incorporated into nucleic acids (Maugeri et al., 2003). The route for glucose incorporation is presumed to be through its conversion to R5P via the PPP. However, this value cannot be used as an estimate of the total PPP flux, because a substantial proportion of the PPP intermediates is channelled back into glycolysis.

In order to describe utilisation of glucose and ribose more clearly, I performed the following metabolomic experiment with differential labelling. WT *L. mexicana* promastigotes were grown in four different types of media where the primary sugar content varied: 1) 16 mM glucose, 50% of which was U-^{13}C-glucose, 2) 16 mM ribose, 50% of which was U-^{13}C-ribose, 3) 8 mM glucose, 50% of which was U-^{13}C-glucose and 8 mM ribose (unlabelled), 4) 8 mM ribose, 50% of which was U-^{13}C-ribose and 8 mM glucose (unlabelled) (Fig 4.1). Subsequently, the labelling patterns of PPP intermediates and other metabolites were analysed.

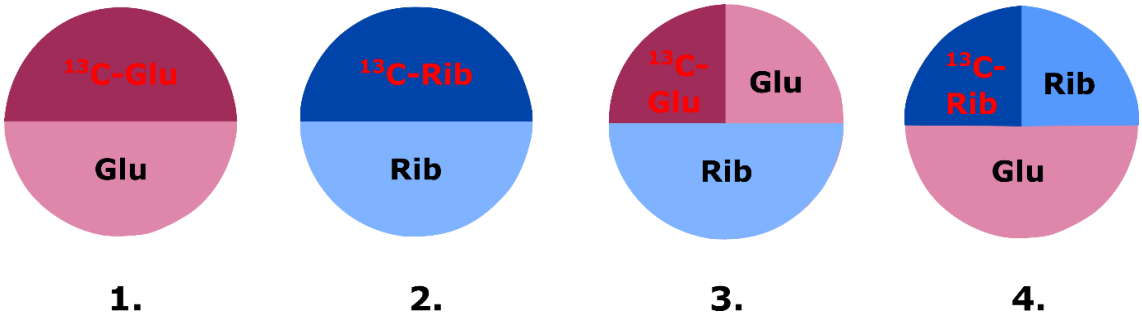

Figure 4.1. Scheme of sugar composition in media used in the four sample groups. ^{13}C-Glu = U-^{13}C-glucose , Glu = glucose, ^{13}C-Rib = U-^{13}C-ribose, Rib = ribose.

4.1.1 Aims

- Grow WT promastigote *L. mexicana* in medium containing 16 mM glucose, 16 mM ribose, or 8 mM glucose and 8 mM ribose. Subsequently prepare the same media containing 50% of the sugars U-^{13}C labelled.
- Prepare metabolomics samples
- Analyse the data with focus on differential utilisation of carbons depending in the type of medium

4.2 Results

Labelling in the separate metabolites was analysed, assessing the proportion of the specific number of carbons labelled in each group. That reflects the origin of the respective metabolites in relation to the labelled sugar source and points to differences that arise in response to the specific medium composition. Changes in the total abundance of respective metabolites were not assessed, unless interesting and significant. The natural abundance of ^{13}C is approximately 1% and this was not subtracted when considering the results, hence a background incorporation of ^{13}C into metabolites irrespective of the labelled source occurs. The intensity of this background depends on size of each metabolite, for example for metabolites composed of 5 carbons 5% of the metabolite will contain one labelled carbon (i.e. 5 x 1%).

The labelling pattern of glucose offers a proof of principle, since 40% of glucose is fully labelled in the cells where 50% of labelled glucose was supplemented in the media, this part decreased to 34% if ribose was supplied in addition (Fig 4.2, Tab 4.1). The labelling pattern looks completely different in hexose phosphates, however, where the labelling is largely similar in the first three sample groups, but minimal in cells which were grown in labelled ribose in the presence of glucose (Fig 4.2). This result indicates that if only ribose is available, it is converted to hexose phosphates to the same extent as glucose. However, when glucose is available too, glucose is preferred and ribose utilisation is massively diminished. The relatively high activity of TKT and TAL is clear since these enzymes shuffle the carbons creating a rich mixture of products containing different numbers of labelled carbon atoms, responsible for the colourful patterns depicted in Fig 4.2. The respective carbon content profile created when labelled ribose is used is similar to that when glucose is used, but shifted with respect to the number of labelled carbons, reflecting the carbon content of the sugar provided. The peaks detected for R5P were of lower intensity and quality, but we can still see a substantial proportion of fully labelled R5P, if the cells were grown in ribose solely, whereas the labelling is much lower in the other groups where glucose was present too (Fig 4.2).

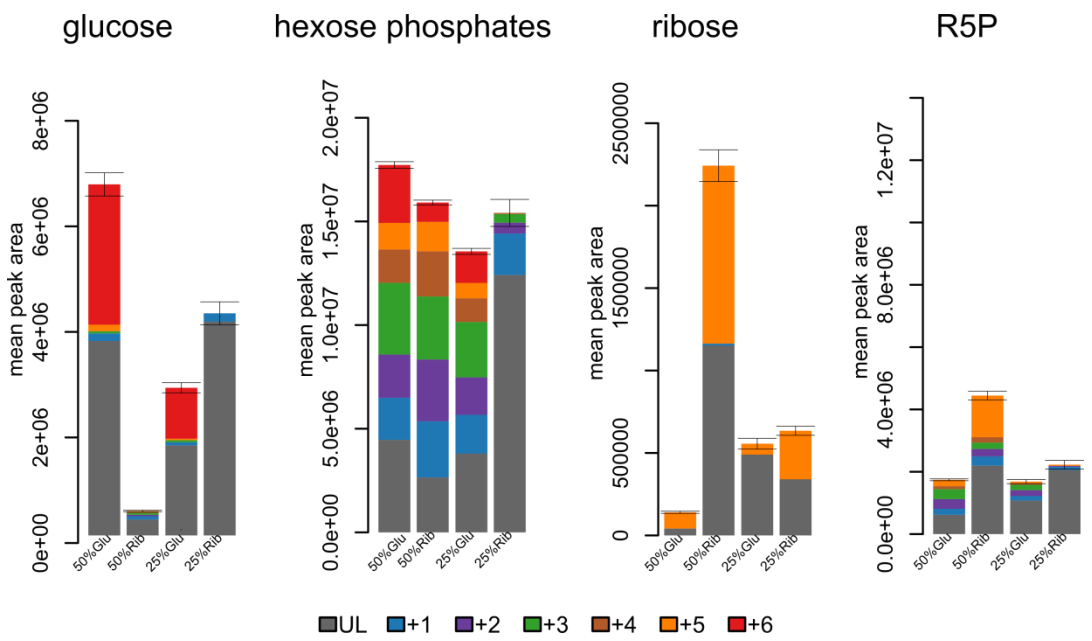

Figure 4.2. Labelling patterns of glucose, hexose phosphates (sum of G6P and F6P), ribose and R5P in the four respective groups described in Fig 4.1. The coloured boxes underneath indicates how colours correspond to number of carbons labelled, UL - unlabelled.

	50% Glu	**50% Rib**	**25% Glu**	**25% Rib**
U-^{13}C-glucose	40%	0	34%	0
U-^{13}C-ribose	70%	48%	12%	46%

Table 4.1. Quantification of fully labelled part of glucose and ribose.

Almost identical labelling patterns were obtained for pyruvate, succinate and malate (Fig 4.3). All of these metabolites have almost the same extent of labelling in the first three sample groups and only minimal labelling in the last group, grown in both sugars with labelled ribose, again indicative of ribose utilisation being suppressed if glucose is available. Pyruvate and succinate are slightly higher in the first group (Tab 4.2), supplied solely with glucose, and this difference is caused mostly by increase in the three carbon part. That indicates that more pyruvate is made directly from glucose through glycolysis, and it is turned into succinate in the succinate fermentation pathway (Saunders et al., 2011).

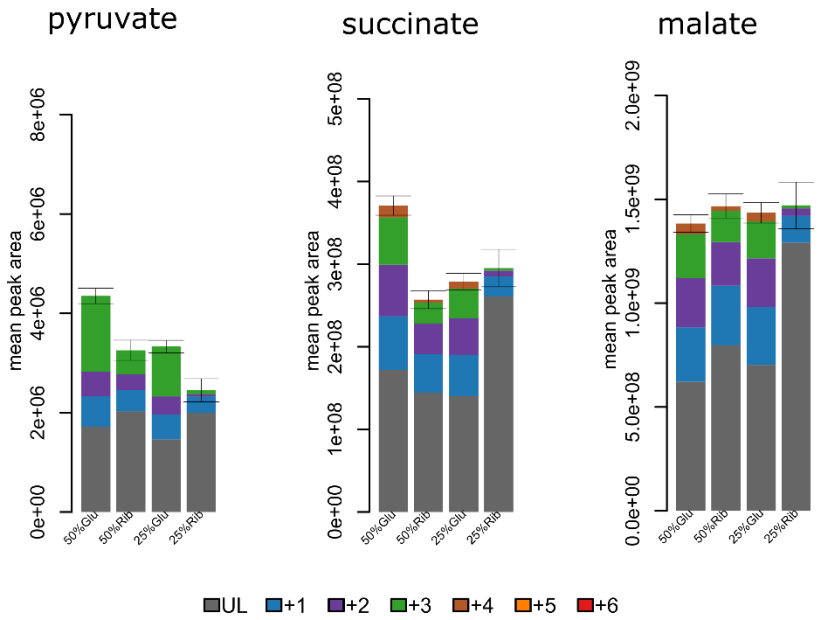

Figure 4.3. Labelling patterns of pyruvate, succinate and malate. The coloured boxes underneath indicates how colours correspond to number of carbons labelled, UL - unlabelled.

pyruvate	50% Glu	50% Rib	25% Glu	25% Rib
0 C labelled	40 %	62 %	44 %	82 %
1 C labelled	14 %	13 %	15 %	13 %
2 C labelled	12 %	9 %	11 %	2 %
3 C labelled	35 %	15 %	30 %	3 %
total abundance	1	0.75	0.76	0.56

Table 4.2. Quantification of labelling in pyruvate. Total abundance is given in values relative to WT.

From the TCA cycle metabolites, citrate, *cis*-aconitate and oxoglutarate were detected. The results of labelling look similar to the previous group of metabolites, since there is substantial and very similar labelling in the first three sample groups and almost nothing labelled in the last group (Fig 4.4).

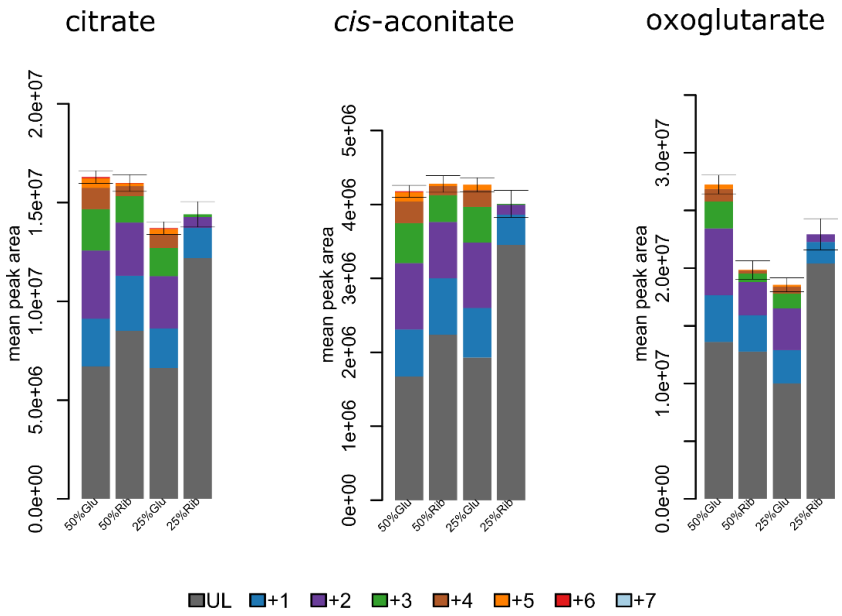

Figure 4.4. Labelling patterns of citrate, *cis*-aconitate, and oxoglutarate. Coloured boxes underneath indicates how colours correspond to number of carbons labelled, UL - unlabelled.

From the metabolites typical for the PPP, only S7P was detected with a peak shape allowing confidence in relative quantification across groups. The labelling pattern of S7P is intriguing. In the first group almost all of the metabolite is labelled from one, all the way to seven carbons, indicating that it comes exclusively from glucose and from no other source (Fig 4.5). Its total levels are the highest in the second group, grown in the presence of 16 mM ribose. The biggest parts are two and five carbons labelled, corresponding to its synthesis by TKT from 5 + 2 carbons. The total abundance is much lower in the third group and in contrast to the first group, labelling of six and seven carbons disappeared, which may be due to depletion of the signal below the detection limit. However, it suggests that S7P is synthesised from both the labelled glucose and unlabelled ribose. The total abundance is relatively high in the last group, but the labelling is very low, which contradicts results of the two previous groups. The proportions of all the respective parts are shown in Tab 4.3. E4P could not be detected, but O8P provided a substantial signal in the second group with high proportion of 5 carbons labelled, indicating synthesis from 5 + 3 carbons.

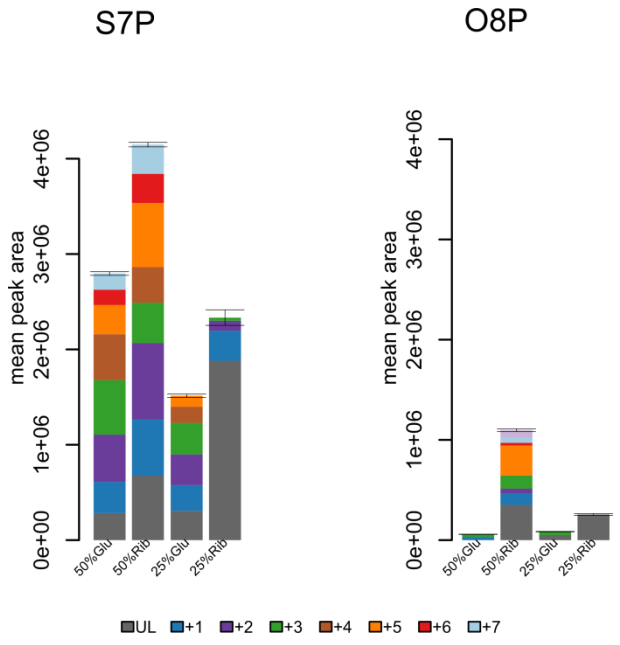

Figure 4.5. Labelling patterns of S7P and O8P. Coloured boxes underneath indicates how colours correspond to number of carbons labelled, UL - unlabelled.

S7P	50% Glu	50% Rib	25% Glu	25% Rib
0 C labelled	10 %	16 %	21 %	83 %
1 C labelled	12 %	14 %	18 %	14 %
2 C labelled	18 %	19 %	22 %	2 %
3 C labelled	21 %	10 %	22 %	0
4 C labelled	18 %	9 %	11 %	0
5 C labelled	11 %	16 %	6 %	0
6 C labelled	6 %	7 %	0	0
7 C labelled	3 %	7 %	0	0
total abundance	1	1.53	0.55	0.83

Table 4.3. Quantification of labelling in S7P. Total abundance is given in values relative to WT.

Metabolites in Fig 4.6 are listed as examples of nucleotide derived metabolites which incorporate R5P (additional examples are in Appendix A4). In some of the sample groups, a five carbon labelled part is of major significance. This part almost certainly represents the R5P part of the nucleotides originating directly from either of the sugars supplied. For example in the second group the 5 carbon labelled part represents 29% of adenosine monophosphate (AMP), 29% of adenosine triphosphate (ATP) and 26% of nicotinamide adenine dinucleotide (NAD^+) (Fig 4.6, Tab 4.4). In all of these compounds, the total labelling is the lowest in the fourth group (labelled ribose in the presence of unlabelled glucose) as was seen previously. However, a substantial proportion with 5 carbons labelled when labelled ribose is available indicates that if both sugars are available, ribose is still used directly for R5P synthesis. A substantial part (8.6%) of NAD^+ containing 10 labelled carbons reflects the presence of two ribose phosphate moieties within this dinucleotide. In uridine triphosphate (UTP), six and seven labelled carbon species are present.

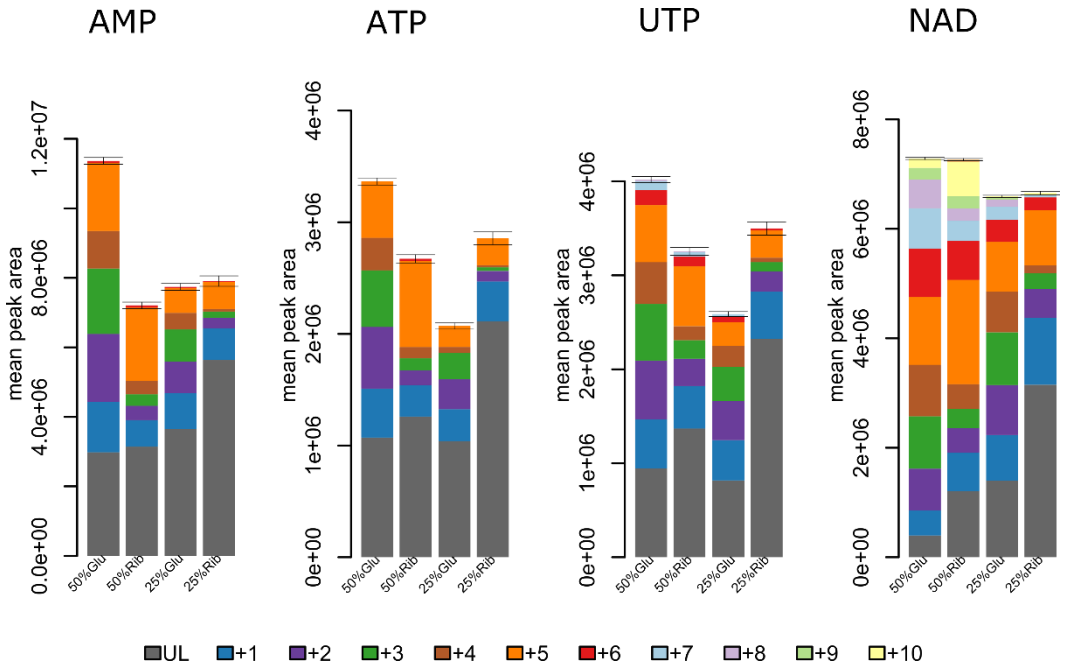

Figure 4.6. Labelling patterns of AMP, ATP, UTP and NAD. Coloured boxes underneath indicate how colours correspond to number of carbons labelled, UL - unlabelled.

AMP	50% Glu	50% Rib	25% Glu	25% Rib
0 C labelled	26 %	44 %	47 %	71 %
1 C labelled	13 %	11 %	13 %	12 %
2 C labelled	17 %	6 %	12 %	4 %
3 C labelled	17 %	5 %	12 %	2 %
4 C labelled	9 %	5 %	6 %	1 %
5 C labelled	17 %	29 %	9 %	10 %
6 C labelled	0	1 %	0	0
total abundance	1	0.63	0.68	0.7

Table 4.4. Quantification of labelling in AMP. Total abundance is given in values relative to WT.

As examples of amino acids, alanine, aspartate, glutamate and glutamine, were analysed (Fig 4.7). The trends observed in some of the previous metabolites are evident here as well. The total abundance and distribution of labelling is almost identical in the first three groups in aspartate and glutamate (Fig 4.7). The data are similar for the other two amino acids, but the total abundance is decreased to 75% for glutamine in the second group and decreased to 56% for alanine. The peak shapes for alanine are good, so the almost two fold depletion in the ribose group is not ambiguous. As with the previous observations, there is almost no labelling in the last group. In general, it is surprising that such relatively large quantities of amino acids are made from sugar substrates, when all amino acids are present in sufficient amounts in medium. The rest of amino acids detected are shown in Appendix A3, but only a minor labelling was detected in serine and asparagine and almost none in any of the others.

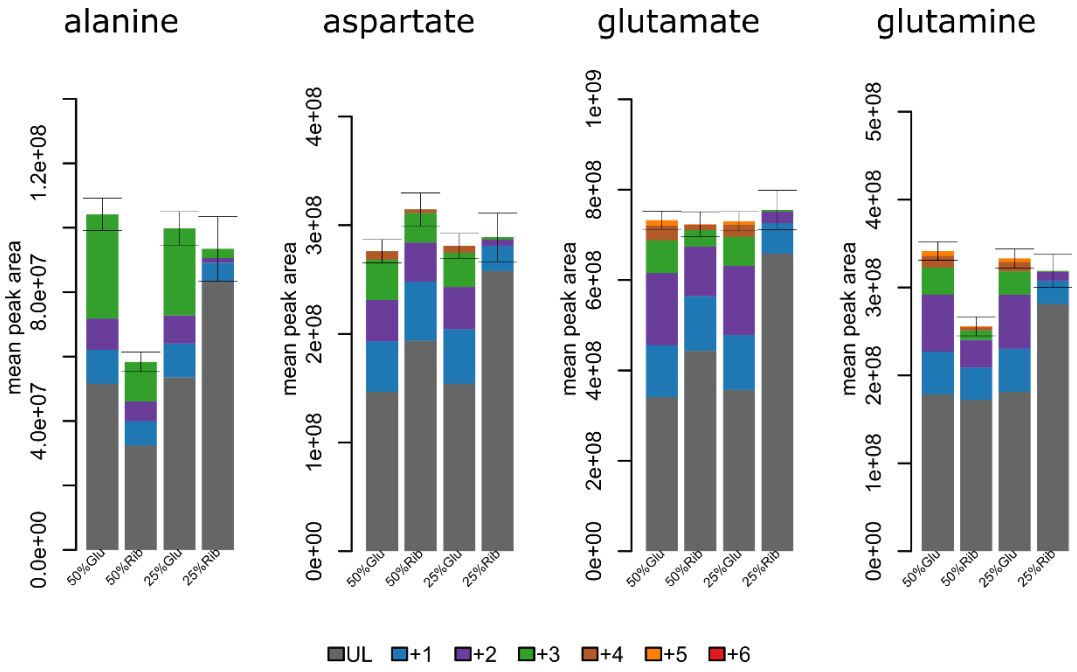

Figure 4.7. Labelling patterns of alanine, aspartate, glutamate and glutamine. Coloured boxes underneath indicates how colours correspond to number of carbons labelled, UL - unlabelled.

4.3 Discussion

The results presented in this chapter reveal a number of general trends. Firstly, the extent and pattern of labelling in the first three groups (i.e. mixed labelled and unlabelled glucose alone, mixed labelled and unlabelled ribose alone, or labelled glucose with unlabelled ribose) is substantial and similar, while the fourth group (labelled ribose with unlabelled glucose) leads to minimal incorporation of label into most metabolites. This suggests that glucose is the preferred carbon source for synthesis of these representatives of various metabolic pathways. If glucose is not available, ribose can completely substitute for it, but if both sugars are supplied, glucose is preferred. Cells in the third and fourth group were grown in effectively the same medium, varying only in whether it was glucose or ribose provided in the labelled form, yet when both sugars are available, label enters many metabolites from glucose, but barely any from ribose.

The first group (glucose alone) produced more labelled pyruvate and succinate than other groups. These metabolites come from glucose's being metabolised to phosphoenolpyruvate and further converted to pyruvate or succinate via the succinate shunt, which is secreted as an end product (Saunders et al., 2011). This indicates a profligate use of glucose, i.e. consumption in excessive quantities with large quantities of carbon and potential energy wasted through secretion of these partially oxidised products. The same explanation holds for alanine, since the total amount of labelled alanine in the second group (ribose as a carbon source without glucose) is two fold lower than in the first group (glucose only). Alanine can be made from pyruvate by transamination (Saunders et al., 2011), and secreted as an end product, as was shown in section 3.3.3. This implies that alanine can be made from ribose, but to produce only half of the amount made in first group is sufficient.

The data provide clear evidence for substantial activity in the PPP, especially the non-oxidative branch. First, there is striking difference between results for glucose and hexose phosphates with respect to labelling, which can be explained by activity of the non-oxidative PPP converting ribose to hexose phosphates. A substantial amount of S7P was detected and almost all of it was labelled to some extent, indicating it originates solely from the sugars. The large proportion of the total S7P that contains two or five labelled carbons is a proof of its synthesis by TKT (product of SBPase would contain more of 3

+ 4 label (Clasquin et al., 2011)). Interestingly, if ribose is present in medium as the only sugar, the total levels of S7P increase by one third, although no specific role is known for its further utilisation in trypanosomatid metabolism. Ribose is phosphorylated to R5P which can be converted in the non-oxidative PPP to GA3P or F6P, a possible entry points for glycolysis. S7P may simply be a by-product of reaction $5 + 5 \rightarrow 3 + 7$, the 7 carbon sugar then being further used in the non-oxidative branch to create other intermediates. Ribose as the main carbon source may trigger activation of TKT, which corresponds with increase in O8P in the same sample group. However, such a potential mechanism has not been reported to date in other organisms. Alternatively, supplementation with ribose may increase the flux through the PPP based on concentration gradients, without affecting the TKT enzyme itself.

Clear regulation of metabolism, however, is apparent depending on which sugars are available. For example, the labelling in the last two groups indicates that if both glucose and ribose are available, ribose is not utilised for S7P synthesis, which is quite surprising. On the other hand, labelling in nucleotides clearly shows that ribose is consumed, phosphorylated and incorporated into nucleotides. This is very intriguing. It suggests that if both sugars are available, ribose is taken up, phosphorylated and used as R5P directly where needed but not fed into the PPP. The PPP is instead somehow separated and independently fed by glucose.

We can only speculate what could make such a barrier. Subcellular localisation could be considered, even though both the PPP and nucleotide synthesis are present both in the cytosol and in glycosomes (Boitz et al., 2012). Localisation of ribokinase has not been investigated in *Leishmania*, but it has a predicted PTS2 (Opperdoes and Szikora, 2006) indicating a glycosomal localisation. In addition R5P should pass through the semi-permeable glycosomal membrane (Achcar et al., 2013). The observed results could be caused by decreased activity of ribokinase and concomitant preferential utilisation of R5P for nucleotide synthesis prior to the non-oxidative PPP. Partial inhibition of *L. mexicana* ribokinase by glucose was reported (Ogbunude et al., 2007), but still the theory has gaps. For example, ribokinase would need to be in a physical complex with phosphoribosyltransferase to enable direct channelling of R5P. However, in *Leishmania* there are multiple phosphoribosyl transferases specific for the different nucleobases. However, if, in principle, ribokinase was partly inhibited and phosphoribosyltransferase

activity was significantly higher than TKT, then this incorporation of R5P into nucleotides but not into the PPP intermediates is feasible.

There is substantial labelling in the nucleotides observed and it has to be interpreted with caution, since these are relatively large metabolites (10 to 21 carbons) and we cannot be sure which of the carbons are labelled. However, the high proportion of a five carbon labelled part indicates incorporation of labelled R5P, which is supported by the fact that this proportion is increased in samples supplied with ribose. The ten carbon labelled part in NAD^+ likely represents two molecules of R5P in the dinucleotide. There is a difference between ATP and UTP, when a clearly distinguishable part of six and seven carbon labelled product is detected in the latter. In the case of UTP this represents the sum of five carbons from R5P plus one or two carbons from the base, since pyrimidine synthesis from glucose through oxaloacetate was shown previously in *T. brucei* (Creek et al., 2015) whereas purines are salvaged (Boitz et al., 2012).

Regarding amino acids, the high proportion of several amino acids derived from sugars is a surprise given the abundance of all of the standard amino acids in medium. Incorporation of label from glucose into alanine, aspartate and glutamate was shown before, while most of the amino acids detected were not labelled (Saunders et al., 2011) which is consistent with the results presented here.

Altogether, these data provide new information about the utilisation of glucose and ribose in *L. mexicana* promastigotes. Clearly, glucose is the preferred source but ribose can fully substitute for it. If both substrates are available, glucose is preferred but ribose is still used for R5P synthesis and for metabolites where it is directly incorporated, such as nucleotides. The most interesting observation is the potential increase in non-oxidative PPP flux if cells are grown on ribose as the major carbon source. Upregulation of the PPP in trypanosomatids was previously observed in response to increased oxidative stress when the mechanism was proposed to be dependent on NADP/NADPH balance (Maugeri and Cazzulo, 2004; Maugeri et al., 2003). Here, however, my results indicate a novel mechanism controlling flux through the non-oxidative branch. It would be of interest to see whether ribose triggers increase in flux in the PPP alone, or whether it induces activation of transketolase and transaldolase.

5 Transketolase

5.1 Introduction

Transketolase has been studied from many angles, including its structure and function, connection with cancer, or biotechnological application, for example as a biocatalyst for asymmetric synthesis (Lindqvist et al., 1992; Nilsson et al., 1997; Ranoux and Hanefeld, 2013; Staiger et al., 2006b). Here, I will focus on the most important aspects and those relevant to its exploitation as a potential drug target in *Leishmania*.

Transketolase is an enzyme that transfers two carbon keto units from a ketose to an aldose, using a wide range of substrates, mostly sugar phosphates from three to seven carbons in size. The enzyme is a homodimer, using as cofactors thiamine pyrophosphate (TPP) and Mg^{2+}, which can be substituted by other bivalent metal ions, such as Ca^{2+}, Mn^{2+}, Co^{2+},Ni^{2+} (Heinrich et al., 1972). Each subunit consists of three domains, an N-terminal pyrophosphate binding domain, a central pyridinium binding domain and a C-terminal domain without any known specific binding function attributed so far (Lindqvist et al., 1992). The crystal structure was resolved for the yeast enzyme first, showing that TPP binds at interface between the two subunits and that there are two catalytic sites at interface of the two subunits (Lindqvist et al., 1992). Later, a crystal structure of *Leishmania* TKT was resolved at 2.2 Å resolution (Veitch et al., 2004). Nilsson and colleagues Nilsson et al., (1997) obtained a structure of the yeast enzyme with bound TPP, Ca^{2+} and E4P showing that the structure in complex is very similar to the holoenzyme. They identified conserved amino acid residues which are responsible for the cofactor and substrate binding, which enabled them to prepare various amino acid

substitution mutants. The enzyme with Asp477 replaced by Ala conveyed only 1.7% of WT enzymatic activity (Nilsson et al., 1997). The substrate was shown to bind in a narrow cleft between the two subunits which can accommodate only a single substrate molecule at a time, and not both the donor and acceptor simultaneously (Nilsson et al., 1997). That is consistent with the kinetic ping-pong mechanism of TKT action (Horecker et al., 1963). Kinetic measurements stimulated formulation of an alternative hypothesis, when the non-oxidative PPP is presented as a sum of half-reactions, where donor substrate reacts with the enzyme first, and subsequently any suitable molecule can serve as an acceptor (Kleijn et al., 2005). The range of possible donor and acceptor substrates is relatively large. While the canonical donor ketoses are X5P, F6P, S7P and erythrulose and acceptor aldoses are R5P, E4P, GA3P and glycoaldehyde (Clark et al., 1971; Datta and Racker, 1961), in a modified pH-based TKT assay, lithium hydroxypyruvate combined with a wide range of aldehydes can be used instead (Yi et al., 2012).

Essentiality of TKT and its role in metabolism was studied in classical model organisms including yeast and *E. coli*. TKT deletion mutants in yeast showed no defect in rich growth medium and interestingly, also grew well on gluconeogenic carbon sources (glycerol, pyruvate, lactate, ethanol). However, growth was compromised on fermentable carbon sources (glucose, fructose, mannose, galactose, raffinose) (Sundström et al., 1993). Similarly, after TKT overexpression, yeast cells suffered a growth defect only on fermentable carbon sources, which suggests a regulatory mechanism between glycolysis and the non-oxidative PPP (Sundström et al., 1993). Further, the TKT knock-out (KO) yeast did not grow without aromatic amino acids (tryptophan, tyrosine, phenylalanine) which was explained by the fact that E4P, a product of TKT, is a necessary precursor for their synthesis (Sundström et al., 1993). Cases of TKT deficiency in humans are not known, because mutations are probably lethal at the embryonic stage (reviewed in Stincone et al., 2014). Single TKT KO mice suffered from weight reduction and fewer animals were obtained in the progeny than expected, suggesting that half of the TKT single KO embryos died (Xu et al., 2002). No double KO animals were obtained in their progeny which further confirms essentiality of the gene for mammals (Xu et al., 2002). Similar conclusions were drawn when TKT RNAi was induced in mammalian oocytes, since meiosis arrested at metaphase I stage, and rearrangements of meiotic spindle and chromosomes were observed (Kim et al., 2012). Interestingly, mRNA levels of ribokinase and phosphoribosyl pyrophosphate synthetase decreased after TKT RNAi, but

expression of the other PPP enzymes was unchanged (Kim et al., 2012). The phenotype was partly rescued by supplementation with R5P, which again suggests some kind of feedback control but is very difficult to pinpoint precisely how this occurs (Kim et al., 2012).

In addition to TKT, the human genome encodes TKT-like1 (TKTL1) and TKT-like2 (TKTL2) genes (Coy et al., 1996). Contradictory results were obtained for TKTL1 enzymatic activity (Coy et al., 1996; Meshalkina et al., 2013; Schneider et al., 2012), but it received increased attention recently, since it is specifically overexpressed in tumour cells. The mRNA levels were elevated only in 10% cases but the protein level was increased in 40% of cancer tissues tested (Staiger et al., 2006b). The relevance for tumour growth was examined and it was confirmed that supplementation with thiamine supported further growth (Boros et al., 1997; Comín-Anduix et al., 2001). On the contrary, when oxythiamine, an analogue of TPP was applied as a TKT inhibitor, cell cycle arrest occurred and cells stopped growing (Rais et al., 1999). TKTL1 expression was studied specifically in gastric cancer and was shown to correlate with invasive colon and urothelial tumours' size and poor patient outcome, thus TKTL1 was suggested as a potential biomarker for cancer (Diaz-Moralli et al., 2011; Langbein et al., 2006; Staiger et al., 2006b). A high-throughput screen of 64,320 compounds for new TKT inhibitors was performed, testing selective enzyme inhibition and inhibition of cell proliferation, resulting in two compounds being selected as promising hits with good pharmacokinetic properties (Du et al., 2004). However, no further reports on their follow up have emerged to date.

TKT was also investigated as a potential drug target, in the malaria parasite *Plasmodium falciaprum*, where the enzyme appears to be hexameric (Joshi et al., 2008). Its role is also uncertain given the lack of transaldolase in *Plasmodium* sp. (Bozdech and Ginsburg, 2005). The purified enzyme was inhibited by *p*-hydroxyphenylpyruvate at low concentrations in noncompetitive manner with F6P and competitive with hydroxypyruvate, which differs from a previous report from yeast where the inhibition was competitive to both donors (Joshi et al., 2008; Solovjeva and Kochetov, 1999).

The metabolomics analysis presented in Chapter 3 indicates that the non-oxidative PPP is active in amastigote *L. donovani*, as the levels of the metabolites are comparable to

promastigotes. The analysis with labelled glucose and ribose in Chapter 4 confirmed a substantial flux in the PPP in promastigote *L. mexicana*, which may be potentially increased in response to substrate availability, or increased oxidative stress as reported previously (Maugeri et al., 2003). In this chapter I focus on TKT in *L. mexicana*, I studied various aspects of the enzyme and scrutinized its utilisation as a potential drug target.

TKT was also studied in other trypanosomatids e.g. *T. brucei* and *L. mexicana.* As mentioned earlier, TKT is not expressed in bloodstream *T. brucei* at all (Cronín et al., 1989; Stoffel et al., 2011). Double KO in procyclic stage was generated and the obtained cell line showed no growth defect or any morphological deformation (Stoffel et al., 2011). When examined by LC-MS metabolomics, significant changes in glycolysis and PPP intermediates were detected, indicating that metabolism was altered but without effect on cell growth in rich media. TKT in trypanosomatids contains a well defined peroxisomal targeting signal (PTS) enabling import into glycosomes and about 10% of the protein is located inside glycosomes in procyclic *T. brucei* (Stoffel et al., 2011), whereas it is 30% in promastigote *L. mexicana* (Veitch et al., 2004), and 20% in epimastigote *T. cruzi* (Maugeri and Cazzulo, 2004). Two independent high-throughput proteomic studies found TKT in glycosomes of only procyclic but not bloodstream *T. brucei* (Colasante et al., 2006; Vertommen et al., 2008). Another study of glycosomal proteome using tagged PEX13.1 enrichment followed by SILAC proteomics detected signal for TKT in procyclic *T. brucei* albeit at a level failing to reach statistic significance (Guther et al., 2014).

A cell line was created with both alleles of TKT replaced by antibiotic cassettes (Δtkt) in promastigote *L. mexicana* (Wildridge, 2012). The cells did not demonstrate any growth phenotype nor any morphological deformation compared to WT. The Δtkt cell line was more sensitive to pentamidine but not to methylene blue, a compound used to evaluate oxidative stress response. Δtkt cells consumed the same amount of glucose as WT when assessed over 4 days of cultivation, but produced probably less metabolic end products (Wildridge, 2012). Whereas medium of WT cultures is acidified after few days of cultivation and changes its colour (due to presence of phenol red), medium of Δtkt cells changed very little, suggesting much lower production of acidic metabolic end products, but no further analysis was performed. Targeted metabolomic analysis was performed in collaboration with the Metabolomics Platform in Toulouse showing significant changes

in intermediates of glycolysis and the PPP, corresponding to expected consequences of the deletion (Wildridge, 2012). I continued with deeper and wider characterisation of the Δtkt cell line, especially because infectivity and effects on the amastigote stage were not tested and methodology in metabolomics progressed extensively at Polyomics Glasgow, allowing further and untargeted analyses.

5.2 Aims

- Test sensitivity of Δtkt cell line to oxidative stress, antileishmanial drugs
- Test infectivity of Δtkt to macrophages and mice
- Scrutinize changes in metabolism of Δtkt (untargeted LC-MS, LC-MS with U-^{13}C-glucose, GC-MS, central glycolytic flux)
- Measure PPP flux in WT promastigote *L. mexicana*
- Prepare GFP-TKT constructs with alternations to the C-terminus and assess their subcellular localisation
- Assess functions of TKT in the cytosol and in glycosomes. Prepare cell lines expressing TKT solely in the cytosol or glycosomes and compare their growth, sensitivity to oxidative stress, metabolomes.

5.3 TKT is an essential enzyme and a possible drug target in *Leishmania*

5.3.1 TKT knock-out and complemented cell lines

First, I compared growth of WT, Δtkt and Δtkt + TKT re-expressor cell lines under standard conditions in Homem medium. No significant difference in growth is observed between these cells (Fig 5.1A).

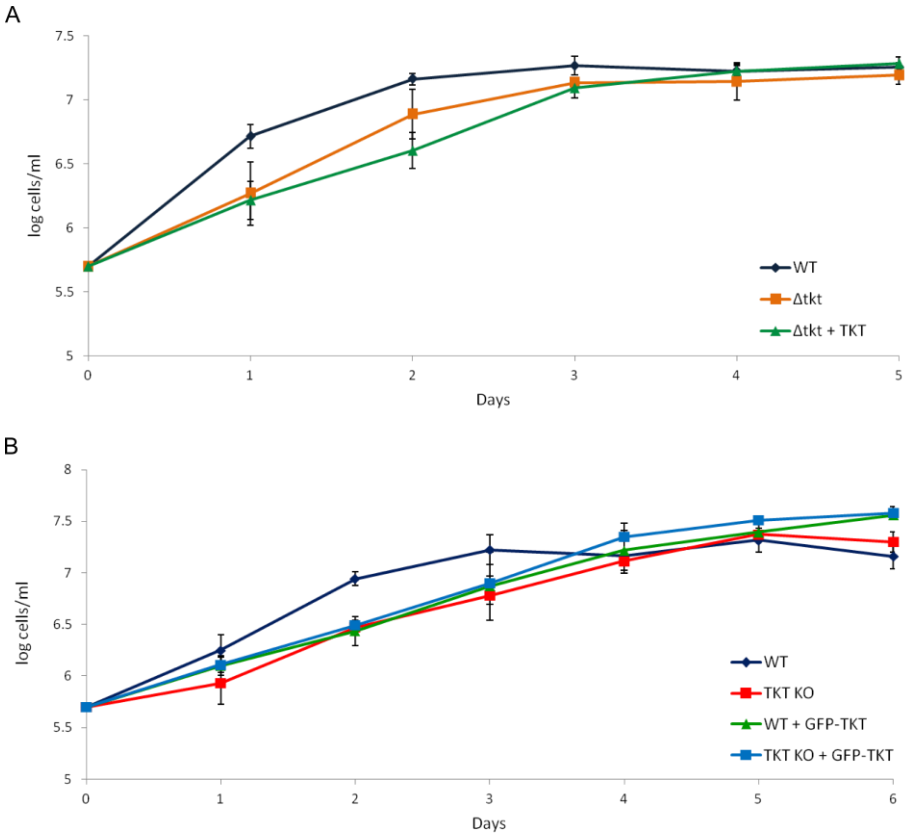

Figure 5.1. Growth curves of TKT cell lines. n = 3, error bars represent standard deviation. A – Growth of WT, Δtkt, and Δtkt + TKT cell lines. B – Growth of WT, Δtkt, WT + GFP-TKT, and Δtkt + GFP-TKT cell lines.

Following from this, I used a plasmid from the pNUS series (http://www.ibgc.u-bordeaux2.fr/pNUS/index.html (Tetaud et al., 2002)) for episomal overexpression in *Leishmania*, and prepared a construct expressing TKT fused with a green fluorescent protein (GFP) to its N-terminus. The successful transfection with the plasmid was verified by fluorescence microscopy, the obtained cell lines were called WT + GFP-TKT and Δtkt + GFP-TKT, respectively (Fig 5.2).

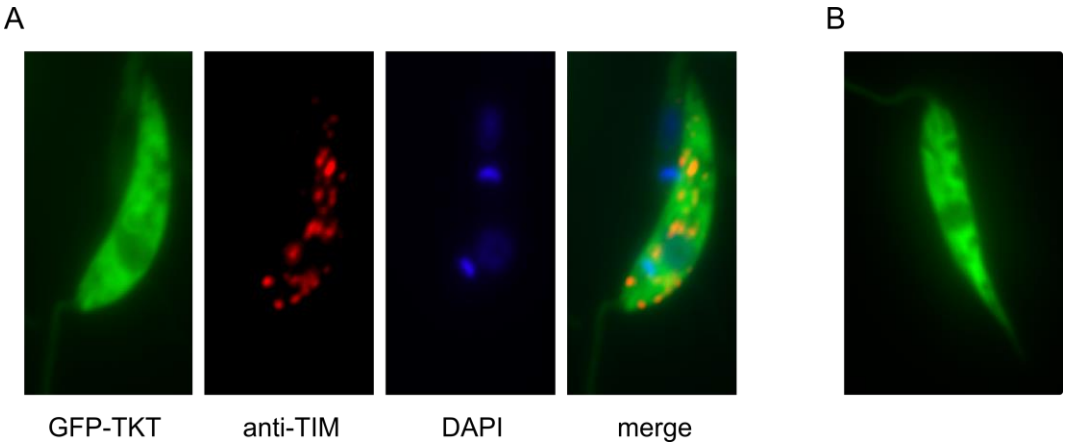

Figure 5.2. Validation of cell lines expressing GFP-TKT. A - WT + GFP-TKT cell line. Antibody against triosephosphate isomerase (TIM) was used as a glycosomal marker. B – Δtkt + GFP-TKT cell line.

Enzyme activity of TKT was measured in all of these cell lines, especially because the fusion with GFP may affect dimerisation and proper function of the enzyme. The enzyme assay using Xu5P and R5P as substrates was used as described by Bergmeyer (Brin, 1974), where coupling with TPI and GA3PDH leads to consumption of NADH, which can be easily measured as change in absorbance at λ=340 nm. An enzyme activity comparable to a previous report was detected in WT cell line (Maugeri et al., 2003), no TKT enzyme activity was detectable in Δtkt, whereas the activity (twice that of WT) was rescued in Δtkt+TKT, probably due to higher expression of the gene from that locus (Tab 5.1). Enzyme activity was even higher in cells expressing GFP-TKT, but over-expression is expected from the construct and it definitely confirmed that the enzyme function is not compromised by the GFP tag (Tab 5.1). TKT activity in axenic amastigotes was four times lower than in promastigotes (31 versus 113 mU, respectively).

	activity (nmol/min/10^7 cells)	
WT	2.9	7.22
Δtkt	-0.19	0.1
Δtkt+TKT	6.16	11.08
WT + GFP-TKT	14.16	14.16
Δtkt + GFP-TKT	24.56	29.86

Table 5.1 TKT activity measured in cell extracts of various cell lines. Two biological replicates are shown.

5.3.2 Viability and oxidative stress sensitivity

In accordance with previous observations, Δtkt promastigote cells grow in rich Homem medium under optimal conditions as fast as WT cells. However, the deletion of the gene may become more apparent under non-optimal conditions, for example under various types of stress.

Sensitivity to oxidative stress was tested using methylene blue, which is commonly used for experiments with bloodstream *T. brucei* (Boda et al., 2005). However, in addition to NADPH depletion (Kelner and Alexander, 1985), it probably interferes with the respiratory chain in not completely defined manner and was reported even to support growth under specific conditions (Rojas et al., 2012; Schirmer et al., 2003). No significant difference was detected in sensitivity to methylene blue (WT EC_{50} = 2.36± 0.422 µM; Δtkt EC_{50} = 1.88±0.155 µM; p=0.137), which corresponds with the previous observation (Wildridge, 2012). A more direct test for oxidative stress involves an Alamar Blue Assay with glucose oxidase, an enzyme which consumes glucose and constitutively produces H_2O_2, a reactive oxygen species which is very unstable itself (adapted from Allmann et al., (2013)). When using this assay, Δtkt cell line was twice as sensitive as WT, while Δtkt+TKT partly reverted to WT levels (Fig 5.3; Tab 5.2).

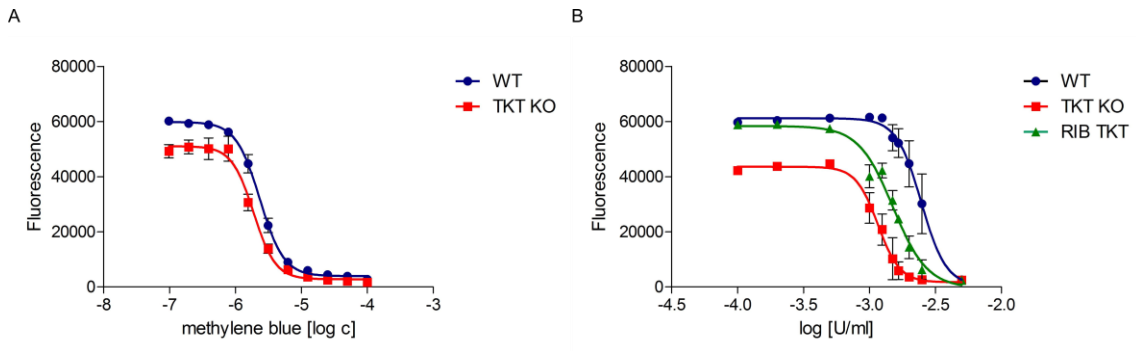

Figure 5.3. Alamar Blue Assays to test sensitivity to oxidative stress.Whereas methylene blue (A) did not show any difference, Δtkt cells were two times more sensitive to glucose oxidase than WT (B). Fluorescence indicated on y axis correlates with viability of cells.

	EC50 [mU/ml]	**p-value**
WT	2.32 ± 0.33	
Δtkt	1.18 ± 0.27	0.01
Δtkt + TKT	1.53 ± 0.14	0.02

Table 5.2. Alamar Blue Assay results for GOX sensitivity, n=3.

The clinically relevant stage of *Leishmania* is the amastigote, thus it was of interest to test the effects of TKT depletion in the amastigote stage. Δtkt cells transformed into amastigotes under increased temperature and low pH, when assessed by microscopy, but the cells never started dividing and growing. Even after repeated attempts, I never obtained a growing culture of Δtkt amastigote cells. Such an observation is interesting in indicating a possibly essential role for TKT to amastigote cells. Even though WT cells transformed into amastigotes and continued to grow, Δtkt + TKT cell line had the same phenotype as Δtkt, thus no conclusions can be made. Moreover, it can be disputed that axenic cultures are artificial and not representative, thus I proceeded to infection assays.

5.3.3 Macrophage infections

Following from the previous observations, I wanted to assess infectivity of Δtkt cells towards macrophages. THP1 cells were activated with PMA, incubated with stationary phase parasites and infection was estimated at different time points as percentage of macrophages infected with amastigotes.

Δtkt cells seem to be around half as infective towards macrophages as WT, although variability is high and the results are not always statistically significant (depending on individual experiment). Two representative examples are shown in Fig 5.4, but additional experiments across different conditions yield less conclusive outputs. Infectivity of Δtkt + TKT cell line seems to be rescued but with overall high variability. Altogether, the results are ambiguous and inconclusive.

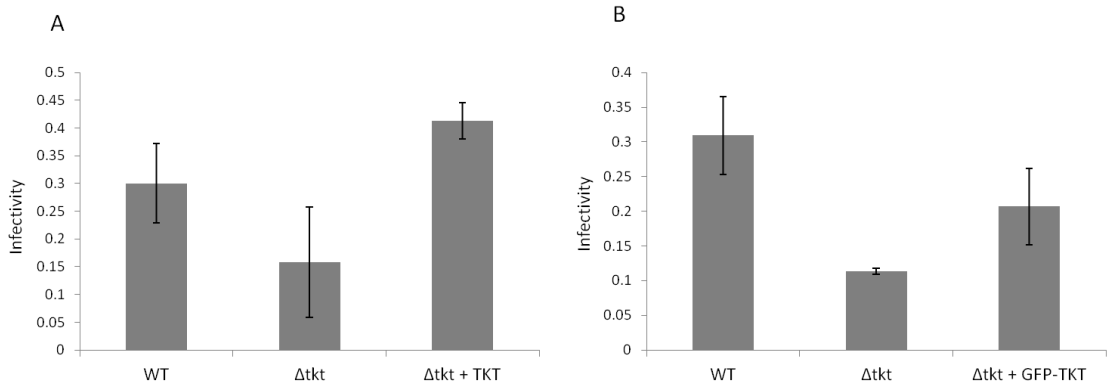

Figure 5.4. Infectivity towards macrophages calculated as proportion of macrophages infected with *Leishmania*, error bars represent standard deviations. A – 24 hours of cultivation, MOI = 5, n = 4, p = 0.018. B – 4 days of cultivation, MOI = 10, n = 4, p = 0.091

5.3.4 Mice infections

The experimental setting closest to real leishmaniasis is infection of mice models and examination of skin lesion development. It is known that ability of *Leishmania* to infect decreases after prolonged *in vitro* cultivation (Pescher et al., 2011), hence first I infected BALB/c mice with my *Leishmania* strains, culled the animals after 3 months, obtained the popliteal lymph nodes from which parasites were recovered. Afterwards, I used these

parasites for an *in vivo* infectivity study. 2 x 10^6 cells (WT, Δtkt, and Δtkt + TKT cells) were injected into foot pads of four BALB/c mice each. Subsequently, size of the foot pads was measured weekly, reflecting swelling and development of skin lesions. Mice infected with WT *Leishmania* developed 4 mm lesions in 13 (20 for the last) weeks, whereas no obvious lesions developed in mice infected with Δtkt parasites even after 23 weeks and no parasites were recovered from the lymph nodes. Most importantly, re-expression of TKT in Δtkt + TKT rescued the infectivity and the skin lesions reached 4 mm in 15 (21 for the last) weeks (Fig 5.5). This experiment confirms that infectivity was decreased due to absence of TKT and that TKT is essential for infectivity and amastigote survival *in vivo*.

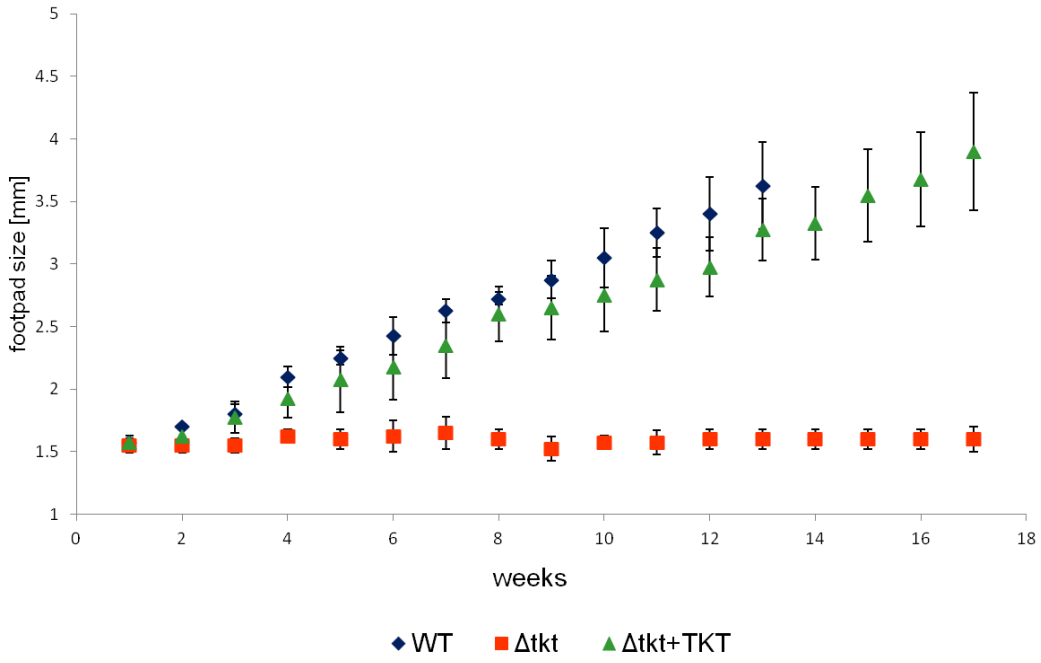

Figure 5.5. Mice infections. Mice were injected into foot pads with 2 x 10^6 *Leishmania* cells. Size of foot pads was measured weekly, each point represents average of 4 mice infected, error bars represent standard deviations.

5.3.5 Screening for TKT inhibitors

5.3.5.1 Common *Leishmania* drugs

One of the persisting questions in parasitology is mode of action of the drugs used to kill the parasites and treat the diseases. For most drugs used against trypanosomatids, their targets inside cells and modes of action are unknown (Croft et al., 2006; Horn and Duraisingh, 2014). Based on the previous experiments, TKT is clearly essential in the amastigote stage and thus a potential drug target. An arising question, therefore, is whether it is targeted by any of the drugs currently in use. To test this possibility, Alamar Blue Assays were performed using the common antileishmanial drugs (AmB, paromomycin, pentamidine, antimonials, miltefosine). However, no difference in sensitivity was detected for antimonials between WT and Δtkt and for AmB, miltefosine, paromomycin, and pentamidine, Δtkt was slightly more sensitive (Fig 5.6; Tab 5.3). We can conclude that TKT is not targeted by any of the drugs tested and its depletion increases sensitivity of the cells towards some of the compounds, probably due to increased overall stress.

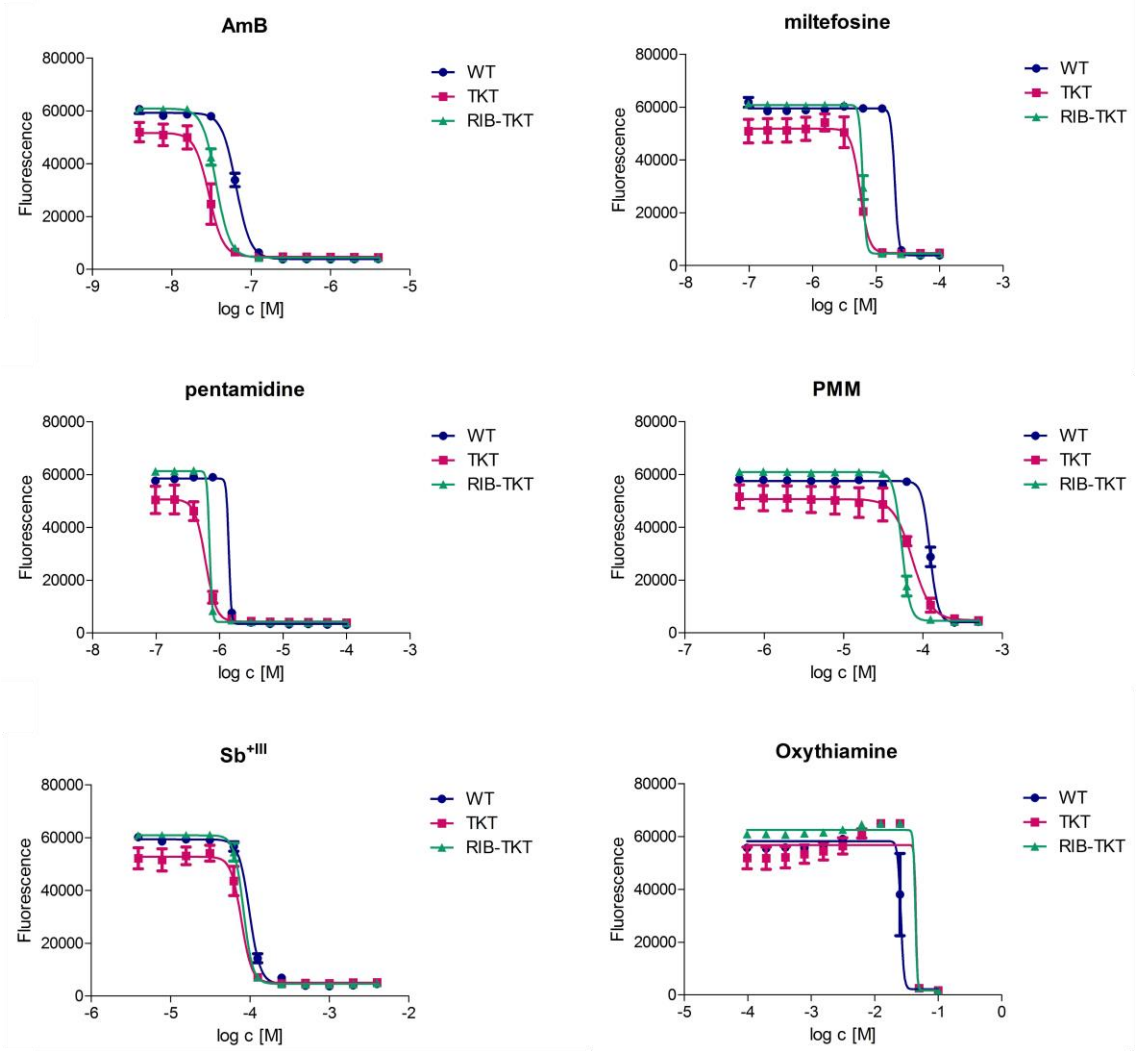

Figure 5.6. Alamar Blue Assays with common antileishmanial drugs and oxythiamine. Effects of drugs commonly used against *Leishmania* were tested against promastigote WT, Δtkt, and Δtkt + TKT cell lines. The efficacy was similar or stronger on Δtkt than WT. Oxythiamine did not inhibit growth until high concentrations were reached; n = 2.

	WT	Δtkt	Δtkt + TKT	fold change Δtkt/WT
AmB	0.0647	0.02945	0.03619	0.46
miltefosine	19.75	5.59	6.166	0.28
pentamidine	1.404	0.5993	0.6966	0.43
paromomycin	122.9	74.04	54.21	0.60
Sb^{+3}	98.46	77.77	82.68	0.79

Table 5.3. EC_{50} values for Alamar Blue Assays from Fig 5.6. Values are averages of two biological replicates, [μM], n = 2.

5.3.5.2 Oxythiamine

Another compound associated with TKT is oxythiamine (Fig 5.7). It is an analogue of thiamine, a precursor of TPP, a cofactor of TKT, and was suggested and tested with promising results as a treatment against cancer, due to PPP inhibition aimed at TKT (Rais et al., 1999). On the other hand, when tested on *P. falciparum*, substantial inhibition was obtained only in thiamine-depleted medium and most importantly, the authors explain the decrease in growth by inhibition of pyruvate and oxoglutarate dehydrogenases, other TPP-dependent enzymes (Chan et al., 2013). Thus, it was of interest to examine the effects of oxythiamine on WT and TKT-depleted *Leishmania* cells. However, no difference was observed between the two cell lines and the EC_{50} values measured are relatively high (WT EC_{50} = 25.82 mM, Δtkt = 44.54 mM, Δtkt + TKT = 43.64 mM) (Fig 5.6). It would be interesting, in the future, to perform the experiment with medium low or free of thiamine.

5.3.5.3 Thiamine analogues

Thanks to collaboration with Dr. Fraser Scott from the University of Strathclyde, we obtained a series of thiamine analogues (Lünse et al., 2014, and unpublished) (Fig. 3.7). The effect of these compounds was tested on WT amastigote *Leishmania* by Alamar Blue Assay. Any of the compounds tested did not show inhibition of growth within the range used and EC_{50} values could not have been determined (Fig. 3.8), thus no further experiments were carried forward.

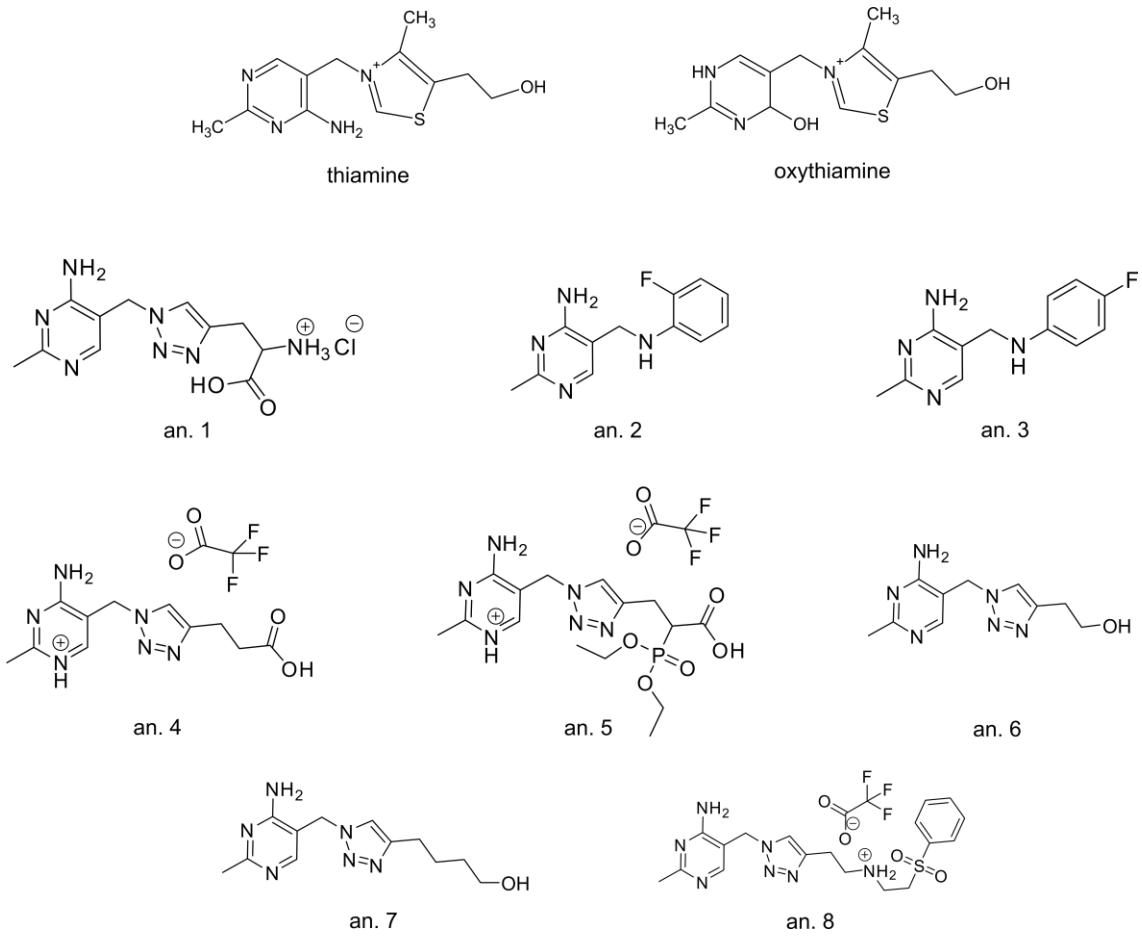

Figure 5.7. Structures of thiamine, oxythiamine and compounds tested as thiamine analogues 1 – 8.

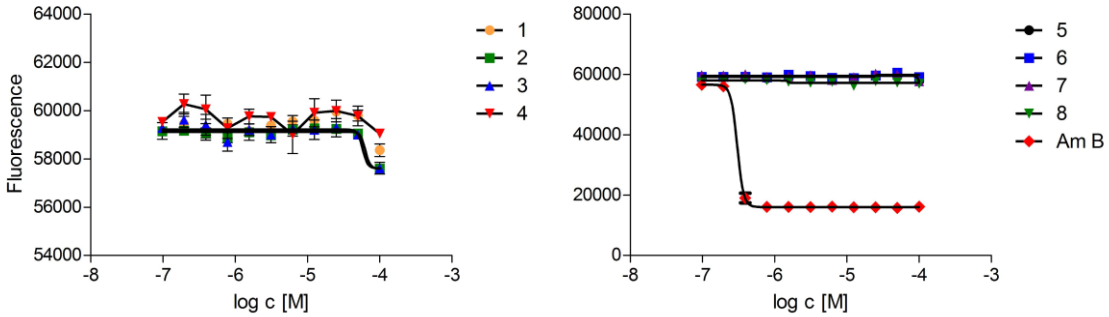

Figure 5.8. Alamar Blue Assays with thiamine analogues. Alamar Blue Assays were performed with compound analogues to TPP on WT amastigote *L. mexicana*, starting from 100 mM with serial dilutions. The compounds are labelled 1 – 8, AmB was used as a control.

5.4 Impacts of TKT deletion on metabolism

A metabolomic analysis of the Δtkt promastigote *L. mexicana* cell line was performed previously (Wildridge, 2012), but the analysis was targeted and provided quantification of relatively low number of metabolites, albeit focusing on those most closely associated with the glucose metabolising pathways directly associated with TKT. Since untargeted LC-MS metabolomics of trypanosomatids is well established at Glasgow Polyomics, it was of interest to analyse Δtkt *Leishmania* by the untargeted method, allowing identification of hundreds of metabolites, both directly related to the pathways associated with TKT, but also extending into the wider metabolic network. Moreover, considering the intriguing phenotype observed, when promastigotes show no defect but amastigotes are not viable, it was of interest to use metabolomics to analyse the changes in metabolism. Although focusing on promastigotes which are more amenable to analysis, the alterations in one stage can allow extrapolation of knowledge to other stages, pointing to why the deletion is lethal for amastigotes. Later, an RNAseq experiment was performed, in order to relate changes in metabolism to those in gene expression, and these are discussed specifically in chapter 3.4.3, but data pertinent to observations within the metabolomics experiments are discussed where appropriate and useful here.

5.4.1 Changes in glycolysis and the PPP detected by LC-MS

We performed untargeted LC-MS metabolomics analysis of WT, Δtkt, and Δtkt + TKT cells. Identifications of most of the metabolites are putative and relative changes in abundance are detected while absolute quantification of metabolites is not feasible with the methodology used. It is indicated where standards were available for confirmation of the identity, otherwise the identification is predicted based on retention time and mass detected.

The general overview of the LC-MS metabolomics results shows that a substantial proportion of the most changing metabolites are saccharides and metabolites directly connected with sugar metabolism (Fig 5.9). Visualisation of the overall data reflects that the changes observed in Δtkt are reverted back towards WT levels in the re-expressor cell line (Fig 5.9). Among the metabolites detected, I searched for those which correspond to intermediates of glycolysis and the PPP and the changes detected are listed in Tabs 3.4 and 3.5 and Fig 5.10.

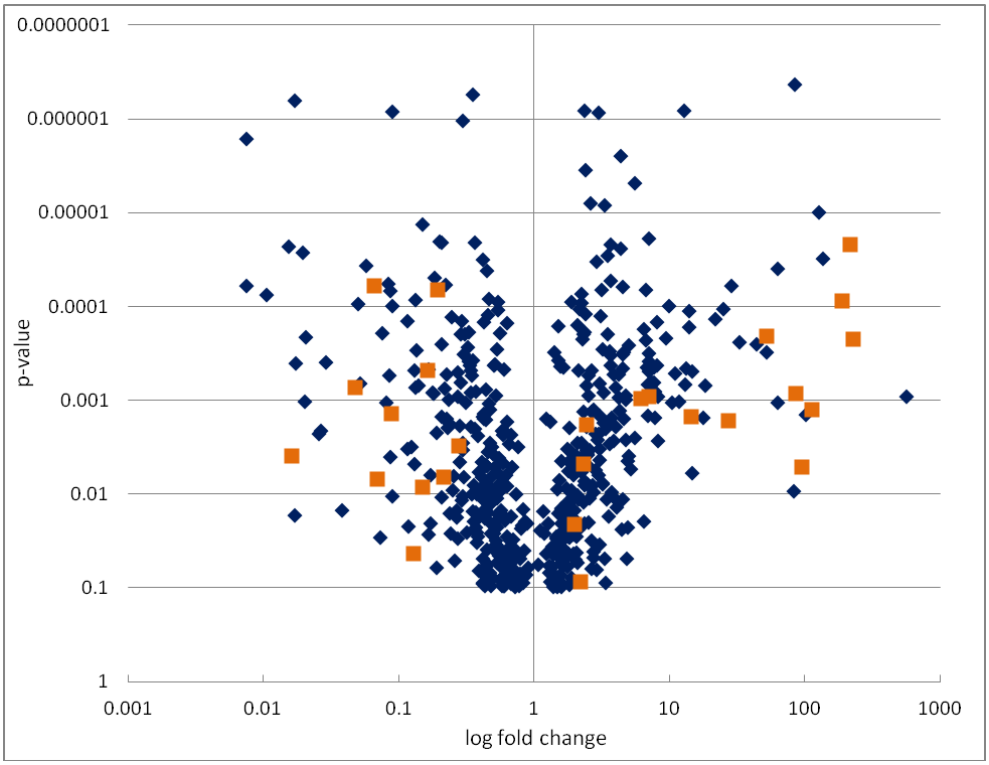

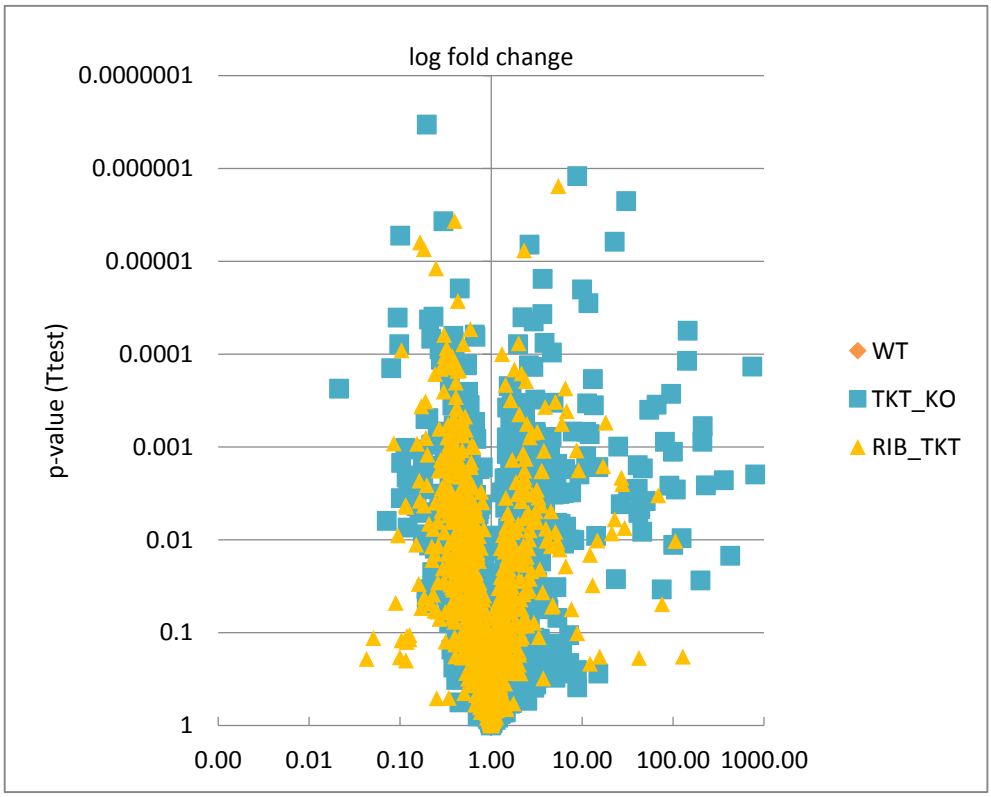

Figure 5.9. Volcano plots showing changes in Δtkt relative to WT as detected by LC-MS metabolomics. In to top plot metabolites directly connected with sugar metabolism are highlighted in orange. The bottom plot shows overall changes in metabolome in Δtkt and re-expressor Δtkt + TKT relative to WT.

In glycolysis, glucose accumulates while all of the subsequent intermediates are depleted. Those metabolites highest in the pathway (hexose phosphates) decrease by less than two fold, whilst subsequent metabolites are diminished by progressively larger amounts, resulting in PEP being seven times decreased in Δtkt compared to WT cells. Pyruvate is not changed, but it can be supplied from additional routes or taken up from the medium. In Δtkt + TKT, most of the metabolites reverted back to WT levels, confirming rescue of the TKT deletion phenotype.

In the PPP, the changes observed correspond with expectations associated with TKT deletion. The metabolites upstream from TKT, 6PG and pentose phosphates are accumulated, 5 and about 200-fold, respectively, whereas S7P, a metabolite downstream from TKT, is three fold decreased (Fig 5.10). The pentose phosphates are massively accumulated and subsequently drive the flux into additional reactions resulting in production of metabolites not detected in WT, such as O8P, alcohol derivatives of pentoses, or alcohol derivatives of pentose phosphates.

glycolysis	**Δtkt**	**Δtkt + TKT**	**p-value (Δtkt/ WT)**
glucose	2.6	1.13	0.022
G6P	0.75	0.77	NS
F1,6bP	0.42	0.53	0.002
GA3P	0.2	0.25	0.023
glycerol-3P	0.2	0.59	3×10^{-7}
1(2),3bPG	increased	ND	-
2PG	0.17	0.65	1×10^{-4}
PEP	0.14	0.67	2×10^{-4}
pyruvate	0.92	1.75	NS

Table 5.4. Metabolites of glycolysis as detected by LC-MS metabolomics. Changes in putative metabolites of glycolysis, numbers indicate relative abundance in Δtkt and Δtkt + TKT compared to WT, metabolites highlighted in bold were confirmed with standards, p-values indicated are for change between WT and Δtkt. In case of bis-phosphoglycerate, no peak was detected in WT but a substantial peak in Δtkt, thus it cannot be quantified. ND = not detected, NS = not significant, p>0.05.

PPP	Δtkt	Δtkt + TKT	p-value (Δtkt / WT)
6PG	5.23	0.58	3×10^{-4}
R5P	212.06	0.81	4×10^{-6}
S7P	0.31	0.77	0.003
O8P	230.02	0.77	8×10^{-5}
N9P	0.26	0.77	6×10^{-4}
ribose	0.7	0.81	NS
xylulose	increased	ND	-
ribitol 5P	increased	ND	-
xylitol	210	0.58	1×10^{-5}

Table 5.5. Metabolites of the PPP as detected by LC-MS metabolomics. Changes in putative metabolites of the PPP, numbers indicate relative abundance in Δtkt and Δtkt + TKT compared to WT, metabolites highlighted in bold were confirmed by standards, p-values indicated are for change between WT and Δtkt. If no value is determined, no peak was detected in WT but a substantial peak in Δtkt, thus it cannot be quantified. ND = not detected, NS = not significant, $p>0.05$.

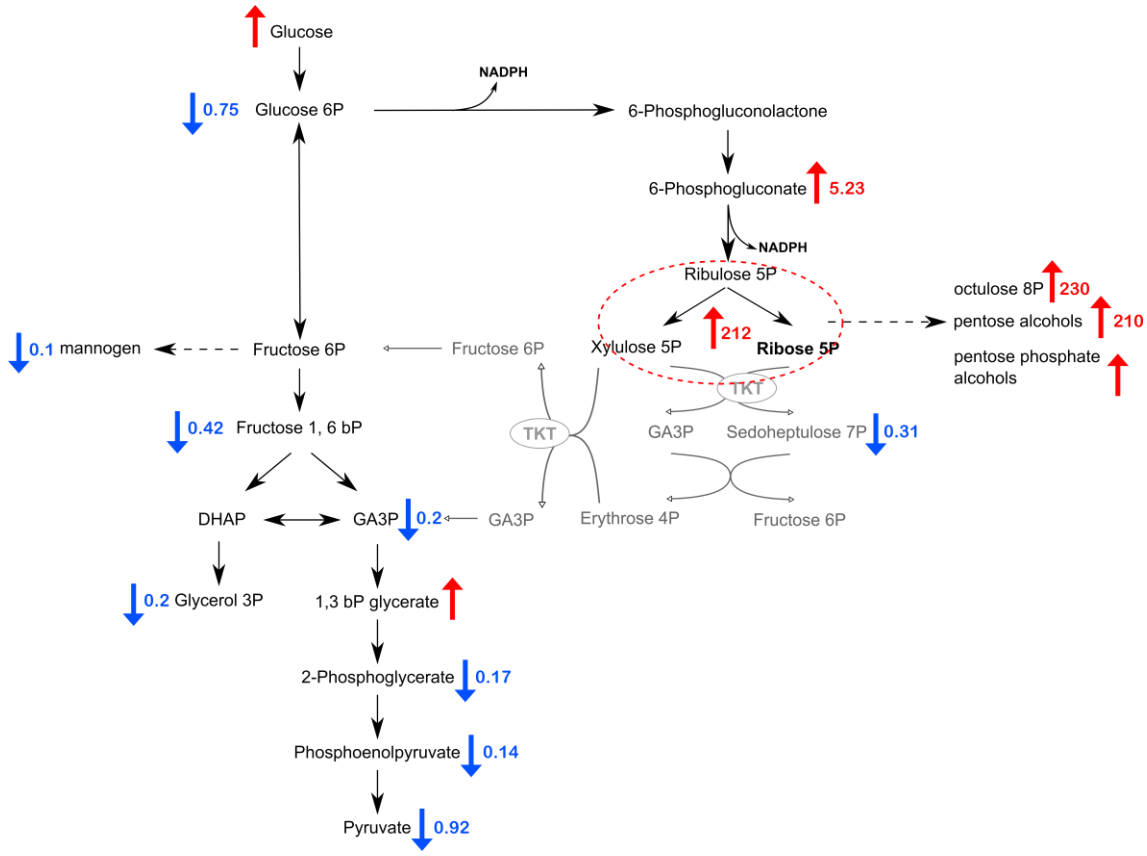

Figure 5.10. Scheme of glycolysis and the PPP with indicated changes as detected by LC-MS metabolomics. Red arrows and numbers indicate accumulation in Δtkt relative to WT and blue colour indicates relative decrease. Where no numbers are given, the peak shapes were not good enough to be quantified.

5.4.2 GC-MS metabolomic analysis

Since LC-MS approach does not enable detection of all sugars and separation of isomers, in our case most importantly G6P and F6P or the separate pentose phosphates, we proceeded with GC-MS analysis, which provides precise identification of lower numbers of metabolites. The metabolites detected and their relative changes in Δtkt are listed in Appendix A2. These metabolites are mapped to the scheme of glycolysis and the PPP shown in Fig 5.11. The general trends overlap with observations from LC-MS, but there are some differences in specific metabolites. Likewise, glucose is accumulated but the other intermediates from glycolysis are depleted, with an exception of fructose 1,6-bisphosphate (F1,6bP), which is here seven times increased compared to WT. Levels of G6P and F6P are comparable (0.46 versus 0.5), indicating that there is high rate of

interconversion between them by PGI. Their labelling profiles are probably also similar (shown in Fig 5.14).

The PPP intermediates are also increased, Ru5P twice as much as R5P. Pentoses in general accumulated substantially: arabinose, ribose and xylulose being nominally 80, 45 and 890-fold increased, respectively. Alcohols derived from sugars were also substantially elevated, confirming the reduction reactions observed in the previous LC-MS experiment. Dulcitol, an alcohol derived from galactose, is 10-fold higher in Δtkt cells compared to WT and xylitol levels enhanced almost three fold (Fig 5.11). Moving to the transcriptome data discussed later, there are two outstanding changes in gene expression detected in this part of metabolism. The first is a two-fold increase in pentose-5-phosphate isomerase while the mRNA of xylulose reductase is two-fold decreased. The reductase turns xylulose to xylitol while consuming NADPH. Such a change may be responsible for high accumulation of xylulose (nominally 890-fold over WT) observed. It is tempting to speculate that it could be a feedback reaction due to depletion of NADPH.

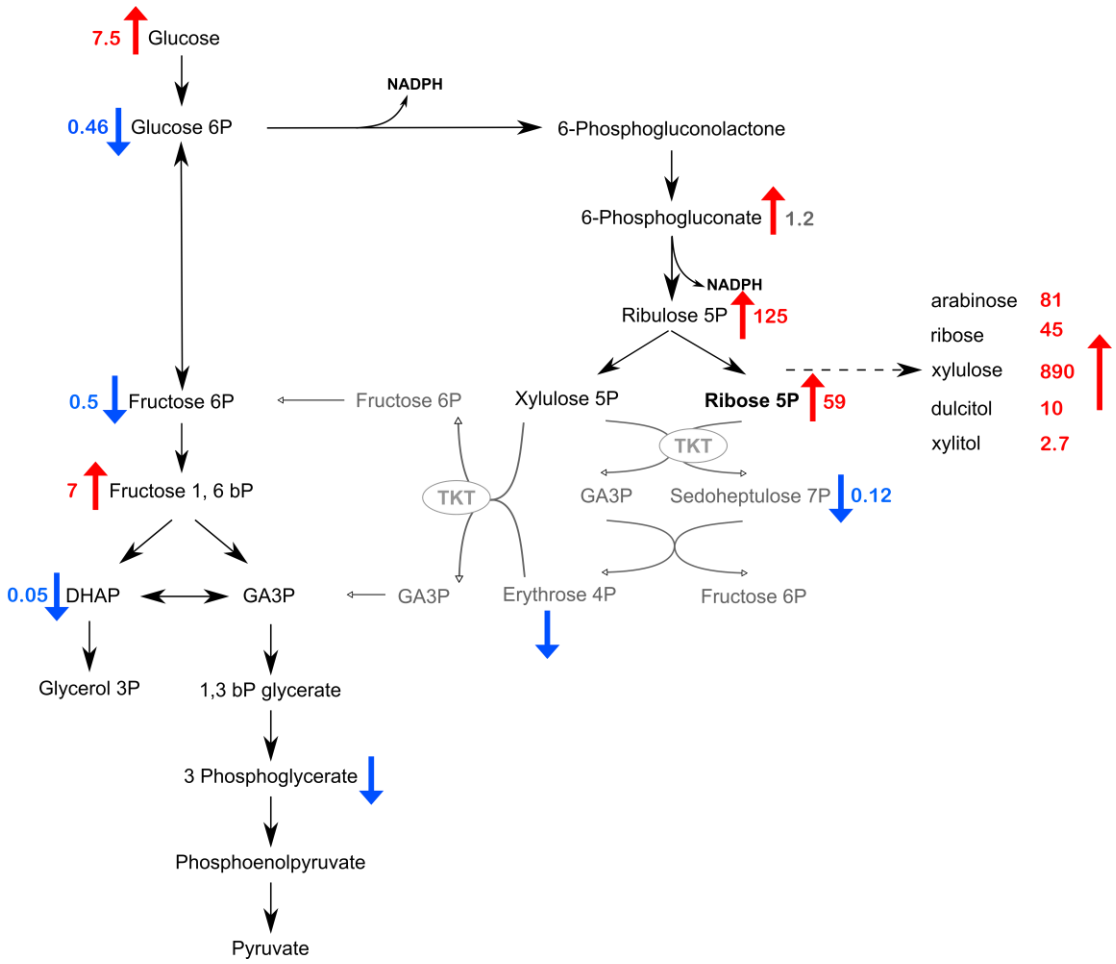

Figure 5.11. Metabolites of glycolysis and the PPP as detected by GC-MS metabolomics. All identifications are based on matches with standards. Red arrows and numbers indicate accumulation in Δtkt relative to WT, and blue colour indicates relative decrease. If no value is determined, the metabolite was detected in WT but not in Δtkt, suggesting decrease.

5.4.3 Central carbon flux

The drop in all glycolytic intermediates post glucose implies that the whole flux through glycolysis may be decreased in the Δtkt cells. To test directly this flux we sought to quantify inputs and outputs of the pathway, i.e. consumption of glucose and production of metabolic end products. Consumption of glucose was measured as a change of concentration in Homem medium containing 1 mM glucose (plus about 0.5 mM present within 10% FCS) in a fast growing culture over 24 hours. Whereas WT cells consumed 3.9 (±0.3) nmol glucose/min/10^8 cells, only 3.2 (±0.3) nmol/min/10^8 cells were consumed by Δtkt cells ($p<0.05$; Fig 5.12). The RNAseq experiment (Section 3.4.3) revealed that

mRNA levels of all three genes for glucose transporters present in the *Leishmania* genome decreased to 75%, which may contribute to the decrease in glucose consumption observed (Appendix B3).

In order to assess the production of metabolic end products, a metabolomic analysis of spent media was performed over 4 days of cultivation. The main metabolites produced were succinate, malate and alanine, which increased in WT over four days 12, 7 and 3.5 fold, respectively (Fig 5.13). In the Δtkt cells, alanine was consumed (30% of the starting concentration being used) instead, whereas levels of succinate and malate increased only 2 and 4 fold, respectively. These experiments point to a significant decrease in the central carbon metabolic flux in the Δtkt cell line.

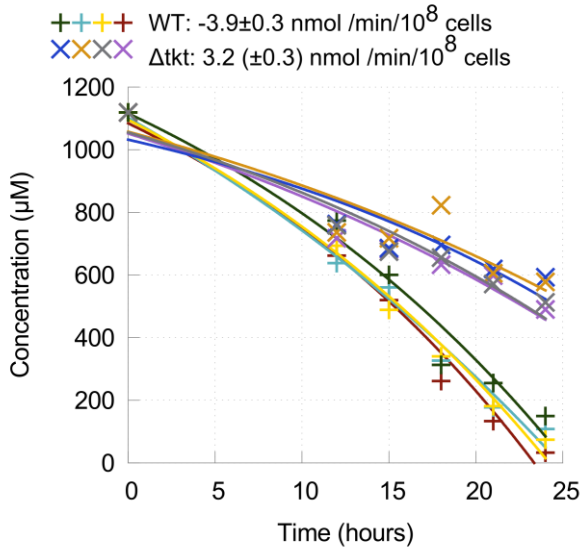

Figure 5.12. Glucose consumption by WT and Δtkt cells over 24 hours, n = 4.

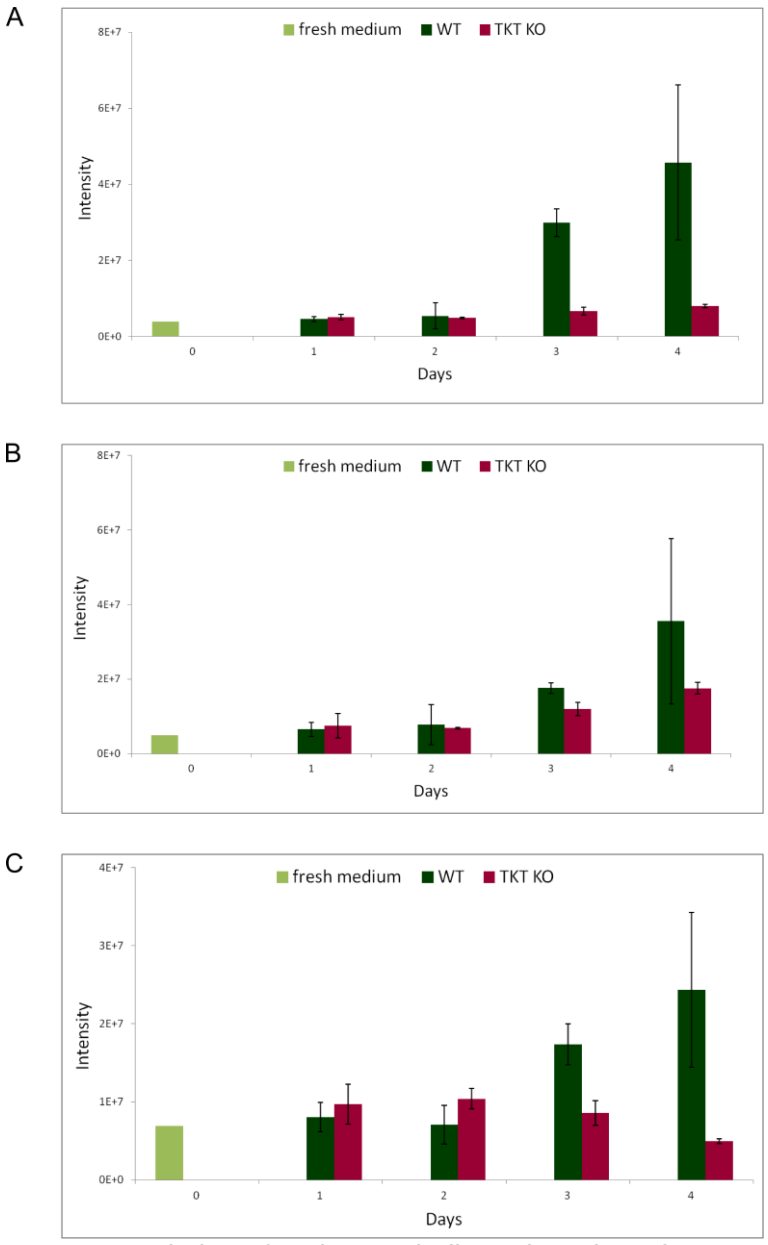

Figure 5.13. Accumulation of main metabolic end products in spent media over 4 days as determined by LC-MS metabolomics. A – succinate, B – malate, C – alanine; n = 4, error bars represent standard deviation.

5.4.4 U-^{13}C-glucose metabolomic analysis reveals changes in TCA cycle metabolism

The primary products of glucose, pyruvate from glycolysis and malate from the succinate fermentation pathway, enter the TCA cycle. In spite of the substantial decrease in abundance of glycolytic intermediates, only mild alternations were observed in metabolites of the TCA cycle (Tab 5.6). TCA cycle intermediates, however, arise from sources other than glycolysis and without using isotope distribution patterns the derivation of intermediates cannot be ascertained. To understand the situation better, a further LC-MS metabolomics analysis was performed, using cells grown in medium containing labelled U-^{13}C-glucose mixed with unlabelled glucose in a 1:1 ratio.

TCA cycle	Δtkt	Δtkt + TKT	p-value (Δtkt / WT)
acetyl-CoA	1.02	0.66	NS
citrate	1.38	0.56	NS
2-oxoglutarate	0.51	0.31	NS
succinate	0.35	1.64	0.001
malate	0.68	1.27	5×10^{-5}

Table 5.6. Metabolites of the TCA cycle as detected by LC-MS metabolomics. Changes in putative metabolites of the TCA cycle, numbers indicate relative abundance in Δtkt and Δtkt + TKT compared to WT, metabolites highlighted in bold were confirmed with standards. p-values indicated are for change between WT and Δtkt. NS = not significant, p>0.05.

The profile of hexose 6-phosphates (a sum of G6P and F6P) in WT cells shows labelling from zero to all six carbons with all variants in between which originate during carbon shuffling in the PPP (Fig 5.14). The labelling pattern is completely different in Δtkt cells, where only zero and six carbon labelled molecules were detected, consistent with disruption of the PPP. Similarly, the proportion of labelling in PEP and pyruvate in Δtkt is substantially reduced when compared to WT.

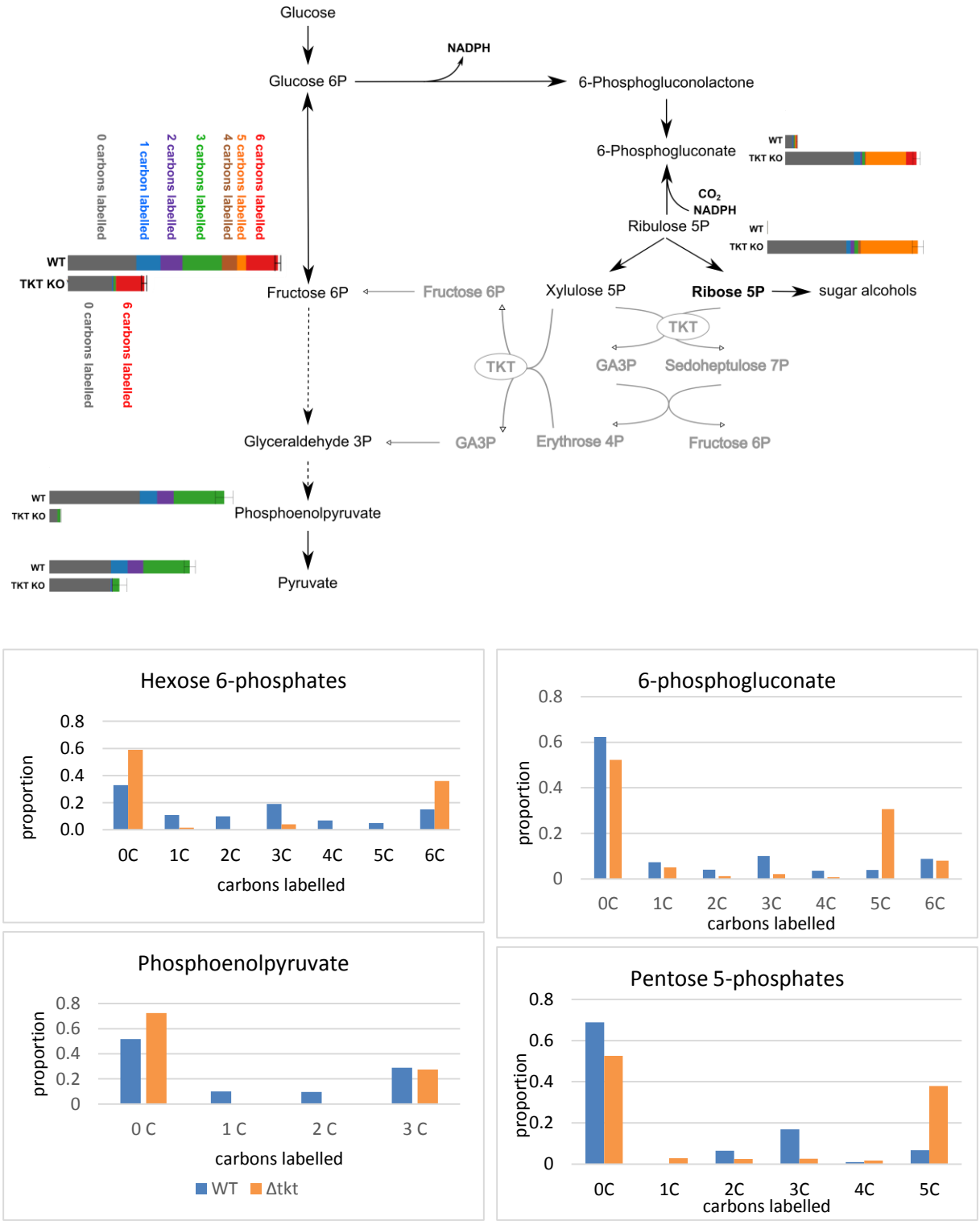

Figure 5.14. Labelling of metabolites of glycolysis and the PPP as determined by LC-MS metabolomics when 50% of glucose is U-^{13}C-glucose. The labelling profile is shown for each metabolite detected. Colour codes for labelling are the same as indicated for hexose phosphates, coloured proportions of each bar represent the relative abundance. Histograms reflect proportion of specific types of labelling in WT in blue and Δtkt in orange.

The labelling experiment provided especially interesting results for the TCA cycle intermediates. Whereas 50 – 60% of the intermediates are labelled to some extent (one to five carbons) in WT, this total sum dropped below 10% in Δtkt (Fig 5.15). This pattern is consistent for succinate, oxoglutarate, pyruvate, glutamate and aspartate. The majority of each of these metabolites is unlabelled indicating they derive from precursors other than glucose. This explains why TCA cycle intermediates do not diminish to the same extent as those of the glycolytic pathway in Δtkt cells, as their derivation involves other carbon sources.

Another intriguing observation arising from this experiment is the labelling pattern of 6PG, where the five carbon labelled species represent 30% of the total in Δtkt cells, a surprisingly large proportion (Fig 5.14). A likely explanation is that the accumulation of Ru5P in the knockout cells causes a change in equilibrium driving the 6PGDH reaction in its "reverse" direction, causing CO_2 assimilation and NADPH consumption, instead of production. The reverse reaction of 6PGDH has been reported previously in sheep liver and *Candida utilis* (Berdis and Cook, 1993; Villet and Dalziel, 1969), but I did not succeed in measuring the enzyme activity in the opposite direction from cell extracts (data not shown).

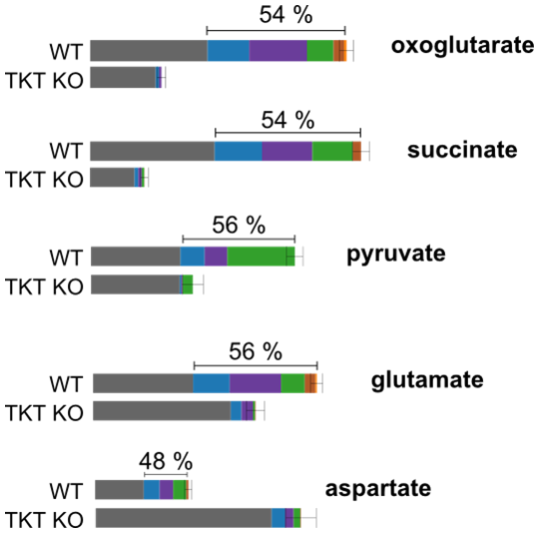

Figure 5.15. Labelling pattern of selected metabolites from LC-MS metabolomics analysis with 50% U-^{13}C-glucose. The grey part represents molecules with no carbons labelled, blue one carbon, purple two carbons, green three carbons, brown four carbons and orange five carbons labelled. Numbers indicate sum of all types of labelling in WT. Natural abundance of ^{13}C is approximately 1%.

5.4.5 Amino acid and fatty acid metabolism

As described above, the TCA cycle in the Δtkt cell line appears to be fed primarily by a carbon source other than glucose. Amino acids and fatty acids are both common carbon sources in various cell types. Hence, I analysed the metabolomics data derived from spent media specifically to assess depletion of amino acids. Aspartate and glutamate are two amino acids previously shown to be incorporated into the TCA cycle intermediates by WT cells to limited extent (Saunders et al., 2011). However, neither of these substrates was consumed more by Δtkt than WT (rather the opposite appeared to be the case on day two (Fig 5.16)). The same is true for other amino acids, all of them either being consumed to the same extent by both cell lines or actually less by Δtkt (Fig 5.16, Appendix A6). It should be noted, that these numbers indicate the relative amounts of each amino acid detected in the media rather than uptake of these amino acids *per se*. In contrast, in spite of no apparent increase in their acquisition from the medium, most of the amino acids were significantly accumulated inside Δtkt cells. Intracellular tryptophan and tyrosine levels accumulated most, about 7 fold and aspartate rose almost 3 times (Tab 5.7). This correlates with data from the RNAseq experiment, where six different genes for amino acid transporters were detected to be two fold increased at the RNA level (whereas one was 5 fold diminished in abundance) (Appendix B3). One of these genes is orthologous to a lysine transporter described in *L. infantum* (Inbar et al., 2012) and two genes are orthologous to an arginine permease AAP3 of *L. donovani* (Shaked-Mishan et al., 2006). All of the amino acids detected reach the same or higher levels in Δtkt as in WT (with an exception of arginine – Tab 5.8) indicating that they are not utilised more for the TCA cycle incorporation than in WT. In addition, no specific amino acid degradation pathway was noted as being upregulated significantly either in the metabolomics or the RNAseq analyses.

The first step in amino acid degradation is transamination producing respective ketoacids. Relatively few ketoacids were detected, but several were slightly increased in Δtkt, and 4-hydroxyphenylpyruvate, the product of tyrosine was more than 4 times higher. Indolepyruvate is detected at higher levels in the spent medium of Δtkt, suggesting that ketoacids are made and secreted from the cells rather than used as source of carbon (Fig 5.17; Tab 5.7). Amino acid metabolism was speculated to be connected with immune system evasion, either by depleting the host of amino acids, or by producing

ketoacids or other intermediates directly affecting host's immune response (Westrop et al., 2015).

Altogether, no straightforward conclusions can be made about amino acid metabolism. They are accumulated inside the cells, but we cannot determine if it is due to higher uptake or lower utilisation. The ambivalence is increased by peptides, since there are numerous peptides of undefined composition present in the media, which become degraded and contribute to the amino acid pool in the media.

Even though fatty acids were shown not to be used in the TCA cycle by WT promastigotes, they are used by amastigotes and it was shown previously that under non-optimal conditions *Leishmania* adapt and change their metabolism (Rodriguez-Contreras and Hamilton, 2014). However, not a single metabolite from the list of fatty acids or all lipids was consumed more by Δtkt than WT (Fig 5.18).

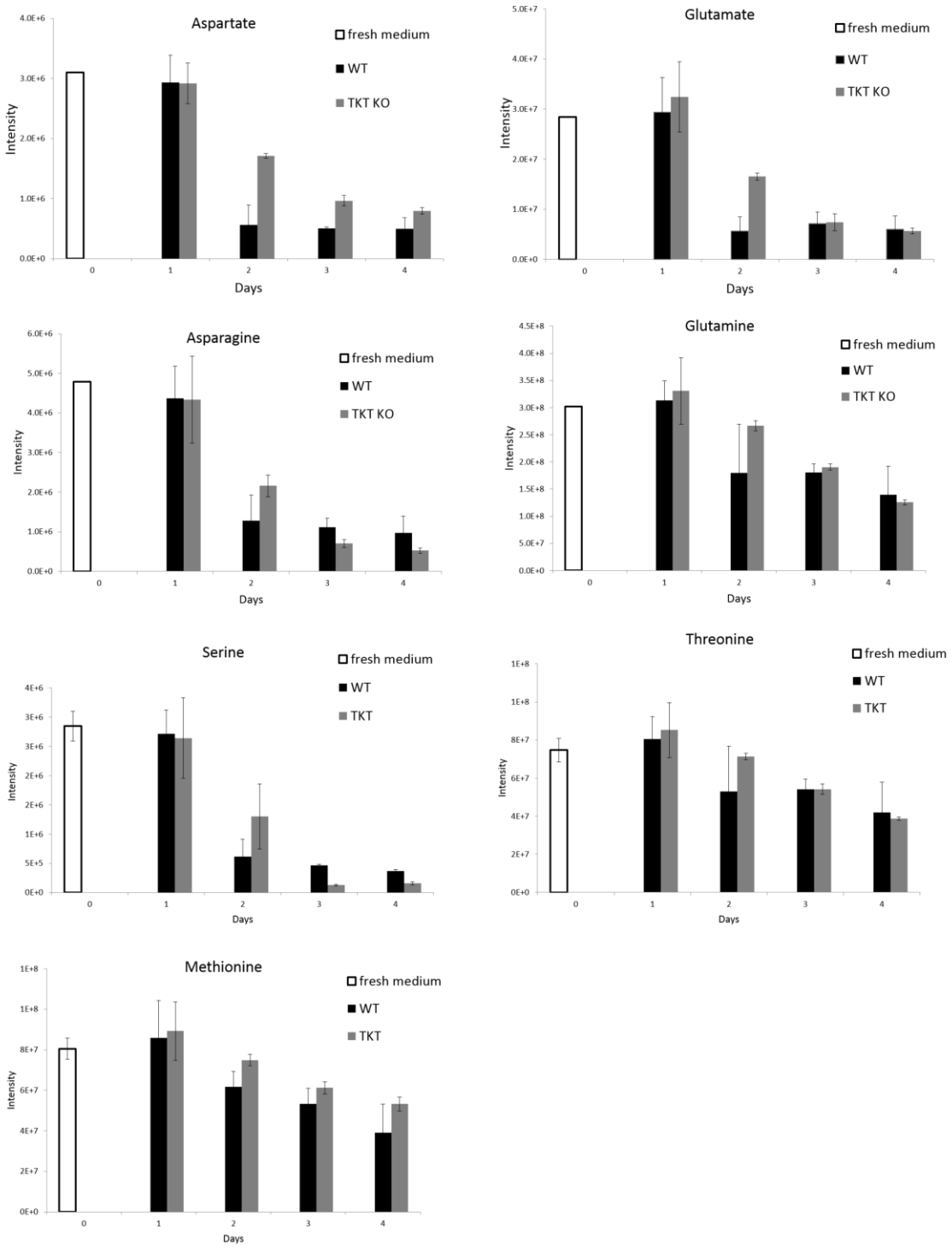

Figure 5.16. LC-MS metabolomics of spent media on days 1 to 4. The most consumed amino acids are shown. White – fresh medium, black – WT, grey – Δtkt. Error bars represent standard deviation, n=4.

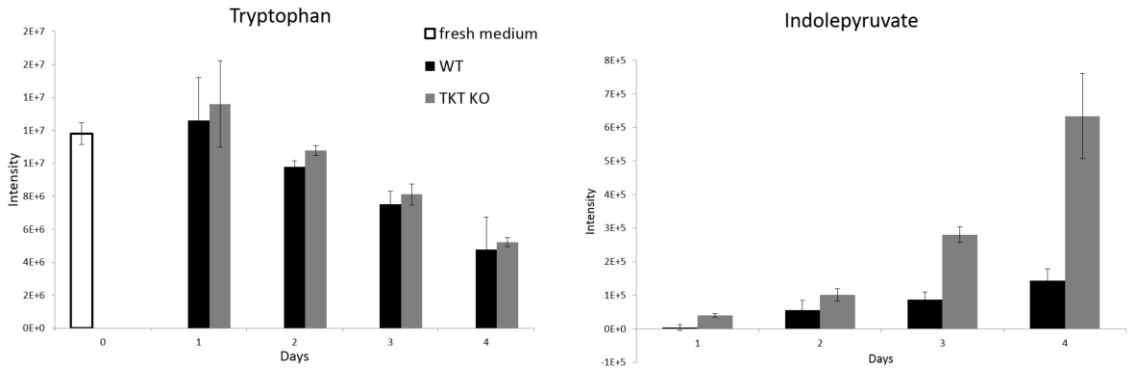

Figure 5.17 LC-MS metabolomics of spent media, abundance of tryptophan and its ketoacid, indolepyruvate. White – fresh medium, black – WT, grey – Δtkt. Error bars represent standard deviation, n=4.

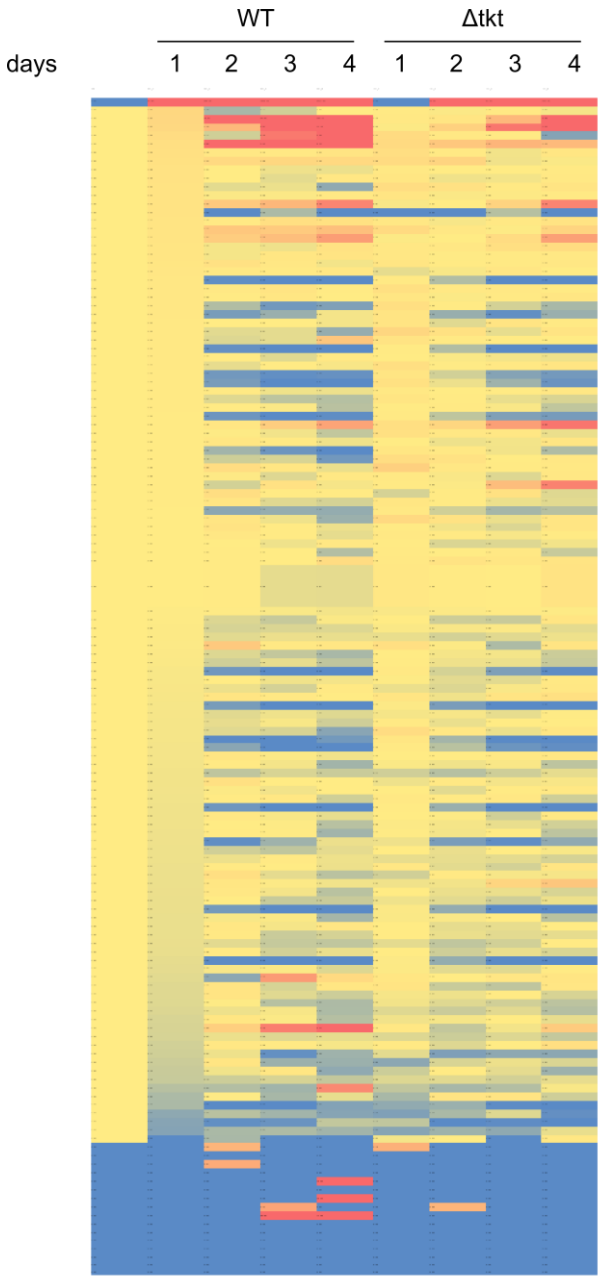

Figure 5.18. Heatmap of lipids in the spent medium over four days, as determined by LC-MS metabolomics. The first column shows fresh medium and the following columns spent medium on days 1 to 4 in WT and Δtkt, respectively. Yellow colour indicates no change, blue decrease and red increase. No big differences were observed between the two cell lines.

Intracellular amino acids				**ketoacids**			
	Δtkt	Δtkt + TKT	p-value (Δtkt/WT)		Δtkt	Δtkt + TKT	p-value (Δtkt/WT)
Tryptophan	7.41	0.52	0.001	**indole-3-pyruvate**	ND *	ND	-
Tyrosine	6.36	2.68	0.002	**4-hydroxyphenylpyruvate**	4.58	2.84	0.04
Leucine	2.41	1.52	2×10^{-5}	**3-methyl-2-oxopentanoate**	1.74	3.19	0.05
Histidine	2.31	1.53	2×10^{-4}	**urocanate**	1.67	1.22	NS
Valine	1.98	1.29	4×10^{-5}	**3-Methyl-2-oxobutanoic acid**	1.2	1.81	NS
Glutamine	1.5	0.37	NS	**2-oxoglutaramate**	1.61	0.8	NS

Table 5.7. Intracellular levels of amino acids and ketoacids as determined by LC-MS metabolomics. Numbers indicate relative abundance in Δtkt and Δtkt + TKT compared to WT. ND = not detected, NS = not significant, p>0.05, * substantial quantities in the spent medium

.

Intracellular amino acids			
	Δtkt	Δtkt + TKT	p-value (Δtkt / WT)
Phenylalanine	3.96	2.56	3×10^{-4}
Methionine	3.56	1.34	4×10^{-4}
Serine	3.2	0.91	2×10^{-4}
Aspartate	2.83	0.72	2×10^{-4}
Glycine	2.38	1.6	2×10^{-4}
Asparagine	2.09	0.72	0.002
Threonine	1.42	1.45	0.04
Lysine	1.28	1.62	NS
Glutamate	0.93	0.53	NS
Proline	0.92	0.62	NS
Alanine	0.89	1.44	NS
Arginine	0.49	0.98	0.002

Table 5.8. Intracellular levels of amino acids as determined by LC-MS metabolomics. Corresponding ketoacids were not detected. Numbers indicate relative abundance in Δtkt and Δtkt + TKT compared to WT. ND = not detected, NS = not significant, $p>0.05$

5.5 Elucidating consequences of TKT deletion

As discussed in the previous chapter, the metabolomics data indicate that TKT deletion caused not only perturbation in the PPP as expected, but also further changes in central carbon metabolism, which indicates cross-talk between pathways involved in glucose metabolism beyond the simple perturbations associated with loss of the individual reactions catalysed by TKT. These extended alterations to metabolism are extremely interesting, because they indicate that mechanisms of adaptation of metabolism and regulatory mechanisms in the parasites are operative. Hence, I strived to dissect the regulatory mechanism, since it may be a novel feedback control of glycolysis in *Leishmania*.

5.5.1 Determination of the PPP flux in WT *L. mexicana*

One explanation for the metabolic flux decrease in glycolysis could be the lack of the metabolites returning from the PPP loop which is disrupted. In order to test this hypothesis, metabolic flux in the PPP in WT promastigote *L. mexicana* was measured according to method published by Lee et al. (1998). Even though the PPP flux was estimated previously in promastigote *L. mexicana* (Maugeri et al., 2003), the authors followed incorporation of labelled glucose into nucleic acids, which may be inaccurate due to preferential utilisation of ribose as I showed in Chapter 4. I used a method when cells are grown in 100% 1,2-^{13}C-glucose and any glucose used in glycolysis produces three carbon intermediates (for example pyruvate) that have two or no carbons labelled. Whereas if 1,2-^{13}C-glucose is channelled into the PPP, one labelled carbon is cleaved off as a CO_2 molecule by the 6PGDH reaction, and subsequent three carbon products have one or no carbons labelled. Thus, the proportion of different labelling in three carbon intermediates indicates the relative utilisation of glucose in glycolysis or the PPP (scheme shown in Fig 5.19). I assessed the labelling distribution in PEP and 3-PG and calculated that 14% of glucose enters the PPP, which is a number matching with previous reports (Maugeri and Cazzulo, 2004; Maugeri et al., 2003). Considering the overall glucose consumption established in chapter 3.3.3, an estimated 0.546 nmol of glucose enters the PPP in 10^8 cells/min.

However, this calculation indicates that the disruption of the PPP in Δtkt is unlikely to account for the substantial decrease in glycolytic flux. Glucose consumption dropped by

25% and production of succinate and malate indicates an even bigger decrease. Most likely, such big drop is caused by a mechanism beyond a 14% reduction in glucose flux.

A significant labelling with different numbers of carbons labelled was observed in hexose phosphates in WT cells in two different experiments, first using 50% U-^{13}C-glucose and second, using 100% 1,2-^{13}C-glucose (Fig 5.20). Presumably, this high proportion of different types of labelling comes from the carbon shuffling in the non-oxidative branch of the PPP, as can be verified by its disappearance in Δtkt. Both of these labelling patterns indicate a flux involving much more than 14% of total glucose. 14% represents the PPP net flux, but there may be high reverse flux in the non-oxidative branch, which would account for the variable labelling patterns in individual metabolites However, considering the nature of the TKT and TAL reactions, they do not operate in the unidirectional pathway usually depicted in textbooks, but rather act to exchange carbons between sugar phosphates in various combinations and order.

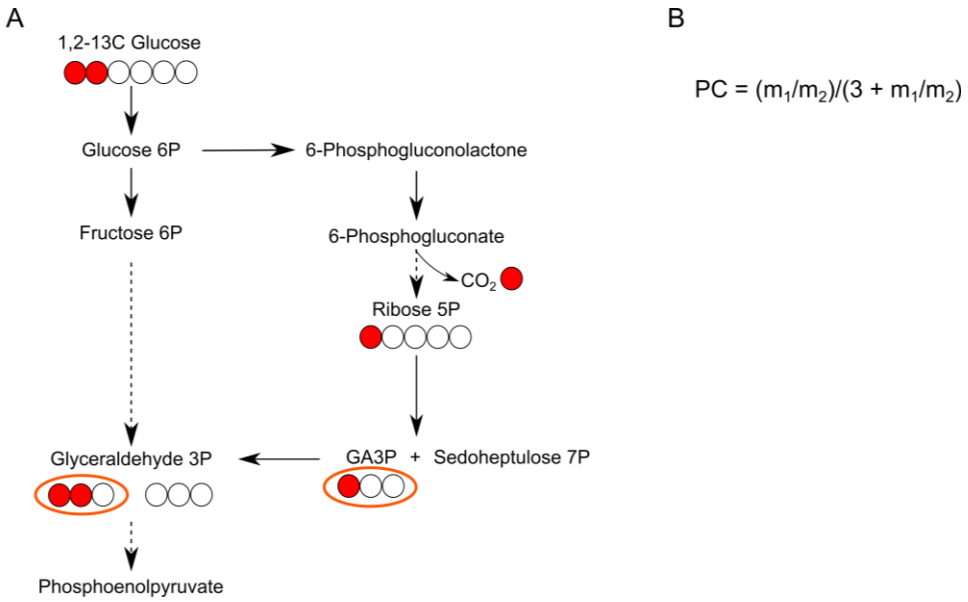

Figure 5.19.The PPP flux. A - Scheme of experiment design for the PPP flux calculation. B - Equation used to calculate the PPP flux, PC – pentose cycle flux, m_1 – intensity of molecules containing one ^{13}C substitution, m_2 – intensity of molecules containing two ^{13}C substitutions, adapted from Lee et al., (1998).

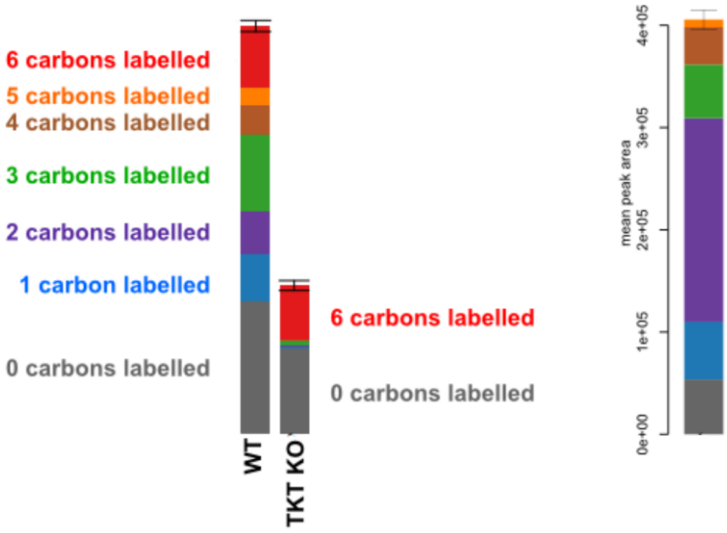

Figure 5.20. Labelling patterns of hexose phosphates, when 50% of U-^{13}C-glucose (A) and 100% 1,2-^{13}C-glucose (B) is used. Colour codes are the same.

5.5.2 Metabolomics of Δtkt supplemented with fructose

Another potential explanation for the observed decrease in glycolytic flux is inhibition of PGI. It is well established that PGI can by inhibited by 6PG *in vitro* (Milewski et al., 2006; Tsuboi et al., 1971). High accumulation of 6PG in our study then sparks a hypothesis, that the glycolytic flux may be decreased as a consequence of PGI inhibition by 6PG. If it was the case, then feeding Δtkt cells on fructose should rescue the phenotype, since fructose can be phosphorylated by hexokinase and enter glycolysis downstream of PGI. I performed LC-MS metabolomics analysis with WT and Δtkt cells grown in the presence of either glucose or fructose. However, the results showed almost no difference in the metabolomics profiles of Δtkt cells irrespective of which sugar was used (Fig 5.21). Glycolytic intermediates were decreased to the same extent in both cases. The only metabolite which was partly rescued was mannogen, the storage polysaccharide of *Leishmania*. We can detect tetra-, penta- and hexamers of glucose, which consistently show the same trend and they all probably represent mannogen subunits (Fig 5.21 B). The mannogen pathway is shown in Fig 5.25, but it does not offer a clear explanation as to why the levels are higher in the presence of fructose. Thus, these results are not consistent with inhibition of PGI as the control mechanism of glycolysis in Δtkt.

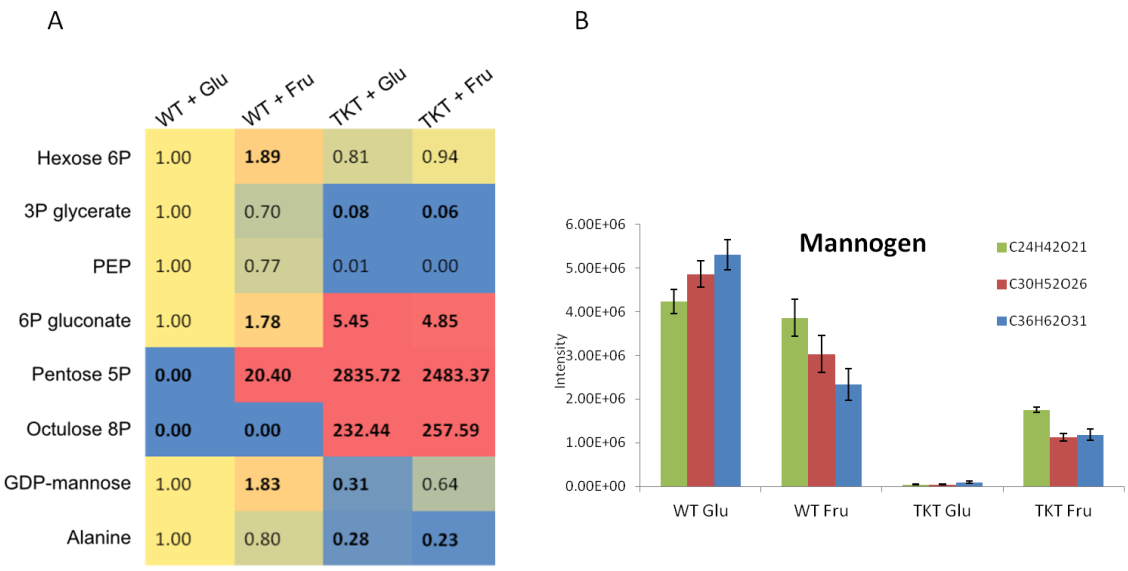

Figure 5.21. WT and Δtkt cells grown solely in the presence of glucose or fructose. A – Overview of representative and most changing metabolites. B – Levels of sugar polymers, presumably all representing mannogen.

5.5.3 RNAseq analysis of Δtkt

To obtain an overall image of the changes happening at the RNA level, I performed RNAseq analysis of WT, Δtkt and Δtkt + TKT promastigote cells harvested in mid-log growth phase. We wanted to examine if diminished glycolysis correlated with reduced mRNA levels and if there were any other changes in mRNA abundance, which would explain the downstream effects in metabolism observed.

Overall, there were about 150 genes which were two fold or more abundant in Δtkt cells, of which only 14 genes were overexpressed three times or more, and a similar number of genes was downregulated (Fig 5.22). Fig 5.23 shows relative changes in mRNA levels of glycolytic and PPP enzymes in Δtkt compared to WT. mRNA of most glycolytic enzymes dropped to about 70% of their WT levels, which does not seem to be enough to cause such a big perturbation to the metabolism. Since the ways by which glycolysis in *Leishmania* is controlled has not been investigated, no clear conclusions can be drawn, but no single enzyme stands out as offering control at the mRNA level. Enzymes of the PPP did not show substantial changes either; only ribose 5-phosphate isomerase mRNA was present at higher levels (almost two fold increased) while the other enzymes were slightly downregulated.

One of the biggest changes, a three-fold decrease, was observed for mannose 1-phosphate guanysyltransferase. This enzyme was not considered in the core mannogen biosynthesis pathway previously (Naderer et al., 2010), but because it produces GDP-mannose from mannose and GTP, it may be contributing to the polysaccharide biosynthesis substantially (Fig 5.24). Hence, this decrease in mRNA level may be responsible for the drop in mannogen in Δtkt. Whether this decrease relates directly to the loss of TKT, however, is not certa in, since mannogen levels were not restored when re-expressing TKT.

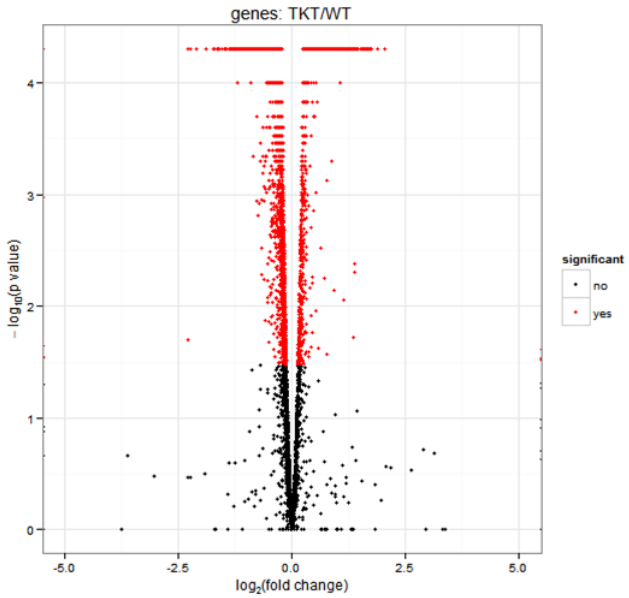

Figure 5.22. Volcano plot of RNAseq analysis.

mRNAs encoding three enzymes putatively involved in oxidative stress defence: ornithine decarboxylase, putative acetylornithine deactylase, and ascorbate peroxidise are increased by more than two fold, which might represent an adaptation to the increased oxidative stress related to diminished NADPH production. The RNAseq analysis did not offer a clear, simple explanation for the decrease in central metabolic flux in the Δtkt mutant, not indicate possible alternative carbon source usage. Control mechanisms in *Leishmania* do not, therefore, have their basis primarily in the levels of mRNA of metabolic enzymes, but further downstream, on translation or enzyme activity levels.

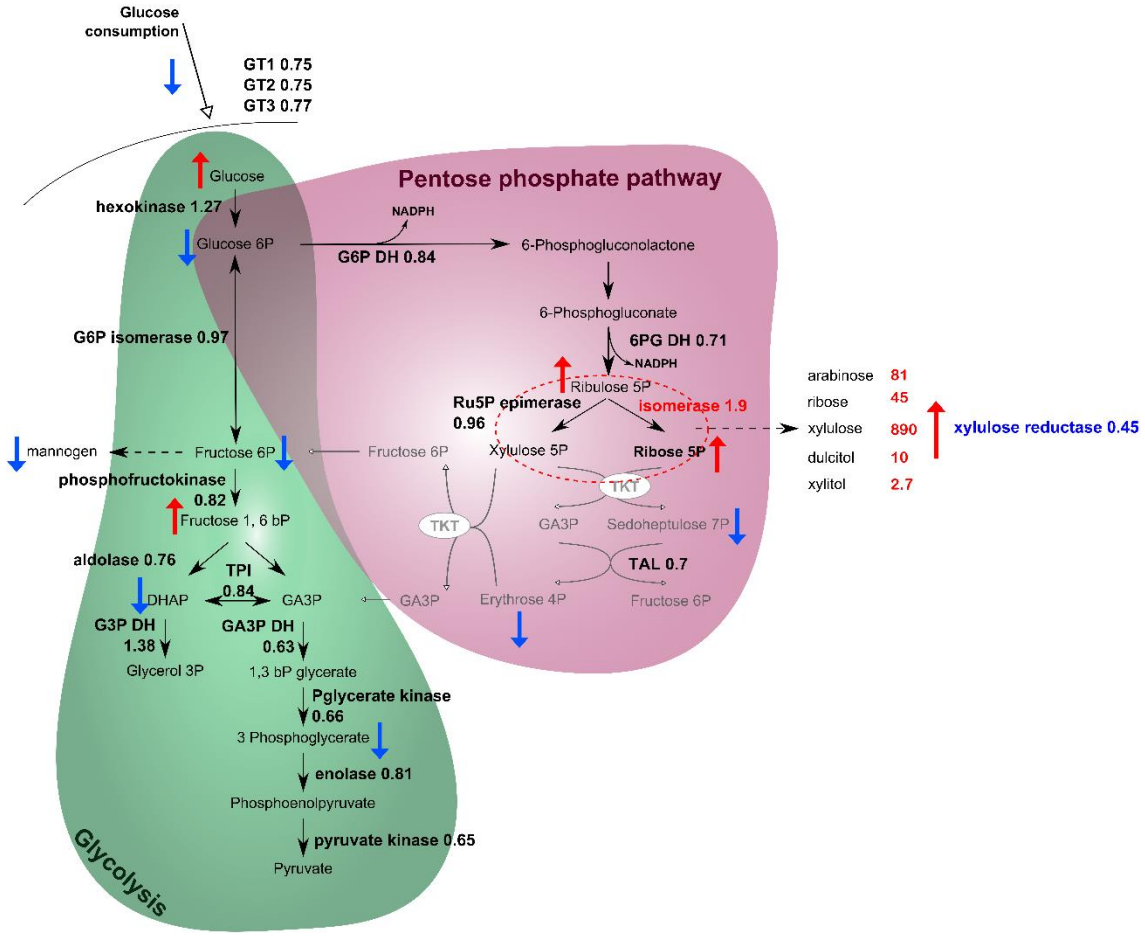

Figure 5.23. A scheme of glycolysis and the PPP with indicated changes in mRNA levels of the respective enzymes, values represent relative amount in Δtkt when compared to WT. The coloured arrows indicate changes in metabolites as detected by GC-MS metabolomics (from Fig 5.11).

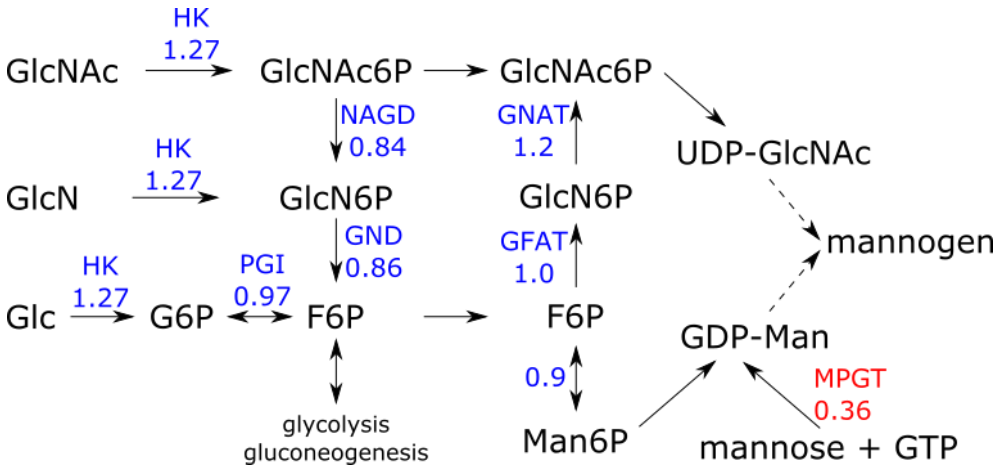

Figure 5.24. Scheme of mannogen biosynthesis, blue and red colours indicate enzymes and relative mRNA abundance in Δtkt when compared to WT. GlcNAc – N-acetylglucosamine, GlcN – glucosamine, Glc – glucose, GlcNAc6P – N-acetylglucosamine 6-phosphate, GlcN6P – glucosamine 6-phosphate, G6P – glucose 6-phosphate, F6P – fructose 6-phosphate, Man6P – mannose 6-phosphate, UDP-GlcNAc – uridine diphosphate N-acetylglucosamine, GDP-Man – guanosine diphosphate mannose, GTP – guanidine triphosphate, HK – hexokinase, PGI – glucose-6-phosphate isomerase, NAGD – N-acetylglucosamine-6-phosphate deacetylase, GND – glucosamine-6-phosphate deaminase, GNAT – glucosamine-6-phosphate acetylase, GFAT – glutamine:Fru6P aminotransferase, MPGT – mannose-1-phosphate guanylyltransferase; adapted from Naderer et al. (2010).

5.5.4 Measurement of activities of glycolytic enzymes

RNA levels merely point to the degree to which a gene is transcribed and its message retained at a steady state level. Translational control can mean that the enzyme produced is not directly related to the levels of that RNA and further regulation of enzyme activity (e.g. by post-translational modification, or allosteric control) can lead to phenotypic changes that have no direct correlation to RNA levels. Measuring the specific activity of individual enzymes has been used classically to determine contributions of enzymes to the metabolic network, thus I measured several enzyme activities to assess if there is any difference between WT and Δtkt.

Activities of hexokinase, glucose 6-phosphate isomerase, fructose 1,6-bisphosphate aldolase, and the two dehydrogenases from the PPP were measured and the values are in Tab 5.9. Both glucose 6-phosphate and 6-phosphogluconate dehydrogenases are not changed after TKT deletion. The only enzyme, showing significantly changed activity was fructose 1,6-bisphosphate aldolase (FbPase) which decreased two fold in Δtkt ($p=0.0005$). This is especially interesting because this correlates with the GC-MS data (chapter 3.3.2), where F1,6bP, the substrate of FbPase, was accumulated and DHAP, its product was twenty fold decreased. From a broader perspective it also corresponds with the LC-MS data, where the largest measured decreases in metabolite levels occurred in the lower part of glycolysis.

	activity (nmol/min/mg protein)	
	WT	**Δtkt**
hexokinase	296 (±161)	429 (±139)
glucose-6-phosphate isomerase	338 (± 55)	232 (±28)
fructose-1,6-bisphosphate aldolase	202 (±15)	95 (±11)
glucose-6-phosphate dehydrogenase	128 (±15)	107 (±25)
6-phosphogluconate dehydrogenase	131 (±20)	101 (±23)

Table 5.9. Activities of selected enzymes of glycolysis and the PPP as measured on whole cell extracts. n = 4 – 5, values in brackets represent standard error of mean.

5.6 Localisation of TKT in *L. mexicana*

It is known that the PPP has dual localisation in all trypanosomatids, as it is present both in the cytosol and in glycosomes (Igoillo-Esteve et al., 2007). The same is true for TKT in *L. mexicana*, as was shown by digitonin fractionation and enzyme activity measurement (Veitch et al., 2004). Due to instability and flexibility of the C-terminal part, its precise structure could not be resolved using X-ray crystallography (Veitch et al., 2004). Later, a preliminary experiment suggested that the addition of different substrates to TKT influences its ability to bind to PEX5 (Wildridge, 2012). Since this interaction depends upon the PTS1 sequence, which is represented by the last three amino acid residues (SKM), these data suggest there may be a connection between the flexibility of the C-terminus and binding to PEX machinery. Hypothetically, binding of different substrates could trigger conformational changes in the enzyme structure, which subsequently determine the exposure and availability of the PTS1 sequence for PEX5. Subsequently, this would determine if the enzyme is retained in the cytosol, or imported into a glycosome. I addressed this hypothesis and the first results led to further experiments and studies about consequences of different subcellular localisation of TKT.

5.6.1 Localisation of TKT with varied C-termini

Presuming the hypothesis formulated above is correct, then an enzyme variant with an artificially extended C-terminus may have its PTS1 always exposed and, therefore, be always imported into glycosomes. Based on this premise, I prepared a series of constructs using a pNUS family vector for episomal overexpression of proteins in *Leishmania*, with a GFP tag attached to the N-terminus of TKT (Fig 5.25). These constructs had alternations in the C-termini, so that TKT was elongated by 10, 20 or 30 amino acids, or else truncated by 10 or 20 amino acids. The extension was made by repeating the amino acids of the flexible C-terminus preceding the SKM targeting sequence and similarly, the deletions were cut by the residues preceding the terminal tripeptide, but retaining the SKM sequence itself. All of these constructs were transfected into both WT and Δtkt cell lines. Fig 5.26 shows the results of immunofluorescence analysis (IFA) with varied GFP-TKTs and antibody against triosephosphate isomerase used as a glycosomal marker, and Fig 5.27 shows control Western blot analyses.

WT GFP-TKT is distributed throughout the leishmanial cell. Different mutant proteins, however, are found in the two compartments in variable proportions. The most interesting is the variant of TKT shorter by 10 AA, which is present primarily in glycosomes. The proteins elongated by 10 and 20 AA also seem to be mostly glycosomal but with a more notable proportion remaining in the cytosol. The other constructs: TKT plus 30 AA and TKT minus 20 AA show the same localisation as WT TKT. These results confirm that C-terminus controls subcellular localisation of TKT but not in the manner hypothesised earlier. There is no clear pattern in the results, so it is impossible to dissect how exactly the localisation control works.

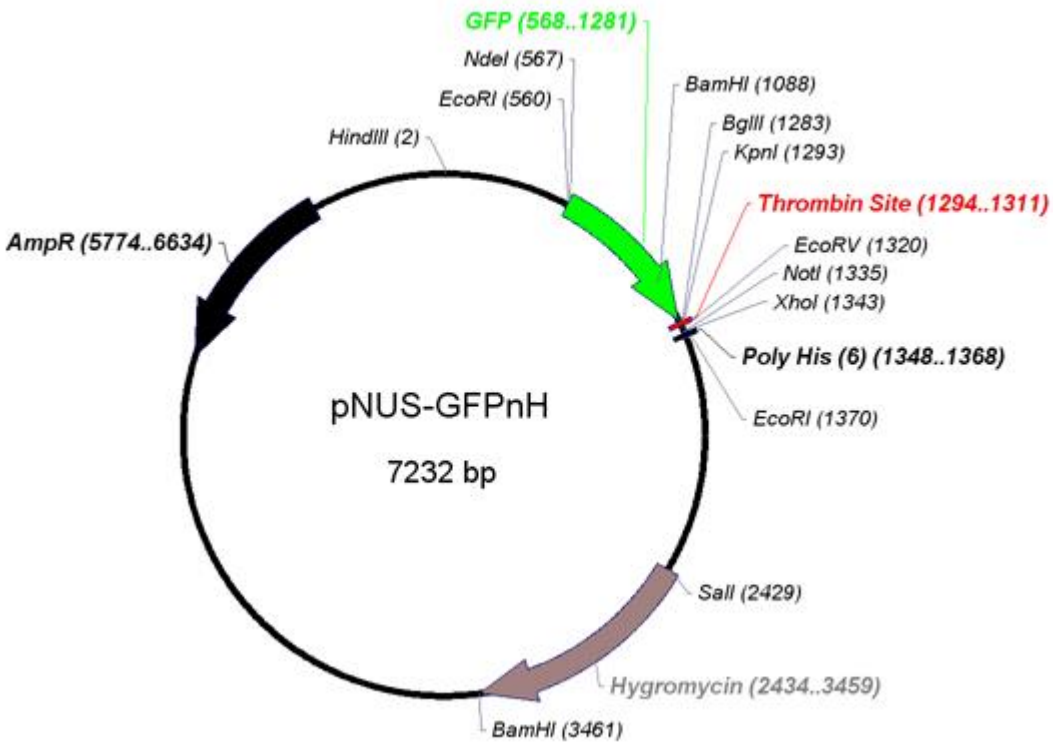

Figure 5.25. Scheme of the pNUS-GFPnH plasmid used for GFP-TKT expression. TKT was ligated into *Bgl*II and *Xho*I restriction sites (http://www.ibgc.u-bordeaux2.fr/pNUS/greenvectors.html#map).

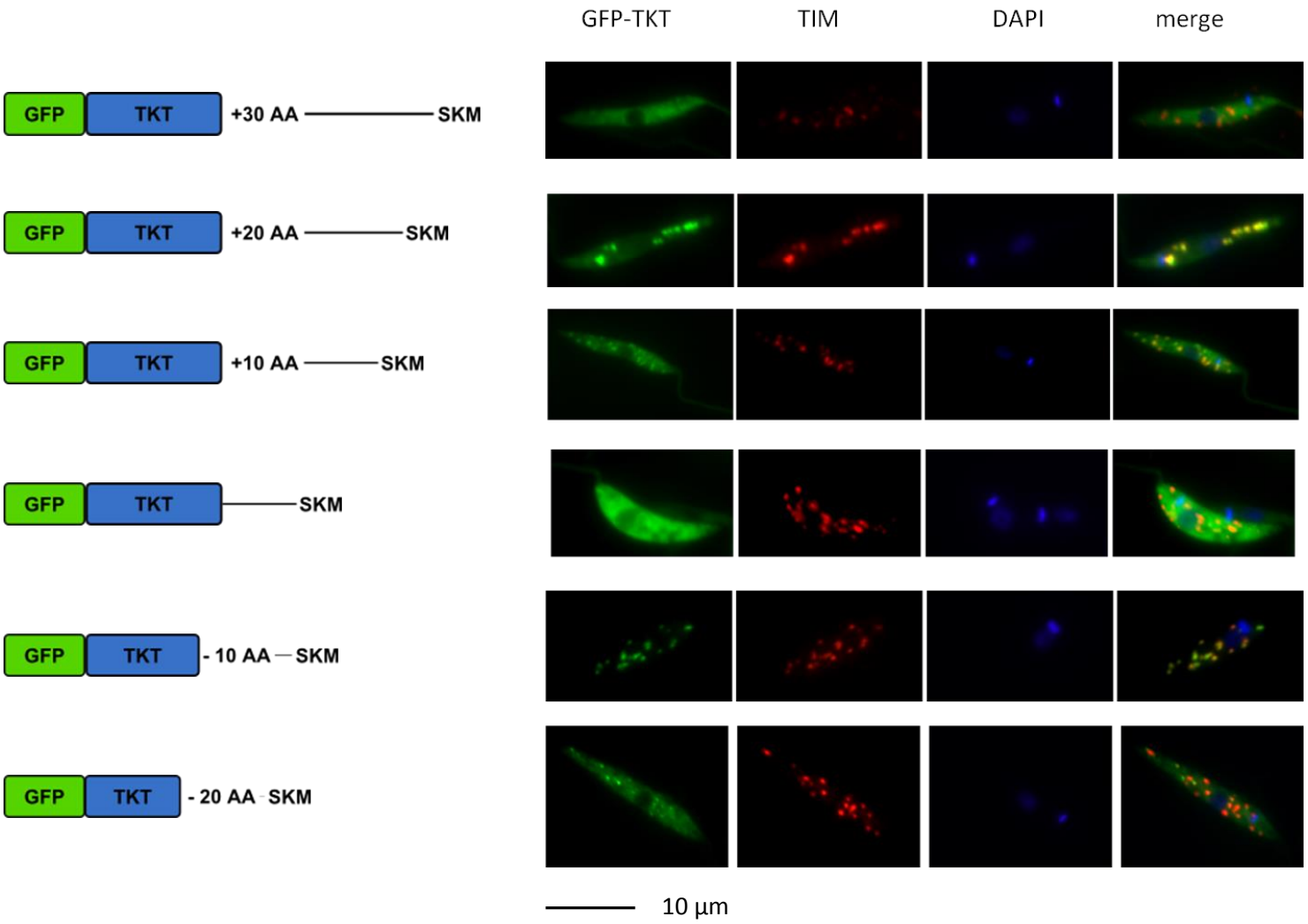

Figure 5.26. Immunofluorescence microscopy of WT cells transfected with all variants of altered GFP-TKT constructs. Cartoons on the left represent the variants from the longest at the top to the shortest at the bottom. TIM was used as a glycosomal marker.

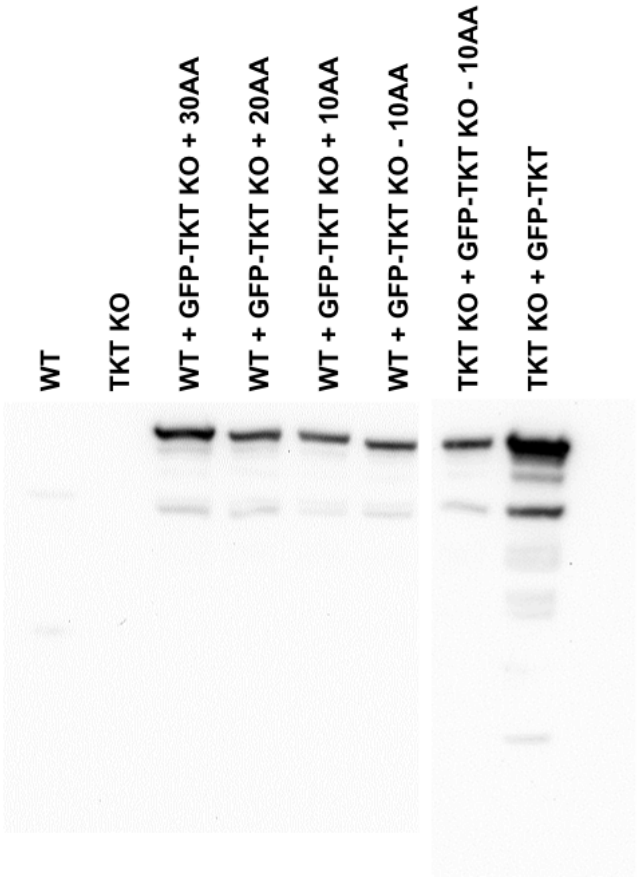

Figure 5.27. Control WB for the cell lines depicted in Fig 5.26, staining with α-GFP antibody.

5.6.2 Digitonin fractionation

Another method used to study subcellular localisation of proteins in trypanosomatids is digitonin fractionation followed by Western blot analysis or enzyme activity measurement. Hence, I used the transfected cell lines for the experiment, incubating cell samples with increasing amounts of digitonin and using the lysates for Western blot analysis. I used enolase as a marker for the cytosol and glycerol-3-phosphate dehydrogenase (GDH) as a marker of glycosomes, which showed that glycosomes were disrupted by 0.8 mg/ml digitonin (Fig 5.28 B). When using cells expressing GFP-TKT, the α-GFP signal was detected in all fractions, and the signal in the first fraction seemed relatively strong compared to the enolase signal. Most probably expression of GFP-TKT

was so high, that the protein contaminated all fractions, even those where WT TKT is not present. High TKT overexpression was indicated by enzyme activity measurements in these cell lines (Tab 5.1).

Subsequently, I repeated the digitonin fractionation experiment with the Δtkt + glyco GFP-TKT cell line. However, TKT was again released even in fractions treated with the lowest concentration of detergent used, whereas GDH was released only by 0.8 mg/ml digitonin (Fig 5.29). Similarly as in the previous case, that is most likely caused by high expression of the GFP-TKT-10AA protein, which contaminated all the fractions. Hence, no conclusions can be made from this set of experiments and I was not able to confirm the IFA data by digitonin fractionation.

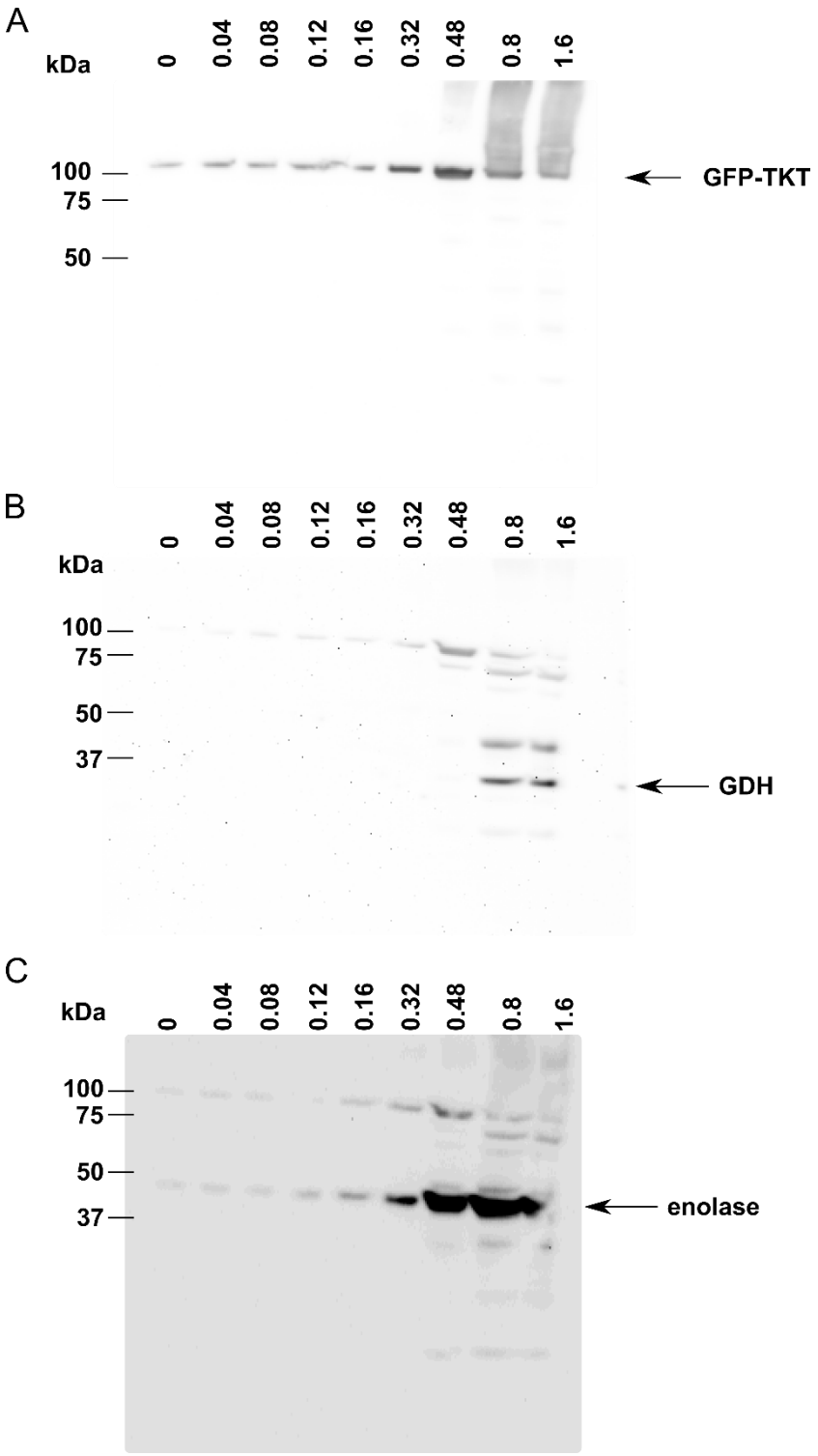

Figure 5.28. Western blots of digitonin fractionation of Δtkt + GFP-TKT cell line. Numbers at the top indicate concentration of digitonin (mg/ml) in the respective fractions. A – α-GFP antibody staining for detection of GFP-TKT, B – α-GDH antibody staining as a glycosomal marker, C – α-enolase staining as a cytosolic marker; GFP-TKT is 100 kDa in size, GDH 39 kDa and enolase 46 kDa. .

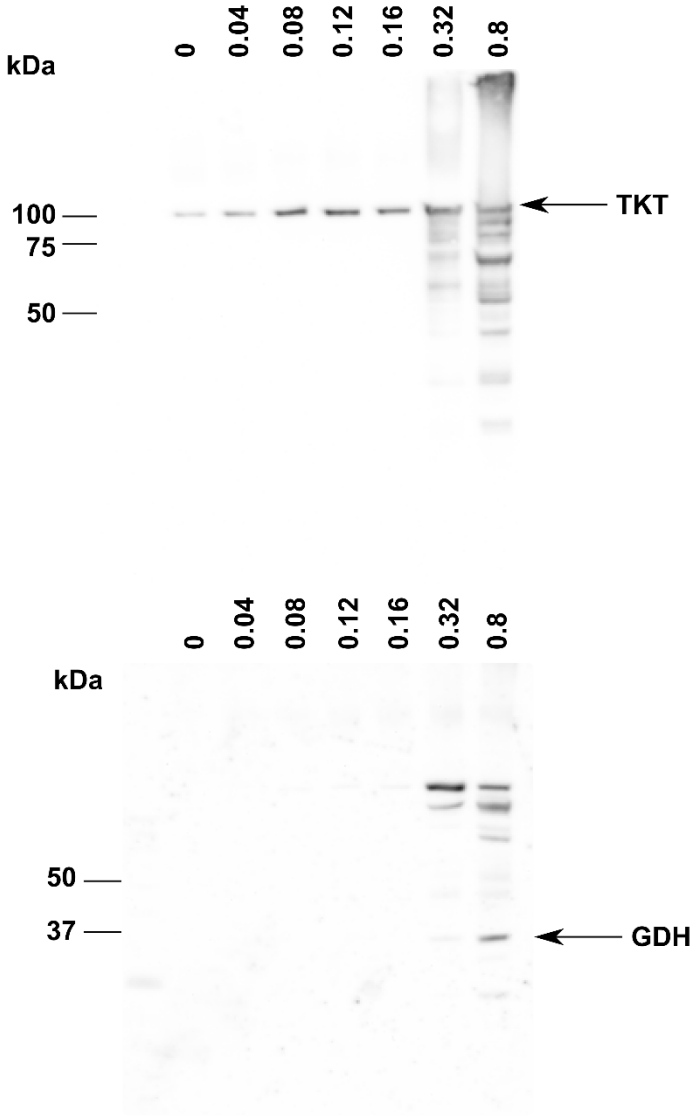

Figure 5.29. Western blots of digitonin fractionation of Δtkt + GFP-TKT-10AA cell line. Numbers at the top indicate concentration of digitonin (mg/ml) in the respective fractions. A – α-GFP antibody staining for detection of GFP-TKT, B – α-GDH antibody staining as a glycosomal marker.

5.6.3 Phenotypic and metabolomic comparison of cells expressing solely cytosolic or solely glycosomal TKT

The cell line Δtkt + GFP-TKT-10AA (later called Δtkt + glyco GFP-TKT) has TKT present solely in glycosomes. To give a comparison between cells in which TKT is found primarily in the glycosome with one where it is found only in the cytosol, the Δtkt cells were transfected with a GFP-TKT construct from which the PTS1 tripeptide was truncated (called Δtkt + cyto GFP-TKT). Subsequently, I performed a series of experiments focused on comparison of these two cell lines. I expected that such major manipulation with localisation of TKT should cause negative effects on the cells and thus indicate what specific functions TKT has in the respective compartments.

First, I assessed the growth of promastigotes and there was no difference in growth rate between cells expressing solely cytosolic or solely glycosomal TKT (Fig 5.30). Next, I tested sensitivity to oxidative stress by Alamar Blue Assay with glucose oxidase as described earlier, nevertheless both the cell lines were susceptible to the same extent (Fig 5.31). Finally, I performed LC-MS metabolomic experiment with these two cell lines. Surprisingly, there were, once again, only minimal differences between them and metabolites of the highest interest, i.e. those from glycolysis and the PPP did not differ (Fig 5.32). The only differences were in ribose 1,5-bisphosphate which reaches only half the abundance in Δtkt + glyco GFP-TKT than in Δtkt + cyto GFP-TKT, and O8P which is decreased in the cell line with the glycosomal TKT compared to the line expressing the cytosolic variant.

Based on this data, I can conclude that subcellular localisation of TKT in the promastigote stage plays no demonstrable role and the cells are apparently not affected by having the enzyme only in a single compartment.

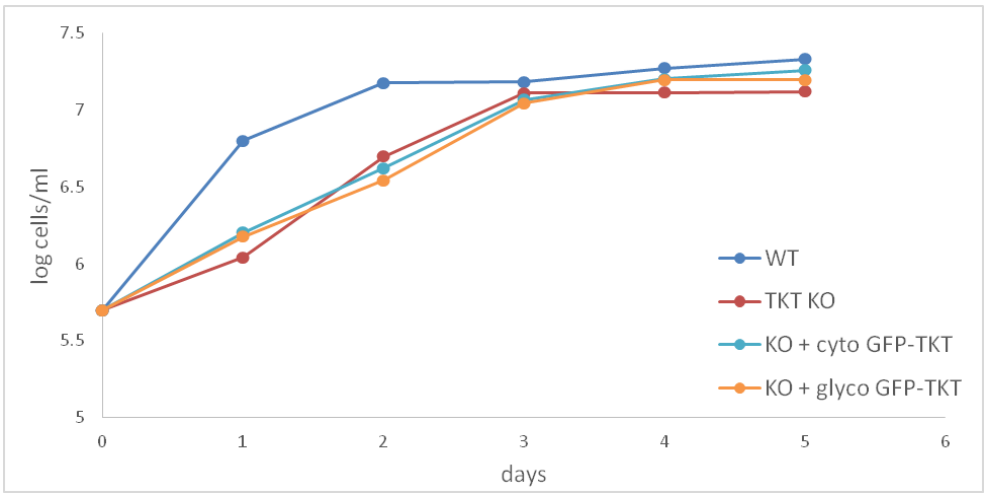

Figure 5.30. Growth curves of Δtkt cells expressing cyto GFP-TKT or glyco GFP-TKT.

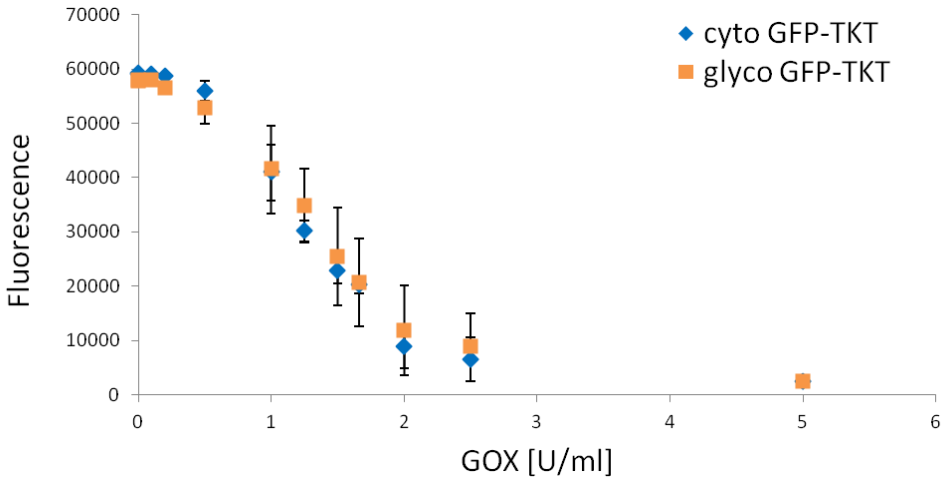

Figure 5.31. Alamar Blue Assay with GOX and Δtkt cells expressing cyto GFP-TKT or glyco GFP-TKT, fluorescence detected corresponds with viability of cells.

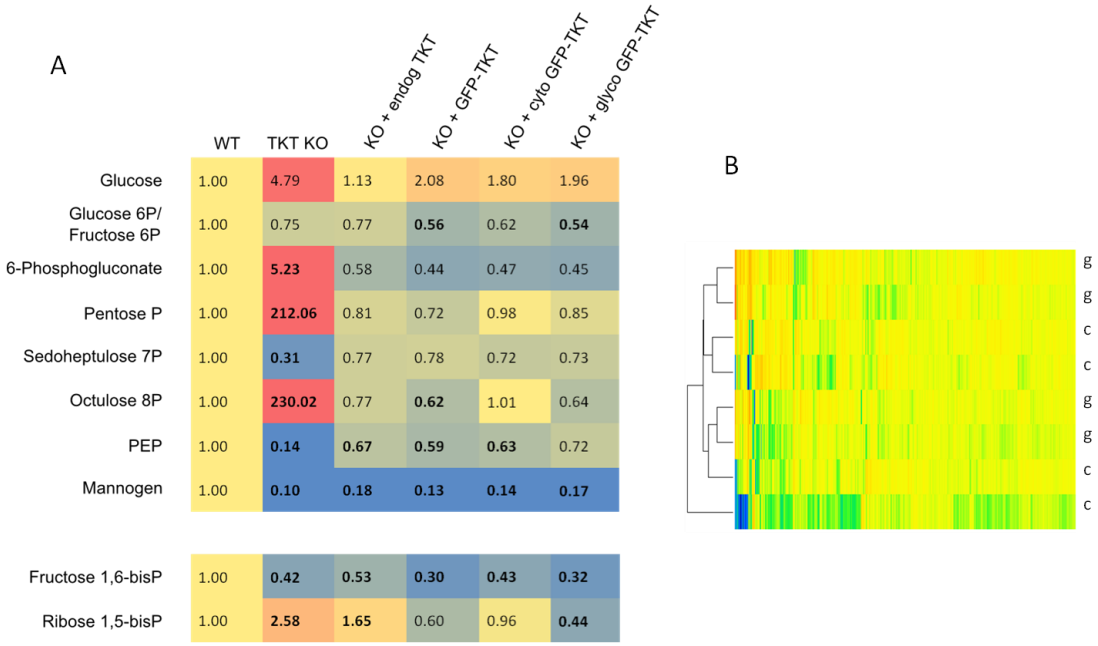

Figure 5.32. LC-MS metabolomics comparison between Δtkt + cyto GFP-TKT and Δtkt + glyco GFP-TKT. A - Selected metabolites of glycolysis and the PPP for various TKT cell lines, the numbers represent relative abundance compared to WT. B – Heat map of all the metabolites detected, each line represents one biological replicate, g = Δtkt + glyco GFP-TKT, c = Δtkt + cyto GFP-TKT, yellow indicates no change, red increase and green decrease.

5.7 Discussion

5.7.1 Growth, sensitivity to stress, infectivity

It is very interesting that the *L. mexicana* Δtkt cell line has no visible phenotype in the promastigote stage but is of reduced viability in the amastigote stage. This underlines the diversity of the two life stages, but also it points towards flexibility and adaptability of the cells, given how promastigote metabolism is clearly altered to a fairly large degree and yet no growth or morphological defect is evident, and even sensitivity to oxidative stress and various drugs is only marginally increased. When assessing oxidative stress sensitivity, I obtained different results for methylene blue and for glucose oxidase (which constitutively produced hydrogen peroxide). Since the mode of action of methylene blue is not precisely known, glucose oxidase is more reliable agent, in addition, it creates oxidative stress continuously, assuming the enzyme was stable in the growth medium. Still, the sensitivity in Δtkt was increased only two times.

When working with axenic amastigotes, I observed that Δtkt cells differentiated into the amastigote form, but did not grow thereafter. However, the Δtkt + TKT cell line did not grow as amastigotes either, indicating that a change other than loss of TKT *per se* might have been acquired during cultivation that precludes growth of amastigotes, thus no conclusions can be made at this point. I proceeded with macrophage infection assays. It was the case that Δtkt cells infected two times fewer macrophages, but the data were inconclusive due to high variability. Some of the later infection time points showed increased infection rates due to continuing infection with extracellular parasites. Moreover, we could not be sure about fitness of the *Leishmania* cells as they had been maintained in culture for long time and it is known that *Leishmania* lose infectivity *in vitro* (Pescher et al., 2011).

In contrast to the lack of clarity in macrophage infections, mice infections provided clear results as animals injected with Δtkt *Leishmania* did not develop any leishmaniasis related lesions and the parasites could not be recovered from lymph nodes. At the same time, Δtkt + TKT cell line caused infection to the same extent as WT, albeit slightly delayed, proving that the loss of fitness *in vivo* was caused by TKT deletion. It seems that Δtkt cells are able to infect the host cells but do not survive for long, which is encouraging for further drug studies. Importantly, these results suggest that TKT is a

potential drug target for leishmaniasis. It would also be of interest to assess immunogenicity of this cell line, i.e. to determine whether its interaction with the host as a viable agent is sufficient to provoke a robust immune response, including development of immunological memory that could render the strain a potential live-attenuated vaccine for leishmaniasis.

I performed further experiments exploring the possibilities of using TKT as a potential drug target. In summary, the Δtkt promastigote cells are marginally more sensitive to several leishmanicides, probably due to additive effects of different types of stress. If the drugs are acting by increasing intracellular oxidative stress, a possible additive effect with PPP dysfunction is possible. TKT is, however, not itself targeted by any of the drugs currently in use which I tested. I will screen GSK LeishBox (Peña et al., 2015) for inhibition of TKT enzyme activity with an aim to search for potential hits for inhibitors.

5.7.2 Metabolomics

Using various methods and focusing on different parts of metabolism, we can conclude that the Δtkt cell line displays a stringent metabolic response, akin to that described as promastigotes transform to amastigotes (Saunders et al., 2014). Significantly less glucose is consumed, the flux in the central metabolism is decreased and significantly less succinate, malate, and no alanine or proline are produced and secreted to the spent media. In addition, carbon source utilisation is changed since the relatively high levels of amino acids are used to substitute for glucose, albeit without increasing their total consumption as the metabolism is not profligate as found in WT.

Metabolomics results have to be treated with caution as identification of most of the metabolites is only putative, changes in quantity detected are relative and if the peak is low or has a poor quality shape, the quantification can be inaccurate. However, the amount of data obtained is enormous, standards were used for many important metabolites and the same changes in related metabolites support that the trends observed are real. Most importantly, very similar results obtained from LC-MS and GC-MS analyses increase the credibility of assignments.

The LC-MS data are complemented and concordant with the GC-MS data, the former allowing putative identification of large numbers of metabolite, while the latter enables

precise quantification and identification of fewer compounds. In general, the GC-MS analysis supports the LC-MS results. Isomers of sugar phosphates cannot be separated reliably by LC-MS and they are important in these pathways, but we were able to distinguish them by GC-MS. Hence, we confirmed that G6P and F6P levels are similar (two fold decreased), whereas increases in different pentose phosphates is specific for each compound. For example, glucose was detected in WT by LC-MS, but the peak was of low quality and thus the relative change in Δtkt cannot be quantified, whereas the other approach showed clear 7 fold increase. The biggest difference in results between the two methods is a 5-fold accumulation of F1,6bP measured by GC-MS, whereas a two-fold decrease was indicated by LC-MS. However, that is one example of a metabolite, identification of which is only predicted and detection is poor by LC-MS, thus GC-MS is much more reliable. Bisphosphoglycerate showed an unexpected increase by LC-MS but we cannot distinguish 1,3- or 2,3- bisphosphoglycerate and the peak quality is poor. Unfortunately, the standard was not available for GC-MS analysis and the question remains open. Both analyses, however, concur that metabolites from the bottom part of glycolysis are substantially depleted (DHAP 20 fold, 2PG and 3PG dropping below the detection limit).

The GC-MS analysis contributed additional intermediates, which were not detected previously, such as E4P, DHAP, or quantification for glucose. Further, by focusing on carbohydrates, the profound accumulation of pentoses and compounds related to them was confirmed. The magnitude of some of the changes (up to 200 fold) may be startling, but abundance of these metabolites in WT is probably very low, thus the accumulation after TKT depletion causes high relative change. The fact that it is not a single metabolite, but a group of interlinked ones, supports that it is a coherent change. Surprisingly, xylose seems to be decreased below detection limit, suggesting that the utilisation and metabolism of separate pentoses is not uniform.

The observation that the direction of the 6PGDH reaction may be reversed after TKT deletion is intriguing, which is the most plausible explanation for high proportion of 5 carbon labelling in 6PG, even though it is only indirect proof. 6PGDH running in the opposite direction was reported previously in sheep liver and fungi (Silverberg and Dalziel, 1975; Villet and Dalziel, 1969), although I did not succeed when measuring it, possibly due to insufficient concentrations of CO_2. It would be of interest to establish

whether such an alteration also occurs in other instances where pentose phosphates are accumulated, as was observed for example in TAL or RPI deficiency in humans (Engelke et al., 2010; Huck et al., 2004; Vas et al., 2006). It is of importance because the reaction in this direction consumes NADPH instead of producing it, which must significantly affect the redox balance inside the cells.

The Δtkt + TKT re-expressor cell line retains some differences from WT, despite expressing active TKT (and in levels exceeding those of WT), but most of the changes in metabolism are reverted to WT levels..

Changes in mannogen in Δtkt are of interest as the level decreased under normal conditions but increased again in presence of fructose. It is not clear why mannogen is decreased in Δtkt at the first place, although clearly TKT does play a role in carbohydrate metabolism and mannogen is a part of that extended network. From the RNAseq analysis it seems to be due to decrease in expression (or faster degradation) of mRNA for mannose-1-phosphate guanylyltransferase. We cannot exclude a random mutation, due to long term cultivation of the cell line. Of note, re-expression of TKT does not restore mannogen levels and mRNA for mannose-1-phosphate guanylyltransferase is also three fold decreased, indicating it is indeed possible that this change has occurred independently, prior to selecting the Δtkt line. To test this it would be desirable to produce a second, independent knock-out line to determine whether the same change to mannogen levels occurs or not. However, that observation strengthens the presumed importance of mannose-1-phosphate guanylyltransferase in mannogen biosynthesis, or maintenance.

The central carbon flux is significantly decreased in the Δtkt cell line. Consumption of glucose measured here is close to value reported previously (about 3.3 nmol (Saunders et al., 2014)). Although Wildridge did not detect any difference between WT and Δtkt (Wildridge, 2012), he used medium with 16 mM glucose and fewer, but more spaced out time points thus he may have missed the difference I detected. The decrease in secreted metabolic end products matches the observation that the media in Δtkt culture becomes much less acidic (Wildridge, 2012). Glucose uptake may be downregulated in response to accumulation of glucose inside cells or due to decreased levels of glucose transporter gene expression as identified through RNAseq. Why glucose accumulates inside the cells is another question. A complex regulatory mechanism stimulating the stringent metabolic

response, as described in amastigotes (Saunders et al., 2014) may be occurring, albeit triggered by different mechanism. It could be possibly a general stress response.

There does not seem to be clear downregulation of the TCA cycle as observed in the other pathways of glucose metabolism. This appears to be due to the fact that multiple carbon sources e.g. a mixture of different amino acids fuel the TCA cycle. The changes detected in the TCA cycle are not consistent between metabolites nor across different experiments, for example there are differences in the overall levels in Fig 5.15 and Tab 5.5. RNAseq data show similar trends, levels of some of the enzymes are slightly decreased, other increased but the changes are small.

It is difficult to make clear conclusions about changes in amino acid metabolism. mRNA levels of most of the amino acid transporter genes are increased, supporting use of amino acids to compensate for glucose (expression levels of the glucose transporter genes are diminished). On the other hand, amino acids in the spent media are not obviously consumed more by Δtkt cells than WT. All amino acids accumulate inside cells, which would rather indicate decreased catabolism. A possible explanation for some of these changes is that under standard conditions, they are transaminated using pyruvate as amino group acceptor to produce alanine. But because of pyruvate depletion in Δtkt, the whole process is disrupted and there is an accumulation of aminoacids. None of the data indicated increased flux into the TCA cycle, or any amino acid degradation pathway, on the other hand, that may be interpreted as more efficient use of resources in contrast to profligate WT metabolism. It is possible that amino acids are taken up from medium the same way by both cell lines, but used inside the cells differently. If Δtkt does not prefer a single amino acid, but uses a mixture of different ones, then the changes in specific metabolites or genes may be too subtle to generate significant differences in abundance, while the net contribution is sufficient. It may be hypothesised that due to stringent metabolic response, carbon sources are utilised more efficiently and no substantial replacement is needed. The labelling data of the TCA cycle intermediates, however, clearly showed that these metabolites originate from a different source than glucose.

5.7.3 PPP flux

The 14% flux of glucose into the PPP calculated here corresponds with previous reports in other organisms. It was reported to be 10% in *T. cruzi* (Maugeri and Cazzulo, 2004),

7% in healthy humans (Dusick et al., 2007), 5.7% in human hepatoma cells (Lee, 1998), 10% in *Corynebacterium* but increased to 30–60% under stress (Moritz et al., 2002). Maugeri (2003) estimated that 11% of radiolabelled glucose is incorporated into DNA in promastigote *L. mexicana*, meaning that it is channelled into the PPP and turned into R5P. This method may not be very precise because ribose can also be taken up from medium, phosphorylated by ribokinase and incorporated into nucleic acids preferentially. Nevertheless, the two values obtained by different techniques are very close.

Based on the labelling experiments here, it seems that 14% flux measured in the PPP represents the net flux via the pathway. Flux via the oxidative branch is possibly the same, but a higher flux in the non-oxidative branch, including cycling between the intermediates, is not reflected in these measurements. The non-oxidative PPP should be considered as allowing free interconversion of carbons between various substrates in no particular order rather than a straightforward pathway with a prevailing direction as depicted classically (Fig 5.33). The sensitivity of the metabolomics methodology has shown that unusual metabolites such as O8P and N9P also appear in the non-oxidative branch of the pathway. These large monosaccharides (at least O8P) are associated with sugar cycling in the Calvin cycle or biosynthesis of lipopolysaccharides for bacterial cell wall (Kneidinger et al., 2002; Williams and MacLeod, 2006), but roles for these metabolites are not clear in trypanosomatids. However, it is possible that they are simply the inevitable products of the non-oxidative PPP given the promiscuity of the enzymes and their ability to remove and add carbon units.

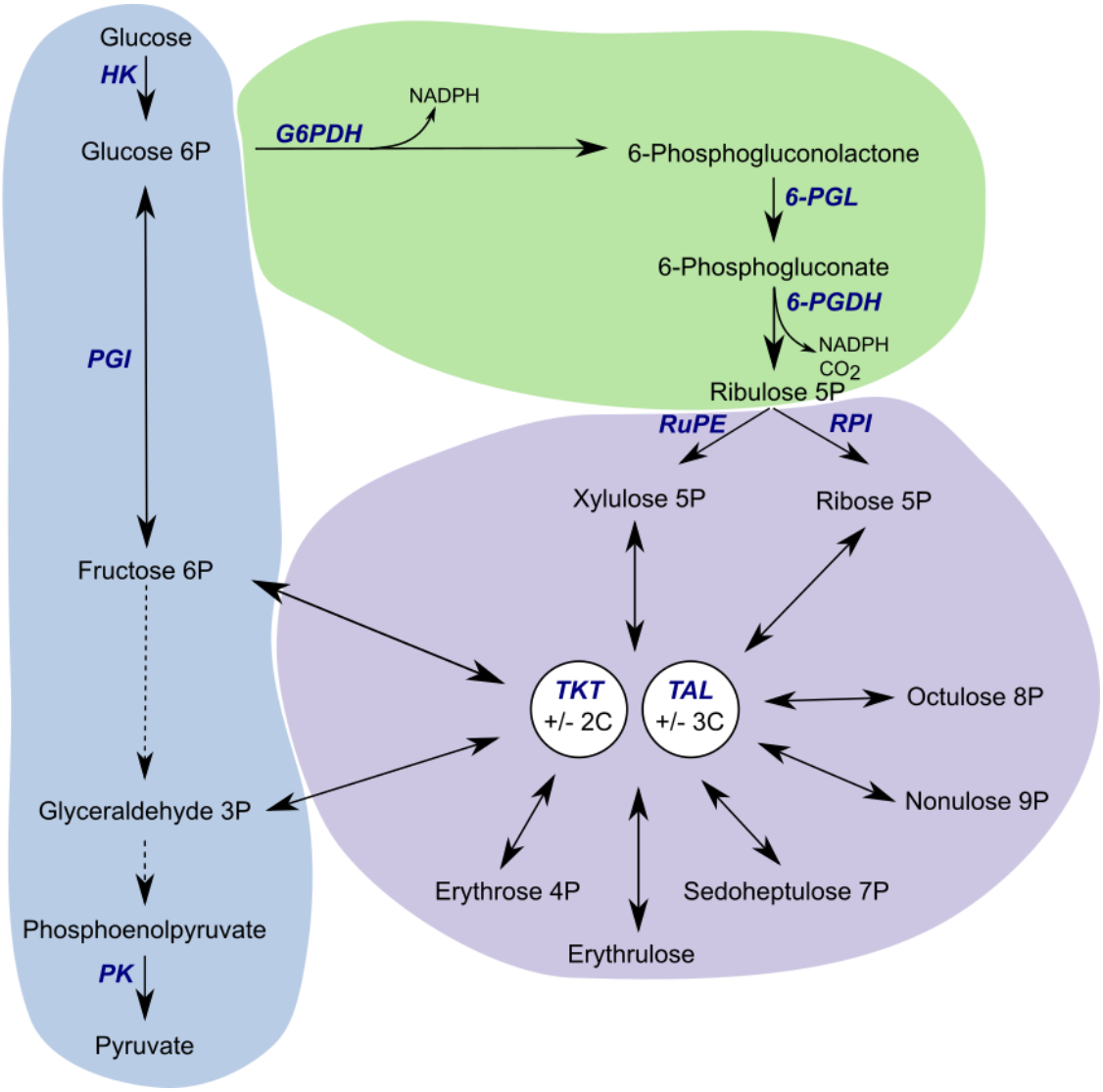

Figure 5.33. An alternative scheme of the PPP, reflecting the mode of action of TKT and TAL.

After observing downregulation of central carbon metabolism as a consequence of TKT deletion, I tested various hypotheses in order to find the control point. Purified PGI was shown to be inhibited by 6PG, although it was never proven inside cells. This work disproves this as an explanation for diminished glycolysis through PGI inhibition in *L. mexicana*, since using fructose rather than glucose did not alter the overall metabolic network distribution, in spite of the fact that fructose enters the pathway beneath the isomerase reaction. Nevertheless due to the compartmentalisation of glucose catabolism in trypanosomatids, the hypothesis could still hold for other organisms. Of the possibilities tested, inhibition of FbPase activity seems to be the mechanism most likely

responsible for the block in glycolysis. This corresponds with the metabolomics data and explains the drastic drop in the lower part of glycolysis, and accumulation of metabolites upstream. It was reported previously that FbPase is inhibited by R5P and 6PG in various organisms (Bais et al., 1985; Lal et al., 2005; Moorhead and Plaxton, 1990) and I observed high accumulation of both of these metabolites. The protein sequences are similar, and amino acid residues responsible for substrate binding are conserved across species, including *Leishmania* (Fig 5.34). To test this hypothesis, the enzyme from *Leishmania* would need to be purified and the inhibition established, but at the moment it seems to be the most likely explanation.

We cannot exclude that additional regulatory and feedback mechanisms take place concomitantly. The stringent metabolic response which was observed could be the outcome of coordinated control mechanisms responding to stress, or it could be outcome of additive effects of random changes triggered by artificial deletion of the TKT gene.

Figure 5.34. Alignment of FBPase protein sequences. Representatives of the enzymes reported to be inhibited by PPP intermediates and *L. mexicana* sequences are shown. Arrows indicate the conserved amino acid residues crucial for substrate binding and activity. The alignment was made using PRALINE tool (Heringa, 2002).

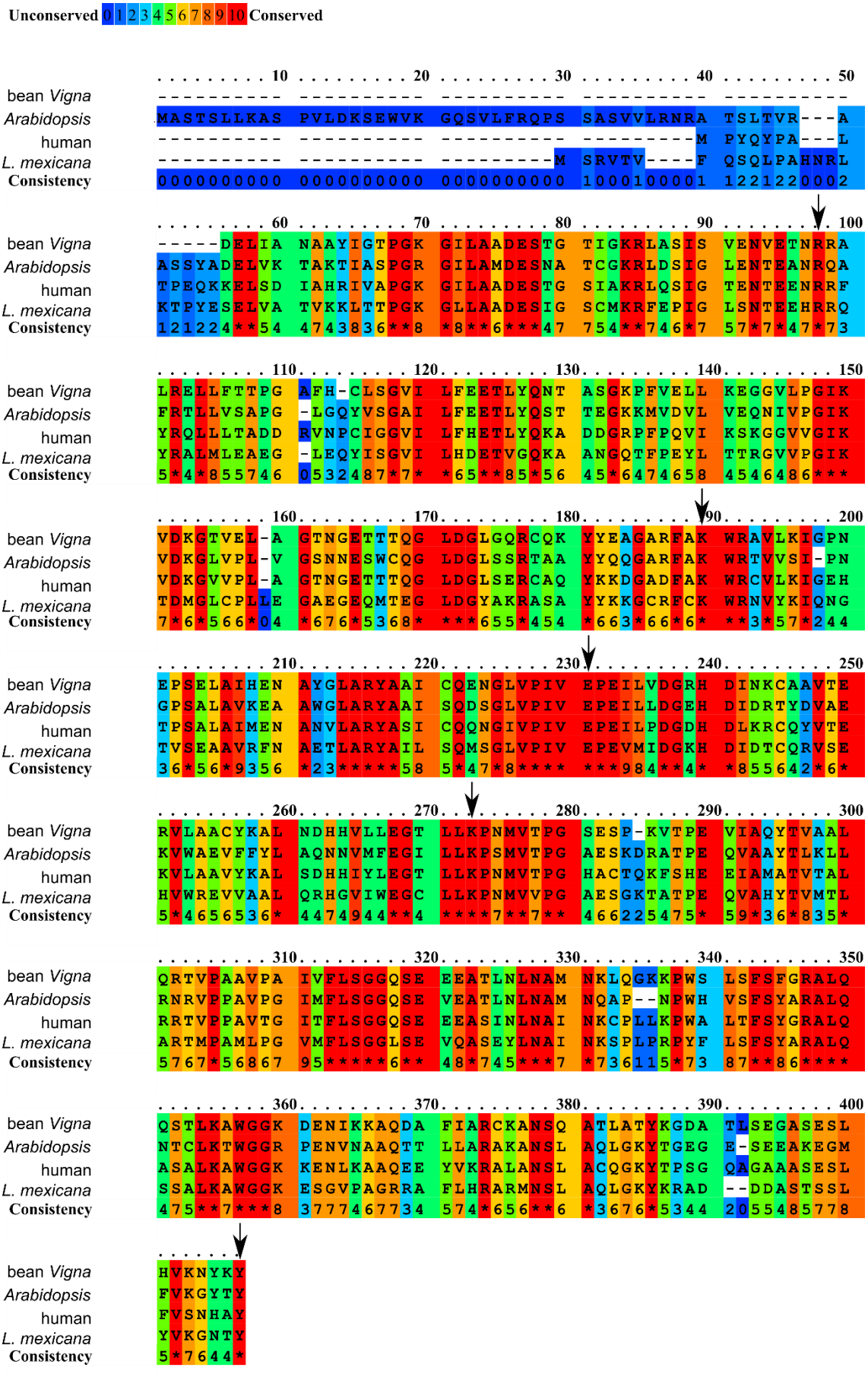
Unconserved 0 1 2 3 4 5 6 7 8 9 10 Conserved
bean Vigna
Arabidopsis
human
L. mexicana
Consistency

5.7.4 Why is the infectivity of amastigotes decreased?

I did not manage to bring a straightforward answer to the question regarding the causes of a detrimental effect of TKT deletion to the amastigote stage. It seems that Δtkt amastigotes are able to infect host cells, but they do not survive inside for long term. Under natural conditions, amastigotes are exposed to high oxidative stress and their defence mechanisms may be disabled by the PPP disruption and decreased NADPH production. Promastigote Δtkt were only twice as sensitive to GOX as WT, but the situation may be completely different in the amastigote stage. The highest demand for NADPH is in trypanothione reductase recycling, but other NADPH consuming pathways are found in lipid metabolism, notably ergosterol biosynthesis (De Vas et al., 2011) and fatty acid synthesis (Lee et al., 2007), which may be operative and relevant to the amastigote stage, and thus decrease in their activity could contribute to Δtkt lethality. Further, glutamate dehydrogenase catalyses transamination of oxoglutarate to glutamate at concomitant consumption of NADPH, but that step is not expected to be essential (Saunders et al., 2011). On the other hand, the PPP is not the only NADPH producing pathway, as it is made in addition by malic enzyme (Mottram and Coombs, 1985b), isocitrate dehydrogenase in the TCA cycle (Saunders et al., 2014), and possibly in tetrahydrofolate metabolic pathway (Vickers and Beverley, 2011).

Mannogen was reported to be essential for amastigotes (Ralton et al., 2003) and it is highly decreased in Δtkt. However, infectivity is restored in the TKT re-expression line, in spite of mannogen levels remaining low, pointing to TKT being the determinant of infectivity in both of these cell lines. TKT deletion may have caused intracellular stresses within the promastigote lines in which they were selected, but adaptive mechanisms might have evolved to permit survival in this stage. However, transformation to amastigotes within the host system, might then have over-ridden any such bypass mechanism after which death ensued.

5.7.5 Localisation

The results of experiments focused on localisation of TKT are quite surprising, especially the solely glycosomal localisation of the TKT protein truncated by 10 amino acids. Although Western blot analysis following digitonin lysis did not confirm the IFA observation, the latter technique is more reliable and shows unambiguously the

localisation of the protein inside the cells. Considering the differences in localisation that vary as the C-terminus varies, it is clear that this part of the protein does play a role in cellular targeting, although a better understanding of exactly how this works will require further work. The mechanism is not as simple as hypothesised originally, where it was considered possible that it was a simple case of extending a flexible tail that enabled binding to PEX components of the glycosomal targeting pathway, whilst withdrawing the tail would prevent that. Possibly, the flexible C-terminus forms a particular structure depending on the amino acid sequence from which it is composed, in which case this structure differs between the constructs I made, and it is this that influences availability of the PTS1 sequence and the final localisation. A possible way to approach the question could by through X-ray crystallography or protein NMR, which can provide detailed information about structure. To address this question from a different angle, we are collaborating with Ylva Lindqvist's crystallography group from the Karolinska Institute, in order to obtain structure of TKT in complex with different substrates. One of the objectives is to examine whether the conformation of the C-terminus differs depending on the binding of different substrates.

When comparing the cells expressing TKT solely in one compartment, I expected to detect significant differences at the level of the metabolome, between them. However, no substantial changes were found. At the moment, it seems curious that cells have a presumably very complex mechanism of localisation control, when no difference to metabolism is apparent irrespective of localisation. On the other hand, I did not manage to compare these variants in the amastigote stage, and it is possible that a particular phenotype becomes obvious only in a specific stage (amastigote, or even other parts of the life cycle), or under specific conditions. However, these results confirm the presumed semi-permeable nature of the glycosomal membrane (Achcar et al., 2013), because it does not matter where the enzyme is present, if the substrates and products can pass across the membrane and access the enzyme freely irrespective of its localisation.

6 General discussion

My work was focused on *Leishmania* metabolism, which I studied using various metabolomic approaches and the data presented here are connected by two common topics: the pentose phosphate pathway and stringent metabolism. Using labelled glucose and ribose for a metabolomics study provided us with information on utilisation of these sugars in overall cellular metabolism and on the activity of the PPP. Further, I used an *L. mexicana* cell line depleted of transketolase, which answered questions on the essentiality of this gene and consequently the non-oxidative branch of the PPP. Interestingly the Δtkt cell line shows characteristics of a stringent metabolic response, described previously for amastigotes. That is the main topic of the last part of my work, where I compared metabolomics data for promastigote and amastigote *L. donovani*.

6.1 Metabolomics approach

A key benefit of untargeted LC-MS metabolomics approaches is that they provide a large amount of unbiased data. Nevertheless, certain drawbacks are evident too. The method of separation (GC versus LC, column and gradient choice) prior to MS analysis can be chosen specifically depending on the group of metabolites of interest, but no method is optimal for all metabolites. The predominant method used here (LC-MS with ZIC-pHILIc) is suitable for amino acids, carboxylic acids, glycolytic intermediates, but not for fatty acids and other non-polar molecules, or very small molecules. Metabolites are identified based on matches with standards used, of which there are around 200 in our case, leaving most of the identifications as only putative. Unless calibration standards are used, relative quantification only is possible (Kim et al., 2015). In addition, if the peak detected is of poor quality, even the relative quantification is unreliable and this may lead to misleading results. The reproducibility was very good in my experience, i. e. the major

changes appearing consistently in different datasets. When I used a GC-MS method for the same sample analysis, I obtained precise quantification albeit with far fewer metabolites with confident identification. However, the sample and data processing is much more demanding.

6.2 Amastigotes

The metabolomics data on amastigotes presented here are in general consistent with stringent metabolism reported for this stage previously (Saunders et al., 2014). A key hallmark of the amastigote dataset, and an observation not reported before, is the decrease in levels of all amino acids (except for methionine and histidine). Amastigotes produce lower quantities of the metabolic end products, succinate and malate, and the data are consistent with a decrease in glycolysis too. Levels of sugar polymers are high in amastigotes, corresponding to mannogen being essential in the mammalian infective stage (Naderer et al., 2006; Ralton et al., 2003). Axenic and splenic amastigotes seem to be fairly similar based on the total metabolic profile as well as examination of specific metabolites of interest.

An alternative to describing amastigote metabolism as a 'stringent metabolic response' would be to describe WT promastigote metabolism as 'profligate', since the cells seem to consume unnecessary high amounts of substrates and to secrete large quantities of incompletely oxidized products such as succinate and alanine. This can be concisely concluded from the analysis of metabolic end products, comparison of glucose and ribose utilisation as carbon sources, and the comparison between promastigotes and amastigotes in this work, and has also been concluded based on previous observations too (McConville et al., 2015). It would be of interest to establish how promastigote metabolism observed *in vitro* relates to *in vivo* conditions in the sand fly which are practically unknown. The 'profligate metabolic response' could be an artefact induced by the very rich *in vitro* conditions. Amastigotes, however, are also cultured in similar rich medium, but their metabolism does not become profligate and they seem fairly similar to lesion-derived parasites. Hence there remains much to learn about the triggers and mechanisms that cause different *Leishmania* forms to metabolise in different ways.

6.3 Utilisation of glucose and ribose

The data obtained from metabolomics with labelled glucose and ribose in different combinations showed clearly that glucose is the preferred carbon source. The two sugars are preferentially carried by different transporters, phosphorylated by specific kinases and whereas G6P enter glycolysis directly, R5P transits the PPP first. Ribose can be utilised to the same extent and incorporated into the same metabolites, since it is channelled through the non-oxidative PPP as can be seen through increases in the intermediates and the labelling patterns. Hence feeding cells on ribose alone seems to increase flux in the non-oxidative PPP. If both sugars are available, glucose is preferred and ribose is used only to a minor extent. Surprisingly, when glucose is abundant, ribose was phosphorylated to R5P and incorporated into nucleotides, but not transformed into other metabolites. That indicates on an intriguing regulatory mechanism, the details of which remain elusive. It may involve subcellular localisation or inhibitory effects of the sugars and could be a part of the parasite's adaptive mechanisms to different environments and energetic sources. Possibly, using TKT mutant cell lines expressing the enzyme in a single compartment may help to explain the mechanisms involved. In addition, detailed functional characterisation of ribokinase in *Leishmania* may provide more insight into its regulation.

We may speculate whether utilisation of ribose for nucleotide synthesis and fructose for mannogen biosynthesis may have a similar regulatory control. Glucose seems to be the preferred carbon source, but if unavailable the parasites can replace it with other sugars. When different sugars are available, glucose seems to be preferred for central metabolism, but ribose for incorporation into nucleotides and fructose is favoured for mannogen biosynthesis. Learning more about the regulatory mechanism controlling preferential use of different carbon sources for different biochemical pathways will be an interesting topic of future investigation.

6.4 TKT deletion triggers stringent metabolic response

It was surprising to see no growth or morphological defect in Δtkt promastigote *L. mexicana*. Looking at a scheme of the PPP, function of TKT does not seem crucial *per se*, but the oxidative branch of the PPP produces NADPH, which is, in addition to other functions in metabolism, essential in defence against oxidative stress, specifically for recovery of trypanothione reductase, a process itself essential for the parasite (reviewed in Leroux and Krauth-Siegel, 2015). Blocking the non-oxidative branch is expected to cause accumulation of intermediates upstream and to disrupt flux in the whole pathway. Both G6PDH and 6PGDH, the two NADPH producing enzymes, are known to be essential in bloodstream form but not procyclic form *T. brucei* (Cordeiro et al., 2009). The depletion of G6PDH in promastigote *L. mexicana* resulted in a growth defect and increased sensitivity to Sb^{3+} (Mukherjee et al., 2013), but further effects were not investigated, and comparison across the two genera may be misleading, even though in both cases oxidative stress is expected to be higher in the mammalian infective stage. The fact that TKT is essential only in amastigote *L. mexicana* stage is in agreement with this speculation.

By employing a metabolomics approach I showed that even though Δtkt cells did not demonstrate any obvious phenotype, they underwent substantial changes in metabolism. That demonstrates that the parasites have high flexibility and adaptability with regard to metabolism, which was demonstrated again in other parts of my work, such as when WT cells were shown to be able to utilise both glucose and ribose in similar ways, even though the entry points into metabolism are different. In addition to the metabolic changes, TKT deletion is accompanied by increases in general sensitivity to stress. For example, the cells are more sensitive to oxidative stress and almost all of the current anti-leishmanial compounds tested, activity of which is partly conveyed by oxidative stress too. However, the rise in sensitivity is rather small, definitely smaller than predicted when considering that what is presumed to be the major source of NADPH for these cells is disrupted. No data is available on relative production and consumption of NADPH by the respective pathways in *Leishmania*, and the data reported for mammalian cells show high variability (Fan et al., 2014). Moreover, the labelling data presented here indicate that huge accumulation of pentose phosphates leads to reversion of the 6PGDH reaction, resulting in consumption of an NADPH molecule instead of production. It is difficult to predict

the final outcome of such a situation, since it would involve 6PGDH consuming NADPH and producing 6PG, and then G6PDH reaction would be driven by NADPH demand against high level of its product, 6PG. The final outcome of the reactions' activity would depend on the more energetically favourable directions, but most likely the canonical flux would not be very high. Possibly, accumulation of intermediates may spread upstream of the pathway resulting in blockage and total destruction of the flux.

The Δtkt cells may be compensating for this block by increasing other enzymes involved in oxidative stress defence such as ascorbate peroxidase, mRNA of which was 2.3 fold increased in Δtkt. In addition two enzymes from polyamine metabolism, ornithine decarboxylase and putative acetylornithine deacetylase, were more than two fold elevated and they may possibly increase trypanothione biosynthesis. In addition, other NADPH producing enzymes are present such as malic enzyme and isocitrate dehydrogenase, and dispensability of G6PDH indicates that production of NADPH from other pathways than the PPP may be sufficient (Mukherjee et al., 2013).

I measured 14% of glucose used in WT *L. mexicana* passes through the PPP, which is similar to flux reported for other organisms (10% in *T. cruzi* (Maugeri and Cazzulo, 2004), 7% in humans (Dusick et al., 2007)) and corresponds with previous studies on the PPP in *L. mexicana* (Mancilla et al., 1965; Maugeri et al., 2003). It was shown previously that the flux increases in response to oxidative stress (Maugeri et al., 2003) and the ribose labelling data presented here suggest that the flux also increases when ribose is the major carbon source, and the non-oxidative PPP is needed for its conversion to glycolytic intermediates. The flux calculation represents the net flux and could possibly measure only the oxidative branch, but the two branches seem to be independent in this regard. It may be impossible to measure flux in the non-oxidative PPP, because the straightforward pathway with a clear direction as depicted in textbooks, doesn't really exist, instead a mosaic of carbon interconversions between various substrates in variable combinations, performed by TKT and TAL occurs, as indicated in an alternative scheme I present in Fig 5.33.

Some of the metabolic changes following TKT deletion corresponded with anticipated outcomes, but other changes went beyond expectation and impact on distant branches of the metabolic network. Even though there are some minor differences between the data

from GC-MS and LC-MS, there is good correlation between the two and the same trends are seen. Accumulation of metabolites upstream of TKT (6PG, pentose phosphates) were expected, even though the extent of the increase was surprising. Accumulation of pentose phosphates drives flux into reactions which are otherwise not detected, such as conversion into alcohols or O8P, whilst metabolites downstream from TKT (S7P, GA3P) were depleted. E4P signal completely disappeared in Δtkt based on GC-MS. Whereas O8P levels increased a lot, N9P decreased significantly, because these sugars are most likely produced by TAL in 5 + 3 and 6 + 3 carbon reactions, respectively, thus the production depends on availability of the substrates. Most importantly, the changes observed in the metabolome are consistent with previous analyses of Δtkt *L. mexicana* (Wildridge, 2012) and *T. brucei* (Stoffel et al., 2011) (Appendix A1).

Interestingly, the flux in central carbon metabolism is decreased in Δtkt. Consumption of glucose is decreased by 25% and glycolytic intermediates dropped up to 20% of their WT concentrations. Decrease in glucose uptake is probably caused by depletion of mRNA for all three major glucose transporters by 25%. It is tempting to speculate that it is a feedback reaction to accumulation of glucose inside cells (by 7.5 fold), even though no such mechanism has been reported in trypanosomatids so far. Trypanosomatids have polycistronic transcription and mRNA regulation is conveyed by a balance between stability and degradation of mRNA, but no details are known about glucose transporters (Boucher et al., 2002; Clayton, 2002; Quijada et al., 2000). Hexokinase inhibition is also a possible explanation, since glucose is accumulated while G6P decreases. mRNA levels for hexokinase are increased by 27% and hexokinase activity was higher in lysates of the Δtkt cell line (although not significant due to high variability) (Tab 5.8). Translational or allosteric regulation within the cellular system may therefore be responsible for the decrease in activity *in situ*. *L. mexicana* depleted for all three glucose transporter genes was assessed for changes in mRNA levels, and among the most upregulated genes were hexokinase and ribokinase (Feng et al., 2011), which indicates that the cells sense a shortage of these sugars and attempt to compensate for it by enhancing enzymes that can utilise sugars at the gene expression level. The other genes reported as overexpressed in that glucose transporter KO study do not overlap with my data on the Δtkt line, except for serine hydroxymethyltransferase, mRNA of which was 2.5 fold increased in Δtkt and 7.7 fold increased in the glucose transporter knock-out, although there is no clear connection with sugar metabolism (Feng et al., 2011).

Since production of all the major metabolic end products which were detected (succinate, pyruvate, alanine) decreased substantially, the phenotype resembles stringent metabolic response described in amastigotes (Saunders et al., 2014). However, a big difference between the stringent metabolic response reported for amastigotes and the Δtkt line relates to amino acids. These are greatly decreased intracellularly in amastigotes compared with promastigotes, while they increase within the Δtkt line. TKT itself is a good example of amastigote stringent metabolism, because the enzyme activity is four fold lower in amastigotes, but it is essential in these cells in contrast to promastigotes. There is no obvious reason why deletion of TKT causes a similar induction of a stringent response as seen in amastigotes. Stringent metabolism may be part of a general stress response for *Leishmania*, as has been suggested by McConville *et al.* (McConville et al., 2015). It would be of interest but challenging to dissect the signalling and feedback mechanisms.

Flux through glycolysis could be disrupted due to inhibition of F1,6bPase by 6PG or R5P. Δtkt cells displayed half of the F1,6bPase activity compared to WT and the metabolomics data point at disruption in this step (accumulation of F1,6bP, depletion of the products), and such inhibition was described previously for mammalian and plant enzymes (Bais, 1985; Lal, 2005; Moorhead, 1990). To confirm this hypothesis, the *Leishmania* enzyme needs to be purified and the inhibition tested. Unfortunately, I did not have sufficient time to proceed with this work. However, the amino acid residues in the enzyme's active site responsible for substrate binding are conserved in the leishmanial one (Fig 5.34).

Another change in Δtkt metabolism is replacement of glucose by a different carbon source. Since the cells switch to stringent metabolism, they should, by definition, use less carbon. Whereas in WT about 50% of TCA cycle intermediates come from a source other than glucose, 90% of these intermediates are from non-glucose sources in Δtkt, while the total amount of these intermediates is the same or lower in absolute numbers. We have not been able to ascertain these alternative carbon sources. It was observed in WT *L. mexicana* that next to glucose, aspartate and glutamate are used to minor extent (Saunders et al., 2014). Hence, most likely it is the same situation for Δtkt, and possibly a wider range of amino acids may be used. In order to clearly answer the question, multiple metabolomic analyses would need to be performed with various amino acids carbon-

labelled to dissect which are fed into the TCA cycle. The Δtkt cells do not consume more amino acids, but they use them differently. Since the metabolism is stringent, levels of TCA cycle intermediates are decreased, and the same amounts of amino acids make up for much higher proportion of carbon in TCA cycle intermediates. Levels of mRNA for amino acid transporters are elevated in Δtkt, possibly indicating feedback in response to the block in carbon metabolism. Intracellular levels of many amino acids are increased (eleven amino acids are elevated 2 fold or more).

6.5 Why are Δtkt amastigotes not viable?

Whereas Δtkt cells have no growth defect as promastigotes, they are not viable as amastigotes. Experiments with axenic amastigotes indicated this to be the case, but the data were not conclusive, since I did not obtain a growing culture of the Δtkt + TKT cell line either. Infections of macrophages indicated decreased infectivity, but the parasites were still able to infect the host cells. Infections of mice, however, showed that Δtkt cells failed to develop leishmaniasis lesions even after 23 weeks. It seems that Δtkt cells can infect phagocytic host cells and survive inside short term, but not long enough to establish infection.

The reason for this loss of viability, however, remains unclear. A suspected possible reason would be loss of oxidative stress defence. However, Δtkt promastigotes are only two times more sensitive to glucose oxidase and Δtkt + TKT cell line reverted to WT levels only partly in the same assay (but this re-expressor line caused normal infection in mice). On the other hand, it is unknown how promastigote and amastigote defence systems compare and in general it seems that promastigotes can handle more disruption and higher stress. A second possible explanation would be that inhibition of F1,6bPase and subsequent decrease in glycolytic flux is intolerable for amastigotes. If the switch to stringent metabolism results in parasites that use only what is needed, then even only partial inhibition may have lethal consequences. mRNA for F1,6bPase was detected to be around two fold decreased in amastigotes in three independent transcriptomic studies (Alcolea et al., 2010a, 2010b; Holzer et al., 2006). Intriguingly, leishmanial F1,6bPase was also shown to be present in the cytosol of infected macrophages and suggested to

activate tyrosine phosphatase SHP-1 and inhibit expression of mammalian nitric oxid synthase (Nandan et al., 2007).

In addition, I also observed a significant drop in levels of mannogen, a storage sugar essential for amastigotes. No direct connection with TKT is obvious, but decreases in mRNA for mannose 1-phosphate guanylyltransferase seemed to be responsible for mannogen depletion. We do not know if it is due to some kind of feedback in consequence of the metabolic changes, or if it is a random additional mutation in the original Δtkt cell line. In order to test that, an independent Δtkt cell line would need to be made. Nevertheless, mannogen levels are still low in Δtkt + TKT, but the cells caused infection, which excludes this as a reason for loss of viability. Finally, it is possible that different types of stress contribute together resulting in detrimental effect on Δtkt amastigote cells. Altogether, TKT is a potential drug target against *Leishmania*, and I am planning to screen the LeishBox of leishmanicidal agents from GSK (Peña et al., 2015) for potential inhibitors of the enzyme's activity.

6.6 Localisation of TKT

Another interesting feature of TKT is its subcellular localisation. Previously it was shown that about 30% of the enzyme is confined to glycosomes in promastigote *L. mexicana* with the majority being cytosolic (Veitch et al., 2004). A crystal structure of the protein was resolved and it was noted that the C-terminal residues were unstructured with a possible explanation that this part of the protein is flexible (Veitch et al., 2004). Additional preliminary data indicated that binding of TKT to the PEX machinery varied depending on different sugar substrates added to the protein (Wildridge, 2012). These pieces of information led to formulation of hypothesis that binding of various substrates induces conformational changes in the enzyme including the C-terminal part containing PTS1 targeting sequence, having impact on its final intracellular localisation.

In order to shed more light on these data, I prepared a series of five TKT constructs with a C-terminus of varied length prior to the PTS1 sequence. Surprisingly, a version of the protein truncated by ten amino acids located solely into glycosomes. Some of the other mutants showed an increased proportion localised to the glycosomal part too, whilst

localisation of the others was the same as WT TKT. Altogether, no clear conclusions can be drawn solely from this data. The total net length of the C-terminal tail is not the decisive aspect in driving localisation. Instead it may be the secondary structure of the C-terminal part, dependent on its composition and interaction with the rest of the protein that is responsible for different localisation. The C-terminus plays a key role in the final localisation of the enzyme and the dual localisation in WT may be caused by its flexibility and changing availability of the recognition site for the PEX machinery. On the other hand, the whole PPP has the same dual localisation (with slightly varied proportions for different enzymes) and it is unknown how the dual localisation is controlled for the other components. In addition, proteins can be imported into peroxisomes in oligomeric complexes (Glover et al., 1994; McNew and Goodman, 1994; Opperdoes and Szikora, 2006) and such a scenario has not been investigated for the other PPP enzymes.

Having obtained a cell line expressing TKT with a purely glycosomal location, I prepared another mutant, lacking the C-terminal glycosomal targeting sequence which was solely cytosolic. Surprisingly there were no differences between these two cell lines. They were sensitive to oxidative stress to the same extent and metabolomics analysis showed only minimal changes in general, and none in the levels of metabolites of carbohydrate metabolism. This seems to confirm the presumed semi-permeable character of glycosomal membrane, when substrates and products of the enzyme (up to six carbons) can freely pass through the membrane (Achcar et al., 2013), and thus it does not matter where TKT is localised. It is intriguing, therefore, that a complicated regulatory mechanism of dual localisation takes place, given the final localisation of TKT appears irrelevant. On the other hand, the localisation may play a particular role under different conditions or in the amastigote, or other stages of the life cycle. It would be of interest to test infectivity of these mutated TKT cell lines in animals in future.

6.7 Conclusions and future work

- Metabolomics analysis of *in vivo* grown *L. donovani* amastigotes is presented. Metabolomes of splenic amastigotes, axenic amastigotes and promastigotes are reflected as three separate groups. In general, the data are consistent with stringent metabolic response in amastigotes. Both types of amastigotes had very low intracellular levels of amino acids compared to promastigotes, independent of their environment.
- Glucose is the preferred carbon source for WT promastigote *L. mexicana*, but it can be replaced by ribose. Ribose is the preferred source only for R5P part of nucleotides. Supplementation with ribose increases the flux in the non-oxidative PPP.
- WT promastigote metabolism under standard culture conditions is profligate.
- TKT deletion in promastigote *L. mexicana* causes no obvious phenotype (growth rate, oxidative stress and drug sensitivity), but substantial changes in metabolism were observed beyond the PPP.
- TKT deletion causes decreases in central carbon flux, possibly due to inhibition of fructose-1,6-bisphosphate aldolase by the accumulated PPP intermediates.
- The PPP consumes 14% of all glucose in promastigote *L. mexicana*, but in the non-oxidative PPP carbons are shuffled in a stochastic way, which cannot be quantified easily.
- Conformation of the C-terminus of TKT determines the final subcellular localisation of the protein. If the C-terminus is truncated by 10 AA, TKT is present exclusively in glycosomes.
- Changes in subcellular localisation have no effect on growth rate, oxidative stress sensitivity or metabolism.

This thesis has shown that the PPP enzyme TKT is essential to amastigote forms of *L. mexicana* even though its loss has little impact on the promastigote stage. The enzyme may therefore be considered as a drug target. Metabolomics analysis has shown that loss of TKT causes changes in the levels of substrates of the PPP but also leads to a decrease in use of glucose through glycolysis, pointing to novel regulatory cross-talk between these pathways. Whether the enzyme is localised solely to the glycosome, solely to the cytosol or dually localised to both compartments, neither promastigote parasite viability,

nor metabolism was altered. This supports a model where smaller metabolites are free to move between the glycosome and cytosol. Comparative analysis of metabolism in promastigote and amastigote forms of the parasite reveals metabolism to be stringent in the amastigote form and yet profligate in the promastigote form. The TKT knockout cells reproduced the stringent response even as promastigotes. Transcriptomic analysis indicated that much of the switch to a stringent response during differentiation occurs at stages in the gene regulatory flow beyond the level of RNA abundance.

Considering the progress in development of tools for genetic manipulation, it would be possible and desirable to prepare an inducible TKT knock-out cell line in the future. Use of DiCre (Duncan et al., 2016) and CRISPR-Cas9 (Sollelis et al., 2015) mediated systems was demonstrated in *Leishmania* already. That would enable to assess the phenotype in early time points after induction, which may allow to distinguish between direct and subsequent downstream effects. In the current study, I was not able to do any experiments with Δtkt axenic amastigotes because they are not viable. An inducible knock-out system would possibly overcome this issue, and more studies of these cells may provide useful information and indications why Δtkt are not infectious. In addition, expression of mannose-1-phosphate guanylyltransferase and levels of mannogen could be assessed in the new knock-out cell line, which would answer the question if the changes observed here are direct consequences of TKT deletion, or an additional random mutation in our original cell line.

Further, it would be technically challenging but desirable to perform metabolomics analysis of metacyclics as another *Leishmania* stage. Similarly, it would be interesting to compare promastigotes obtained from sand flies to *in vitro* cultured parasites. I did not observe any substantial difference between promastigote cells expressing TKT solely in the cytosol, or glycosomes. It would be of interest to test this perturbation in the amastigote stage, where a stronger phenotype or defect in infectivity may be observed. Further, it would be desirable to measure the flux in the PPP in the amastigote stage too. The activity of the pathway may differ in each stage, being increased in amastigotes due to higher demands for NADPH. The metabolomics data are consistent with stringent metabolic response in amastigotes, but the PPP activity may be the same in both stages and thus relatively higher to glycolysis in amastigotes.

Appendix A Metabolomics

Appendix A1. Comparison of metabolomics data from this work with previous publications (Stoffel et al., 2011; Wildridge, 2012). All values are relative to WT.

	Stoffel, 2011, *T. brucei*	Wildridge, 2012		this work, LC-MS		this work GC-MS
cell line	TKT KO	TKT KO	re-expressor	TKT KO	RIB TKT	TKT KO
G6P	0.94	0.80	0.28	0.75	0.77	0.46
F6P	0.63	0.70	0.25	-	-	0.5
6-PG	1.78	1.00	0.12	5.23	0.58	1.21
Pen5P	7.91	11.43	0.43	212	0.81	58.8
F1,6bP	1.03	0.60	0.40	0.42	0.53	6.86
2/3-phosphoglycerate	0.57	1.73	0.50	0.17	0.65	-
glycerol 3P	0.31	0.41	0.36	0.2	0.59	-
PEP	0.22	0.13	0.47	0.14	0.67	-
Pen1P	1.16	1.80	0.91	-	-	-
M6P	0.58	0.25	0.20	-	-	-
fumarate	0.76	0.67	0.53	-	-	-
succinate	0.80	0.81	2.43	0.35	1.64	-
malate	0.25	0.69	0.67	0.68	1.27	-
ketoglutarate	0.13	1.18	0.68	0.51	0.31	-
citrate	1.17	1.57	1.15	1.38	0.56	-
cis-aconitate	0.89	1.00	1.00	1.41	0.78	-
orotic acid	0.99	1.00	1.00	1.06	0.9	-
E4P	-	23.45	0.72	-	-	-
S7P	-	0.07	0.18	0.31	0.77	0.12
G1P	-	0.60	0.18	-	-	-

Appendix A2. All metabolites detected in GC-MS analysis. Values indicate relative abundance in Δtkt compared to WT. ND = not detected.

	Δtkt relative abundance
2-Deoxy-ribose	0.26
2-Phosphoglycerate	ND
3-Phosphoglycerate	ND
6-Phosphogluconic acid	1.21
D-Arabinose	80.76
D-Erythrose	ND
D-Erythrose 4-phosphate	ND
D-Fructose 1,6-bisphosphate	6.86
D-Fructose 1-phosphate	ND
D-Fructose 6-phosphate	0.50
D-Glucose	7.47
D-Glucose 6-phosphate	0.46
Dihydroxyacetone phosphate	0.05
D-Lactose	0.05
D-Mannose	0.34
D-Ribose	44.97
D-Ribose 5-phosphate	58.79
D-Sorbitol	10.39
D-Threose	ND
Dulcitol	9.99
D-Xylose	ND
D-Xylulose	890.23
Fructose	5.81
Fucose	2.79
Lactic Acid	0.42
L-Alanine	0.15
L-Glutamine	5.36
L-Rhamnose	1.36
L-Tryptophan	5.56
Maltose	1.47
myo-Inositol	2.77
myo-Inositol 1-phosphate	0.88
Octadecanoic acid	0.98
Palmitic acid	1.13
Ribulose 5-phosphate	125.15
scyllo-Inositol	0.93
Sedoheptulose 7-phosphate	0.12
Serine	0.19
Sucrose	0.80
Xylitol	2.72

Appendix A3. Labelling of amino acids depending on the presence of labelled glucose or ribose in the medium.

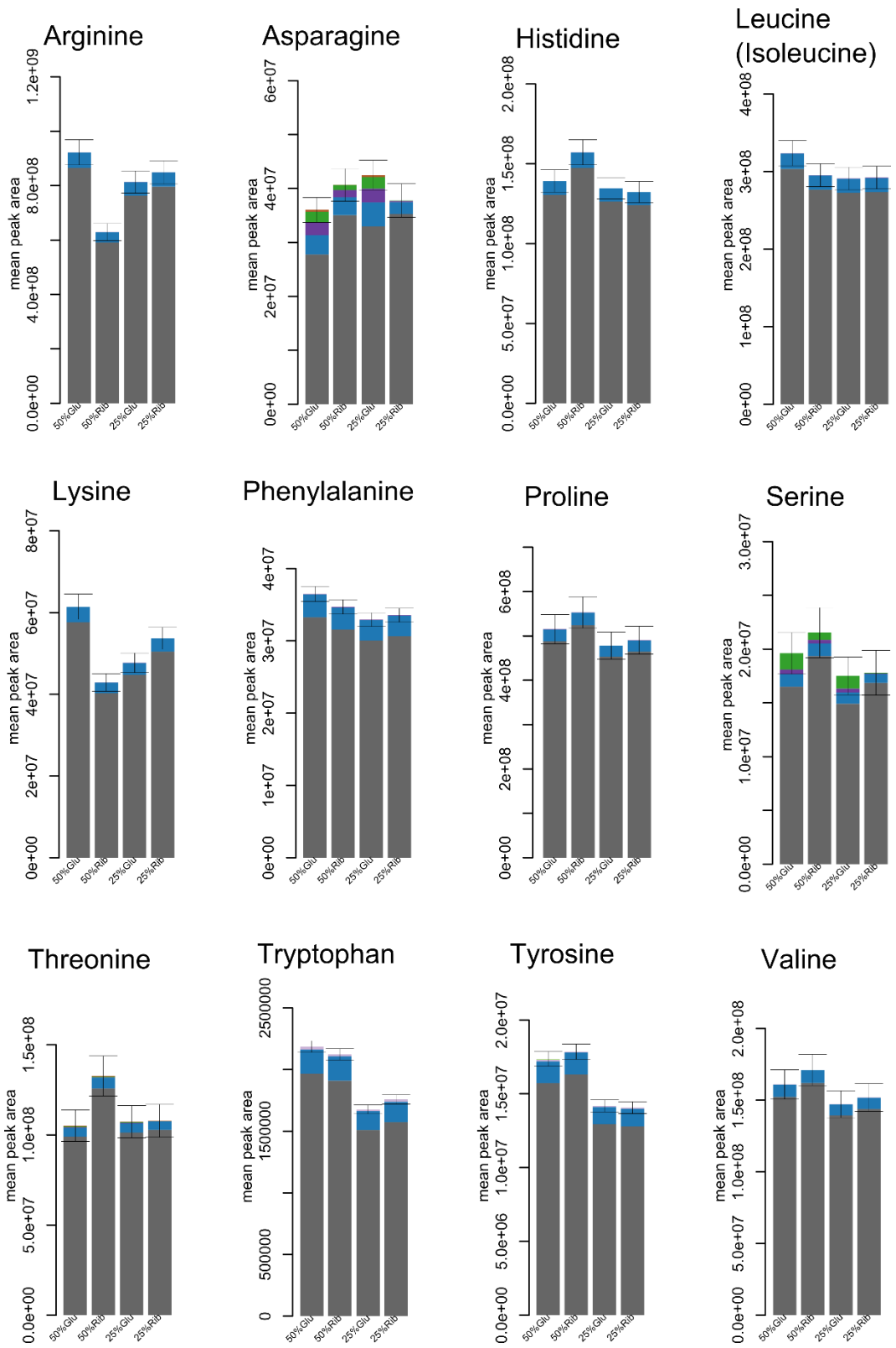

Appendix A4. Labelling of nucleotides and coenzyme A depending on the presence of labelled glucose or ribose in the medium.

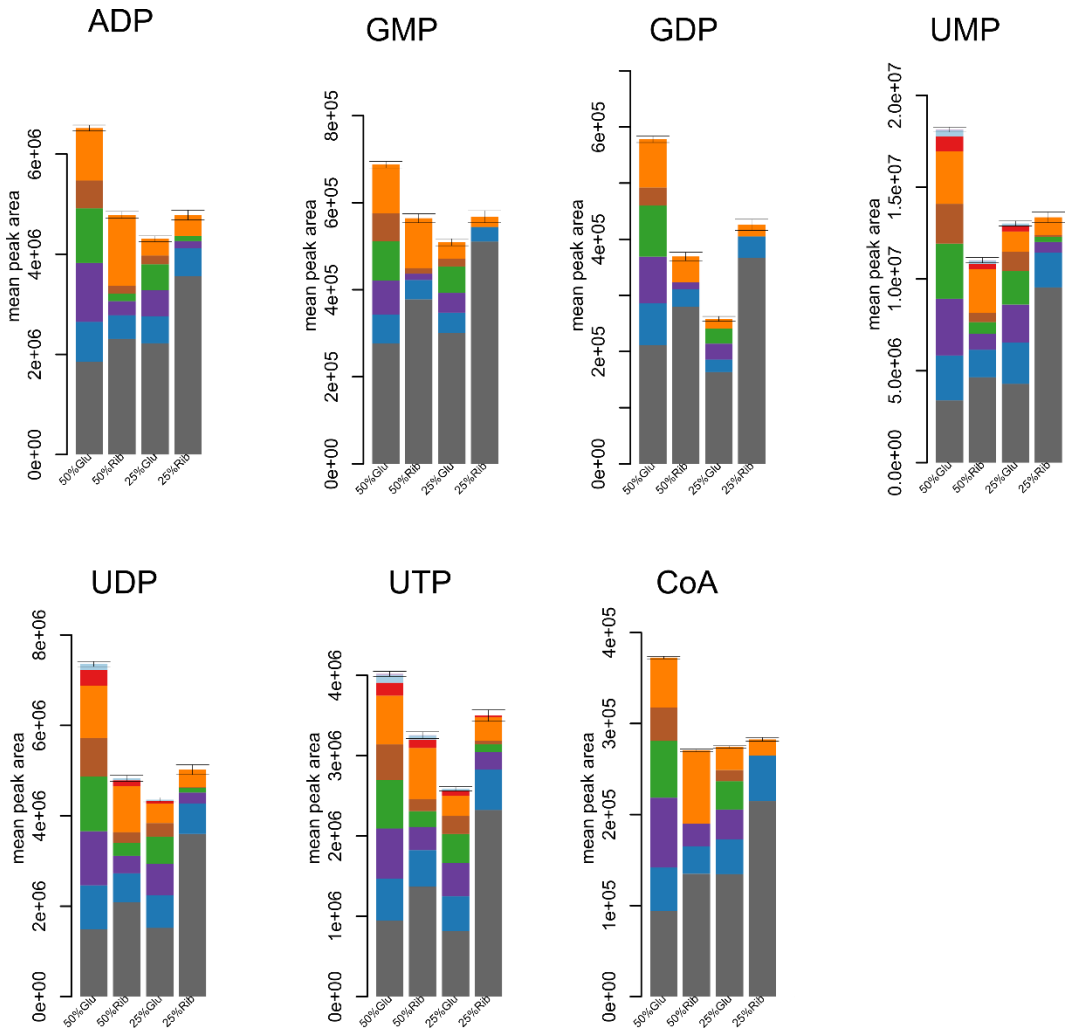

Appendix A5. The top 20 metabolites of the loading plot shown in Fig 5.2 for each principal component.

PC1	**PC 2**
Hexadecanoic acid	Hexadecanoic acid
Octadecanoic acid	Octadecanoic acid
L-Glutamine	D-Glucose
L-Glutamate	MES
4-Imidazolone-5-propanoate	(R)-2-Hydroxyglutarate
Isobutyronitrile	[FA (18:1)] 9Z-octadecenoic acid
D-Glucose	Taurine
Orthophosphate.1	sn-Glycerol 3-phosphate
L-Threonine	[GL (20:0/22:2)] 1-eicosanoyl-2-(13Z_16Z-docosadienoyl)-sn-glycerol
Choline	Choline
[FA (18:1)] 9Z-octadecenoic acid	D-Glucose 6-phosphate
MES	Ala-Val-Val-Pro
L-Leucine	L-Histidine
L-Lysine	[FA trihydroxy(4:0)] 2_3_4-trihydroxy-butanoic acid
Pyrimidine.2	Dodecanoic acid
sn-Glycerol 3-phosphate	Hypoxanthine
HEPES	D-Sorbitol
Theophylline	sodium dodecyl sulfate
L-1-Pyrroline-3-hydroxy-5-carboxylate	L-Methionine

Appendix A6. Amino acids detected in spent medium metabolomics analysis. White – fresh medium, black – WT, grey – Δtkt. Error bars represent standard deviation.

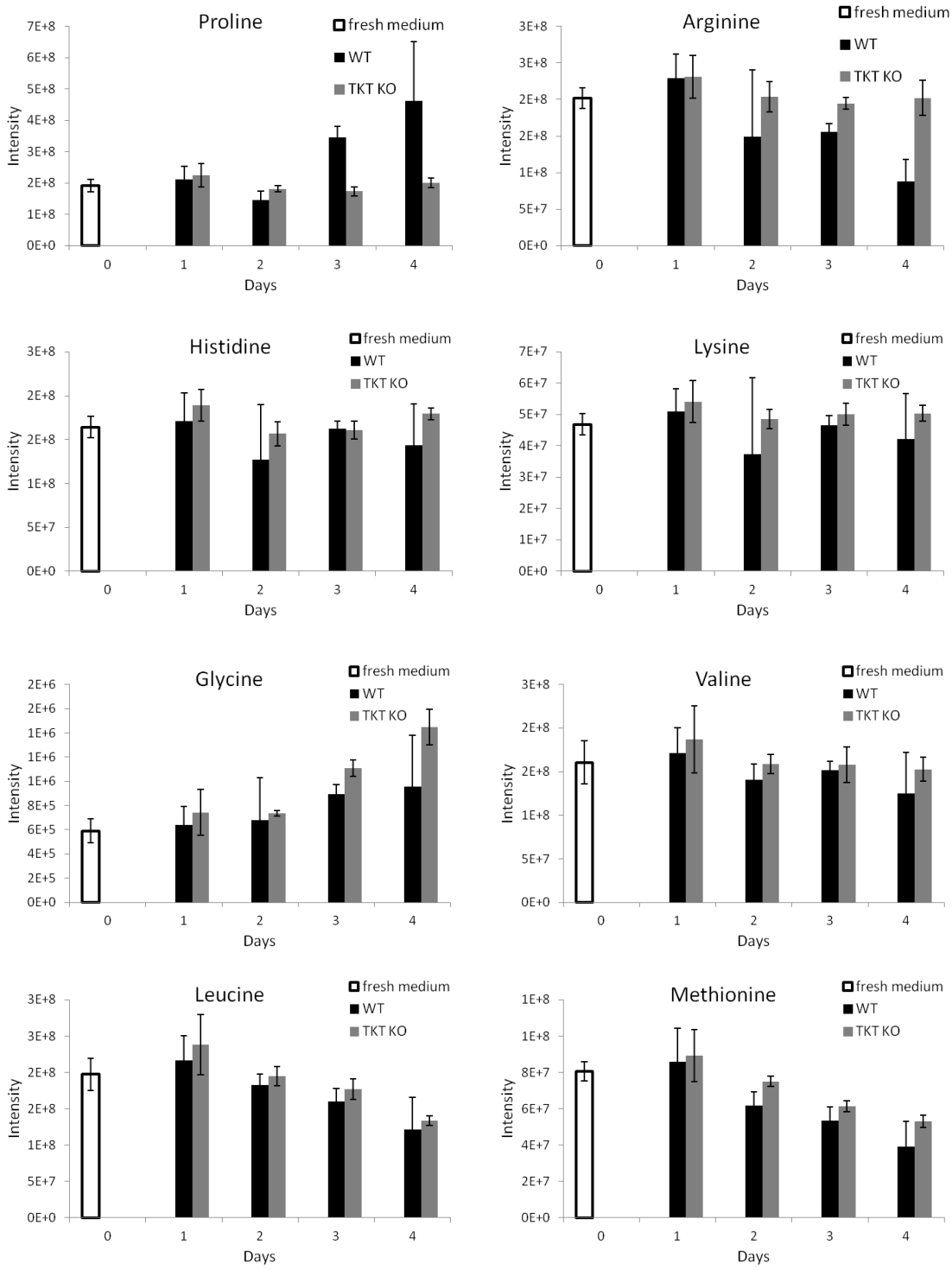

Appendix B Transcriptomics

Appendix B1. Genes detected in the trasncriptomic analysis when comparing WT and ΔTKT upregulated with fold change 2<.

gene	Annotation_TriTrypDB	p_value	Fold-change
LmxM.30.0880	amino acid permease 3	0.00005	4.092
LmxM.12.1090	promastigote surface antigen protein PSA	0.00005	3.670
LmxM.04.0210	surface antigen-like protein	0.00005	3.369
LmxM.23.1050	small hydrophilic endoplasmic reticulum-associated protein (sherp)	0.00005	3.357
LmxM.04.0130	unspecified product	0.00005	3.312
LmxM.28.1050	hypothetical protein, conserved	0.00005	3.213
LmxM.10.0470	GP63, leishmanolysin	0.00005	3.169
LmxM.16.1660	hypothetical protein, conserved	0.00005	3.164
LmxM.22.1150	hypothetical protein, conserved	0.00005	3.101
LmxM.30.0771	hypothetical protein	0.00005	3.089
LmxM.28.1060	hypothetical protein, conserved	0.00005	3.088
LmxM.28.1930	unspecified product	0.00005	3.069
LmxM.30.0760	hypothetical protein, unknown function	0.00005	3.017
LmxM.23.1061	small hydrophilic endoplasmic reticulum-associated protein (sherp)	0.00005	3.005

gene	Annotation_TriTrypDB	p_value	Fold-change
LmxM.25.1700	hypothetical protein, conserved	0.00005	2.999
LmxM.26.1340	DNA ligase k alpha, putative	0.00005	2.978
LmxM.30.0900	hypothetical protein, conserved	0.00005	2.967
LmxM.04.0390	hypothetical protein	0.00005	2.960
LmxM.28.1930	zinc transporter, putative	0.00005	2.949
LmxM.05.0900	surface antigen-like protein	0.00005	2.921
LmxM.04.0040	hypothetical protein	0.00005	2.905
LmxM.21.1350	hypothetical protein, conserved	0.00005	2.877
LmxM.34.0460	hypothetical protein, conserved	0.00005	2.826
LmxM.10.0380	unspecified product	0.00005	2.769
LmxM.23.1665	hypothetical protein	0.00005	2.767
LmxM.33.2479	hypothetical protein, conserved	0.00005	2.757
LmxM.28.1120	hypothetical protein, conserved	0.00005	2.728
LmxM.28.2740	activated protein kinase c receptor (LACK)	0.00005	2.721
LmxM.07.0025	hypothetical protein, conserved	0.00005	2.720
LmxM.28.2740a	unspecified product	0.00005	2.715
LmxM.28.2750	unspecified product	0.00005	2.703
LmxM.28.1280	phenylalanine-4-hydroxylase, putative	0.00005	2.662
LmxM.12.0890	surface antigen protein 2, putative	0.00005	2.657
LmxM.22.0100	hypothetical protein, conserved	0.00005	2.615
LmxM.12.0990	surface antigen protein, putative	0.00005	2.596
LmxM.29.2960	hypothetical protein, conserved	0.00005	2.594
LmxM.12.0980	promastigote surface antigen protein 2 PSA2	0.00005	2.592
LmxM.32.1460	hypothetical protein, conserved	0.005	2.587
LmxM.33.0010	hypothetical protein, conserved	0.00005	2.561
LmxM.28.0240	glycerol-3-phosphate dehydrogenase, putative	0.00005	2.561
LmxM.28.2205	ribosomal protein S29, putative	0.00005	2.558
LmxM.12.0470	hypothetical protein, unknown function	0.00005	2.548

gene	Annotation_TriTrypDB	p_value	Fold-change
LmxM.28.1430	DNA polymerase kappa, putative	0.00005	2.546
LmxM.09.0690	hypothetical protein, conserved	0.01875	2.538
LmxM.36.3140	hypothetical protein, conserved	0.00005	2.537
LmxM.12.0891	surface antigen protein 2, putative	0.00005	2.530
LmxM.32.0990	hypothetical protein, unknown function	0.00005	2.521
LmxM.34.5200	hypothetical protein, conserved	0.00005	2.515
LmxM.28.1030	ribosomal protein S20, putative	0.00005	2.488
LmxM.01.0450	alpha/beta-hydrolase-like protein	0.00005	2.483
LmxM.04.0625	hypothetical protein	0.00005	2.481
LmxM.09.0150	ATG8/AUT7/APG8/PAZ2, putative (ATG8C.1)	0.00005	2.470
LmxM.28.2370	serine hydroxymethyltransferase	0.00005	2.457
LmxM.16.0500	hypothetical protein, unknown function	0.00005	2.454
LmxM.28.1011	ribosomal protein S20, putative	0.00005	2.441
LmxM.24.0290	hypothetical protein, conserved	0.00005	2.436
LmxM.27.1080	hypothetical protein, conserved	0.00005	2.434
LmxM.09.0180	unspecified product	0.00005	2.434
LmxM.05.1110	hypothetical protein, conserved	0.00005	2.431
LmxM.31.2660	amino acid transporter, putative,amino acid permease, putative	0.00005	2.413
LmxM.23.1267	hypothetical protein, unknown function	0.00005	2.409
LmxM.04.0310	beta-fructofuranosidase, putative	0.00005	2.401
LmxM.28.1010	ribosomal protein S20, putative	0.00005	2.372
LmxM.08.0810	unspecified product	0.00005	2.365
LmxM.21.1480	hypothetical protein, conserved	0.00005	2.364
LmxM.28.2950	hypothetical protein, conserved	0.00005	2.364
LmxM.30.2800	hypothetical protein, unknown function	0.00005	2.361
LmxM.15.0630	hypothetical protein, unknown function	0.00005	2.360
LmxM.29.1920	hypothetical protein, unknown function	0.00005	2.359
LmxM.10.0390	GP63, leishmanolysin	0.00005	2.356

gene	Annotation_TriTrypDB	p_value	Fold-change
LmxM.12.0870	surface antigen protein 2, putative	0.00005	2.352
LmxM.36.2730	D-tyrosyl-tRNA deacylase, putative	0.00005	2.342
LmxM.08_29.0940	hypothetical protein, conserved	0.00005	2.340
LmxM.07.0400	hypothetical protein, conserved	0.00005	2.336
LmxM.10.0405	GP63, leishmanolysin	0.00005	2.328
LmxM.12.0280	ornithine decarboxylase, putative	0.00005	2.321
LmxM.28.2560	40S ribosomal protein S17, putative	0.00005	2.303
LmxM.14.1100	unspecified product	0.00005	2.303
LmxM.33.0070	ascorbate-dependent peroxidase, putative	0.00005	2.294
LmxM.24.1280	amastin-like surface protein-like protein	0.00005	2.286
LmxM.28.2555	40S ribosomal protein S17, putative	0.00005	2.280
LmxM.12.0850	surface antigen protein 2, putative	0.00005	2.264
LmxM.12.0860	surface antigen, putative	0.00005	2.263
LmxM.31.2640	cystathionine beta-lyase, putative	0.00005	2.260
LmxM.07.0270	acetylornithine deacetylase-like protein	0.00005	2.242
LmxM.30.1760	hypothetical protein, unknown function	0.00005	2.241
LmxM.20.0030	histone-lysine N-methyltransferase, putative	0.00005	2.233
LmxM.25.0280	hypothetical protein, conserved	0.00005	2.231
LmxM.07.0500	60S ribosomal protein L7a, putative	0.00005	2.219
LmxM.07.0510	60S ribosomal protein L7a, putative	0.00005	2.206
LmxM.12.0910	promastigote surface antigen protein PSA	0.00005	2.205
LmxM.03.0380	unspecified product	0.00005	2.202
LmxM.11.0660a	protein associated with differentiation 4, putative	0.00005	2.197
LmxM.28.0540	ribosomal protein S26, putative	0.00005	2.194
LmxM.34.1020	hypothetical protein, unknown function	0.00005	2.171
LmxM.10.0370	folate/biopterin transporter, putative	0.00005	2.168
LmxM.06.1260	pteridine transporter, putative	0.00005	2.160

gene	Annotation_TriTrypDB	p_value	Fold-change
LmxM.24.1620	hypothetical protein, conserved	0.00005	2.160
LmxM.15.1040	tryparedoxin peroxidase	0.00005	2.159
LmxM.30.1170	hypothetical protein, unknown function	0.00005	2.159
LmxM.34.0380	hypothetical protein, conserved	0.00005	2.151
LmxM.31.2155	hypothetical protein, conserved	0.00005	2.145
LmxM.14.1110	kinesin K39, putative	0.00005	2.142
LmxM.28.2780	heat-shock protein hsp70, putative	0.00005	2.137
LmxM.20.0700	hypothetical protein, conserved	0.00005	2.128
LmxM.14.0020	phosphatidylinositol 3-kinase, putative	0.00005	2.126
LmxM.30.0350	amino acid transporter aATP11, putative	0.00005	2.124
LmxM.28.2770	heat-shock protein hsp70, putative	0.00005	2.117
LmxM.26.2530	serine/threonine protein phosphatase, putative	0.00005	2.109
LmxM.07.1160	transmembrane amino acid transporter, putative	0.00005	2.096
LmxM.27.1440	hypothetical protein, conserved	0.00005	2.088
LmxM.36.0730	hypothetical protein, conserved	0.0001	2.085
LmxM.04.0320	unspecified product	0.00005	2.084
LmxM.27.2020	D-lactate dehydrogenase-like protein	0.00005	2.083
LmxM.34.5350	amino acid permease, putative	0.00005	2.073
LmxM.30.0870	amino acid permease 3	0.00005	2.072
LmxM.26.0160	nuclear lim interactor-interacting factor-like	0.00005	2.071
LmxM.22.1690a	unspecified product	0.00005	2.065
LmxM.07.0890	hypothetical protein, unknown function	0.00005	2.046
LmxM.28.1300	hypothetical protein, conserved	0.00005	2.046
LmxM.24.0680	sugar transporter, putative	0.00005	2.046
LmxM.28.1940	hypothetical protein, conserved	0.00005	2.044
LmxM.28.0080	hypothetical protein, unknown function	0.00005	2.042
LmxM.03.0400	unspecified product	0.00005	2.041

gene	Annotation_TriTrypDB	p_value	Fold-change
LmxM.18.1580	nonspecific nucleoside hydrolase	0.00005	2.031
LmxM.28.2460	ribosomal protein S29, putative	0.00005	2.031
LmxM.23.1025	hypothetical protein, conserved	0.00005	2.028
LmxM.04.0200	surface antigen-like protein	0.00005	2.025
LmxM.33.3645	unspecified product	0.00005	2.023
LmxM.28.3000	protein kinase, putative	0.00005	2.017
LmxM.25.0920	hypothetical protein, conserved	0.00005	2.013
LmxM.31.0630	hypothetical protein, conserved	0.00005	2.009
LmxM.28.0130	hypothetical protein, conserved	0.00005	2.006
LmxM.36.6570	hypothetical protein, conserved,y113g7b.23 protein-like protein	0.00005	2.003
LmxM.28.0210	histone H2B variant	0.00005	2.001
LmxM.36.2760	hypothetical protein, conserved	0.00005	2.001

Appendix B2. Genes detected in the trasncriptomic analysis when comparing WT and ΔTKT downregulated with fold change 2>.

gene	Annotation_TriTrypDB	p_value	Fold-change
LmxM.24.2060	transketolase, putative	0.00105	-1716.56
LmxM.30.0571	amino acid transporter aATP11, putative	0.00005	-4.90
LmxM.30.1440b	unspecified product	0.00005	-4.74
LmxM.21.1360	hypothetical protein, conserved	0.00005	-4.33
LmxM.30.1440	hypothetical protein, unknown function	0.00005	-4.29
LmxM.02.0170	unspecified product	0.00005	-3.74
LmxM.30.1440a	unspecified product	0.00005	-3.36
LmxM.19.1485	hypothetical protein, conserved	0.00005	-3.32
LmxM.15.0150	hypothetical protein, unknown function	0.00005	-3.25
LmxM.30.1442	hypothetical protein, unknown function	0.00005	-3.25
LmxM.25.0590	hypothetical protein, conserved	0.00005	-3.14
LmxM.02.0160	unspecified product	0.00005	-3.11
LmxM.18.1110	methyltransferase, putative	0.00005	-3.03
LmxM.08.1222	hypothetical protein, conserved	0.00005	-3.02
LmxM.36.5780	hypothetical protein, conserved	0.00005	-2.94
LmxM.27.0230	hypothetical protein, conserved	0.00005	-2.93
LmxM.17.0770	hypothetical protein, conserved	0.00005	-2.93
LmxM.22.1230	hypothetical protein, conserved	0.00005	-2.91
LmxM.30.2620	hypothetical protein, conserved	0.00005	-2.82
LmxM.03.0690	hypothetical protein, conserved	0.00005	-2.78
LmxM.23.0110	mannose-1-phosphate guanyltransferase	0.00005	-2.76
LmxM.29.0720	hypothetical protein, conserved	0.00005	-2.74
LmxM.36.6530	hypothetical protein, conserved	0.00005	-2.71
LmxM.36.5610	hypothetical protein, conserved	0.00005	-2.64

gene	Annotation_TriTrypDB	p_value	Fold-change
LmxM.25.1620	hypothetical protein, conserved	0.00005	-2.63
LmxM.29.0640	hypothetical protein, conserved	0.00005	-2.63
LmxM.36.2685	hypothetical protein, conserved	0.00005	-2.59
LmxM.20.1360	RNasePH-like protein,exosome associated protein 1 (Rrp42 homologue), putative	0.00005	-2.55
LmxM.33.1410	d-isomer specific 2-hydroxyacid dehydrogenase- like protein	0.00005	-2.51
LmxM.36.6920	hypothetical protein, conserved	0.00005	-2.47
LmxM.36.4145	transcription factor S-II-like protein	0.00005	-2.45
LmxM.36.4460	hypothetical protein, conserved	0.00005	-2.44
LmxM.25.0140	hypothetical protein, conserved	0.00005	-2.43
LmxM.36.6350	hypothetical protein, conserved	0.00005	-2.43
LmxM.31.3610	hypothetical protein, conserved	0.00005	-2.43
LmxM.26.2710	glutamate 5-kinase, putative	0.02195	-2.43
LmxM.33.1430	tyrosine phosphatase isoform, putative	0.00005	-2.42
LmxM.21.0340	mitochondrial processing peptidase alpha subunit, putative,metallo-peptidase, Clan ME, Family M16	0.00005	-2.41
LmxM.23.1640	hypothetical protein	0.00005	-2.40
LmxM.24.1840	lysophospholipase, putative	0.00005	-2.38
LmxM.09.0120	kinesin, putative	0.00005	-2.38
LmxM.29.0205	hypothetical protein, conserved	0.00005	-2.37
LmxM.22.1610	hypothetical protein, conserved	0.00005	-2.37
LmxM.33.3120	lipophosphoglycan biosynthetic protein (lpg2)	0.00005	-2.36
LmxM.17.0550	RNA-binding protein, putative	0.00005	-2.36
LmxM.33.3440	DNA topoisomerase IB, large subunit	0.00005	-2.35
LmxM.08_29.2450	heat shock protein 20, putative	0.00005	-2.35
LmxM.30.1140	monoglyceride lipase, putative	0.00005	-2.34
LmxM.22.1450	cyclophilin, putative	0.00005	-2.34
LmxM.34.0560	phosphatidylinositol-4-phosphate 5-kinase-like, putative	0.00005	-2.34

gene	Annotation_TriTrypDB	p_value	Fold-change
LmxM.34.3540	hypothetical protein, conserved	0.00005	-2.34
LmxM.33.1415	d-isomer specific 2-hydroxyacid dehydrogenase- like protein	0.00005	-2.33
LmxM.30.2580	ubiquinol-cytochrome-c reductase-like protein	0.00005	-2.33
LmxM.22.0090	methyltransferase, putative,mRNA cap methyltransferase-like protein	0.00005	-2.33
LmxM.33.1400	d-isomer specific 2-hydroxyacid dehydrogenase- like protein	0.00005	-2.32
LmxM.24.2220	hypothetical protein, conserved	0.00005	-2.32
LmxM.30.1550	hypothetical protein, conserved	0.00005	-2.29
LmxM.32.1090	guanylate kinase, putative	0.00005	-2.29
LmxM.29.1130	hypothetical protein, conserved	0.00005	-2.28
LmxM.34.0720	hypothetical protein, conserved	0.00005	-2.28
LmxM.27.0180	hypothetical protein, conserved	0.00005	-2.28
LmxM.04.0370	hypothetical protein, conserved	0.00005	-2.27
LmxM.36.6760	hypothetical protein, conserved	0.00005	-2.26
LmxM.18.1490	chaperone protein DNAj, putative	0.00005	-2.25
LmxM.07.1170	phosphoglycan beta 1,3 galactosyltransferase 1	0.00005	-2.25
LmxM.24.0600	hypothetical protein, conserved	0.00005	-2.25
LmxM.23.1060	hydrophilic surface protein	0.00005	-2.25
LmxM.27.0220	hypothetical protein, conserved	0.00005	-2.24
LmxM.34.2670	ankyrin repeat protein, putative	0.00005	-2.24
LmxM.29.1890	hypothetical protein, conserved	0.00005	-2.24
LmxM.32.2060	hypothetical protein, conserved	0.00005	-2.24
LmxM.26.2290	hypothetical protein, conserved	0.00005	-2.23
LmxM.09.1350	hypothetical protein, conserved	0.00005	-2.23
LmxM.36.1660	tRNA pseudouridine synthase A, putative	0.00005	-2.23
LmxM.30.2000	GP63-like protein, leishmanolysin-like protein,metallo-peptidase, Clan MA(M), Family M8	0.00005	-2.23
LmxM.32.1140	hypothetical protein, conserved	0.00005	-2.23
LmxM.09.0580	surface antigen-like protein	0.00005	-2.23

gene	Annotation_TriTrypDB	p_value	Fold-change
LmxM.32.0150	hypothetical protein, conserved	0.00005	-2.22
LmxM.26.2495	phosphatidylinositol-4-phosphate 5-kinase, putative	0.00005	-2.22
LmxM.20.0820	hypothetical protein, conserved	0.00005	-2.22
LmxM.21.1555	hypothetical protein, conserved	0.00005	-2.21
LmxM.25.0010	beta galactofuranosyl transferase	0.00005	-2.21
LmxM.32.0520	d-xylulose reductase, putative	0.00005	-2.21
LmxM.30.3190	phosphoglycan beta 1,3 galactosyltransferase 5	0.00005	-2.20
LmxM.29.2820	chaperonin HSP60/CNP60, putative	0.00005	-2.20
LmxM.33.4230	hypothetical protein, conserved	0.00005	-2.20
LmxM.36.2570	membrane-bound acid phosphatase precursor	0.00005	-2.20
LmxM.26.2500	hypothetical protein, conserved	0.00005	-2.19
LmxM.36.4710	hypothetical protein, conserved	0.0014	-2.18
LmxM.30.2600	calreticulin, putative	0.00005	-2.17
LmxM.27.0640	hypothetical protein, unknown function	0.00005	-2.17
LmxM.18.1610	hypothetical protein, conserved	0.00005	-2.17
LmxM.30.1165	hypothetical protein	0.00005	-2.16
LmxM.08.0940	hypothetical protein, conserved	0.00005	-2.15
LmxM.33.2240	hypothetical protein, conserved	0.00005	-2.15
LmxM.11.1030	hypothetical protein, conserved	0.00005	-2.15
LmxM.03.0680	hypothetical protein	0.00005	-2.15
LmxM.34.0890	hypothetical protein, conserved	0.00005	-2.15
LmxM.36.5060	hypothetical protein, conserved	0.0001	-2.14
LmxM.36.5365	hypothetical protein, conserved	0.00005	-2.14
LmxM.36.5040	hypothetical protein, conserved	0.00005	-2.13
LmxM.36.1330	hypothetical protein, conserved	0.00005	-2.13
LmxM.34.5090	hypothetical protein, conserved	0.00005	-2.12
LmxM.10.1320	fatty acid desaturase, putative	0.00005	-2.12
LmxM.08_29.1400	hypothetical protein, conserved	0.00005	-2.11

gene	Annotation_TriTrypDB	p_value	Fold-change
LmxM.30.1885	mannosyltransferase-like protein	0.00005	-2.11
LmxM.36.5670	RNA helicase, putative	0.00005	-2.11
LmxM.32.0240	thiol-dependent reductase 1	0.00005	-2.10
LmxM.34.4300	hypothetical protein, conserved	0.00005	-2.09
LmxM.23.0030	beta propeller protein, putative	0.00005	-2.08
LmxM.24.1710	ubiquitin-conjugating enzyme e2, putative	0.00005	-2.07
LmxM.27.2210	dual specificity protein phosphatase, putative	0.00005	-2.07
LmxM.25.0620	RNA polymerase I second largest subunit, putative	0.00005	-2.07
LmxM.29.2750	hypothetical protein, conserved	0.00005	-2.07
LmxM.27.1690	hypothetical protein, conserved	0.00005	-2.07
LmxM.31.3710	hypothetical protein, conserved	0.00005	-2.06
LmxM.34.2860	hypothetical protein, conserved	0.00005	-2.06
LmxM.20.0020	hypothetical protein, conserved	0.00005	-2.06
LmxM.29.0730	co-chaperone GrpE, putative	0.00005	-2.06
LmxM.29.3120	S-adenosylmethionine decarboxylase proenzyme- like, putative	0.00005	-2.05
LmxM.26.2305	hypothetical protein, conserved	0.00005	-2.05
LmxM.36.1770	hypothetical protein, conserved	0.00005	-2.05
LmxM.33.1440	hypothetical protein, conserved	0.00005	-2.05
LmxM.32.0270	hypothetical protein, conserved	0.00005	-2.04
LmxM.24.1850	hypothetical predicted multi-pass transmembrane protein	0.00005	-2.04
LmxM.27.0050	DEAD-box helicase-like protein	0.00005	-2.04
LmxM.23.0700	hypothetical protein, conserved	0.00005	-2.04
LmxM.19.1190	hypothetical protein, conserved	0.00005	-2.04
LmxM.26.2580	hypothetical protein, conserved	0.00005	-2.03
LmxM.32.2080	hypothetical protein, conserved	0.00005	-2.03
LmxM.22.0010	hypothetical protein, conserved	0.00005	-2.03
LmxM.33.4590	hypothetical protein, conserved	0.00005	-2.03

gene	Annotation_TriTrypDB	p_value	Fold-change
LmxM.34.1990	hypothetical protein, conserved	0.00005	-2.02
LmxM.33.1450	hypothetical protein, conserved	0.00005	-2.02
LmxM.21.0725	hypothetical protein, conserved	0.00005	-2.02
LmxM.34.1030	hypothetical protein, unknown function	0.00005	-2.01
LmxM.08_29.1020	hypothetical protein, conserved	0.00005	-2.01
LmxM.34.1610	hypothetical protein, conserved	0.00005	-2.01
LmxM.32.2980	hypothetical protein, conserved	0.00005	-2.01
LmxM.23.1350	acetyltransferase-like protein	0.00005	-2.01
LmxM.34.0070	prohibitin, putative	0.03265	-2.00
LmxM.22.0210	hypothetical protein, conserved	0.00005	-2.00

Appendix B3. Results of the transcriptomic analysis for genes of interest. Values indicate fold change relative to WT.

gene ID	glucose transporters	TKT KO	RIB-TKT
LmxM.36.6300	GT1	0.75	1.34
LmxM.36.6290	GT2	0.75	1
LmxM.36.6280	GT3	0.77	1.02
LmxM.24.0680	myo-inositol/proton symporter	2.05	1.7
	glycolysis		
LmxM.21.0240	hexokinase	1.27	0.88
LmxM.12.0530	PGI	0.97	1.3
LmxM.08_29.2510	phosphofructokinase	0.82	0.95
LmxM.36.1260	aldolase	0.76	0.99
LmxM.24.0850	TPI	0.84	1.1
LmxM.29.2980	GA3PDH glycosomal	0.63	0.79
LmxM.20.0100	PGK glycosomal	0.66	0.92
LmxM.36.2350	GA3PDH cytosolic	1.33	1.81
LmxM.20.0110	PGK cytosolic	0.67	0.9
LmxM.10.0510	G3PDH glycosomal	1.38	1.01
LmxM.28.0240	G3PDH mitochondrial	2.56	1.19
LmxM.14.1160	enolase	0.81	0.77
LmxM.34.0020	PYK	0.65	0.85
	succinate shunt		
LmxM.27.1805	PEPCK	0.66	0.91
LmxM.28.2860	malate DH cytosolic	0.8	0.65
LmxM.19.0710	malate DH glycosomal	0.58	0.64
LmxM.24.0320	fumarase	1.88	1.59
LmxM.23.0110	mannose-1P guanyltransferase	0.36	0.35
	AA transporters		
LmxM.30.0350	aATP11	2.12	2.73
LmxM.07.1160	transmembrane transporter, putative	2.1	1.65
LmxM.31.2660	amino acid transporter, putative	2.41	2.1
LmxM.30.0320	amino acid transporter, putative	1.7	2.02
LmxM.34.5350	amino acid permease, putative	2.07	1.17
LmxM.30.0880	amino acid permease 3	4.09	4.27
LmxM.30.0870	amino acid permease 3	2.07	2.22
LmxM.30.0571	amino acid transporter aATP11, putative	0.20	0.29

Bibliography

Achcar, F., Barrett, M.P., and Breitling, R. (2013). Explicit consideration of topological and parameter uncertainty gives new insights into a well-established model of glycolysis. FEBS J. *280*, 4640–4651.

Afgan, E., Chapman, B., Jadan, M., Franke, V., and Taylor, J. (2012). Using cloud computing infrastructure with CloudBioLinux, CloudMan, and Galaxy. Curr. Protoc. Bioinformatics *Chapter 11*, Unit11.9.

Akopyants, N.S., Matlib, R.S., Bukanova, E.N., Smeds, M.R., Brownstein, B.H., Stormo, G.D., and Beverley, S.M. (2004). Expression profiling using random genomic DNA microarrays identifies differentially expressed genes associated with three major developmental stages of the protozoan parasite *Leishmania major*. Mol. Biochem. Parasitol. *136*, 71–86.

Alawieh, A., Musharrafieh, U., Jaber, A., Berry, A., Ghosn, N., and Bizri, A.R. (2014). Revisiting leishmaniasis in the time of war: the Syrian conflict and the Lebanese outbreak. Int. J. Infect. Dis. *29*, 115–119.

Alcolea, P.J., Alonso, A., Gómez, M.J., Sánchez-Gorostiaga, A., Moreno-Paz, M., González-Pastor, E., Toraño, A., Parro, V., and Larraga, V. (2010a). Temperature increase prevails over acidification in gene expression modulation of amastigote differentiation in *Leishmania infantum*. BMC Genomics *11*, 31.

Alcolea, P.J., Alonso, A., Gómez, M.J., Moreno, I., Dominguez, M., Parro, V., and Larraga, V. (2010b). Transcriptomics throughout the life cycle of *Leishmania infantum*: High down-regulation rate in the amastigote stage. Int. J. Parasitol. *40*, 1497–1516.

Alcolea, P.J., Alonso, A., Gómez, M.J., Postigo, M., Molina, R., Jiménez, M., and Larraga, V. (2014). Stage-specific differential gene expression in *Leishmania infantum*: from the foregut of Phlebotomus perniciosus to the human phagocyte. BMC Genomics *15*, 849.

Allmann, S., Morand, P., Ebikeme, C., Gales, L., Biran, M., Hubert, J., Brennand, A., Mazet, M., Franconi, J.-M., Michels, P. a M., et al. (2013). Cytosolic NADPH homeostasis in glucose-starved procyclic *Trypanosoma brucei* relies on malic enzyme and the pentose phosphate pathway fed by gluconeogenic flux. J. Biol. Chem.

Almeida, R., Gilmartin, B.J., McCann, S.H., Norrish, A., Ivens, A.C., Lawson, D., Levick, M.P., Smith, D.F., Dyall, S.D., Vetrie, D., et al. (2004). Expression profiling of the Leishmania life cycle: cDNA arrays identify developmentally regulated genes present but not annotated in the genome. Mol. Biochem. Parasitol. *136*, 87–100.

Al-Salabi, M.I., and De Koning, H.P. (2005). Purine nucleobase transport in amastigotes of *Leishmania mexicana*: Involvement in allopurinol uptake. Antimicrob. Agents Chemother. *49*, 3682–3689.

Alsford, S., Turner, D.J., Obado, S.O., Sanchez-flores, A., Glover, L., Berriman, M.,

Hertz-fowler, C., and Horn, D. (2011). High-throughput phenotyping using parallel sequencing of RNA interference targets in the African trypanosome. Genome Res *21*, 915–924.

Alvar, J., Yactayo, S., and Bern, C. (2006). Leishmaniasis and poverty. Trends Parasitol. *22*, 552–557.

Alvar, J., Vélez, I.D., Bern, C., Herrero, M., Desjeux, P., Cano, J., Jannin, J., and de Boer, M. (2012). Leishmaniasis worldwide and global estimates of its incidence. PLoS One *7*.

Anstead, G.M., Chandrasekar, B., Zhao, W., Yang, J., Perez, L.E., and Melby, P.C. (2001). Malnutrition Alters the Innate Immune Response and Increases Early Visceralization following Leishmania donovani Infection. Infect. Immun. *69*, 4709–4718.

Bais, R., James, H.M., Rofe, A.M., and Conyers, R.A. (1985). The purification and properties of human liver ketohexokinase. A role for ketohexokinase and fructose-bisphosphate aldolase in the metabolic production of oxalate from xylitol. Biochem. J. *230*, 53–60.

Bakker, B.M., Michels, P.A., Opperdoes, F.R., and Westerhoff, H. V (1997). Glycolysis in bloodstream form *Trypanosoma brucei* can be understood in terms of the kinetics of the glycolytic enzymes. J. Biol. Chem. *272*, 3207–3215.

Bakker, B.M., Michels, P.A., Opperdoes, F.R., and Westerhoff, H. V (1999). What controls glycolysis in bloodstream form *Trypanosoma brucei*? J. Biol. Chem. *274*, 14551–14559.

Bakker, B.M., Mensonides, F.I.C., Teusink, B., Van Hoek, P., Michels, P. a M., and Westerhoff, H. V (2000). Compartmentation protects trypanosomes from the dangerous design of glycolysis. Proc. Natl. Acad. Sci. U. S. A. *97*, 2087–2092.

Barrett, M.P., and Le Page, R.W. (1993). A 6-phosphogluconate dehydrogenase gene from *Trypanosoma brucei*. Mol. Biochem. Parasitol. *57*, 89–100.

Bates, P.A. (2007). Transmission of Leishmania metacyclic promastigotes by phlebotomine sand flies. Int. J. Parasitol. *37*, 1097–1106.

Bates, P.A., Robertson, C.D., Tetley, L., and Coombs, G.H. (1992). Axenic cultivation and characterization of *Leishmania mexicana* amastigote-like forms. Parasitology *105 (Pt 2*, 193–202.

Bente, M., Harder, S., Wiesgigl, M., Heukeshoven, J., Gelhaus, C., Krause, E., Clos, J., and Bruchhaus, I. (2003). Developmentally induced changes of the proteome in the protozoan parasite *Leishmania donovani*. Proteomics *3*, 1811–1829.

Berdis, A.J., and Cook, P.F. (1993). Overall kinetic mechanism of 6-phosphogluconate dehydrogenase from *Candida utilis*. Biochemistry *32*, 2036–2040.

Berens, R.L., Brun, R., and Krassner, S.M. (1976). A simple monophasic medium for axenic culture of hemoflagellates. J. Parasitol. *62*, 360–365.

Berriman, M., Ghedin, E., Hertz-Fowler, C., Bartholomeu, D.C., Lennard, N.J., Caler, E., Hamlin, N.E., Haas, B., Bo, U., Hannick, L., et al. (2005). The Genome of the African Trypanosome *Trypanosoma brucei*. Science (80-). *309*, 416–423.

Blum, J.J. (1990). Effects of culture age and hexoses on fatty acid oxidation by *Leishmania major*. J. Protozool. *37*, 505–510.

Blum, J.J., and Opperdoes, F.R. (1994). Secretion of sucrase by *Leishmania donovani*. J. Eukaryot. Microbiol. *41*, 228–231.

Boda, C., Enanga, B., Courtioux, B., Breton, J.C., and Bouteille, B. (2005). Trypanocidal activity of methylene blue: Evidence for in vitro efficacy and in vivo failure. Chemotherapy *52*, 16–19.

Boitz, J.M., Ullman, B., Jardim, A., and Carter, N.S. (2012). Purine salvage in Leishmania: complex or simple by design? Trends Parasitol. *28*, 345–352.

Boros, L.G., Puigjaner, J., Cascante, M., Lee, W.N.P., Brandes, J.L., Bassilian, S., Yusuf, F.I., Williams, R.D., Muscarella, P., Melvin, W.S., et al. (1997). Oxythiamine and dehydroepiandrosterone inhibit the nonoxidative synthesis of ribose and tumor cell proliferation. Cancer Res. *57*, 4242–4248.

Bouatra, S., Aziat, F., Mandal, R., Guo, A.C., Wilson, M.R., Knox, C., Bjorndahl, T.C., Krishnamurthy, R., Saleem, F., Liu, P., et al. (2013). The Human Urine Metabolome. PLoS One *8*, e73076.

Boucher, N., Wu, Y., Dumas, C., Dube, M., Sereno, D., Breton, M., and Papadopoulou, B. (2002). A common mechanism of stage-regulated gene expression in Leishmania mediated by a conserved 3'-untranslated region element. J. Biol. Chem. *277*, 19511–19520.

Bozdech, Z., and Ginsburg, H. (2005). Data mining of the transcriptome of *Plasmodium falciparum*: the pentose phosphate pathway and ancillary processes. Malar. J. *4*, 17.

Braus, G.H. (1991). Aromatic Amino Acid Biosynthesis in the Yeast *Saccharomyces cerevisiae* : a Model System for the Regulation of a Eukaryotic Biosynthetic Pathway. Microbiol. Rev. *55*, 349–370.

Brin, M. (1974). Transketolase A2 - Bergmeyer, Hans Ulrich BT - Methods of Enzymatic Analysis (Second Edition). In Methods of Enzymatic Analysis, (Academic Press), pp. 703–709.

Burchmore, R.J.S., Rodriguez-Contreras, D., McBride, K., Merkel, P., Barrett, M.P., Modi, G., Sacks, D., and Landfear, S.M. (2003). Genetic characterization of glucose transporter function in *Leishmania mexicana*. Proc. Natl. Acad. Sci. U. S. A. *100*, 3901–3906.

Bursell, E., Billing, K.J., Hargrove, J.W., McCabe, C.T., and Slack, E. (1973). The supply of substrates to the flight muscle of tsetse flies. Trans. R. Soc. Trop. Med. Hyg. *67*, 296.

Calligari, P.A., Salgado, G.F., Pelupessy, P., Lopes, P., Ouazzani, J., Bodenhausen, G., and Abergel, D. (2012). Insights into internal dynamics of 6-phosphogluconolactonase from *Trypanosoma brucei* studied by nuclear magnetic resonance and molecular dynamics. Proteins *80*, 1196–1210.

Cantacessi, C., Dantas-Torres, F., Nolan, M.J., and Otranto, D. (2015). The past, present, and future of Leishmania genomics and transcriptomics. Trends Parasitol. *31*, 100–108.

Caradonna, K.L., Engel, J.C., Jacobi, D., Lee, C.-H., and Burleigh, B.A. (2013). Host metabolism regulates intracellular growth of *Trypanosoma cruzi*. Cell Host Microbe *13*, 108–117.

Carter, N.S., Yates, P., Arendt, C.S., Boitz, J.M., and Ullman, B. (2008). Purine and Pyrimidine Metabolism in Leishmania. Adv Exp Med Biol *625*, 141-154.

Cavalier-Smith, T. (2010). Kingdoms Protozoa and Chromista and the eozoan root of the eukaryotic tree. Biol. Lett. *6*, 342–345.

Cecilio, P., Perez-Cabezas, B., Santarem, N., Maciel, J., Rodrigues, V., and da Silva, A.C. (2014). Deception and manipulation: The arms of Leishmania, a successful parasite. Front. Immunol. *5*, 1–16.

Cerf, B.J., Jones, T.C., Badaro, R., Sampaio, D., Teixeira, R., and Johnson, W.D.J. (1987). Malnutrition as a risk factor for severe visceral leishmaniasis. J. Infect. Dis. *156*, 1030–1033.

Chan, X.W.A., Wrenger, C., Stahl, K., Bergmann, B., Winterberg, M., Müller, I.B., and Saliba, K.J. (2013). Chemical and genetic validation of thiamine utilization as an antimalarial drug target. Nat. Commun. *4*, 2060.

Chokkathukalam, A., Jankevics, A., Creek, D.J., Achcar, F., Barrett, M.P., and Breitling, R. (2013). mzMatch-ISO: an R tool for the annotation and relative quantification of isotope-labelled mass spectrometry data. Bioinformatics *29*, 281–283.

Clark, M.G., Williams, J.F., and Blackmore, P.F. (1971). The Transketolase Exchange Reaction *in vitro*. Biochem J *125*, 381–384.

Clasquin, M.F., Melamud, E., Singer, A., Gooding, J.R., Xu, X., Dong, A., Cui, H., Campagna, S.R., Savchenko, A., Yakunin, A.F., et al. (2011). Riboneogenesis in yeast. Cell *145*, 969–980.

Clayton, C. (2013). The regulation of trypanosome gene expression by RNA-binding proteins. PLoS Pathog. *9*, e1003680.

Clayton, C.E. (2002). Life without transcriptional control? From fly to man and back again. EMBO J. *21*, 1881–1888.

Clayton, C.E. (2014). Networks of gene expression regulation in *Trypanosoma brucei*. Mol. Biochem. Parasitol. *195*, 96–106.

Cohen-Freue, G., Holzer, T.R., Forney, J.D., and McMaster, W.R. (2007). Global gene expression in Leishmania. Int. J. Parasitol. *37*, 1077–1086.

Colasante, C., Ellis, M., Ruppert, T., and Voncken, F. (2006). Comparative proteomics of glycosomes from bloodstream form and procyclic culture form *Trypanosoma brucei brucei*. Proteomics *6*, 3275–3293.

Comín-Anduix, B., Boren, J., Martinez, S., Moro, C., Centelles, J., Trebukhina, R., Petushok, N., Lee, W., Boros, L., and Cascante, M. (2001). The effect of thiamine supplementation on tumour proliferation. A metabolic control analysis study. Eff. Thiamine Suppl. Tumour Proliferation. A Metab. Control Anal. Study. *268*, 4177–4182.

Comini, M.A., Ortíz, C., and Cazzulo, J.J. (2013). Drug Targets in Trypanosomal and Leishmanial Pentose Phosphate Pathway. In Trypanosomatid Diseases, (Wiley-VCH Verlag GmbH & Co. KGaA), 297–313.

Coombs, G.H., Craft, J.A., and Hart, D.T. (1982). A comparative study of *Leishmania mexicana* amastigotes and promastigotes, enzyme activities and subcellular locations. Mol. Biochem. Parasitol. *5*, 199–211.

Cordeiro, A.T., and Thiemann, O.H. (2010). 16-bromoepiandrosterone, an activator of the mammalian immune system, inhibits glucose 6-phosphate dehydrogenase from *Trypanosoma cruzi* and is toxic to these parasites grown in culture. Bioorg. Med. Chem. *18*, 4762–4768.

Cordeiro, A.T., Thiemann, O.H., and Michels, P. a M. (2009). Inhibition of Trypanosoma brucei glucose-6-phosphate dehydrogenase by human steroids and their effects on the viability of cultured parasites. Bioorg. Med. Chem. *17*, 2483–2489.

Coy, J.F., Dübel, S., Kioschis, P., Thomas, K., Micklem, G., Delius, H., and Poustka, A. (1996). Molecular cloning of tissue-specific transcripts of a transketolase-related gene: implications for the evolution of new vertebrate genes. Genomics *32*, 309–316.

Creek, D.J., Jankevics, A., Breitling, R., Watson, D.G., Barrett, M.P., and Burgess, K.E. V (2011). Toward global metabolomics analysis with hydrophilic interaction liquid chromatography-mass spectrometry: Improved metabolite identification by retention time prediction. Anal. Chem. *83*, 8703–8710.

Creek, D.J., Chokkathukalam, A., Jankevics, A., Burgess, K.E. V, Breitling, R., and Barrett, M.P. (2012a). Stable isotope-assisted metabolomics for network-wide metabolic pathway elucidation. Anal. Chem. *84*, 8442–8447.

Creek, D.J., Anderson, J., McConville, M.J., and Barrett, M.P. (2012b). Metabolomic analysis of trypanosomatid protozoa. Mol. Biochem. Parasitol. *181*, 73–84.

Creek, D.J., Jankevics, A., Burgess, K.E. V., Breitling, R., and Barrett, M.P. (2012c). IDEOM: an Excel interface for analysis of LC-MS-based metabolomics data. Bioinformatics *28*, 1048–1049.

Creek, D.J., Nijagal, B., Kim, D.-H., Rojas, F., Matthews, K.R., and Barrett, M.P. (2013). Metabolomics guides rational development of a simplified cell culture medium for drug screening against Trypanosoma brucei. Antimicrob. Agents Chemother. *57*, 2768–2779.

Creek, D.J., Mazet, M., Achcar, F., Anderson, J., Kim, D.-H., Kamour, R., Morand, P., Millerioux, Y., Biran, M., Kerkhoven, E.J., et al. (2015). Probing the metabolic network in bloodstream-form *Trypanosoma brucei* using untargeted metabolomics with stable isotope labelled glucose. PLoS Pathog. *11*, e1004689.

Croft, S.L., Sundar, S., and Fairlamb, A.H. (2006). Drug Resistance in Leishmaniasis Drug Resistance in Leishmaniasis. Society *19*, 111–126.

Cronín, C.N., Nolan, D.P., and Voorheis, H.P. (1989). The enzymes of the classical pentose phosphate pathway display differential activities in procyclic and bloodstream forms of *Trypanosoma brucei*. FEBS Lett. *244*, 26–30.

Cull, B., Godinho, J.L.P., Rodrigues, J.C.F., Frank, B., Schurigt, U., Williams, R.A.M., Coombs, G.H., and Mottram, J.C. (2014). Glycosome turnover in *Leishmania major* is mediated by autophagy. Autophagy *10*, 2143–2157.

Dardonville, C., Rinaldi, E., Hanau, S., Barrett, M.P., Brun, R., and Gilbert, I.H. (2003). Synthesis and biological evaluation of substrate-based inhibitors of 6-phosphogluconate dehydrogenase as potential drugs against African trypanosomiasis. Bioorganic Med. Chem. *11*, 3205–3214.

Dardonville, C., Rinaldi, E., Barrett, M.P., Brun, R., Gilbert, I.H., and Hanau, S. (2004). Selective inhibition of *Trypanosoma brucei* 6-phosphogluconate

dehydrogenase by high-energy intermediate and transition-state analogues. J. Med. Chem. *47*, 3427–3437.

Das, S., Freier, A., Boussoffara, T., Das, S., Oswald, D., Losch, F.O., Selka, M., Sacerdoti-Sierra, N., Schönian, G., Wiesmüller, K.-H., et al. (2014). Modular multiantigen T cell epitope-enriched DNA vaccine against human leishmaniasis. Sci. Transl. Med. *6*, 234ra56.

Datta, A., and Racker, E. (1961). Mechanism of action of transketolase. J. Biol. Chem *236*, 617–623.

Debrabant, A., Joshi, M.B., Pimenta, P.F.P., and Dwyer, D.M. (2004). Generation of *Leishmania donovani* axenic amastigotes: Their growth and biological characteristics. Int. J. Parasitol. *34*, 205–217.

Delarue, M., Duclert-Savatier, N., Miclet, E., Haouz, A., Giganti, D., Ouazzani, J., Lopez, P., Nilges, M., and Stoven, V. (2007). Three Dimensional Structure and Implications for the Catalytic Mechanism of 6-Phosphogluconolactonase from *Trypanosoma brucei*. J. Mol. Biol. *366*, 868–881.

Depledge, D.P., Evans, K.J., Ivens, A.C., Aziz, N., Maroof, A., Kaye, P.M., and Smith, D.F. (2009). Comparative expression profiling of Leishmania: Modulation in gene expression between species and in different host genetic backgrounds. PLoS Negl. Trop. Dis. *3*.

Desjeux, P. (2004). Leishmaniasis: Current situation and new perspectives. Comp. Immunol. Microbiol. Infect. Dis. *27*, 305–318.

Diaz-Moralli, S., Tarrado-Castellarnau, M., Alenda, C., Castells, A., and Cascante, M. (2011). Transketolase-like 1 expression is modulated during colorectal cancer progression and metastasis formation. PLoS One *6*, e25323.

Du, M.X., Sim, J., Fang, L., Yin, Z., Koh, S., Stratton, J., Pons, J., Wang, J.J., and Carte, B. (2004). Identification of Novel Small-Molecule Inhibitors for Human Transketolase by High-Throughput Screening with Fluorescent Intensity (FLINT) Assay. J. Biomol. Screen. *9*, 427–433.

Du, R., Hotez, P.J., Al-Salem, W., and Acosta-Serrano, A. (2016). Old World Cutaneous Leishmaniasis and Refugee Crises in the Middle East and North Africa. PLoS Negl. Trop. Dis. *In press*.

Duffieux, F., Van Roy, J., Michels, P. a, and Opperdoes, F.R. (2000). Molecular characterization of the first two enzymes of the pentose-phosphate pathway of *Trypanosoma brucei*. Glucose-6-phosphate dehydrogenase and 6-phosphogluconolactonase. J. Biol. Chem. *275*, 27559–27565.

Duncan, S., Myburgh, E., Philipon, C., Brown, E., Meissner, M., Brewer, J., and Mottram, J.C. (2016). Conditional gene deletion with DiCre demonstrates an essential role for CRK3 in *Leishmania mexicana* cell cycle regulation. Mol. Micorbiol. *16*, DOI: 10.1111/mmi.13375.

Dusick, J.R., Glenn, T.C., Lee, W.N.P., Vespa, P.M., Kelly, D.F., Lee, S.M., Hovda, D., and Martin, N. (2007). Increased pentose phosphate pathway flux after clinical traumatic brain injury: a [1,2-13C2]glucose labeling study in humans. J. Cereb. Blood Flow Metab. *27*, 1593–1602.

Engelke, U.F.H., Zijlstra, F.S.M., Mochel, F., Valayannopoulos, V., Rabier, D.,

Kluijtmans, L.A.J., Perl, A., Verhoeven-Duif, N.M., de Lonlay, P., Wamelink, M.M.C., et al. (2010). Mitochondrial involvement and erythronic acid as a novel biomarker in transaldolase deficiency. Biochim. Biophys. Acta *1802*, 1028–1035.

Engwerda, C.R., and Kaye, P.M. (2000). Organ-specific immune responses associated with infectious disease. Immunol. Today *21*, 73–78.

Esteve, M.I., and Cazzulo, J.J. (2004). The 6-phosphogluconate dehydrogenase from *Trypanosoma cruzi*: The absence of two inter-subunit salt bridges as a reason for enzyme instability. Mol. Biochem. Parasitol. *133*, 197–207.

Evans, K.J., and Kedzierski, L. (2012). Development of Vaccines against Visceral Leishmaniasis. J. Trop. Med. *2012*, 892817.

Fairlamb, A.H., Blackburn, P., Ulrich, P., Chait, B.T., and Cerami, A. (1985). Trypanothione: a novel bis(glutathionyl)spermidine cofactor for glutathione reductase in trypanosomatids. Science *227*, 1485–1487.

Fan, J., Ye, J., Kamphorst, J.J., Shlomi, T., Thompson, C.B., and Rabinowitz, J.D. (2014). Quantitative flux analysis reveals folate-dependent NADPH production. Nature *510*, 298–302.

Feng, X., Rodriguez-Contreras, D., Buffalo, C., Bouwer, H.G.A., Kruvand, E., Beverley, S.M., and Landfear, S.M. (2009). Amplification of an alternate transporter gene suppresses the avirulent phenotype of glucose transporter null mutants in *Leishmania mexicana*. Mol. Microbiol. *71*, 369–381.

Feng, X., Feistel, T., Buffalo, C., McCormack, A., Kruvand, E., Rodriguez-Contreras, D., Akopyants, N.S., Umasankar, P.K., David, L., Jardim, A., et al. (2011). Remodeling of protein and mRNA expression in *Leishmania mexicana* induced by deletion of glucose transporter genes. Mol. Biochem. Parasitol. *175*, 39–48.

Garami, A., and Ilg, T. (2001). Disruption of mannose activation in *Leishmania mexicana*: GDP-mannose pyrophosphorylase is required for virulence, but not for viability. EMBO J. *20*, 3657–3666.

Garami, A., Mehlert, A., and Ilg, T. (2001). Glycosylation defects and virulence phenotypes of *Leishmania mexicana* phosphomannomutase and dolicholphosphate-mannose synthase gene deletion mutants. Mol. Cell. Biol. *21*, 8168–8183.

Ghosh, A.K., Sardar, A.H., Mandal, A., Saini, S., Abhishek, K., Kumar, A., Purkait, B., Singh, R., Das, S., Mukhopadhyay, R., et al. (2015). Metabolic reconfiguration of the central glucose metabolism: A crucial strategy of *Leishmania donovani* for its survival during oxidative stress. FASEB J. *29*, 2081–2098.

Giardine, B., Riemer, C., Hardison, R.C., Burhans, R., Elnitski, L., Shah, P., Zhang, Y., Blankenberg, D., Albert, I., Taylor, J., et al. (2005). Galaxy: a platform for interactive large-scale genome analysis. Genome Res. *15*, 1451–1455.

Glover, J.R., Andrews, D.W., and Rachubinski, R.A. (1994). *Saccharomyces cerevisiae* peroxisomal thiolase is imported as a dimer. Proc. Natl. Acad. Sci. U. S. A. *91*, 10541–10545.

Gluenz, E., Ginger, M.L., and McKean, P.G. (2010). Flagellum assembly and function during the Leishmania life cycle. Curr. Opin. Microbiol. *13*, 473–479.

González, D., Pérez, J.L., Serrano, M.L., Igoillo-Esteve, M., Cazzulo, J.J., Barrett,

M.P., Bubis, J., and Mendoza-León, A. (2010). The 6-phosphogluconate dehydrogenase of *Leishmania (Leishmania) mexicana*: gene characterization and protein structure prediction. J. Mol. Microbiol. Biotechnol. *19*, 213–223.

Gould, S.J., Keller, G. a, Hosken, N., Wilkinson, J., and Subramani, S. (1989). A conserved tripeptide sorts proteins to peroxisomes. J. Cell Biol. *108*, 1657–1664.

Greenblatt, C.L., Schnur, L.F., Bar-Gal, G.K., Ermolaev, H., Peleg, N., and Barrett, M.P. (2002). Polymorphism among alleles of the 6-phosphogluconate dehydrogenase gene from *Leishmania major* and *Leishmania tropica*. Mol. Biochem. Parasitol. *125*, 185–188.

Van Grinsven, K.W.A., Van Den Abbeele, J., Van Den Bossche, P., Van Hellemond, J.J., and Tielens, A.G.M. (2009). Adaptations in the glucose metabolism of procyclic *Trypanosoma brucei* isolates from tsetse flies and during differentiation of bloodstream forms. Eukaryot. Cell *8*, 1307–1311.

Gualdrón-López, M., Brennand, A., Avilán, L., and Michels, P. a M. (2013). Translocation of solutes and proteins across the glycosomal membrane of trypanosomes; possibilities and limitations for targeting with trypanocidal drugs. Parasitology *140*, 1–20.

Gupta, S., Cordeiro, A.T., and Michels, P. a M. (2011). Glucose-6-phosphate dehydrogenase is the target for the trypanocidal action of human steroids. Mol. Biochem. Parasitol. *176*, 112–115.

Guther, M.L.S., Urbaniak, M.D., Tavendale, A., Prescott, A., and Ferguson, M.A.J. (2014). High-confidence glycosome proteome for procyclic form *Trypanosoma brucei* by epitope-tag organelle enrichment and SILAC proteomics. J. Proteome Res. *13*, 2796–2806.

Haanstra, J.R., Van Tuijl, A., Kessler, P., Reijnders, W., Michels, P. a M., Westerhoff, H. V, Parsons, M., and Bakker, B.M. (2008). Compartmentation prevents a lethal turbo-explosion of glycolysis in trypanosomes. Proc. Natl. Acad. Sci. U. S. A. *105*, 17718–17723.

Hadighi, R., Mohebali, M., Boucher, P., Hajjaran, H., Khamesipour, A., and Ouellette, M. (2006). Unresponsiveness to Glucantime Treatment in Iranian Cutaneous Leishmaniasis due to Drug-Resistant *Leishmania tropica* Parasites . PLoS Med. *3*, e162.

Hadighi, R., Boucher, P., Khamesipour, A., Meamar, A.R., Roy, G., Ouellette, M., and Mohebali, M. (2007). Glucantime-resistant *Leishmania tropica* isolated from Iranian patients with cutaneous leishmaniasis are sensitive to alternative antileishmania drugs. Parasitol. Res. *101*, 1319–1322.

Harrison, L.H., Naidu, T.G., Drew, J.S., de Alencar, J.E., and Pearson, R.D. (1986). Reciprocal relationships between undernutrition and the parasitic disease visceral leishmaniasis. Rev. Infect. Dis. *8*, 447–453.

Hart, D.T., and Coombs, G.H. (1982). *Leishmania mexicana*: energy metabolism of amastigotes and promastigotes. Exp. Parasitol. *54*, 397–409.

Hayani, K., Dandashli, A., and Weisshaar, E. (2015). Cutaneous Leishmaniasis in Syria: Clinical Features, Current Status and the Effects of War. Acta Derm. Venereol. *95*, 62–66.

Heinrich, P.C., Steffen, H., Janser, P., and Wiss, O. (1972). Studies on the reconstitution of apotransketolase with thiamine pyrophosphate and analogs of the coenzyme. Eur. J. Biochem. *30*, 533–541.

Heise, N., and Opperdoes, F.R. (1999). Purification, localisation and characterisation of glucose-6-phosphate dehydrogenase of *Trypanosoma brucei*. Mol. Biochem. Parasitol. *99*, 21–32.

Helfert, S., Estévez, A.M., Bakker, B., Michels, P., and Clayton, C. (2001). Roles of triosephosphate isomerase and aerobic metabolism in *Trypanosoma brucei*. Biochem. J. *357*, 117–125.

Hellemond, J.J. Van, and Tielens, A.G.M. (1997). Inhibition of the respiratory chain results in a reversible metabolic arrest in Leishmania promastigotes. *85*, 135–138.

Heringa, J. (2002). Local weighting schemes for protein multiple sequence alignment. Comput. Chem. *26*, 459–477.

Holzer, T.R., McMaster, W.R., and Forney, J.D. (2006). Expression profiling by whole-genome interspecies microarray hybridization reveals differential gene expression in procyclic promastigotes, lesion-derived amastigotes, and axenic amastigotes in *Leishmania mexicana*. Mol. Biochem. Parasitol. *146*, 198–218.

Horecker, B.L., Cheng, T., and Pontremoli, S. (1963). The coupled reaction catalyzed by the enzymes transketolase and transaldolase. II. Reaction of erythrose 4-phosphate and the transaldolase-dihydroxyacetone complex. J. Biol. Chem. *238*, 3428–3431.

Horn, D., and Duraisingh, M.T. (2014). Antiparasitic chemotherapy – from genomes to mechanisms. Annu Rev Pharmacol Toxicol *54*, 71–94.

Huck, J.H.J., Verhoeven, N.M., Struys, E. a, Salomons, G.S., Jakobs, C., and van der Knaap, M.S. (2004). Ribose-5-phosphate isomerase deficiency: new inborn error in the pentose phosphate pathway associated with a slowly progressive leukoencephalopathy. Am. J. Hum. Genet. *74*, 745–751.

Hughes, M.B., and Lucchesi, J.C. (1976). Genetic Rescue of a Lethal "Null" Activity Allele of 6-Phosphogluconate Dehydrogenase in *Drosophila melanogaster*. Science (80-.). *196*, 1114–1115.

Igoillo-Esteve, M., and Cazzulo, J.J. (2006). The glucose-6-phosphate dehydrogenase from *Trypanosoma cruzi*: Its role in the defense of the parasite against oxidative stress. Mol. Biochem. Parasitol. *149*, 170–181.

Igoillo-Esteve, M., Maugeri, D., Stern, A.L., Beluardi, P., and Cazzulo, J.J. (2007). The pentose phosphate pathway in *Trypanosoma cruzi*: a potential target for the chemotherapy of Chagas disease. An. Acad. Bras. Cienc. *79*, 649–663.

Ilg, T., Stierhof, Y.D., Craik, D., Simpson, R., Handman, E., and Bacic, A. (1996). Purification and structural characterization of a filamentous, mucin-like proteophosphoglycan secreted by Leishmania parasites. J. Biol. Chem. *271*, 21583–21596.

Inbar, E., Canepa, G.E., Carrillo, C., Glaser, F., Suter Grotemeyer, M., Rentsch, D., Zilberstein, D., and Pereira, C.A. (2012). Lysine transporters in human trypanosomatid pathogens. Amino Acids *42*, 347–360.

Inci, R., Fatih, I.M., Ozturk, P., Mulayim, M.K., Ozyurt, K., and Alatas, E.T.A.

(2015). Effect of the Syrian Civil War on Prevalence of Cutaneous Leishmaniasis in Southeastern Anatolia, Turkey. Med. Sci. Monit. *21*, 2100–2104.

Isnard, a D., Thomas, D., and Surdin-Kerjan, Y. (1996). The study of methionine uptake in *Saccharomyces cerevisiae* reveals a new family of amino acid permeases. J. Mol. Biol. *262*, 473–484.

Ivens, A.C., Peacock, C.S., Worthey, E.A., Murphy, L., Aggarwal, G., Berriman, M., Sisk, E., Rajandream, M., Adlem, E., Aert, R., et al. (2005). The Genome of the Kinetoplastid Parasite, *Leishmania major*. Science (80). *309*, 436–443.

Ives, A., Ronet, C., Prevel, F., Ruzzante, G., Fuertes-Marraco, S., Schutz, F., Zangger, H., Revaz-Breton, M., Lye, L.-F., Hickerson, S.M., et al. (2011). Leishmania RNA virus controls the severity of mucocutaneous leishmaniasis. Science *331*, 775–778.

Jamdhade, M.D., Pawar, H., Chavan, S., Sathe, G., Umasankar, P.K., Mahale, K.N., Dixit, T., Madugundu, A.K., Prasad, T.S.K., Gowda, H., et al. (2015). Comprehensive proteomics analysis of glycosomes from *Leishmania donovani*. OMICS *19*, 157–170.

Jhingran, A., Chawla, B., Saxena, S., Barrett, M.P., and Madhubala, R. (2009). Paromomycin: uptake and resistance in *Leishmania donovani*. Mol. Biochem. Parasitol. *164*, 111–117.

Johnston, K.L. (2015). Metabolomic approaches for the identification of metabolic pathways in *Trypanosoma brucei*. University of Glasgow.

Joshi, S., Singh, A.R., Kumar, A., Misra, P.C., Siddiqi, M.I., and Saxena, J.K. (2008). Molecular cloning and characterization of *Plasmodium falciparum* transketolase. Mol. Biochem. Parasitol. *160*, 32–41.

Kacser, H. (1995). Recent developments beyond metabolic control analysis. Biochem. Soc. Trans. *23*, 387–391.

Kardon, T., Stroobant, V., Veiga-da-Cunha, M., and Schaftingen, E. Van (2008). Characterization of mammalian sedoheptulokinase and mechanism of formation of erythritol in sedoheptulokinase deficiency. FEBS Lett. *582*, 3330–3334.

Kaye, P., and Scott, P. (2011). Leishmaniasis: complexity at the host-pathogen interface. Nat. Rev. Microbiol. *9*, 604–615.

Kelner, M.J., and Alexander, N.M. (1985). Methylene blue directly oxidizes glutathione without the intermediate formation of hydrogen peroxide. J. Biol. Chem. *260*, 15168–15171.

Kerkhoven, E.J., Achcar, F., Alibu, V.P., Burchmore, R.J., Gilbert, I.H., Trybiło, M., Driessen, N.N., Gilbert, D., Breitling, R., Bakker, B.M., et al. (2013). Handling uncertainty in dynamic models: the pentose phosphate pathway in *Trypanosoma brucei*. PLoS Comput. Biol. *9*, e1003371.

Kim, D.H., Achcar, F., Breitling, R., Burgess, K.E., and Barrett, M.P. (2015). LC/MS-based absolute metabolite quantification: application to metabolic flux measurement in trypanosomes. Metabolomics *11*, 1721–1732.

Kim, Y., Kim, E.Y., Seo, Y.M., Yoon, T.K., Lee, W.S., and Lee, K.A. (2012). Function of the pentose phosphate pathway and its key enzyme, transketolase, in the regulation of the meiotic cell cycle in oocytes. Clin. Exp. Reprod. Med. *39*, 58–67.

Kleijn, R.J., van Winden, W. a, van Gulik, W.M., and Heijnen, J.J. (2005). Revisiting the 13C-label distribution of the non-oxidative branch of the pentose phosphate pathway based upon kinetic and genetic evidence. FEBS J. *272*, 4970–4982.

Kloehn, J., Saunders, E.C., O'Callaghan, S., Dagley, M.J., and McConville, M.J. (2015). Characterization of Metabolically Quiescent Leishmania Parasites in Murine Lesions Using Heavy Water Labeling. PLoS Pathog. *11*, 1–19.

Kneidinger, B., Marolda, C., Graninger, M., Zamyatina, A., McArthur, F., Kosma, P., Valvano, M.A., and Messner, P. (2002). Biosynthesis pathway of ADP-L-glycero-beta-D-manno-heptose in *Escherichia coli*. J. Bacteriol. *184*, 363–369.

Kohl, L., Drmota, T., Do Thi, C.-D., Callens, M., Van Beeumen, J., Opperdoes, F.R., and Michels, P.A.M. (1996). Cloning and characterization of the NAD-linked glycerol-3-phosphate dehydrogenases of *Trypanosoma brucei brucei* and *Leishmania mexicana mexicana* and expression of the trypanosome enzyme in *Escherichia coli*. Mol. Biochem. Parasitol. *76*, 159–173.

Kumar, R., Gupta, S., Srivastava, R., Sahasrabuddhe, A.A., and Gupta, C.M. (2010). Expression of a PTS2-truncated hexokinase produces glucose toxicity in *Leishmania donovani*. Mol. Biochem. Parasitol. *170*, 41–44.

Lal, A., Plaxton, W.C., and Kayastha, A.M. (2005). Purification and characterization of an allosteric fructose-1,6- bisphosphate aldolase from germinating mung beans (*Vigna radiata*). Phytochemistry *66*, 968–974.

Lam, H., and Winkler, M.E. (1990). Metabolic Relationships between Pyridoxine (Vitamin B6) and Serine Biosynthesis in *Escherichia coli* K-12. J. Bacteriol. *172*, 6518–6528.

Lamour, N., Rivière, L., Coustou, V., Coombs, G.H., Barrett, M.P., and Bringaud, F. (2005). Proline metabolism in procyclic *Trypanosoma brucei* is down-regulated in the presence of glucose. J. Biol. Chem. *280*, 11902–11910.

Langbein, S., Zerilli, M., zur Hausen, A., Staiger, W., Rensch-Boschert, K., Lukan, N., Popa, J., Ternullo, M.P., Steidler, A., Weiss, C., et al. (2006). Expression of transketolase TKTL1 predicts colon and urothelial cancer patient survival: Warburg effect reinterpreted. Br. J. Cancer *94*, 578–585.

Langmead, B., and Salzberg, S.L. (2012). Fast gapped-read alignment with Bowtie 2. Nat Methods *9*, 357–359.

Laskay, T., Van Zandbergen, G., and Solbach, W. (2003). Neutrophil granulocytes - Trojan horses for *Leishmania major* and other intracellular microbes? Trends Microbiol. *11*, 210–214.

LeBowitz, J.H., Smith, H.Q., Rusche, L., and Beverley, S.M. (1993). Coupling of poly(A) site selection and trans-splicing in Leishmania. Genes Dev. *7*, 996–1007.

Lee, S.H., Stephens, J.L., and Englund, P.T. (2007). A fatty-acid synthesis mechanism specialized for parasitism. Nat. Rev. Microbiol. *5*, 287–297.

Lee, W.P., Boros, L.G., Puigjaner, J., Bassilian, S., Lim, S.H.U., Cascante, M., Paul, W., Puig-, J., and Lim, S. (1998). Mass isotopomer study of the nonoxidative pathways of the pentose cycle with [1 ,2-13 C2] glucose. Am J Physiol *274*, 843–851.

Leifso, K., Cohen-Freue, G., Dogra, N., Murray, A., and McMaster, W.R. (2007). Genomic and proteomic expression analysis of Leishmania promastigote and amastigote life stages: The Leishmania genome is constitutively expressed. Mol. Biochem. Parasitol. *152*, 35–46.

Leroux, A.E., and Krauth-Siegel, R.L. (2015). Thiol redox biology of trypanosomatids and potential targets for chemotherapy. Mol. Biochem. Parasitol.

Lindqvist, Y., Schneider, G., Ermler, U., and Sundstrom, M. (1992). Three-dimensional structure of transketolase, a thiamine diphosphate dependent enzyme, at 2.5 A resolution. EMBO J. *11*, 2373–2379.

Lobo, Z., and Miatra, P.K. (1982). Pentose Phosphate Pathway Mutants of Yeast. Mol Gen Genet *185*, 367–368.

Loureiro, I., Faria, J., Clayton, C., Macedo-Ribeiro, S., Santarém, N., Roy, N., Cordeiro-da-Siva, A., and Tavares, J. (2015). Ribose 5-Phosphate Isomerase B Knockdown Compromises Trypanosoma brucei Bloodstream Form Infectivity. PLoS Negl. Trop. Dis. *9*, 1–11.

Lünse, C.E., Scott, F.J., Suckling, C.J., and Mayer, G. (2014). Novel TPP-riboswitch activators bypass metabolic enzyme dependency. Front. Chem. *2*, 53.

Lux, H., Heise, N., Klenner, T., Hart, D., and Opperdoes, F.R. (2000). Ether-lipid (alkyl-phospholipid) metabolism and the mechanism of action of ether-lipid analogues in Leishmania. Mol. Biochem. Parasitol. *111*, 1–14.

Maarouf, M., Adeline, M.T., Solignac, M., Vautrin, D., and Robert-Gero, M. (1998). Development and characterization of paromomycin-resistant *Leishmania donovani* promastigotes. Parasite *5*, 167–173.

Mancilla, R., and Naquira, C. (1964). Comparative metabolism of C14-glucose in two strains of *Trypanosoma cruzi*. J. Protozool. *11*, 509–513.

Mancilla, R., Naquira, C., and Lanas, C. (1965). Metabolism of glucose labelled with carbon - 14 in *Leishmania enriettii*. Nature *206*, 27–28.

Martin, E., Simon, M.W., Schaefer, F.W. 3rd, and Mukkada, A.J. (1976). Enzymes of carbohydrate metabolism in four human species of Leishmania: a comparative survey. J. Protozool. *23*, 600–607.

Mathieu, C., Gonzalez Salgado, A., Wirdnam, C., Meier, S., Suter Grotemeyer, M., Inbar, E., Mäser, P., Zilberstein, D., Sigel, E., Butikofer, P., et al. (2014). *Trypanosoma brucei* eflornithine transporter AAT6 is a low affinity, low selective transporter for neutral amino acids. Biochem J *18*, 9–18.

Maugeri, D. a, and Cazzulo, J.J. (2004). The pentose phosphate pathway in *Trypanosoma cruzi*. FEMS Microbiol. Lett. *234*, 117–123.

Maugeri, D.A., Cazzulo, J.J., Burchmore, R.J.S., Barrett, M.P., and Ogbunude, P.O.J. (2003). Pentose phosphate metabolism in *Leishmania mexicana*. Mol. Biochem. Parasitol. *130*, 117–125.

Mazet, M., Morand, P., Biran, M., Bouyssou, G., Courtois, P., Daulouède, S., Millerioux, Y., Franconi, J.M., Vincendeau, P., Moreau, P., et al. (2013). Revisiting the Central Metabolism of the Bloodstream Forms of *Trypanosoma brucei*: Production of Acetate in the Mitochondrion Is Essential for Parasite Viability. PLoS Negl. Trop. Dis. *7*, 1–14.

Mbongo, N., Loiseau, P.M., and Billion, M.A. (1998). Mechanism of Amphotericin B Resistance in *Leishmania donovani* Promastigotes. Antimicrob Agents Chemother *42*, 352-7.

McConville, M.J., Saunders, E.C., Kloehn, J., and Dagley, M.J. (2015). Leishmania carbon metabolism in the macrophage phagolysosome- feast or famine? F1000Research *4*, 938.

McNew, J.A., and Goodman, J.M. (1994). An oligomeric protein is imported into peroxisomes in vivo. J. Cell Biol. *127*, 1245–1257.

McNicoll, F., Drummelsmith, J., Muller, M., Madore, E., Boilard, N., Ouellette, M., and Papadopoulou, B. (2006). A combined proteomic and transcriptomic approach to the study of stage differentiation in *Leishmania infantum*. Proteomics *6*, 3567–3581.

Melaku, Y., Collin, S.M., Keus, K., Gatluak, F., Ritmeijer, K., and Davidson, R.N. (2007). Treatment of kala-azar in southern Sudan using a 17-day regimen of sodium stibogluconate combined with paromomycin: a retrospective comparison with 30-day sodium stibogluconate monotherapy. Am. J. Trop. Med. Hyg. *77*, 89–94.

Mercaldi, G.F., Ranzani, A.T., and Cordeiro, A.T. (2014). Discovery of new uncompetitive inhibitors of glucose-6-phosphate dehydrogenase. J. Biomol. Screen. *19*, 1362–1371.

Meshalkina, L.E., Drutsa, V.L., Koroleva, O.N., Solovjeva, O.N., and Kochetov, G.A. (2013). Is transketolase-like protein, TKTL1, transketolase? Biochim. Biophys. Acta - Mol. Basis Dis. *1832*, 387–390.

Michels, P. a, Hannaert, V., and Bringaud, F. (2000). Metabolic aspects of glycosomes in trypanosomatidae - new data and views. Parasitol. Today Pers. Ed *16*, 482–489.

Michels, P. a M., Bringaud, F., Herman, M., and Hannaert, V. (2006). Metabolic functions of glycosomes in trypanosomatids. Biochim. Biophys. Acta *1763*, 1463–1477.

Miclet, E., Stoven, V., Michels, P.A.M., Opperdoes, F.R., Lallemand, J.Y., and Duffieux, F. (2001). NMR Spectroscopic Analysis of the First Two Steps of the Pentose-Phosphate Pathway Elucidates the Role of 6-Phosphogluconolactonase. J. Biol. Chem. *276*, 34840–34846.

Milewski, S., Janiak, A., and Wojciechowski, M. (2006). Structural analogues of reactive intermediates as inhibitors of glucosamine-6-phosphate synthase and phosphoglucose isomerase. Arch. Biochem. Biophys. *450*, 39–49.

Millerioux, Y., Ebikeme, C., Biran, M., Morand, P., Bouyssou, G., Vincent, I.M., Mazet, M., Riviere, L., Franconi, J.M., Burchmore, R.J.S., et al. (2013). The threonine degradation pathway of the *Trypanosoma brucei* procyclic form: The main carbon source for lipid biosynthesis is under metabolic control. Mol. Microbiol. *90*, 114–129.

Mishra, K.K., Holzer, T.R., Moore, L.L., and LeBowitz, J.H. (2003). A negative regulatory element controls mRNA abundance of the *Leishmania mexicana* Paraflagellar rod gene PFR2. Eukaryot. Cell *2*, 1009–1017.

Moorhead, G.B., and Plaxton, W.C. (1990). Purification and characterization of

cytosolic aldolase from carrot storage root. Biochem. J. *269*, 133–139.

Moritz, B., Striegel, K., de Graaf, A.A., and Sahm, H. (2002). Changes of pentose phosphate pathway flux in vivo in *Corynebacterium glutamicum* during leucine-limited batch cultivation as determined from intracellular metabolite concentration measurements. Metab. Eng. *4*, 295–305.

Mottram, J.C., and Coombs, G.H. (1985a). *Leishmania mexicana*: subcellular distribution of enzymes in amastigotes and promastigotes. Exp. Parasitol. *59*, 265–274.

Mottram, J.C., and Coombs, G.H. (1985b). *Leishmania mexicana*: Enzyme activities of amastigotes and promastigotes and their inhibition by antimonials and arsenicals. Exp. Parasitol. *59*, 151–160.

Mukherjee, A., Boisvert, S., Monte-Neto, R.L. do, Coelho, A.C., Raymond, F., Mukhopadhyay, R., Corbeil, J., and Ouellette, M. (2013). Telomeric gene deletion and intrachromosomal amplification in antimony-resistant Leishmania. Mol. Microbiol. *88*, 189–202.

Murray, A., Fu, C., Habibi, G., and McMaster, W.R. (2007). Regions in the 3' untranslated region confer stage-specific expression to the *Leishmania mexicana* a600-4 gene. Mol. Biochem. Parasitol. *153*, 125–132.

Murray, H.W., Berman, J.D., Davies, C.R., and Saravia, N.G. (2005). Advances in leishmaniasis. Lancet *366*, 1561–1577.

Naderer, T., Ellis, M. a, Sernee, M.F., De Souza, D.P., Curtis, J., Handman, E., and McConville, M.J. (2006). Virulence of Leishmania major in macrophages and mice requires the gluconeogenic enzyme fructose-1,6-bisphosphatase. Proc. Natl. Acad. Sci. U. S. A. *103*, 5502–5507.

Naderer, T., Wee, E., and McConville, M.J. (2008). Role of hexosamine biosynthesis in Leishmania growth and virulence. Mol. Microbiol. *69*, 858–869.

Naderer, T., Heng, J., and McConville, M.J. (2010). Evidence that intracellular stages of *Leishmania major* utilize amino sugars as a major carbon source. PLoS Pathog. *6*.

Naderer, T., Heng, J., Saunders, E.C., Kloehn, J., Rupasinghe, T.W., Brown, T.J., and McConville, M.J. (2015). Intracellular Survival of *Leishmania major* Depends on Uptake and Degradation of Extracellular Matrix Glycosaminoglycans by Macrophages. PLoS Pathog. *11*, 1–20.

Nandan, D., Tran, T., Trinh, E., Silverman, J.M., and Lopez, M. (2007). Identification of leishmania fructose-1,6-bisphosphate aldolase as a novel activator of host macrophage Src homology 2 domain containing protein tyrosine phosphatase SHP-1. Biochem. Biophys. Res. Commun. *364*, 601–607.

Naula, C.M., Logan, F.M., Wong, P.E., Barrett, M.P., and Burchmore, R.J. (2010). A glucose transporter can mediate ribose uptake: Definition of residues that confer substrate specificity in a sugar transporter. J. Biol. Chem. *285*, 29721–29728.

Nilsson, U., Meshalkina, L., Lindqvist, Y., and Schneidere, G. (1997). Examination of substrate binding in thiamin diphosphate-dependent transketolase by protein crystallography and site-directed mutagenesis. J. Biol. Chem. *272*, 1864–1869.

Nugent, P.G., Karsani, S.A., Wait, R., Tempero, J., and Smith, D.F. (2004).

Proteomic analysis of *Leishmania mexicana* differentiation. Mol. Biochem. Parasitol. *136*, 51–62.

Ogbunude, P.O.J., Lamour, N., and Barrett, M.P. (2007). Molecular Cloning, Expression and Characterization of Ribokinase of *Leishmania major*. Acta Biochim. Biophys. Sin. (Shanghai). *39*, 462–466.

Opperdoes, F.R., and Coombs, G.H. (2007). Metabolism of Leishmania: proven and predicted. Trends Parasitol. *23*, 149–158.

Opperdoes, F.R., and Szikora, J.-P. (2006). In silico prediction of the glycosomal enzymes of *Leishmania major* and trypanosomes. Mol. Biochem. Parasitol. *147*, 193–206.

Ostyn, B., Gidwani, K., Khanal, B., Picado, A., Chappuis, F., Singh, S.P., Rijal, S., Sundar, S., and Boelaert, M. (2011). Incidence of symptomatic and asymptomatic *Leishmania donovani* infections in High-Endemic foci in India and Nepal: A prospective study. PLoS Negl. Trop. Dis. *5*, 1–7.

Paape, D., Lippuner, C., Schmid, M., Ackermann, R., Barrios-Llerena, M.E., Zimny-Arndt, U., Brinkmann, V., Arndt, B., Pleissner, K.P., Jungblut, P.R., et al. (2008). Transgenic, fluorescent *Leishmania mexicana* allow direct analysis of the proteome of intracellular amastigotes. Mol. Cell. Proteomics MCP *7*, 1688–1701.

Pace, D. (2014). Leishmaniasis. J. Infect. *69*, S10–S18.

Pages, M., Bastien, P., Veas, F., Rossi, V., Bellis, M., Wincker, P., Rioux, J.A., and Roizes, G. (1989). Chromosome size and number polymorphisms in *Leishmania infantum* suggest amplification/deletion and possible genetic exchange. Mol. Biochem. Parasitol. *36*, 161–168.

Palumbo, E. (2008). Oral miltefosine treatment in children with visceral leishmaniasis: a brief review. Braz. J. Infect. Dis. *12*, 2–4.

Pan, a a, Duboise, S.M., Eperon, S., Rivas, L., Hodgkinson, V., Traub-Cseko, Y., and McMahon-Pratt, D. (1993). Developmental life cycle of Leishmania-cultivation and characterization of cultured extracellular amastigotes. J Eukaryot Microbiol *40*, 213–223.

Parkin, D.W. (1996). Purine-specific nucleoside N-ribohydrolase from *Trypanosoma brucei brucei*. Purification, specificity, and kinetic mechanism. J. Biol. Chem. *271*, 21713–21719.

Pasti, C., Rinaldi, E., Cervellati, C., Dallocchio, F., Hardré, R., Salmon, L., and Hanau, S. (2003). Sugar derivatives as new 6-phosphogluconate dehydrogenase inhibitors selective for the parasite *Trypanosoma brucei*. Bioorganic Med. Chem. *11*, 1207–1214.

Peña, I., Pilar Manzano, M., Cantizani, J., Kessler, A., Alonso-Padilla, J., Bardera, A.I., Alvarez, E., Colmenarejo, G., Cotillo, I., Roquero, I., et al. (2015). New compound sets identified from high throughput phenotypic screening against three kinetoplastid parasites: an open resource. Sci. Rep. *5*, 8771.

Perry, M.R., Wyllie, S., Raab, A., Feldmann, J., and Fairlamb, A.H. (2013). Chronic exposure to arsenic in drinking water can lead to resistance to antimonial drugs in a mouse model of visceral leishmaniasis. Proc. Natl. Acad. Sci. U. S. A. *110*, 19932–19937.

Perry, M.R., Prajapati, V.K., Menten, J., Raab, A., Feldmann, J., Chakraborti, D., Sundar, S., Fairlamb, A.H., Boelaert, M., and Picado, A. (2015). Arsenic exposure and outcomes of antimonial treatment in visceral leishmaniasis patients in Bihar, India: a retrospective cohort study. PLoS Negl. Trop. Dis. *9*, e0003518.

Pescher, P., Blisnick, T., Bastin, P., and Spath, G.F. (2011). Quantitative proteome profiling informs on phenotypic traits that adapt *Leishmania donovani* for axenic and intracellular proliferation. Cell. Microbiol. *13*, 978–991.

Peters, N.C., Egen, J.G., Secundino, N., Debrabant, A., Kimblin, N., Kamhawi, S., Lawyer, P., Fay, M.P., Germain, R.N., and Sacks, D. (2008). *In vivo* imaging reveals an essential role for neutrophils in leishmaniasis transmitted by sand flies. Science *321*, 970–974.

Petrareanu, G., Balasu, M.C., Vacaru, A.M., Munteanu, C.V.A., Ionescu, A.E., Matei, I., and Szedlacsek, S.E. (2014). Phosphoketolases from *Lactococcus lactis*, *Leuconostoc mesenteroides* and *Pseudomonas aeruginosa*: Dissimilar sequences, similar substrates but distinct enzymatic characteristics. Appl. Microbiol. Biotechnol. *98*, 7855–7867.

Phillips, C., Dohnalek, J., Gover, S., Barrett, M.P., and Adams, M.J. (1998). A 2.8 A resolution structure of 6-phosphogluconate dehydrogenase from the protozoan parasite *Trypanosoma brucei*: comparison with the sheep enzyme accounts for differences in activity with coenzyme and substrate analogues. J. Mol. Biol. *282*, 667–681.

Pral, E.M., da Moitinho, M.L., Balanco, J.M., Teixeira, V.R., Milder, R. V, and Alfieri, S.C. (2003). Growth phase and medium ph modulate the expression of proteinase activities and the development of megasomes in axenically cultivated *Leishmania (Leishmania) amazonensis* amastigote-like organisms. J Parasitol *89*, 35–43.

Purkait, B., Kumar, A., Nandi, N., Sardar, A.H., Das, S., Kumar, S., Pandey, K., Ravidas, V., Kumar, M., De, T., et al. (2012). Mechanism of amphotericin B resistance in clinical isolates of *Leishmania donovani*. Antimicrob. Agents Chemother. *56*, 1031–1041.

Quijada, L., Soto, M., Alonso, C., and Requena, J.M. (2000). Identification of a putative regulatory element in the 3'-untranslated region that controls expression of HSP70 in *Leishmania infantum*. Mol. Biochem. Parasitol. *110*, 79–91.

Rais, B., Comin, B., Puigjaner, J., Brandes, J.L., Creppy, E., Saboureau, D., Ennamany, R., Lee, W.P., Boros, L.G., and Cascante, M. (1999). Oxythiamine and dehydroepiandrosterone induce a G 1 phase cycle arrest in Ehrlich's tumor cells through inhibition of the pentose cycle. FEBS Lett. *456*, 113–118.

Ralton, J.E., Naderer, T., Piraino, H.L., Bashtannyk, T.A., Callaghan, J.M., and McConville, M.J. (2003). Evidence that Intracellular 1-2 Mannan Is a Virulence Factor in Leishmania Parasites. J. Biol. Chem. *278*, 40757–40763.

Ranoux, A., and Hanefeld, U. (2013). Improving transketolase. Top. Catal. *56*, 750–764.

Räz, B., Iten, M., Grether-Bühler, Y., Kaminsky, R., and Brun, R. (1997). The Alamar Blue assay to determine drug sensitivity of African trypanosomes (T.b. rhodesiense and T.b. gambiense) in vitro. Acta Trop. *68*, 139–147.

Rochette, A., Raymond, F., Ubeda, J.-M., Smith, M., Messier, N., Boisvert, S., Rigault, P., Corbeil, J., Ouellette, M., and Papadopoulou, B. (2008). Genome-wide gene expression profiling analysis of *Leishmania major* and *Leishmania infantum* developmental stages reveals substantial differences between the two species. BMC Genomics *9*, 255.

Rochette, A., Raymond, F., Corbeil, J., Ouellette, M., and Papadopoulou, B. (2009). Whole-genome comparative RNA expression profiling of axenic and intracellular amastigote forms of *Leishmania infantum*. Mol. Biochem. Parasitol. *165*, 32–47.

Rodriguez-Contreras, D., and Hamilton, N. (2014). Gluconeogenesis in *Leishmania mexicana*: Contribution of glycerol kinase, phosphoenolpyruvate carboxykinase, and pyruvate phosphate dikinase. J. Biol. Chem. *289*, 32989–33000.

Rodriguez-Contreras, D., and Landfear, S.M. (2006). Metabolic changes in glucose transporter-deficient *Leishmania mexicana* and parasite virulence. J. Biol. Chem. *281*, 20068–20076.

Rodriguez-Contreras, D., Feng, X., Keeney, K.M., Archie, H.G., and Landfear, S.M. (2007). Phenotypic characterization of a glucose transporter null mutant in *Leishmania mexicana*. *153*, 9–18.

Rodriguez-Contreras, D., Aslan, H., Feng, X., Tran, K., Yates, P.A., Kamhawi, S., and Landfear, S.M. (2015). Regulation and biological function of a flagellar glucose transporter in *Leishmania mexicana*: A potential glucose sensor. FASEB J. *29*, 11–24.

Rogers, M.E., Chance, M.L., and Bates, P.A. (2002). The role of promastigote secretory gel in the origin and transmission of the infective stage of *Leishmania mexicana* by the sandfly *Lutzomyia longipalpis*. Parasitology *124*, 495–507.

Rojas, J.C., Bruchey, A.K., and Gonzalez-Lima, F. (2012). Neurometabolic mechanisms for memory enhancement and neuroprotection of methylene blue. Prog. Neurobiol. *96*, 32–45.

Ruda, G.F., Alibu, V.P., Mitsos, C., Bidet, O., Kaiser, M., Brun, R., Barrett, M.P., and Gilbert, I.H. (2007). Synthesis and biological evaluation of phosphate prodrugs of 4-phospho-D-erythronohydroxamic acid, an inhibitor of 6-phosphogluconate dehydrogenase. ChemMedChem *2*, 1169–1180.

Ruda, G.F., Campbell, G., Alibu, V.P., Barrett, M.P., Brenk, R., and Gilbert, I.H. (2010a). Virtual fragment screening for novel inhibitors of 6-phosphogluconate dehydrogenase. Bioorganic Med. Chem. *18*, 5056–5062.

Ruda, G.F., Alibu, V.P., Mitsos, C., Bidet, O., Kaiser, M., Brun, R., Barrett, M.P., Gilbert, I.H., Wong, P.E., Alibu, V.P., et al. (2010b). Aryl phosphoramidates of 5-phospho erythronohydroxamic acid, a new class of potent trypanocidal compounds. J. Med. Chem. *18*, 1169–1180.

Ryley, J.F. (1962). Studies on the metabolism of the protozoa. 9. Comparative metabolism of blood-stream and culture forms of *Trypanosoma rhodesiense*. Biochem. J. *85*, 211–223.

Saar, Y., Ransford, A., Waldman, E., Mazareb, S., Amin-Spector, S., Plumblee, J., Turco, S.J., and Zilberstein, D. (1998). Characterization of developmentally-regulated activities in axenic amastigotes of *Leishmania donovani*. Mol. Biochem. Parasitol. *95*, 9–20.

Sacks, D.L., Modi, G., Rowton, E., Spath, G., Epstein, L., Turco, S.J., and Beverley, S.M. (2000). The role of phosphoglycans in Leishmania-sand fly interactions. Proc. Natl. Acad. Sci. U. S. A. *97*, 406–411.

Salam, N., Al-Shaqha, W.M., and Azzi, A. (2014). Leishmaniasis in the Middle East: Incidence and Epidemiology. PLoS Negl. Trop. Dis. *8*, 1–8.

Saunders, E.C., Ng, W.W., Chambers, J.M., Ng, M., Naderer, T., Krömer, J.O., Likic, V. a, and McConville, M.J. (2011). Isotopomer profiling of *Leishmania mexicana* promastigotes reveals important roles for succinate fermentation and aspartate uptake in tricarboxylic acid cycle (TCA) anaplerosis, glutamate synthesis, and growth. J. Biol. Chem. *286*, 27706–27717.

Saunders, E.C., Ng, W.W., Kloehn, J., Chambers, J.M., Ng, M., and McConville, M.J. (2014). Induction of a stringent metabolic response in intracellular stages of *Leishmania mexicana* leads to increased dependence on mitochondrial metabolism. PLoS Pathog. *10*, e1003888.

Savoia, D. (2015). Recent updates and perspectives on leishmaniasis. J. Infect. Dev. Ctries. *9*, 588–596.

Saxena, A., Worthey, E.A., Yan, S., Leland, A., Stuart, K.D., and Myler, P.J. (2003). Evaluation of differential gene expression in *Leishmania major* Friedlin procyclics and metacyclics using DNA microarray analysis. Mol. Biochem. Parasitol. *129*, 103–114.

Schaaff-Gerstenschläger, I., and Zimmermann, F.K. (1993). Pentose-phosphate pathway in *Saccharomyces cerevisiae*: analysis of deletion mutants for transketolase, transaldolase, and glucose 6-phosphate dehydrogenase. Curr. Genet. *24*, 373–376.

Scheltema, R.A., Jankevics, A., Jansen, R.C., Swertz, M.A., and Breitling, R. (2011). PeakML/mzMatch: a file format, Java library, R library, and tool-chain for mass spectrometry data analysis. Anal. Chem. *83*, 2786–2793.

Schirmer, R.H., Coulibaly, B., Stich, A., Scheiwein, M., Merkle, H., Eubel, J., Becker, K., Becher, H., Müller, O., Zich, T., et al. (2003). Methylene blue as an antimalarial agent. Redox Rep. *8*, 272–275.

Schneider, S., Lüdtke, S., Schröder-Tittmann, K., Wechsler, C., Meyer, D., and Tittmann, K. (2012). A Δ38 Deletion Variant of Human Transketolase as a Model of Transketolase-Like Protein 1 Exhibits No Enzymatic Activity. PLoS One *7*, 1–9.

Seifert, K., and Croft, S.L. (2006). *In vitro* and *in vivo* interactions between miltefosine and other antileishmanial drugs. Antimicrob. Agents Chemother. *50*, 73–79.

Seyfang, A., and Landfear, S.M. (1999). Substrate depletion upregulates uptake of myo-inositol, glucose and adenosine in Leishmania. Mol. Biochem. Parasitol. *104*, 121–130.

Shaked-Mishan, P., Suter-Grotemeyer, M., Yoel-Almagor, T., Holland, N., Zilberstein, D., and Rentsch, D. (2006). A novel high-affinity arginine transporter from the human parasitic protozoan *Leishmania donovani*. Mol. Microbiol. *60*, 30–38.

Shalev, M., Rozenberg, H., Smolkin, B., Nasereddin, A., Kopelyanskiy, D., Belakhov, V., Schrepfer, T., Schacht, J., Jaffe, C.L., Adir, N., et al. (2015).

Structural basis for selective targeting of leishmanial ribosomes: aminoglycoside derivatives as promising therapeutics. Nucleic Acids Res. *43*, 8601–8613.

Shulaev, V. (2006). Metabolomics technology and bioinformatics. Briefings Bioinforma. *7*, 128–139.

Silva, A.M., Cordeiro-da-Silva, A., and Coombs, G.H. (2011). Metabolic variation during development in culture of *Leishmania donovani* promastigotes. PLoS Negl. Trop. Dis. *5*, e1451.

Silverberg, M., and Dalziel, K. (1975). 6-Phospho-D-gluconate Dehydrogenase from Sheep Liver. Methods Enzymol. *41*, 214–220.

Sollelis, L., Ghorbal, M., MacPherson, C.R., Martinus, R.M., Kuk, N., Crobu, L., Bastien, P., Scherf, A., Lopez-Rubio, J.J., and Sterkers, Y. First efficient CRISPR-Cas9-mediated genome editing in *Leishmania* parasites. Cell Micorbiol *17*, 1405-1412.

Solovjeva, O.N., and Kochetov, G.A. (1999). Inhibition of transketolase by p - hydroxyphenylpyruvate. *462*, 246–248.

Srivastava, P., Prajapati, V.K., Rai, M., and Sundar, S. (2011). Unusual case of resistance to amphotericin B in visceral leishmaniasis in a region in India where leishmaniasis is not endemic. J. Clin. Microbiol. *49*, 3088–3091.

Staiger, W.I., Coy, J.F., Grobholz, R., Hofheinz, R.-D., Lukan, N., Post, S., Schwarzbach, M.H., and Willeke, F. (2006a). Expression of the mutated transketolase TKTL1, a molecular marker in gastric cancer. Oncol. Rep. *16*, 657–661.

Staiger, W.I., Coy, J.F., Grobholz, R., Hofheinz, R.D., Lukan, N., Post, S., Schwarzbach, M.H., and Willeke, F. (2006b). Expression of the mutated transketolase TKTL1, a molecular marker in gastric cancer. Oncol. Rep. *16*, 657–661.

Stern, A.L., Burgos, E., Salmon, L., and Cazzulo, J.J. (2007). Ribose 5-phosphate isomerase type B from *Trypanosoma cruzi*: kinetic properties and site-directed mutagenesis reveal information about the reaction mechanism. Biochem. J. *401*, 279–285.

Stern, A.L., Naworyta, A., Cazzulo, J.J., and Mowbray, S.L. (2011). Structures of type B ribose 5-phosphate isomerase from *Trypanosoma cruzi* shed light on the determinants of sugar specificity in the structural family. FEBS J. *278*, 793–808.

Stincone, A., Prigione, A., Cramer, T., Wamelink, M.M.C., Campbell, K., Cheung, E., Olin-Sandoval, V., Grüning, N.-M., Krüger, A., Tauqeer Alam, M., et al. (2014). The return of metabolism: biochemistry and physiology of the pentose phosphate pathway. Biol. Rev. Camb. Philos. Soc.

Stoffel, S. a, Alibu, V.P., Hubert, J., Ebikeme, C., Portais, J.-C., Bringaud, F., Schweingruber, M.E., and Barrett, M.P. (2011). Transketolase in *Trypanosoma brucei*. Mol. Biochem. Parasitol. *179*, 1–7.

Stuart, K. (1983). Kinetoplast DNA, mitochondrial DNA with a difference. Mol. Biochem. Parasitol. *9*, 93–104.

Sundar, S., Jha, T.K., Thakur, C.P., Engel, J., Sindermann, H., Fischer, C., Junge, K., Bryceson, A., and Berman, J. (2002). Oral miltefosine for Indian visceral

leishmaniasis. N. Engl. J. Med. *347*, 1739–1746.

Sundar, S., Sinha, P.K., Rai, M., Verma, D.K., Nawin, K., Alam, S., Chakravarty, J., Vaillant, M., Verma, N., Pandey, K., et al. (2011). Comparison of short-course multidrug treatment with standard therapy for visceral leishmaniasis in India: an open-label, non-inferiority, randomised controlled trial. Lancet (London, England) *377*, 477–486.

Sundström, M., Lindqvist, Y., Schneidert, G., Hellman, U., and Ronne, H. (1993). Yeast TKL1 gene encodes a transketolase that is required for efficient glycolysis and biosynthesis of aromatic amino acids. J. Biol. Chem. *268*, 24346–24352.

Swinkels, B.W., Gould, S.J., Bodnar, A.G., Rachubinski, R.A., and Subramani, S. (1991). A novel, cleavable peroxisomal targeting signal at the amino-terminus of the rat 3-ketoacyl-CoA thiolase. EMBO J. *10*, 3255–3262.

Tait, A., Barry, J.D., Wink, R., Sanderson, A., and Crowe, J.S. (1985). Enzyme variation in *T. brucei* ssp. II. Evidence for *T. b. rhodesiense* being a set of variants of *T. b. brucei*. Parasitology *90 (Pt 1)*, 89–100.

Tetaud, E., Lecuix, I., Sheldrake, T., Baltz, T., and Fairlamb, A.H. (2002). A new expression vector for *Crithidia fasciculata* and Leishmania. Mol. Biochem. Parasitol. *120*, 195–204.

Titus, R.G., and Ribeiro, J.M. (1988). Salivary gland lysates from the sand fly *Lutzomyia longipalpis* enhance Leishmania infectivity. Science *239*, 1306–1308.

Trager, W. (1957). Nutrition of a Hemoflagellate (*Leishmania tarentolae*) Having an Interchangeable Requirement for Choline or Pyridoxal. J. Protozool. *4*, 269–276.

Trapnell, C., Williams, B.A., Pertea, G., Mortazavi, A., Kwan, G., van Baren, M.J., Salzberg, S.L., Wold, B.J., and Pachter, L. (2010). Transcript assembly and quantification by RNA-Seq reveals unannotated transcripts and isoform switching during cell differentiation. Nat. Biotechnol. *28*, 511–515.

Trinconi, C.T., Reimao, J.Q., Coelho, A.C., and Uliana, S.R.B. (2016). Efficacy of tamoxifen and miltefosine combined therapy for cutaneous leishmaniasis in the murine model of infection with Leishmania amazonensis. J. Antimicrob. Chemother.

Trochine, A., Creek, D.J., Faral-Tello, P., Barrett, M.P., and Robello, C. (2014). Benznidazole biotransformation and multiple targets in *Trypanosoma cruzi* revealed by metabolomics. PLoS Negl. Trop. Dis. *8*, e2844.

Tsuboi, K.K., Fukunaga, K., and Chervenka, C.H. (1971). Phosphogluconase isomerase from human erythrocyte. J. Biol. Chem. *24*, 7586–7595.

Uniting to Combat NTDs (2014). Country Leadership and Collaboration on Neglected Tropical Diseases (London).

Vas, G., Conkrite, K., Amidon, W., Qian, Y., Banki, K., and Perl, A. (2006). Study of transaldolase deficiency in urine samples by capillary LC-MS/MS. J. Mass Spectrom. *41*, 463–469.

De Vas, M.G., Portal, P., Alonso, G.D., Schlesinger, M., Flawia, M.M., Torres, H.N., Fernandez Villamil, S., and Paveto, C. (2011). The NADPH-cytochrome P450 reductase family in *Trypanosoma cruzi* is involved in the sterol biosynthesis pathway. Int. J. Parasitol. *41*, 99–108.

Vasquez, J.J., Hon, C.C., Vanselow, J.T., Schlosser, A., and Siegel, T.N. (2014).

Comparative ribosome profiling reveals extensive translational complexity in different *Trypanosoma brucei* life cycle stages. Nucleic Acids Res. *42*, 3623–3637.

Veitch, N.J., Maugeri, D. a, Cazzulo, J.J., Lindqvist, Y., and Barrett, M.P. (2004). Transketolase from *Leishmania mexicana* has a dual subcellular localization. Biochem. J. *382*, 759–767.

Vercesi, A.E., Moreno, S.N., and Docampo, R. (1994). Ca^{2+}/H^{+} exchange in acidic vacuoles of *Trypanosoma brucei*. Biochem. J. *304*, 227–233.

Vertommen, D., Van Roy, J., Szikora, J.-P., Rider, M.H., Michels, P. a M., and Opperdoes, F.R. (2008). Differential expression of glycosomal and mitochondrial proteins in the two major life-cycle stages of *Trypanosoma brucei*. Mol. Biochem. Parasitol. *158*, 189–201.

Vickers, T.J., and Beverley, S.M. (2011). Folate metabolic pathways in *Leishmania*. Essays Biochem. *51*, 63–80.

Villet, R.H., and Dalziel, K. (1969). The nature of the carbon dioxide substrate and equilibrium constant of the 6-phosphogluconate dehydrogenase reaction. Biochem. J. *115*, 633–638.

Vincent, I.M., Creek, D., Watson, D.G., Kamleh, M.A., Woods, D.J., Wong, P.E., Burchmore, R.J.S., and Barrett, M.P. (2010). A molecular mechanism for eflornithine resistance in African trypanosomes. PLoS Pathog. *6*, e1001204.

Vincent, I.M., Creek, D.J., Burgess, K., Woods, D.J., Burchmore, R.J.S., and Barrett, M.P. (2012). Untargeted metabolomics reveals a lack of synergy between nifurtimox and eflornithine against *Trypanosoma brucei*. PLoS Negl. Trop. Dis. *6*, e1618.

de Vries, H.J.C., Reedijk, S.H., and Schallig, H.D.F.H. (2015). Cutaneous leishmaniasis: recent developments in diagnosis and management. Am. J. Clin. Dermatol. *16*, 99–109.

Westrop, G.D., Williams, R.A.M., Wang, L., Zhang, T., Watson, D.G., Silva, A.M., and Coombs, G.H. (2015). Metabolomic analyses of Leishmania reveal multiple species differences and large differences in Amino Acid Metabolism. PLoS One *10*.

WHO (2010). Control of the Leishmaniases (Geneva).

Wildridge, D. (2012). Metabolism and drug resistance in trypanosomatids. University of Glasgow.

Williams, J.F., and MacLeod, J.K. (2006). The metabolic significance of octulose phosphates in the photosynthetic carbon reduction cycle in spinach. Photosynth. Res. *90*, 125–148.

Wilson, Z.N., Gilroy, C. a, Boitz, J.M., Ullman, B., and Yates, P. a (2012). Genetic dissection of pyrimidine biosynthesis and salvage in *Leishmania donovani*. J. Biol. Chem. *287*, 12759–12770.

Xia, J., Sinelnikov, I. V, Han, B., and Wishart, D.S. (2015). MetaboAnalyst 3.0--making metabolomics more meaningful. Nucleic Acids Res. *43*, W251–W257.

Xu, Z., Wawrousek, E.F., and Piatigorsky, J. (2002). Transketolase Haploinsufficiency Reduces Adipose Tissue and Female Fertility in Mice These include : Transketolase Haploinsufficiency Reduces Adipose Tissue and Female Fertility in Mice. *22*, 6142–6147.

Yi, D., Devamani, T., Abdoul-Zabar, J., Charmantray, F., Helaine, V., Hecquet, L., and Fessner, W.D. (2012). A pH-Based High-Throughput Assay for Transketolase: Fingerprinting of Substrate Tolerance and Quantitative Kinetics. ChemBioChem *13*, 2290–2300.

Zhao, G., and Winkler, M.E. (1994). An *Escherichia coli* K-12 tktA tktB mutant deficient in transketolase activity requires pyridoxine (vitamin B6) as well as the aromatic amino acids and vitamins for growth. J. Bacteriol. *176*, 6134–6138.